ECASIA·24

ABSTRACTS

9-14 June 2024, Gothenburg, Sweden

Abstract Book for European Conference on Applications of Surface and Interface Analysis

Editors:
Professor Lars Nyborg, ECASIA 2024 Chair
Professor Emmy Cao, ECASIA 2024 Co-chair
Technical production: Andreas Andersson

Sessions and chairpersons

Monday			Tuesday		
Morning			Morning		
Opening session			Plenary no. 2		
ECASIA award lecture			DPR2 Lars P.H. Jeurgens	CER1 Guillaume Monier	DAT2 Alexander Shard
Plenary no. 1			MET1 Philippe Marcus	CAT1 Ute Cappel	DPR2 Anna Regoutz
Afternoon			Afternoon		
TEC1 Lars Nyborg	NRG1 Francesco Fumagalli	DPR1 Emmy Cao	IMA2 Sven Tougaard	BIO2 Andreas Dahlin	NRG2 Julia Maybach
IMA1 Peter Sjövall	BIO1 Madeleine Ramstedt	DAT1 Alexander Shard	TEC2 Georg Held	CAT2 Jörg Radnik	NRG3 Wolfgang Werner
			Poster session		

Wednesday			Thursday			Friday	
Morning			Morning			Morning	
Plenary no. 3			Plenary no. 4			DAT6 Donald R Baer	DPR8 Lars Nyborg
COR1 Özlem Özcan Sandikcioglu	CAT3 Julia Maibach	DPR3 Lars P.H. Jeurgens	TEC2 Georg Held	ADH1 Mats Norell	DPR5+ DAT3 Ian Gilmore		
COR2 Philippe Marcus	CAT4 Eduard Hryha	DPR4 Anna Regoutz	NRG4 Anass Benayad	CAT5 Martin Hantusch	DPR6 Ian Gilmore	DAT7 Donald R Baer	DPR9 Lars Nyborg
						Closing ceremony	
Afternoon			Afternoon				
Excursion			MET2 Eduard Hryha	TEC3 Fransisco Yubero	DAT4 Mark Biesinger		
			BIO2 John Fletcher	DAT5 Mark Baker	DPR7 Jules Galipaud		
Dinner							

ADH: Adhesion and Tribology	BIO: Bio-Interfaces, Biomaterials and Life Science
CAT: Catalysis and Surface functionalization	CER: Ceramics; Glass; Oxides
COR: Corrosion	DAT: Data Analysis and Metrology
DPR: Thin Films, Coatings and Depth Profiling	ELC: Micro-, Opto-, and Organic Electronics
IMA: Nanomaterials and Imaging	MET: Metals
NRG: Energy, Environment, Geology And Heritage	POL: Polymers
TEC: Technical Development and New Instrumentation	

Contents

ECASIA Awardee Presentation 12

AS1 - Evolution and revolution in SIMS 13

Plenaries 14

PS1 - From model system to devices – Gaining insight into solar cells with photoelectron spectroscopy 15

PS2 - Active Chiral Surfaces Driving Left-Right Symmetry Breaking in Living Systems 16

PS3 - Advancing X-ray Photoelectron Spectroscopy (XPS) Methodologies for Materials Research 17

PS4 - Atom probe tomography as an amazing tool for the chemical analysis of soft matter and complex interfaces 18

Keynotes 19

K1 - Characterisation of microbial surface chemistry using cryo-XPS 20

K2 - Oxide Films and Corrosion 21

K3 - Electron Beam Attenuation and Energy Dissipation between 0 eV and Relativistic Energies. 22

K4 - Underused Information from XPS and Avoiding Common Errors 23

K5 - XPS, NAP-XPS, and HAXPES inelastic electrons to characterize nano-structured materials 25

K6 - Hard X-ray photoelectron spectroscopy and its application to the bonding and electronic structure of metal dihydrides 27

K7 - Powder for metal additive manufacturing: Properties, reuse and degradation from surface chemistry point of view 28

K8 - A journey towards operando X-ray photoelectron spectroscopy to follow reactions at battery interfaces 29

K9 - The Development of High Energy Sources for XPS 30

Orals 31

1. ADH – Adhesion and Tribology 32

O1 - Practical approach for standardization of surface free energy and piezoelectric constant using atomic force microscopy 33

O2 - REELS and AES applied to amorphous carbon surface imaging for tribological applications 35

2. BIO – Bio-interfaces, Biomaterials and Life Science 37

O3 - Biocompatibility investigations of laser-induced periodic surface structures on 316L stainless steel 38

O4 - Data analysis challenges associated with gas cluster ion beam secondary ion mass spectrometry in the life science arena. 39

O5 - GCIB-SIMS studies of skin cancer 40

O6 - Immunoglobulin stability in contact with elastomer surfaces 41

O7 - Oligopeptides on metallic surfaces: A molecular level description of the interface 43

O8 - Optimal mechanical properties and high cellular proliferation on hybrid PLC/HaP/SA scaffolds for tissue engineering 45

O9 - Physicochemical characterization of nanocellulose materials for food applications 47

O10 - Protein immobilzation on ultrananocrystalline diamond films with different surface terminations 49

O11 - Purification of biopharmaceuticals by electrochemical polymer brush chromatography 50

O12 - Surface analysis of PEGylated liposomes for nanomedicine applications 52

O13 - Surface treatment and functionalization of 2D and 3D titanium alloys for biomedical applications 54

3. CAT – Catalysis and Surface Functionalization 56

O14 - A guided tour around LEIS spectra 57

O15 - A synergy of light and water: unveiling the self-breakdown of organophosphonic acid grafted titanium dioxide 59

O16 - Advanced photoelectron spectroscopy: A tool to characterise the nature of oxygen defects?! 61

O17 - Ammonia decomposition over MgFe2O4 and MgFeCoO4 catalysts: An operando soft X-ray spectroscopy study 62

O18 - Electrocatalytic carbon dioxide reduction on electrodeposited multi-principal element alloy (MPEA) catalysts 64

O19 - Hard X-ray photoelectron spectroscopy reveals Fe segregation in NiFe electrodes during oxygen evolution reaction 65

O20 - Multi-Technique Characterization of PtNi Nanowires for Enhanced Durability and Efficiency 66

O21 - On the combination of UPS with optical absorption to investigate Cu2O||TiO2 direct Z-schemes with different Cu2O loading 67

O22 - Reliable measurements of the chemical composition of graphene-related 2D materials with X-ray photoelectron spectroscopy 69

O23 - Steel surface engineering by non-oxidising wet quenching 71

O24 - Surface Modification of Aged CuO Nanopowders as guided by XPS 72

O25 - Surface reactivity of cerium oxides thin films 73

O26 - The competition of CO oxy-chlorination and oxidation 74

O27 - The use of surface characterization techniques in phosphor materials 76

O28 - Ultrafast surface hydrophilicity transition in TiO2/Si, ZnO/Si, and multilayer heterojunctions 77

O29 - Understanding the enhanced activity of Pd/CeO2 thin films in hydrogen oxidation reaction in alkaline media 79

4. CER – Ceramics; Glass; Oxides 81

O30 - Barrier heights from XPS without “busting the bank”: In-chamber metal deposition on solution-processed zinc-tin oxide 82

O31 - Influence of dopant ion size and valence on CeO2 properties 84

O32 - Thin film deposition of tin and zinc oxide for positional photodetectors 85

5. COR – Corrosion 86

O33 - Contribution of imaging X-ray photoelectron spectroscopy (XPS) to characterize corrosion mechanism of chrome free layer 87

O34 - Full energy range examination of NiCrFeVCuTi high entropy oxide using XPS, HAXPES and UPS-LEIPS 89

O35 - The interplay of transpassive dissolution and oxygen evolution on multi-principal element alloys (MPEAs) 90

6. DAT – Data analysis and Metrology 91

O36 - Advanced characterization of GaN-based compounds by XPS: a new process of nitrogen and gallium content extraction 92

O37 - Combination of SIMS and machine learning as a screening technique in an industrial context 94

O38 - Combining XPS and HAXPES data to get beneath the surface 95

O39 - EnviroMETROS – A novel surface and multilayer thin film analysis tool 96

O40 - In situ determination of indium content in InxGa1-x droplets on GaAs(111)A based on the REELS/XPS complementarity 97

O41 - New insights into the reduction of ceria morphologies in X-ray photoelectron spectroscopy 99

O42 - Non-destructive characterization of multi-layered thin films using XPS, HAXPES and structure modeling in StrataPHI 101

O43 - NXmpes: a unified data transfer standard for photoemission spectroscopy 102

O44 - Obstacles and how to approach them – three examples in X-ray photoelectron spectroscopy measurement and analysis 103

O45 - Reliability of XPS analyses of perovskites: evolution of chemical and optoelectronic properties during X-ray irradiation 104

O46 - ToF-SIMS depth profiling and quantitative analysis of metals and alloys in a UHV, oxygen, and hydrogen Atmosphere 106

O47 - Understanding the fundamentals for A.I. interpretation of X-ray photoelectron spectra 107

O48 - Impact of powder properties and powder reuse on additive manufacturing of copper ... 108

O49 - Using X-ray induced Auger electron spectroscopy transitions to explore the surface reactivity of CIGS 110

O50 - XPS characterisation of brasses 112

7. DPR – Thin films, Coatings and Depth Profiling 113

O51 - Integration of 2D Nanolayers in opto-electronic and photonic devices 114

O52 - Uptake of water and ions in organic coatings on metals: an in situ spectro-electrochemical approach 116

O53 - 3D ToF-SIMS analysis of drug distribution and Mg stearate coating on lactose carrier particles 117

O54 - Air-stable PdSe2 crystal growth and characterization 118

O55 - Angle resolved XPS depth profiling for extreme ultraviolet lithography optics research-monoatomic vs cluster ion source 120

O56 - Carbide-rich nano-layers produced by ion beam mixing 121

O57 - Chemical state analysis of differently miscible interfaces in metallic multilayers 122

O58 - Combined XPS/ToF-SIMS investigation of the adsorption of an amine curing agent on converted HDG steel 123

O59 - Comparative study on advanced preparation techniques for internal structure analysis of organic coatings 124

O60 - Effect of hydrogen on the chemical state of amorphous alumina films grown by thermal atomic layer deposition 126

O61 - Exploiting the anion exchange properties of layered double hydroxide films for the design of functional coatings 128

O62 - Fabrication of multilayered biofilms using gas cluster ion beam assisted deposition 130

O63 - Femtosecond laser ablation (fs-LA) XPS depth profiling of lead halide perovskite thin film solar cells 131

O64 - Femtosecond laser ablation (fs-LA) – A new approach to XPS depth profiling 132

O65 - Highly transparent, stable, and superhydrophobic coatings for glass and PV panels 133

O66 - Interactions of a latent curing agent and metal oxides – relation of pH of the varnish and isoelectric point of surfaces 134

O67 - Interferometric NIR optics for liquid analysis 135

O68 - Multidimensional Elemental and Molecular Analysis for Surface & Interface studies 136

O69 - Optimal conditions for depth profiling with hard/soft multilayers using small cluster beams of C60, Ar and CO2 137

O70 - P-ARXPS analysis and ion profiling of nanometer-thick polyphosphazene (PPP) films on n-InP 139

O71 - Polyelectrolyte adsorption on different surfaces evaluated by XPS using two different quantification approaches 141

O72 - Stability investigation of atomic layer deposited cerium oxide depending on oxidant choice 143

O73 - Surface Analysis of Nanolayers by LEIS, SIMS and XPS 144

O74 - Synthesis of ultra-thin advanced MOF-like materials by use of ALD and their characterization 145

O75 - The effects of substrate interaction on the chemical properties of atomic layer deposited ultrathin ceria layers 147

O76 - Towards a high-entropy alloy thin-film reference material 149

O77 - Tuning the surface chemistry and structure of a phosphated zinc coating by hot active plasma 151

O78 - Unraveling Photostability of Multi-cation Hybrid Perovskites via Surface Analysis Techniques 152

O79 - XPS characterization of thermochemical nitriding MoS2 template sub-layer to prevent AlN delamination during regrowth 153

O80 - XPS depth profiling of highly porous black metal films 155

8. ELC – Micro-, Opto- and Organic Electronics 156

O81 - Advanced optimization of C&O species adsorbed on highly reactive surfaces during vacuum transfer step in microelectronic 157

O82 - Damage-free depth profiling of organic LEDs: a tool for understanding degradation mechanisms 159

9. IMA – Nanomaterials and Imaging 160

O83 - A new XPS test material for more reliable surface analysis of microstructures 161

O84 - Chemical analysis of functionalized graphene along the production process 163

O85 - Engineering materials at the atomic scale for the development of 3D-printed complex architecture 164

O86 - Growth of high density and crystalline GaN nanostructures on GaAs by droplet epitaxy 165

O87 - Modelling method for quantitative analysis of complex responses in piezo-response force microscopy 167

O88 - New HDR approach for TOF-SIMS data acquisition 169

O89 - Sample preparation methods for ToF-SIMS surface analysis of TiO2 nanoparticles: An interlaboratory comparison 170

O90 - Surface analysis of graphene oxide films reduced by thermal treatments 172

10. MET – Metallic Materials 173

O91 - Advancing X-ray photoelectron spectroscopy (XPS) methodologies for materials research 174

O92 - Exploring the impact of pure copper powder reuse on surface chemistry during powder bed fusion electron beam 176

O93 - Fracture surface analysis of LPBF-produced Ti-6Al-4V by XPS and AES 177

O94 - Preparation and characterization of refractory high-entropy alloys for nuclear fusion reactors 178

O95 - Reduction of iron oxides with in situ hydrogen charging of DP1000 steel in X-ray photoelectron spectroscopy XPS 179

O96 - Surface oxide chemistry of β-titanium Ti-Nb-Ta-Zr alloy powder and its changes during additive manufacturing 180

O97 - Wear behavior of an experimental boron-containing advanced high-strength complex-phase steel 181

11. NRG – Energy, Environment, geology and heritage 182

O98 - A Study of the chemistry of Mary-Rose timber hull core samples using XPS and ToF-SIMS 183

O99 - Charge compensation mechanism in LixNiO2 electrode studied by experimental and theoretical HAXPES 184

O100 - Comparison of different deposition procedures of SAMs on their distribution in perovskite solar cells by ToF-SIMS 185

O101 - Correlating electronic structure to material formation, growth, and chemistry in BaZrS3 thin films: from bands to bonds 186

O102 - Cryogenic XPS: 20 years probing intact interfaces in nature and life 188

O103 - Effect of ethylene sulphate on electrode interphases in full cell potassium ion batteries 190

O104 - From the outer surface to the bulk: an overview of Cu(In0.7Ga0.3)Se2 degradation... 191

O105 - High-Performance Li-ion Battery negative electrode of porous Silicon Nanowires Modifies with CHx (No show) 192

O106 - Interface optimization through XPS and UPS in high-efficiency Sb2Se3 solar cells synthesized at high pressure 193

O107 - Laser induced plasma spectroscopy as surface analytical tool for quality control gas diffusion layers of fuel cells 195

O108 - Potential of thermally evaporated thin Li and Na films for the development of next generation alkali metal batteries 197

O109 - Probing electron and ion dynamics of lead halide perovskite single crystals via time-resolved photoelectron spectroscopy 198

O110 - Protein preservation in fossils studied by artificial maturation using ToF-SIMS and N1s-NEXAFS 199

O111 - Surface analysis of engineered particles for improved battery performance and stability 201

O112 - Understanding and solving the issue of photodecomposition of PEO-LiTFSI polymer electrolytes in XPS analysis 202

O113 - XPS analysis of solid state composite cathodes – discriminating degradation from electric potential gradients 204

12. POL – Polymers 206

O114 - Optimized surface functionalization of food-grade PVC with polyhexamethylene guanidine for antimicrobial food packaging........ 207

13. TEC – Technical Development and New Instrumentation........ 209

O115 - A study on electron spectrum imaging measurements using electron microprobe........ 210

O116 - Battery analysis with high-resolution and high-throughput XPS 212

O117 - Evaluation of the high energy resolution spectra acquired by newly developed fast hemi-spherical analyzer (f-HSA) 213

O118 - Exploring the power of TOF-SIMS by coupling collision-induced dissociation and surface-induced dissociation 215

O119 - Hard X-ray photoelectron spectroscopy with photon energy up to 30 keV for characterization of semiconductor materials 217

O120 - Neural network for high-throughput XPS analysis using the simulation of electron spectra for surface analysis code 219

O121 - Non-destructive depth differentiated analysis of surfaces using Ion Scattering Spectroscopy (ISS), XPS and HAXPES........ 221

O122 - Operando Cells for high-pressure solid-gas and solid-liquid interface analysis 222

O123 - Operando/in-situ coupling of XPS and EIS to study solid-state Li-ion batteries........ 224

O124 - Photoelectron spectroscopy laboratory at the European XFEL 226

O125 - Quantitative secondary electron spectroscopy using a concentric hemispherical analyzer and Monte-Carlo simulations 227

O126 - Visualization of Fermi level difference at p-n-p junction in transistor device by spectrum image method of AES 229

Posters 231

1. ADH – Adhesion and Tribology 232

P1 - Effects of laser-processed surface texturing on wear behaviors of Ti alloys in contact with ZrO2 for dental applications........ 233

P2 - Surface coating of graphene oxide/Polyaniline/Cu by co-deposition for improved tribological performance........ 234

2. BIO – Bio-interfaces, Biomaterials and Life Science 236

P3 - Characterization of the biomedical surface by the XPS and HPXPS........ 237

P4 - Isolation of extracellular vesicles based on functionalized beads and a microfluidic device for biomarkers analysis........ 238

P5 - Surface characterisation of electrically poled polylactic acid using sessile drop method.. 239

P6 - XPS and ToF-SIMS characterization of cholesterol-based nanoparticles for Huntington disease 241

3. CAT – Catalysis and Surface Functionalization 243

P7 – Combining theory and experiments: spectra validation through DFT studies of metal-phosphonate properties in NU-1000 244

P8 - Conduction and valence bands investigation of CuInS2@ZnS for gas sensing purposes . 245

P9 - Methane dehydroaromatization on Mo/HZSM-5 and Nb doped Mo/HZSM-5 catalysts: A NAP-XPS study 247

P10 - XPS, TEM and DFT characterization of mnemonic TiO2 rutile–rutile interfaces triggering spontaneous dissociation of water 249

4. CER – Ceramics; Glass; Oxides 250

P11 - Optical response of 2D waveguides in silicate glass created via ion implantation with varying thick of optical barriers 251

P12 - Influences of Cr contents on oxidation behavior of WC-Co-Ni-Cr cemented carbides at 900℃ 252

5. COR – Corrosion 253

P13 - Corrosion behavior of low-temperature carburised AISI 304 austenitic stainless steel after hydrogen uptake 254

P14 - Dominant characteristic of an anodized NiTi alloy surface that suppress a Ni ion release in biological environment 255

P15 - Effect of hydrogen on the passivity of steels by an electrochemical-surface analytical approach 257

P16 - EIS study of the influence of sputtering parameters of SIN thin films deposited on 316 stainless steel. 258

P17 - Influence of current on the surface and corrosion behavior of Ni-obsidian coatings electrodeposited on ductile iron 259

P18 - On the interpretation of the XPS and XAES spectra of Ni compounds 260

P19 - Steel oxidation: reaction mechanisms, kinetics and scale morphology (No show) 262

6. DAT – Data Analysis and Metrology 263

P20 - Correlation analysis for X-ray radiation damage studies on double vacancy ordered halide perovskites 264

P21 - Do different XPS systems give the same result? 265

P22 - HAXPES spectra and quantification of bulk Mo and MoSe2 compound 266

P23 - HAXPES spectra and quantification of bulk W and WSe2 compound 267

P24 - Improved estimation of the spectrometer-transmission function with UNIFIT 2022 269

P25 - Quantitative investigation of SiP and SiGe binary layers using lab-scale HAXPES & ToF-SIMS 270

P26 - UNIFIT 2024 – the improved spectrum processing, analysis and presentation software for XPS, AES, XAS, RAMAN Spectroscopy 271

P27 - UNIFIT 2025 – the improved spectrum processing, analysis and presentation software for XPS, AES, XAS, RAMAN Spectroscopy 272

7. DPR – Thin films, Coatings and Depth Profiling 273

P28 - A comparative study of various analytical techniques to investigate Ni-Si thin film characteristics 274

P29 - Characterization of diamond-like carbon (DLC) coatings and effect of sputter depth profiling on these materials 275

P30 - Deep probing of buried layers with HAXPES, chemical analysis with bias applied operando setup for electronic devices 276

P31 – Inelastic background analysis from lab-based HAXPES spectra for critical interfaces in nano-electronics 278

P32 - Metal thin film morphology suitable for multilayer diffusion study 280

P33 - Surface analysis of the drug-eluting chitosan coatings on 3D-printed TiAl6V4 alloy for orthopedic applications 281

P34 - Thermoelectric and structural properties of sputtered AZO thin films with varying Al doping ratios (No show) 282

P35 - Tungsten coating as hydrogen permeation barrier: a surface characterization 284

8. ELC – Micro-, Opto- and Organic Electronics 285

P36 - Development of plasma surface treatment on GaN analyzed by quasi in-situ pARXPS . 286

P37 - Microstructures prepared by ion beam writing and ion implantation through mask in graphene derivatives and polymers 287

9. IMA – Nanomaterials and Imaging 288

P38 - Comparative chemical analysis of Ni-Fe oxide nanoparticles 289

P39 - Correlative imaging to reveal the nature of different graphene materials 290

P40 - Correlative XPS & SEM analysis to determine 2D material structures 292

P41 - Investigation of the MoS2 / substrate interaction using surface analysis techniques 293

P42 - Method development for inner-channel surface analysis of quartz nanopipettes with chemical modification 294

P43 - Nanoscale secondary ion mass spectrometry imaging (NanoSIMS) – A new tool to unveil nanostructures in life science, material and environmental science 296

P44 - Substrate Effects, Shapes, and Morphologies of Chemical Vapor Deposited 2D WSe2 . 297

10. MET – Metallic Materials 298

P45 - 316L steel prepared by L-PBF: surface effects of plasma low temperature carburizing . 299

P46 - Impact of gaseous hydrogen on low cycle fatigue performance: Fractographic insights from surface analysis 300

P47 - Segregation and crack formation in laser welded IN792 equiaxed superalloy 301

P48 - Tailoring Multi-properties of Fe-6.5Si Magnetic Alloys Through Laser Fluence in Powder Bed Fusion Process 302

P49 - XPS study of Co28Cr6Mo biocompatible alloy 303

11. NRG – Energy, Environment, Geology and Heritage 304

P50 - Effects of voltage holds on graphite electrode surfaces layers and X-ray photoelectron spectroscopy post-mortem studies 305

P51 - Electron spectroscopic investigations at alkaline-based battery-relevant reference material 306

P52 - Improvement of magnetic domain structures and magnetic properties of GO FeSi steels by laser surface treatment 308

P53 - Manufacturer discrepancies in potassium metal: Impact on battery performance and detection of sodium traces 309

P54 - Probing the solid electrolyte interphases in modified hard carbon-based negative electrodes for sodium ion batteries 310

P55 - Shielding surface for cathode material protection in lithium-ion batteries: Atomic layer fluorination 311

P56 - Understanding the surface chemistry of tin halide perovskite thin films 313

12. POL – Polymers 314

P57 - Controlled tunning of the wettability of aromatic polymers by precise dosing of oxygen atoms (No show) 315

P58 - In-situ spectroscopic analysis of thin organosilicon plasma film deposition on polylactide substrates 316

P59 - Revealing surface functionalities of micro- and nanoplastic particles' surface by means of XPS 318

13. TEC – Technical Development and New Instrumentation 320

P60 - Behavior of aniline molecules in the strong electric field by thermal ionization method (No Show) 321

P61 - Optical Surface Roughness Estimation using Artificial Intelligence Classification 322

P62 - Surface investigation of Layered Double Hydroxides grown on the biodegradable AZ31 alloy 323

ECASIA Awardee Presentation

AS1 - Evolution and revolution in SIMS

Award Speaker
Ian Gilmore
National Physical Laboratory, United Kingdom

Since the origins of secondary ion mass spectrometry (SIMS), almost nine decades ago, the field has evolved along distinct pathways where a process of natural selection has seen the emergence and decline of techniques as they, in turn, are superseded by new innovations.

This has resulted in today's powerful SIMS instruments that are having extraordinary impact in almost every area of materials science and increasingly in the life-sciences [1]. However, independent evolutionary lineages have led to segmentation of the community. Recent advances in instrumentation and advances in fundamental understanding are now beginning to show prospects for evolutionary convergence.

To put this in context, recent developments driven by a fundamental analytical challenge will be discussed. Techniques, like nuclear magnetic resonance, provide high confidence in identification but with limited information on localisation. Whilst techniques like electron microscopy, give high confidence in localisation but low confidence in identification. This has been termed the "molecular uncertainty principle" [2]. In 2017, NPL introduced the OrbiSIMS technology [3] with an objective to simultaneously provide molecular identification and localisation as close to this limit as possible. Since then, the number of OrbiSIMS instruments around the world has increased significantly and the community of users and range of applications has grown. In this presentation, we briefly introduce the OrbiSIMS and use examples of the applications in advanced materials [4] and life-sciences [5] to highlight a convergence of "static SIMS" and "dynamic SIMS" as some of the traditional barriers begin to disappear. In a look to the future, further advances in mass spectrometers are expected, for example multiple reflection Time of Flight analysers, ion mobility and other novel hybrid analysers as well as improved sensitivity using quantum detection.

Selected references

[1] N. P. Lockyer et al. Secondary ion mass spectrometry, Nature reviews, methods primer, 2024
[2] A Ali et al, Single cell metabolism: current and future trends. Metabolomics, 2022. 18 (10):
[3] M K Passarelli et al., The 3D OrbiSIMS-label-free metabolic imaging with subcellular lateral resolution and high mass-resolving power, Nature Methods, 2017. 14 (12): p. 1175-
[4] G F Trindade et al., Direct identification of interfacial degradation in blue OLEDs using nanoscale chemical depth profiling. Nature Communications, 2023. 14 (1): p. 8066.
[5] F Zani et al., The dietary sweetener sucralose is a negative modulator of T cell-mediated responses. Nature, 2023. 615 (7953): p. 705-711.

Plenaries

PS1 - From model system to devices – Gaining insight into solar cells with photoelectron spectroscopy

Ute Cappel
Department of Physics and Astronomy, Uppsala University, Sweden

Gaining atomic level understanding of materials properties as well as processes in devices is crucial for the development of applications relying on these materials. This talk will address how we use photoelectron spectroscopy to gain fundamental insights into materials for solar cells.

The direct conversion of sunlight to electricity (photovoltaics) is expected to play a significant role in the future electricity supply due to the great potential of solar energy as a renewable source. To be used on a larger scale, future solar cell technologies must use abundant materials, be inexpensive to produce and stable under device operation. In the last years, much research has focused on developing new solar cells made from organic or hybrid materials, which can be fabricated by cheap methods. This includes solar cells with a hybrid organic inorganic perovskite as the active layer in the solar cell, which have now reached power conversion efficiencies of more than 25%. In a typical solar cell, the perovskite layer is sandwiched between two selective contacts, one for holes and one for electrons.

The future success of these developments crucially depends on understanding the details charge separation, charge transport and charge recombination at the interfaces between the different layers in a solar cell as well as what parameters limit solar cell stability. X-ray based techniques such as photoelectron spectroscopy (PES) are powerful tools for obtaining electronic structure information of materials at an atomic level. By varying the photon energy from soft to hard X-rays, photoelectron spectroscopy can be used for non-destructive depth profiling of the solar cell interfaces giving information about the energy alignment and chemical structure and composition at the interface. Furthermore, time-resolved photoelectron spectroscopy can be used to investigate dynamics within devices relating to charge transport and material stability.

In this presentation, I will discuss how we have used photoelectron spectroscopy to gain fundamental insights into materials for solar cells by carrying out investigations ranging from single crystal model systems to real devices and moving from static to dynamic, time-resolved measurements.

PS2 - Active Chiral Surfaces Driving Left-Right Symmetry Breaking in Living Systems

Stephan Grill
MPI-CBG Dresden, Germany

One of the most remarkable examples of self-organized structure formation is the development of a complex organism from a single fertilized egg. With the identification of molecules that participate in this process of morphogenesis, attention has now turned to capturing the physical principles that govern the emergence of biological form.

What are the physical laws that govern the dynamics and the formation of structure in living matter? Much of the force generation that drives morphogenesis stems from the actomyosin cortical layer of cells just underneath the cell surface, which endows the surface with the ability to generate active stresses and active torques that can drive reshaping. We combine theory and experiment and investigate how the actomyosin cell surface deforms and how it supports chiral rotations, and how these events together participate in chiral morphogenesis and the establishment of a left-right principal body axis in both the nematode worm and the Japanese quail.

PS3 - Advancing X-ray Photoelectron Spectroscopy (XPS) Methodologies for Materials Research

Mark Biesinger
Surface Science Western, Western University, London ON, Canada
Department of Chemistry, Western University, London ON, Canada

Chemical state X-ray photoelectron spectroscopic (XPS) analysis of first row transition metals and their oxides and hydroxides is challenging due to the complexity of the 2p spectra resulting from peak asymmetries, complex multiplet splitting, shake-up and plasmon loss structure, and uncertain, overlapping binding energies.

Our work has shown that all the values of the spectral fitting parameters for each specific species, i.e. binding energy (eV), full width at half maximum (FWHM) value (eV) for each pass energy, spin-orbit splitting values and asymmetric peak shape fitting parameters, are not all normally provided in the literature and databases, and are necessary for reproducible, quantitative chemical state analysis.

We have worked toward a consistent, practical, and effective approach to curve fitting based on a combination of 1) standard spectra from quality reference samples, 2) a survey of appropriate literature databases and/or a compilation of literature references, 3) specific literature references where fitting procedures are available and 4) theoretical fittings, where available, of multiplet split reference spectra. The use of well characterized standard samples and fitting of the entire peak shape has been shown to increase our ability to accurately identify and (semi) quantify the various species present in mixed oxide/hydroxide systems [1,2]. Additional chemical information has also been elucidated from Auger parameters and by using Wagner plots for compounds of Ni, Cu, Ga, In, Cd, and Zn. The unique spectral shapes of the LMM Auger peaks for these transition metals, particularly for Cu [3], as well as for Zn, In and Cd, have also been shown to be of use for chemical speciation. These methods have been shown to be effective in a wide variety of applications. Additionally, a recent assessment [4] of available charge corrections procedures for insulating samples will also be shown including recent work on defining the nature of adventitious carbon and improving its merit for charge correction usage [5].

Selected references

1. M.C. Biesinger, L.W.M. Lau, A.R. Gerson, R.St.C. Smart, Applied Surface Science 257 (2010) 887.
2. M.C. Biesinger, B.P. Payne, A.P. Grosvenor, L.W.M. Lau, A.R. Gerson, R.St.C. Smart, Applied Surface Science 257 (2011) 2717.
3. M.C. Biesinger, Surface and Interface Analysis 49 (2017) 1325.
4. M.C. Biesinger, Applied Surface Science 597 (2022) 15381.
5. L.H. Grey, H.-Y. Nie, M.C. Biesinger, Applied Surface Science 653 (2024) 159319.

PS4 - Atom probe tomography as an amazing tool for the chemical analysis of soft matter and complex interfaces

Guido Schmitz
Institute of Materials Science, University of Stuttgart, Germany

Atom probe tomography is a method of microscopic analysis that is already well-established in the study of hard materials. It is based on controlled field desorption and stands out by combining single-atom sensitivity with a 3D volume reconstruction.

Particular strongholds are the accurate measurement of chemical segregation to grain boundaries and interfaces in nanostructured matter.

Our recent efforts push forward volume reconstruction methods, the quantum mechanics simulation of the evaporation process and the statistical understanding of chemical fluctuations which even enables a direct measurement of Gibbs energy. We desire to break the materials limitations towards the analysis of softmatter and polymeric materials. Meanwhile, nanometric needles are produced from frozen liquids, even from pure water. Studies are performed with aqueous solutions, liquids of short alkanes, liquid crystals and self-assembling monolayers. The talk discusses the field desorption of complex materials and presents time of flight mass spectra and their dependence on field or laser intensity. The complex mechanisms of field desorption from frozen water surfaces and molecular organic liquids are further elucidated by DFT and Monte-Carlo simulation. By proper evaluating evaporation probabilities and event correlations, even insight in bonding strength and the stability of molecules in strong electrical fields may be provided.

Keynotes

K1 - Characterisation of microbial surface chemistry using cryo-XPS

2. BIO – Bio-interfaces, Biomaterials and Life Science

Andrey Shchukarev[1]
Madeleine Ramstedt[1]
[1] Umeå University, Department of Chemistry

Biological materials such as microbial cells are in their natural condition often highly hydrated. Traditionally, surface analysis of these types of materials have been performed on freeze-dried specimens. However, the drying procedure may introduce artefacts, rearrange the surface morphology and reorganize the distribution of sugars, lipids, and proteins at the interface between the material and air. These changes have the potential to alter the chemical composition at the surface, giving rise to data that do not correspond to what would be observed in hydrated state. In order to avoid this and probe hydrated surfaces, we developed methodologies for analysing microbial samples using cryogenic XPS [1,2]. Through the years, we have applied this to bacterial cells, biofilms, bacterial vesicles, fungal cells, microalgae and viruses [3,4,5]. This talk will describe the methodology used and illustrate the types of data that we have obtained on a few selected microorganisms. In addition, I will compare data we obtained from bacterial cells using cryo-XPS and NAP-XPS and discuss advantages and disadvantages we experienced between the two methods [6].

Selected references

[1] 2011, Ramstedt M, Nakao R, Wai S N, Uhlin B-E, Boily J-F, Monitoring Surface Chemical Changes in the Bacterial Cell Wall – Multivariate analysis of X-ray photoelectron spectroscopy data, Journal of Biological Chemistry, DOI: 10.1074/jbc.M110.209536
[2] 2016, M Ramstedt, A Shchukarev, Analysis of bacterial cell surface chemical composition using cryogenic X-ray photoelectron spectroscopy, chapter 16 in Bacterial Cell Wall Homeostasis (Ed) Hee-Jeon Hong in Methods in Molecular Biology, vol 1440, Springer, New York, pp 215-223, DOI:10.1007/978-1-4939-3676-2_16
[3] 2020, A Shchukarev, Z Gojkovic, C Funk, M Ramstedt, Cryo-XPS analysis reveals surface composition of microalgae, Applied Surface Science, DOI:10.1016/j.apsusc.2020.146538
[4] 2020, A Hagberg, O Rzhepishevska, A Semenets, D Cisneros Armas, M Ramstedt, Surface Analysis of Bacterial Systems Using Cryo-X-ray Photoelectron Spectroscopy, Surface and Interface Analysis, DOI:10.1002/sia.6854
[5] 2021, A Shchukarev, E Backman, S Watts, S Salentinig, C F. Urban, M Ramstedt, Applying cryo-XPS to study the surface chemical composition of fungi and viruses, DOI:10.3389/fchem.2021.666853
[6] 2021, Kjærvik M, Ramstedt M, Schwibbert K, Dietrich P M., Unger E.S. W, Comparative study of NAP-XPS and cryo-XPS for the investigation of surface chemistry of the bacterial cell-envelope, DOI: 10.3389/fchem.2021.666161

K2 - Oxide Films and Corrosion

5. COR – Corrosion

Philippe Marcus[1]
[1] CNRS - Chimie ParisTech, PSL University, Institut de Recherche de Chimie Paris, Physical Chemistry of Surfaces Research Group, Paris, France

This lecture with focus on a surface analytical approach of corrosion and protection of metals and alloys.

Oxide films, such as passive films, occupy a central role in corrosion and protection because without such surface oxides nearly no metal or alloy could be used in our environment.

Therefore it is essential to understand the oxide growth, their protective properties, the origin of defects responsible for their local breakdown. This requires the use of surface analytical techniques including XPS, ToF-SIMS, STM.

The best case is when the oxide forms spontaneously on the metal surface as it does on e.g. aluminium, titanium, stainless steels, and new highly corrosion resistant alloys such as High Entropy Alloys. Oxide layers can also be deposited (e.g. by ALD) on less corrosion resistant alloys.

These various aspects will be presented and exemplified in this lecture, and future trends will be discussed.

K3 - Electron Beam Attenuation and Energy Dissipation between 0 eV and Relativistic Energies.

6. DAT – Data Analysis and Metrology

Wolfgang S.M. Werner[1]
[1] Institut für Angewandte Physik, Technische Universität Wien, Wiedner Hauptstr 8-10, A-1040 Wien, Austria

The status quo of quantitative nanoanalysis using medium energy electrons will be briefly reviewed, demonstrating the impressive progress which has been made over the past fifty years. This is in stark contrast to the understanding of the interaction of low energy electrons (LEEs) with surfaces which is rapidly gaining attention due to its importance for a variety of processes on the nanoscale: LEEs are not only essential for nanoscale analysis such as microscopy, CD metrology or attosecond physics but also act as agents inducing physico-chemical processes as in, e.g., electron lithography, electron beam induced deposition, astrochemistry and, last but not least, DNA-bond breaking induced by high energy ionising radiation striking biological tissue. Improvement in this field is complicated by the lack of benchmark experiments specifically designed to obtain information on individual physical parameters or processes.

In the present talk, a recently proposed experimental approach will be described in which the quantitative knowledge of the medium energy range is used to gain information about the (poorly understood) low energy range. This is done by using medium energy primary electrons as messengers of the depth of creation of low energy secondaries. Measuring the secondary electron intensity as a function of depth of creation, the attenuation law in the low energy range is quantified.

In the case of polymethylmethacrylate, it is found that the attenuation law is non-exponential, but is rather made up of two exponential functions, corresponding to two different groups of electrons playing a role in the energy dissipation process. The attenuation lengths of both groups are measured and essentially agree with a theory used for decades in astrophysics —albeit with units expressed in nm rather than lightyears— and providing electron attenuation lengths in the range between 0 eV and relativistic energies (see figure below).

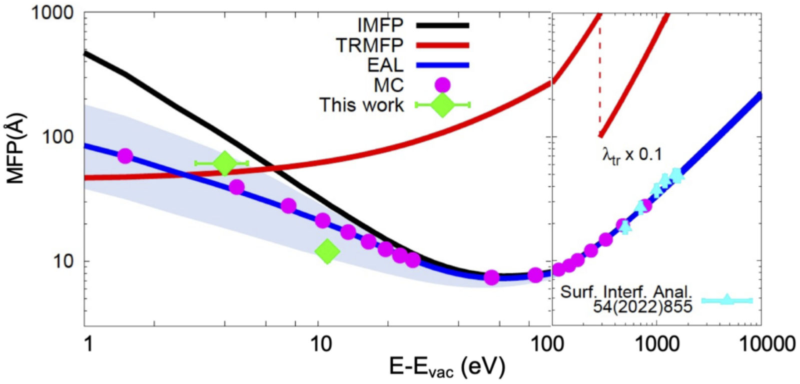

Electron inelastic mean free path (IMFP, black, transport mean free path (TrMFP, red) and effective attenuation length (EAL, blue). Magenta circles: MC model calculations for the EAL; Cyan triangles: earlier experimental data for the IMFP. Green diamond: experiment, present work. Blue shaded region: uncertainty in the EAL when the TrMFP is increased/decreased by a factor of three.

K4 - Underused Information from XPS and Avoiding Common Errors

6. DAT – Data Analysis and Metrology

Donald Baer[1]
[1] Pacific Northwest National Laboratory, Richland WA, USA

The value of information obtained using XPS has fueled significant growth in its use in multiple disciplines and by a new generation of analysts as well as ‘casual’ users less familiar with the method. Accompanying this increased use and changes in the nature of the user community are i) increased presence of erroneous data analysis in literature and ii) fewer analysts taking full advantage of the types of information that can be extracted from well-constructed XPS experiments. This talk will suggest information that experienced XPS analysts can pass along to less experienced XPS users to address both issues. First, the status of several efforts being undertaken to address faulty analysis, and incomplete reporting will be described. These address analysis issues and lack of needed information and parameter reporting. Second, several useful but underused approaches to XPS data collection and analysis will be described.

Examination of literature shows a significant amount of faulty XPS data analysis, often related to peak fitting, and significantly incomplete reporting of data and analysis parameters needed to assess result reliability or enable replication. Recent publications highlight common errors in the effort to encourage analysts to avoid them as well as enable readers and reviewers to recognize them.[1-4] Analyses also indicate that most publications using XPS ask one or more of three interrelated questions: i) What elements are present? ii) How much of each element is on the surface? iii) What are the chemical states of the elements present? Although very appropriate and important uses of XPS, there is a wider range of material and sample information can be obtained that enable XPS to address several analysis needs.

An incomplete list of accessible information includes, sample polarizability and dielectric constants, chemically resolved electrical measurements, local electric field and potentials, band offsets and bending, the nature of electrical double layers and local charge dynamics, and changes in microbe cell walls in response to external stimuli. Common XPS analyses assume that the analyzed surface layer is uniform and ignore the impact of sample structure on XPS signals. Information contained within XPS spectra can provide information about elemental distribution in the surface region, and information about coating thickness and uniformity, and size of nanoparticles. The talk will highlight two approaches that require specialized instrumental capabilities (application of AC or DC fields and cryoXPS) and other approaches primarily involving data analysis (Auger parameter, band information, D-band use, and ‘background’ signals).

Selected references

1. Pinder JW, Major GH, Baer DR, et al. Avoiding common errors in X-ray photoelectron spectroscopy data collection and analysis, and properly reporting instrument parameters. *Applied Surface Science Advances*. 2024/02/01/ 2024;19:100534. doi:https://doi.org/10.1016/j.apsadv.2023.100534
2. Major GH, Pinder JW, Austin DE, et al. Perspective on improving the quality of surface and material data analysis in the scientific literature with a focus on x-ray photoelectron spectroscopy (XPS). *Journal of Vacuum Science & Technology A*. 2023;41(3)doi:10.1116/6.0002437

3. Major GH, Clark BM, Cayabyab K, et al. Insufficient reporting of x-ray photoelectron spectroscopy instrumental and peak fitting parameters (metadata) in the scientific literature. *Journal of Vacuum Science & Technology A*. 2023;41(4)doi:10.1116/6.0002714
4. Greczynski G, Hultman L. A step-by-step guide to perform x-ray photoelectron spectroscopy. *Journal of Applied Physics*. 2022;132(1)doi:10.1063/5.0086359

K5 - XPS, NAP-XPS, and HAXPES inelastic electrons to characterize nano-structured materials

6. DAT – Data analysis and Metrology

Sven Tougaard[1]

[1] Department of Physics, Chem. and Pharm., University of Southern Denmark, Odense M, Denmark

Quantitative characterization of nanostructures by analysis of the inelastic background in photoelectron spectroscopy (XPS and HAXPES) is now a widely used method.[1] In the talk, we report on recent advancements of this method. First, we discuss the application to characterize core-shell nanoparticles (CSNPs) and show that both the shell thickness and its heterogeneity can be accurately determined, and it also correctly proves if the shell material fully encapsulates the core or if part of the core is uncoated [2] (see Figure below). Further, we recently showed how the method can be applied to very accurately correct ambient pressure XPS for the spectral distortion caused by the gas.[3]

The only input in the method, besides the IMFP, is the cross section for inelastic electron scattering. For cases with stacks of layered materials that have widely different cross sections, this quantity is taken as the weighted average of the involved materials.[4] For cases where the involved cross sections are unknown, we recently showed that an optimized cross section, that is determined as part of the fitting procedure, can reliably be determined without any knowledge of the sample composition.[5]

The method is non-destructive, and the probing depth is considerably larger than the usually quoted 3*IMFP because the inelastically scattered electrons originate from larger depths than the electrons in the peak and it is typically ~8*IMFP but can be ~20*IMFP in cases where the background can be followed over several hundred eV. The latter is often the case with HAXPES because the separation between deep lying core electrons can be much larger compared to conventional XPS. With HAXPES, the photoelectron energy and thereby the IMFP and the probing depth is also increased and several examples with analysis of structures at > 100 nm depth have been reported.[4,6] Since lab based HAXPES is now commercially available it is being installed in many labs and its application in nanotechnology is expected to rapidly increase considerably.

Detailed tutorial videos of several of the examples discussed in the talk are available in [7].

Selected references

[1] S. Tougaard, J Vac Sci Technol A. 2021;39:011201 https://doi.org/10.1116/6.0000661;
[2] A. Müller et al, Surf Interface Anal. 2020;52(11):770 https://doi.org/10.1002/sia.6865
[3] S. Tougaard and M. Greiner, Appl Surf Sci. 2020;530:147243. https://doi.org/10.1016/j.apsusc.2020.147243
[4] C. Zborowski, O. Renault, ST. et al J. Appl. Phys 124 (2018) 657
[5] C. Zborowski, ST., Surf Interface Anal. 2021;1–9 https://doi.org/10.1002/sia.7020
[6] B. F. Spencer et al. Appl. Surf Sci (2021) 541, 148635, https://doi.org/10.1016/j.apsusc.2020.148635
[7] S. Tougaard Tutorial videos; https://zenodo.org/search?q=tougaard

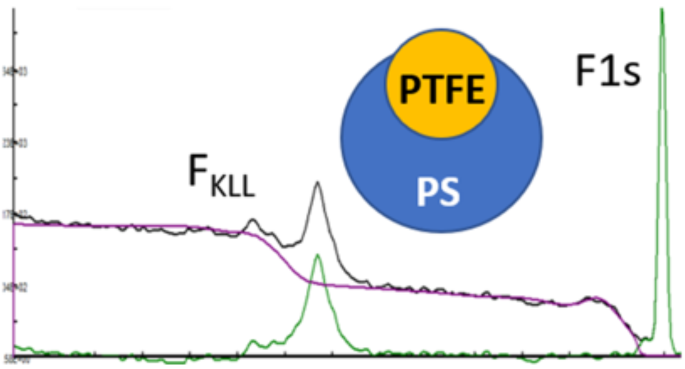

Size and non-completeness of coated nanoparticle found by this method[2]

K6 - Hard X-ray photoelectron spectroscopy and its application to the bonding and electronic structure of metal dihydrides

7. DPR – Thin Films, Coatings and Depth Profiling

Anna Regoutz[1]
[1] University College London

Metal hydrides hold significant promise in various hydrogen-related technologies, encompassing energy storage, hydrogen compression, and hydrogen sensing. Although metal hydrides appear simple compared to many other energy materials, understanding the electronic structure and chemical environment of hydrogen within them remains a key challenge. This work presents a new analytical pathway to explore these aspects in technologically relevant systems using Hard X-ray Photoelectron Spectroscopy (HAXPES) on thin films of two prototypical metal dihydrides: $YH_{2-\delta}$ and $TiH_{2-\delta}$.[1,2] By taking advantage of the tunability of synchrotron radiation, a non-destructive depth profile of the chemical states is obtained using core-level spectra. Combining experimental valence band spectra collected at varying photon energies with theoretical insights from density functional theory (DFT) calculations, a description of the bonding nature and the role of *d* versus *sp* contributions to states near the Fermi energy are provided. Moreover, a reliable determination of the enthalpy of formation is proposed by using experimental values of the energy position of metal *s* band features close to the Fermi energy in the HAXPES valence band spectra.

Selected references

[1] C. Kalha, L. E. Ratcliff, G. Colombi, C. Schlueter, B. Dam, A. Gloskovskii, T.-L. Lee, P. K. Thakur, P. Bhatt, Y. Zhu, J. Osterwalder, F. Offi, G. Panaccione, A. Regoutz, “Revealing the Bonding Nature and Electronic Structure of Early-Transition-Metal Dihydrides”, PRX Energy, 3, 013003, 2024, https://doi.org/10.1103/PRXEnergy.3.013003

[2] C. Kalha, N. K. Fernando, P. Bhatt, F. O. L. Johansson, A. Lindblad, H. Rensmo, L. Zendejas Medina, R. Lindblad, S. Siol, L. P. H. Jeurgens, C. Cancellieri, K. Rossnagel, K. Medjanik, G. Schönhense, M. Simon, A. X. Gray, S. Nemšák, P. Lömker, C. Schlueter, and A. Regoutz, "Hard X-ray Photoelectron Spectroscopy – A Snapshot of the State-of-the-Art in 2020", J. Phys. Condens. Matter, 33, 233001, 2021, https://doi.org/10.1088/1361-648X/abeacd.

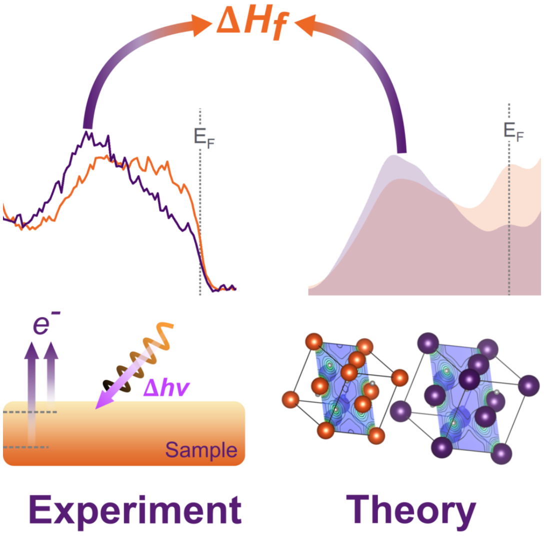

K7 - Powder for metal additive manufacturing: Properties, reuse and degradation from surface chemistry point of view

10. MET – Metallic Materials

Eduard Hryha[1]
Lars Nyborg[1]
[1] Centre for Additive Manufacturing – Metal (CAM2), Department of Industrial and Materials Science, Chalmers University of Technology, Gothenburg, Sweden

Metal powder constitutes the most common feedstock used in metal additive manufacturing (AM), including powder bed fusion (laser beam PBF-LB, and electron beam - PBF-EB), binder jetting (BJT) and powder blown directed energy deposition (DED). Even though the same alloys systems are often used for these technologies, they have different requirements to the powder feedstock when it comes to its physical and chemical characteristics and utilize different size fractions of the metal powder. In addition, this metal powder is exposed to very different conditions during the AM manufacturing cycle in case of different AM technologies. However, importance of powder properties, specifically powder surface chemistry and its changes during powder manufacturing, handling and AM processing is often overlooked. Hence, changes in powder properties during manufacturing cycle and its impact on the final component properties differ significantly.

Metal powder used for additive manufacturing is characterized by large surface area of the powder that leads to high surface reactivity. This, in combination with the alloy composition, will determine powder sensitivity to the powder manufacturing method, handling and AM processing. Powder surface chemistry is initially determined by powder manufacturing method and alloy composition. This initial chemical composition is, however, not stable, and progressively changes with time in dependance on powder handling and processing by metal additive manufacturing. These changes in powder surface chemistry during powder reuse have a strong impact on powder quality and processability by specific AM technologies. This talk summarizes recent experimental observations and thermodynamic simulations of the changes in powder surface chemistry during the whole life-cycle of metal powder: from its manufacturing through powder handling and AM processing by variety of powder-based metal AM technologies. Generic model of the powder degradation in dependance on initial powder properties and alloy composition when processed by different AM processes, is elaborated. Effect of the reused powder on the defect formation during AM processing and its impact on material properties is discussed.

K8 - A journey towards operando X-ray photoelectron spectroscopy to follow reactions at battery interfaces

11. NRG – Energy, Environment, geology and heritage

Julia Maibach[1]
[1] Department of Physics, Chalmers University of Technology, Gothenburg, Sweden

Electrode/electrolyte interfaces are likely the most important and least understood components of Li-ion and next-generation batteries. Improving the understanding of interphases in batteries will undoubtedly lead to breakthroughs in the field. However, obtaining chemical and electronic information with high interface sensitivity is challenging since these interfaces and interphases are typically buried between a solid electrode and liquid electrolyte. Traditionally, evaluating those interphases therefore involves ex situ surface sensitive techniques, even though ex situ sample manipulation is undesirable due to the interphases' dynamic and reactive nature [1].

To resolve this issue, we use near-ambient pressure x-ray photoelectron spectroscopy (NAP-XPS). With this technique, the vacuum constraints of classical UVH-based XPS are relieved and solid/liquid interfaces can be studied. Combing NAP-XPS with specially designed operando setups to study the electrode/electrolyte interface under electrochemical bias, we gain more realistic information on the reactions between electrode and electrolyte.

In this contribution, I will review the journey from first applications of NAP-XPS to battery systems to identifying solid-electrolyte interphase (SEI) formation on model electrodes. As steps along the way I will present NAP-XPS characterizations of electrodes and electrolytes [2,3], tracking electrochemical potential differences over the solid/liquid interface in model battery systems under working conditions [4] and identifying electrode lithiation mechanisms [5].

Selected references

[1] J. Maibach, J. Rizell, A. Matic, N. Mozhzhukhina, ACS Materials Lett., 2023, 5, 2431-2444.
[2] J. Maibach, I. Källquist, M. Andersson, S. Urpelainen, K. Edström, H. Rensmo, H. Siegbahn, and M. Hahlin, *Nat. Commun.*, 2019, 10, 1-7.
[3] P. M. Dietrich, L. Gehrlein, J. Maibach, A. Thissen, *Crystals*, 2020, 10, 1056 .
[4] I. Källquist, F. Lindgren, M.-T. Lee, A. Shavorskiy, K. Edström, H. Rensmo, L. Nyholm, J. Maibach, M. Hahlin, *ACS Appl. Mater. Interfaces*, 2021, 13, 32989–32996.
[5] I. Källquist, T. Ericsson, F. Lindgren, H. chen, A. Shavorskiy, J. Maibach, M. Hahlin, *ACS Appl. Mater Interfaces*, 2022, 14, 6465-6475.

K9 - The Development of High Energy Sources for XPS

13. TEC – Technical Development and New Instrumentation

John Watts[1]
[1] University of Surrey

Over the last fifty years a number of higher energy X-rays sources have been suggested as alternatives for the usual AlKα source found in the first commercial XPS systems, and still the standard anode material for XPS today. This paper reviews the development of a number of such sources, predominantly in the author's laboratory, and the rationale behind the desire to extend the standard binding energy range of XPS. The achromatic sources SiKα, ZrLα and TiKα are described along with monochromatic sources AgLα and CrKβ, both based on the standard quartz monochromator geometry but taking higher orders of diffraction. The driving force for much of this development was the desire to probe deeper core levels and associated CCC Auger transitions. These can be combined into initial (ξ) or final (α) state Auger parameters as described in much of the early work. The highest energy source considered is the CuKα source based around an external X-ray tube, which provide much insight into the electronic structure of steels by measurement of the Fe1s and Fe*KLL* peaks. The last decade or so has seen a significant increase of interest in HAXPES, and all manufacturers of turn-key XPS instruments offer HAXPES options of one form or another, and there are three dedicated HAXPES systems commercially available, which will be briefly described.

Orals

1. ADH – Adhesion and Tribology

O1 - Practical approach for standardization of surface free energy and piezoelectric constant using atomic force microscopy

1. ADH – Adhesion and Tribology

Ehtsham-Ul Haq[1]
Charlie O'Mahony[1], Joseph O'Donnell[1], Yongliang Zhang[1], Krittish Roy[1], Dinesh Barnana[1], Krsitine O'Dwyer[1], Tewfik Soulimane[2], Ning Liu[1], Christophe Silien[1], Tofail Syed[1]
[1] Department of Physics and Bernal Institute University of Limerick V94 T9PX, Ireland, V94 T9PX, Limerick, Ireland
[2] Department of Chemical Sciences, University of Limerick, Limerick V94 T9PX, Ireland, V94 T9PX, Limerick, Ireland

Precise measurement of physical properties at the nanoscale is crucial for designing surfaces with control over chemistry, mechanical, electrical, and morphological properties. The surface free energy (SFE), wetting, adhesion, and friction plays a vital role in tribology, photonics, scaffold materials, drug delivery, and bio-coatings. Similarly, the reliability of electromechanical characterization is crucial for the advancement of materials designed for applications in fields as diverse as energy storage, electronics, biology, and medicine. Atomic force microscopy (AFM) has demonstrated unparalleled efficacy in the characterization of physical properties at the nanoscale. Nevertheless, the precise determination of functional properties using AFM is hindered by theoretical models that fail to account for experimental results and imprecise tip-related characteristics (e.g. contact geometry and surface chemistry). Here we introduce practical approaches for standardization of surface free energy and converse piezoelectric constants obtained from atomic force microscopy.

We present a step-by-step procedure for quantifying measurements of SFE, establishing a dependable link between micrometer-scale measurements and the more traditional macroscopic measurements. For SFE standardization, 10-micron silica and polystyrene (PS) colloids – with a contact area of approximately 1 micron in diameter are utilized. A sequence of consistently uniform calibration specimens, characterized by contact-angle SFEs, are examined with colloids. The colloids are complimentary, and the two colloids work together to refine the SFE result. This process facilitates the calibration of a regression model linking main components derived from AFM with corresponding contact-angle SFEs. As a result, the SFE is calculated through a single model based on contact angles, specifically Owen Wendt's model. The applicability of this SFE analysis method is tested on (biological material) Methionine peptide crystals cast onto an ITO-coated glass substrate. In the subsequent section of this paper, a pragmatic methodology for the standardisation of converse piezoelectric constants derived from piezoresponse force microscopy (PFM) will be detailed. Practical aspects of quantitative PFM, including sample preparation, probe selection, and the utilisation of control samples, will be covered.

Selected references

1. Ehtsham-Ul Haq, Yongliang Zhang, Noel O’Dowd, Ning Liu, Stanislav Leesment, Claude Becker, Edoardo M. Rossi, Marco Sebastiani, Syed A. M. Tofail and Christophe Silien, “Quantitative surface free energy with micro-colloid probe pairs”, RSC advances, 13 (2023) 2718-2726.
2. A.M. Tofail, J. Bauer, Electrically Polarized Biomaterials, Adv Mater, 28 (2016) 5470-5484.

3. P. Koumoulos, S.A.M. Tofail, C. Silien, D. De Felicis, R. Moscatelli, D.A. Dragatogiannis, E. Bemporad, M. Sebastiani, C.A. Charitidis, Metrology and nano-mechanical tests for nano-manufacturing and nano-bio interface: Challenges & future perspectives, Mater Design, 137 (2018) 446-462.
4. Joseph O'Donnell, Ehtsham-Ul Haq, Christophe Silien, Tewfik Soulimane, Damien Thompson, and Syed A. M. Tofail, “A practical approach for standardization of converse piezoelectric constants obtained from piezoresponse force microscopy”, J. Applied Physics 129, (2021) 185104-1-10.
5. Joseph O’Donnell, Sarah Guerin a , Pandeeswar Makam , Pierre-Andre Cazadea , Ehtsham Ul Haq , Kai Tao, Ehud Gazit, Christophe Silien, Tewfik Soulimane, Damien Thompson , Syed A.M. Tofail, “Atomistic-Benchmarking towards a protocol development for rapid quantitative metrology of piezoelectric biomolecular materials”, Applied Materials Today, 21 (2021) 100818.

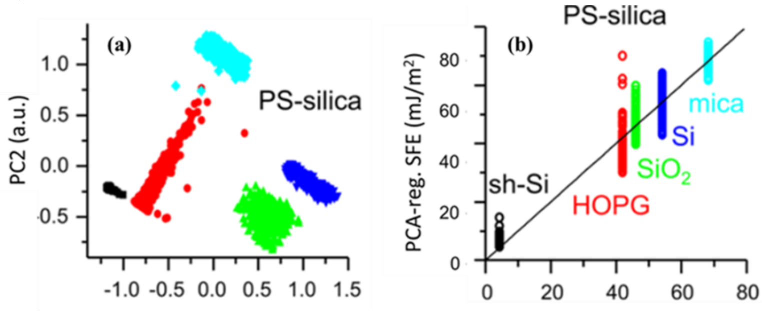

Figure 1 (a) PC2 versus PC1 scatter plots for the training set with PS and Silica colloids. The PCA was computed using AFM-derived values averaged on 10 F(d) curves. The data for sh-Si are shown in black, HOPG in red, silica in green, silicon in blue, and mica in cyan. (b) Second-order regression of the PC1, PC2, and PC3 values on the CA-derived SFE values for the test-set with PS and Silica colloid.

O2 - REELS and AES applied to amorphous carbon surface imaging for tribological applications

1. ADH – Adhesion and Tribology

Jules GALIPAUD[1, 2]
Antoine Normant[1], Julien Fontaine[1]
[1] CNRS, Ecole Centrale de Lyon, ENTPE, LTDS, UMR5513, 69130 Ecully, France
[2] CNRS, INSA Lyon, Universite Claude Bernard Lyon 1, MATEIS, UMR5510, 69621 Villeurbanne, France

Amorphous carbon films have been used widely for solid lubrication purposes with various tribological properties depending on their diamond-like features (ratio of sp2/sp3 carbon) or doping, e.g. hydrogen or fluorine amount [1]. These properties can modify greatly the films' mechanical properties as well as the lubrication mechanism underwent when used against various counterparts. Some formulations, in particular hydrogen-rich amorphous carbons a C:H films, have shown extremely low friction coefficient ($\mu < 0.01$) when rubbed against steel under vacuum [2,3]. This behavior can be partly explained by a modification of the surface physicochemical properties during friction [4]. However, attempts at observing these modifications are hindered by lack of surface sensitive techniques able to probe small rubbed areas without exposing the samples to contamination.

Indeed, amorphous carbon films are a real challenge to study by common photoemission spectroscopy techniques due to the difficulty to separate carbon sp2 and sp3 contributions by XPS and the lack of hydrogen quantification. The addition of XAES C KVV spectra can help unravel some of these films' characteristics properties , in particular the D-parameter has shown some sensitivity to sp2/sp3 carbon ratio and has been used for amorphous carbon coatings[5,6]. However, this technique is limited by the very high signal to noise ratio needed for proper differentiation and analysis.

In this work, we used a combination of X-Ray photoemission techniques and Electron beam techniques (Reflection Electron Energy Loss Spectroscopy and Auger Electron Spectroscopy), to understand the surface modifications induced by friction on hydrogenated amorphous carbon. A comparison of all these techniques and thorough spectral processing shows that the rubbed areas differ quite sensitively at the topmost surface (first nanometer). Analysis of electron induced C KVV maps and REELS spectra evidences a densification and an enrichment in sp2 carbon at the top surface, while XPS reveals a measurable decrease in oxygen content. The hydrogen amount estimated form the hydrogen quasi-elastic peak in REELS spectra, shows no sign of decrease in the friction area.

Selected references

[1] Robertson J. Diamond-like amorphous carbon. Materials Science and Engineering: R: Reports. 2002;37(4–6): 129-281.
[2] Donnet C, Grill A. Friction control of diamond-like carbon coatings. Surface and Coatings Technology. 1997;94-95: 456-462
[3] Antoine Normant, Jules Galipaud, Frédéric Dubreuil, Julien Fontaine. Investigation of Solid Lubrication Processes of DLC Films with a Unique 6 Axes UHV Tribometer. Tribology Online, 2023, 18 (5), pp.239-248. ⟨10.2474/trol.18.239⟩. ⟨hal-04192025⟩

[4] Mangolini F, Koshigan KD, Benthem MHV, Ohlhauson JA, McClimon JB, Hilbert J, Fontaine J, Carpick RW. How hydrogen and oxygen vapor affect the tribochemistry of silicon- and oxygencontaining hydrogenated amorphous carbon under low-friction conditions: a study combining X-ray absorption spectromicroscopy and data science methods. ACS Applied Materials and Interfaces. 2021;13(10): 12610-12621

[5] L. Calliari,AES and core level photoemission in the study of a-C and a-C:H,Diamond and Related Materials,Volume 14, Issue 8, 2005, Pages 1232-1240, ISSN 0925-9635, https://doi.org/10.1016/j.diamond.2004.10.046.

[6] B. Lesiak, L. Kövér, J. Tóth, J. Zemek, P. Jiricek, A. Kromka, N. Rangam, C sp^2/sp^3 hybridisations in carbon nanomaterials – XPS and (X)AES study, Applied Surface Science, Volume 452, 2018, Pages 223-231, ISSN 0169-4332, https://doi.org/10.1016/j.apsusc.2018.04.269.

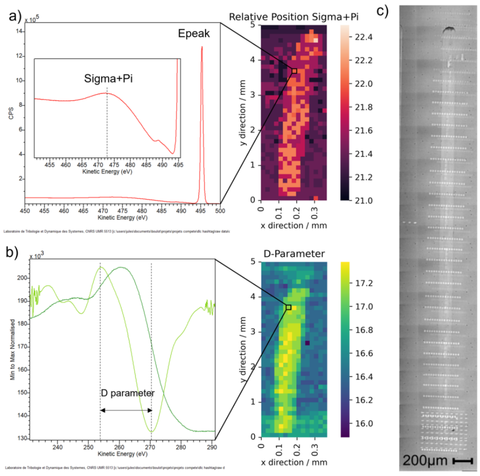

Example of spectra and extracted values for mapping of a) the Sigma+Pi plasmon position taken frome REELS spectra at 500 eV primary energy and b) D-parameter extracted from C KVV measured from Auger spectras taken with 2kV primary energy. c) optical image of the friction track after electron beam analysis.

2. BIO – Bio-interfaces, Biomaterials and Life Science

O3 - Biocompatibility investigations of laser-induced periodic surface structures on 316L stainless steel

2. BIO – Bio-interfaces, biomaterials and life science

Gimmi Guruprasad Engoor[1]
Sowmya Selvaraj[2], Vignesh Muthuvijayan[2], Sujatha Narayanan Unni[1], Nilesh Jayantilal Vasa[3]
[1] Department of Applied Mechanics and Biomedical Engineering, Indian Institute of Technology Madras, Chennai-60036, India
[2] Department of Biotechnology, Bhupat and Jyoti Mehta School of Biosciences, Indian Institute of Technology Madras, Chennai-600036, India
[3] Department of Engineering Design, Indian Institute of Technology Madras, Chennai-60036, India

The biocompatibility of implants is often modeled as a surface phenomenon. Biocompatibility is dependent on the surface chemistry, roughness, wettability, and surface-free energy of the implant. Implant surface modification is used to enhance biocompatibility by tailoring these surface properties. Commonly used surface modification techniques like sand-blasting and acid-etching create random textures on implant surfaces. Comparatively, Laser surface texturing is more environmentally friendly and offers high precision and repeatability.

Antibiofouling implant surfaces are highly essential to prevent bacterial adhesion and proliferation [2]. Laser-induced periodic surface structures (LIPSS) texture is generated on 316L stainless steel through femtosecond LASER texturing. LIPSS are nanostructured self-organized structures that are generated due to the interaction of ultra-short laser pulse with the material [1].

The surface morphology, chemical composition, and elemental maps of the samples are observed through Scanning Electron Microscope (SEM), fitted with Energy Dispersive X-ray Spectroscopy (EDS). Surface roughness and wettability are characterized by an optical profilometer and goniometer respectively. The bacterial cell adhesion on the surface is evaluated by Live/Dead staining of *S. aureus* and *E. coli*, and SEM. The protein adsorption on the samples is studied using ThermoScientific™ Pierce Micro Bicinchoninic acid (BCA) protein assay kit.

Selected references

[1] Pallarés-Aldeiturriaga, David, et al. "Influence of multi-wavelength ultrafast laser texturing and autoclave sterilization on titanium alloy-based surface wettability." *Applied Physics A* 128.10 (2022): 894.
[2] A. H. Lutey, L. Gemini, L. Romoli, G. Lazzini, F. Fuso, M. Faucon, and R. Kling,"Towards laser-textured antibacterial surfaces," *Scientific reports*, vol. 8, no. 1, pp. 1–10, 2018

O4 - Data analysis challenges associated with gas cluster ion beam secondary ion mass spectrometry in the life science arena.

2. BIO – Bio-interfaces, biomaterials and life science

Simon Uzoni[1]
Alfred Fransson[1], John Fletcher[1]
[1] University of Gothenburg, Department of Chemistry and Molecular Biology, Sweden

Gas cluster ion beam secondary ion mass spectrometry (GCIB-SIMS) presents opportunities for extending the SIMS technique into a range of biological application areas where the spatial resolution, surface sensitivity and chemical specificity offer advantages over other, complementary, techniques.[1]

Such samples, and their inherent complexity, produce equally complex data and challenges arise when handling the hyperspectral images from the multiple specimen required for biologically significant studies.[1]

Here we present different approaches for handling and mining different types of SIMS data from microbial samples and human tissue samples. Based on multivariate analysis and machine learning.

Selected references

1: Inci Barut, John S. Fletcher; Cell and tissue imaging by secondary ion mass spectrometry. *Biointerphases* 1 November 2023; 18 (6): 061202. https://doi.org/10.1116/6.0003140

O5 - GCIB-SIMS studies of skin cancer

2. BIO – Bio-interfaces, biomaterials and life science

Noora Neittaanmäki[1, 2]
Oscar Zaar[1, 2], Kevin Sjögren Cehajic[1], Kelly Dimovska Nilsson[1], Dimitrios Katsarelias[1, 2], Roger Olofsson Bagge[1, 2], John Paoli[1, 2], **John Fletcher**[1]
[1] University of Gothenburg
[2] Sahlgrenska University Hospital

The introduction of gas cluster ion beams (GCIBs) for secondary ion mass spectrometry (SIMS) analysis provides softer ejection of biomolecular ions and has created opportunities for meeting the challenges of clinical researchers who require chemical specific imaging of different sample type from cells to tissue biopsies. Here we use a J105 Buncher-ToF SIMS instrument (Ionoptika Ltd, UK) to perform in situ lipidomics of skin cancer samples. GCIB-SIMS analysis enabled detailed spatial-lipidomics that could be directly correlated with conventional histopathological analysis of consecutive H&E slides. Inn this work melanoma cancer samples were the target in order to investigate the chemical changes associated with disease progression and also to investigate if different metastatic pathways could be distinguished based on the chemical signature of the tumours. Primary tumours were analysed along with "healthy" skin from the same subject along with metastatic tumour samples that had spread via either the lymphatic system or through the blood. Significant differences in the lipid profiles were found in primary compared to metastatic melanomas, notably an increase in phosphatidylethanolamine lipids relative to phosphatidylinositol lipids and an increase in GM3 gangliosides in the metastatic samples. Furthermore, analysis of the data from in-transit versus distant metastases samples highlighted that specific phospholipids, and a difference in the long versus shorter chain GM3 gangliosides, discriminated the metastatic routes. Lipidomic changes could serve as a novel biomarker for tumour progression and even serve as a target for novel treatments. Furthermore, analysing the lipid profiles could help to differentiate between primary and metastatic melanomas in challenging cases.

O6 - Immunoglobulin stability in contact with elastomer surfaces

2. BIO – Bio-interfaces, biomaterials and life science

Giorgio Fernando DE AVELAR FRANCISCO[1, 2]
Bruno MORCHAIN[2], Arnaud PONCHE[1]
[1] Université de Haute Alsace
[2] Aptar Pharma Injectables

In 2023, FDA approved 55 new drugs, 13 of which are considered large molecules[1]. These therapeutic proteins, such monoclonal antibodies used to treat a variety of conditions (Alzheimer's disease, rheumatoid arthritis…), may undergo denaturation or changes in their conformation during storage, induced by factors such as temperature, pH levels or exposure to chemical agents[2] and molecules leached from the primary packaging. Additionally, contact with surfaces may cause denaturation and aggregation of these proteins leading to a loss of therapeutic activity over time (Figure 1).

The evaluation of protein interactions with different type of surfaces is important to understand their behavior in pre-filled syringes (PFS) and vials, especially with elastomeric closures such as vial stoppers and syringe plungers. These primary packaging systems are the most widely used for storage of biomolecules because of their capacity to maintain long term container integrity while allowing easy drug delivery[3]. However, aggregation has been reported during storage, which may be induced by a variety of factors.

This work aimed to develop a method to understand which processing parameters of elastomeric closure, such as sterilization processes, surface silicone content and coating, most influence the immunoglobulin (IgG) aggregation process and its interaction with the surfaces. Firstly, stoppers with different processing parameters were surface-characterized. X-ray photoelectron spectroscopy (XPS) analyzed the distribution of silicon, oxygen, carbon, and fluorine atoms within a thin surface layer (approximately 10 nm). Additionally, attenuated total reflectance infrared (ATR-IR) analysis was performed for in-depth surface examination. Finally, static water contact angle measurements assessed the stoppers' wettability. An IgG solution free of surfactants was stored in vials sealed with different stoppers and rotated at various speeds. Following shaking, the amount of desorbed IgG from the stoppers, as well as the size of any nanometer-sized soluble aggregates, IgG monomers, and fragments resulting from protein degradation, were quantified. Factor analysis of mixed data (FAMD) was used to analyze all parameters together and to explain the variability of the data. Using this tool, it was possible to distinguish the influence of each parameter studied on the amount of protein desorbed from the surface and the ratio of monomers and aggregates in solution.

Selected references

1. FDA & Cder. New Drug Therapy Approvals 2023. (2024).
2. Nault, L., Vendrely, C., Bréchet, Y., Bruckert, F. & Weidenhaupt, M. Peptides that form β-sheets on hydrophobic surfaces accelerate surface-induced insulin amyloidal aggregation. *FEBS Lett.* **587**, 1281–1286 (2013).
3. Sacha, G., Rogers, J. A. & Miller, R. L. Pre-filled syringes: a review of the history, manufacturing and challenges. *Pharm. Dev. Technol.* **20**, 1–11 (2015).

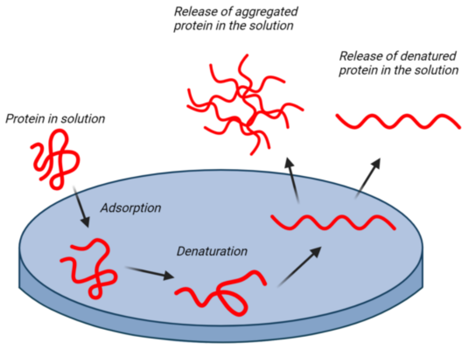

Figure 1: Protein adsorption process on a surface. Image cretaed with Biorender.com

O7 - Oligopeptides on metallic surfaces: A molecular level description of the interface

2. BIO – Bio-interfaces, biomaterials and life science

Christophe Méthivier[1]
Pauline Cornette[1], Joanne Lê-Chesnais[1], Jean-François Lambert[1], Dominique Costa[2], **Jessem Landoulsi**[1]
[1] Sorbonne Université, Laboratoire de Reactivite de Surface, 4 place Jussieu, F-75005 Paris, France
[2] Institut de Recherche de Chimie Paris (IRCP, UMR8247 CNRS), 11 rue Pierre et Marie Curie, 75005 Paris, France

Oligopeptides are short chains of amino acids, which exhibit a remarkable ability to interact with inorganic targets. This has motivated their use in the surface modification of metallic materials, showing promising functionalities, which have been explored in broad biomedical applications. These include the control of cell-material interaction, biosensing and biomineralization. Probing the mechanism by which oligopeptides interact with metallic material in aqueous solution requires, however, coping with the state of "real interfaces" [1]. This is mainly due to (i) the omnipresence of adventitious contaminants, which considerably limits the selectivity of the characterization of the adlayer of interest, and (ii) the surface reactivity, and thus uncontrolled alteration of the metallic surfaces in wet conditions (oxidation, hydration, dissolution, etc.).

Herein, we show that the adsorption behavior of peptides in the liquid phase strongly depends on the reactivity of the metallic surface. Specifically, an unexpected build-up of a hybrid peptide-copper multilayers, whose thickness may reach one hundred of nanometers, was observed [2]. Moreover, it is shown that the driving factors for this layer growth is (i) the generation of Cu^+ ions, due to the dissolution of copper surface in aqueous medium, and (ii) intermolecular interactions between peptide-copper entities mainly through a combination of electrostatic interaction and hydrogen bonds which stabilize the supramolecular edifice.

To cope with the state of "real interfaces", we explore the electrospray-ion beam deposition (ES-IBD) method to adsorb oligopeptides on metallic surfaces. This technique combines an atmospheric pressure ionization source and a vacuum deposition technique to adsorb oligopeptide without alteration [3]. It is particularly relevant when vacuum evaporation fails, due to the molecule disassembling during the sublimation process, or the molecular "landing" at the surface in the form of aggregates. Results show that peptides preserve their molecular structure in the adsorbed state, and their binding mechanisms are highly impacted by the metal crystal face.

As an alternative to the ensemble-average measurements, described above, where a large number of molecules interacts simultaneously in a dynamic chemical equilibrium, the possibility of probing the binding mechanism of oligopeptides at the single-molecule level by means of atomic force microscopy (AFM) is discussed. Specifically, dynamic force spectroscopy measurements are presented and explored to extract kinetic and thermodynamic parameters describing the binding mechanism of oligopeptides on the metallic surface.

Selected references

[1] J. Landoulsi, Surface (bio)-functionalization of metallic materials: How to cope with real interfaces? Advances in Colloid and Interface Science, 2024, 325, 103054.

[2] J. Landoulsi, V. Dupres, C. Méthivier, I. Leteyi Mfiban, P. Cornette, E. Colaço, C.-M. Pradier. Surface-generated copper ions induce multilayer growth of small peptides, Applied Surface Science 2020 507, 145105.

[3] C. Méthivier, P. Cornette, D. Costa, J. Landoulsi. Electrospray ion beam deposition of small peptides on solid surfaces: A molecular level description of the glutathione/copper interface Applied Surface Science 2023, 612, 155895.

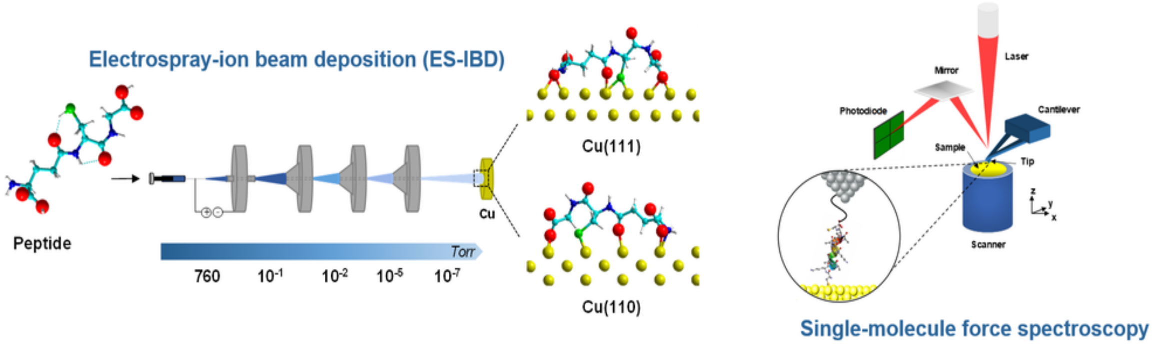

O8 - Optimal mechanical properties and high cellular proliferation on hybrid PLC/HaP/SA scaffolds for tissue engineering

2. BIO – Bio-interfaces, Biomaterials and Life Science

Miguel Hernandez-Gallegos[1]
Rafael González-Parra[1], Arturo Barba[1], Jose Bañuelos[2], Patricia González-Alva[3], Karla Gomez[4]
[1] 1 División de Ingeniería Mecánica e Industrial, (DIMEI), CENISA, Facultad de Ingeniería, UNAM, 04510 Ciudad de México, México
[2] 2 LUCE, Instituto de Ciencias Aplicadas y Tecnología, Universidad Nacional Autónoma de México, Ciudad de México, México
[3] 3 Laboratorio de Bioingeniería de Tejidos, Facultad de Odontología, Universidad Nacional Autónoma de México, Ciudad de México, México
[4] 4 CONACyT-Fellow-Instituto de Materiales, Universidad Nacional Autónoma de México, Ciudad de México, México

A hybrid multilayer electrospunned scaffold consisting of polycaprolactone (PCL) combined with hydroxiapatite (HaP), collagen in acetic acid and sodium alginate (SA) dissolved in poly(vinyl alcohol) (PVA), were mixed to obtain nanofibrous membranes using the electrospinning technique. Four different hydroxyapatite structures were separately incorporated to the different scaffolds: (1) nanometric HaP, (2) micrometric Hap, (3) functionalized nanometric HaP_f and (4) natural-decellularized bovine condyle to produce a hydroxiapatite-lilke compound. These polymeric membranes were seeded with mesenchymal cells to evaluate their biocompatible properties on time. The morphological characterization was carried out using scanning electron microscopy (SEM) and atomic force microscopy (AFM) whereas the mechanical properties were assessed with the tensile test. The cell viability and cellular proliferation properties were evaluated with fluorescent staining against tactin, DAPI and Ki-67 components. The surface and topography results indicated a homogenous crosslinked structure with a low density defects such as porosity. The rounded beads morphology and size varied depending on the HaP conditions onto the membrane. Systems (3) and (4) achieved a well-dispersed beads incorporated into the nanofibrous mats. Despite of the bead formation, the HaP concentration was homogenously dispersed all over the mat architecture without agglomerates formation. The roughness profile of all systems was as follows: (1) 10761.nm, (2) 1458.3 nm, (3) 1977 nm and (4) 2304.3 nm. These data demonstrated that depending on the HaP physico-chemical conditions it was possible to induce a rougher surface or a more hydrophobic membrane. On the other hand, the mechanical tensile test clearly showed that the crosslinked process became more fragile all systems. The mechanical behavior changed in all systems. The highest ultimate tensile strength values corresponded to systems (3) and (4). Concerning the cellular assays, it was demonstrated that the mesenchymal cells did not change their morphology during the cell culture, which revealed that the extracellular matrix (ECM) remained unaltered. This condition proved that the hybrid scaffold was nontoxic and thus, biocompatible with the cell culture. The systems (3) and (4) developed the highest adhesion features with homogenous distribution of mesenchymal cells throughout the polymeric scaffold along the test (Fig 1). The cell culture proliferated on the scaffold showed a thick and compact layer that entirely covered the nanofibers. Therefore, this study demonstrates that these hybrid scaffolds (PCL/collagen/SA) developed optimal preservation and proliferation conditions depending on the nature of the HaP. This material promises an innovative way to generate an effective membrane to restore or repair injured tissue/cartilage/bone.

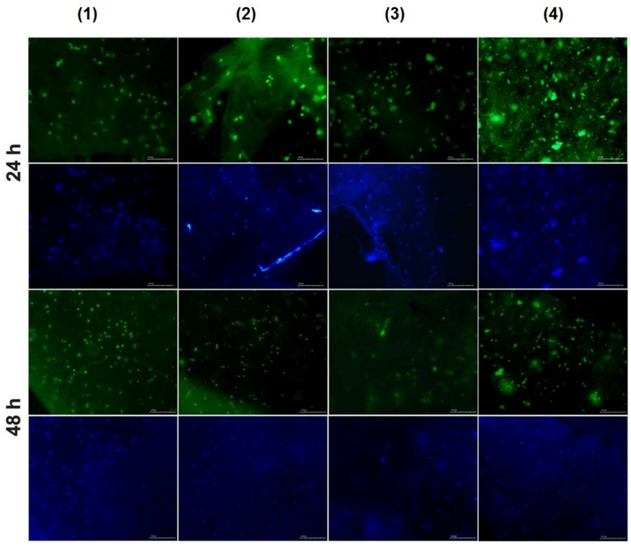
(1)
(2)
(3)
(4)
24 h
48 h

O9 - Physicochemical characterization of nanocellulose materials for food applications

2. BIO – Bio-interfaces, Biomaterials and Life Science

Francesco Fumagalli[1]
Giacomo Ceccone[1], Eveline Verleysen[2], Lisa Siciliani[2, 3], Jan Mast[2], olimpia vicentini[3], francesco cubadda[3]
[1] Joint Research Centre EC
[2] Trace Elements and Nanomaterials, Chemical and Physical Health Risks, Sciensano, Uccle, Belgium
[3] Istituto Superiore di Sanità - National Institute of Health, Rome, Italy

Cellulose is the most abundant organic polymer found in nature and it has been historically exploited for many technological applications. Microcrystalline cellulose (MCM) is a purified, partially depolymerized by-product of fibrous plant cellulose that has already regulated and authorized applications as food additive. Nano-sized cellulose fibres can then be extracted from their micro-counterparts. Nanocellulose (NC) is an emerging advanced nanomaterial with several potential applications in the fields of medicine, energy, food and consumer products. NC can be classified in three types according to its source material: (1) nanofibrillated cellulose (NFC), (2) nanocrystalline cellulose (NCC), and (3) bacterial NC (BNC). Several technological pathways exists for the production of NC, exploiting the different biological sources, which in turn affect many physicochemical properties and ultimately the NC surface chemistry. Understanding the variability in the characteristics of different NC materials is crucial for reliable development of NC-based products and their safety assessment.

Increased attention towards NC use in food applications requires a thorough risk assessment that lays its foundation on a careful evaluation of NC material physicochemical properties. Investigating physicochemical properties of NC materials under the conditions applied for in-vitro testing is a prerequisite for proper hazard assessment and for understanding the underlying biochemical mechanisms occurring during NC interactions with living cells and tissues. Therefore we realized a detailed dataset of the physicochemical properties for each different type of NC material, including a microcrystalline cellulose material reference, using a set of orthogonal nano-analytical techniques. The objective was the realization of an interpretative framework for the subsequent toxicity experiments. The study involved Time-of-Flight Secondary Ions Mass Spectroscopy (ToF-SIMS) for the analysis of macromolecular chemistry, x-ray photoelectron spectroscopy (XPS) and Fourier-transform infrared spectroscopy (FTIR) for the characterization of the functional groups chemistry, X-ray diffraction analyses (XRD) for characterization of the crystalline structure and transmission electron microscopy (TEM) for morphological characterization.

The NC materials were ranked in order of decreasing crystallinity, as measured by XRD. Functional groups chemistry analysis via XPS and FTIR showed the appearance of COO^- functionalities in the NFC-Tempo (i.e. catalytic oxidation) samples that are absent in other formulations. Chemical structure analysis using ToF-SIMS data, processed via multivariate approach (principal component analysis,PCA) is able to separate the samples based on a first component describing the glucose monosaccharide structure and a second component describing oxidized groups. Samples grouping obtained via PCA reflects individual properties differences measured independently with orthogonal techniques.

Acknowledgement and Declaration

This research was performed under NANOCELLUP project. NANOCELLUP has received funding from the European Union through an EFSA grant (GA GP/EFSA/SCER/2020/04). This communication reflects only the author's view and EFSA is not responsible for any use that may be made of the information it contains.

O10 - Protein immobilzation on ultrananocrystalline diamond films with different surface terminations

2. BIO – Bio-interfaces, Biomaterials and Life Science

Rezvaneh Ghasemitabesh[1]
Daniel Merker[1], Daniela Bertinetti[2], Friedrich W. Herberg[2], **Cyril Popov**[1]
[1] Institute of Nanostructure Technologies and Analytics (INA), Center for Interdisciplinary Nanostructure Science and Technology (CINSaT), University of Kassel, Germany
[2] Department of Biochemistry, Institute of Biology, Center for Interdisciplinary Nanostructure Science and Technology (CINSaT), University of Kassel, Germany

Diamond is an ideal candidate for biomedical and biotechnological applications, such as platforms for biosensors and DNA-chips, due to its biocompatibility, excellent mechanical properties, large electro-chemical potential window and high chemical stability. In the current project we are investigating the non-covalent and covalent binding of proteins on the surface of ultrananocrystalline diamond (UNCD) films prepared by microwave plasma chemical vapor deposition. For both pathways green fluorescence protein (GFP) was used allowing direct measurement of the fluorescence signal by a microplate reader. As a first step, the UNCD surface was nanostructured by plasma etching to increase the area for interaction with proteins. In the case of non-covalent immobilization, UNCD surfaces with hydrogen, oxygen or fluorine terminations, achieved after different plasma modifications, were studied. These processes resulted in change of the wettability, revealed by contact angle measurements, and of the surface composition, as shown by X-ray photoelectron spectroscopy (XPS). The intensity of the fluorescence signal due to binding of GFP from solutions with concentrations between 10 μM and 500 pM increased in the order F-UNCD < H-UNCD < O-UNCD, i.e. with the increase of the hydrophilicity of the surface. For the covalent immobilization photochemical grafting of ω-alkene, e.g. of TFAAD (10-Trifluoro-acetamidodec-1-ene), as linker on H-terminated UNCD was firstly applied for direct binding of GFP. In a second series of experiments nanobodies able to bind GFP from solutions were immobilized by the same linker molecules. In order to reduce the physical adsorption and to realize GFP capturing mostly by the binding nanobodies, milk powder was applied as a blocking protein before the exposure to GFP solutions. In both cases the average fluorescence intensity increased with the concentration of GFP in a non-linear relation, which can be attributed to saturation in the higher concentration range and to depletion in the lower one. These initial results can serve as a starting point for further investigations of structured and functionalized UNCD as a bioplatform for immobilization of different binding proteins with high affinity and specificity toward target molecules, e.g. neuropeptides released by neurons plated on it, which play a vital role in the generation and maintenance of the inner clock in different model organisms.

O11 - Purification of biopharmaceuticals by electrochemical polymer brush chromatography

2. BIO – Bio-interfaces, Biomaterials and Life Science

Maria Kiriakidou[1]
Gustav Ferrand Drake del Castillo[1], **Andreas Dahlin**[2]
[1] Nyctea Technologies AB
[2] Chalmers University of Technology

The majority of all new drugs are biological macromolecules rather than small synthetic organic compounds. Such biopharmaceuticals, in particular monoclonal antibodies, can provide treatment of a great range of diseases, but they come at a great cost. Biopharmaceuticals are produced by living cells and although they are efficeint, the target molecule must be purified from the "slurry" produced by the bioreactor. While this is feasible, the purification process is extremely resource intense. Besides being an environmental burden, the costly production also limits availability of biopharmaceuticals in developing countries. In this work we show how polymer brushes and electrochemistry can be used to improve the purification.

Polymer brushes consist of end-grafted chains at high surface density, which enforces stretching in the direction perpendicular to the surface. If polymer brushes are made with weak polyelectrolytes, this can make interfaces pH-responsive, which has attracted a lot of attention for various applications. However, the pH of a given bulk environment, for instance a biological solution, is static and buffered. At the same time, it is well-known that electrochemical control can be used to alter the pH locally at an interface. Still, applying an electrochemical potential tends to destroy the polymer brush or remove the chains. Alternatively, the grafting layer is so dense that it prevents efficient electron transfer and thus the electrochemical activity.

We recently presented the first example of a polymer brush interface fully compatible with electrochemistry by using aryl diazonium salts attached to metals via chemical reduction.[1] This grafting chemistry is stable when an electric potential is applied and Faradaic reactions occur essentially unhindered. By preparing poly(methacrylic acid) (PMAA) brushes, we were able to show complete electrochemical switching over many cycles by pH changes at the interface, i.e. the brush altered between fully ionized and fully protonated (or anywhere in between), even while the bulk environment was buffered.

Furthermore, by immobilizing receptors inside the polymer brush, it can bind large amounts of proteins specifically and release them by electrical control. The system performs excellent with respect to all desirable features: high capacity, specificity and reversibility.[2] Using porous conductive materials, our technology has been upscaled into a functioning chromatography prototype, currently handling quantities on the scale of ~10 mg. The electrochemistry gives precise control of bound species, removes the need for elution chemicals and is much milder for proteins. This reduces the risk of denaturation, which is devastating for therapeutic antibodies.

Selected references

1. Ferrand-Drake del Castillo G*, et al.* Electrically switchable polymer brushes for protein capture and release in biological environments. *Angewandte Chemie International Edition* **61**, e202115745 (2022).

2. de Boer, K.; Schroën, K., Polymer-based stimuli-responsive systems for protein capture: Capacity, reversibility, and selectivity. *Separation and Purification Technology* **337**, 126288 (2024).

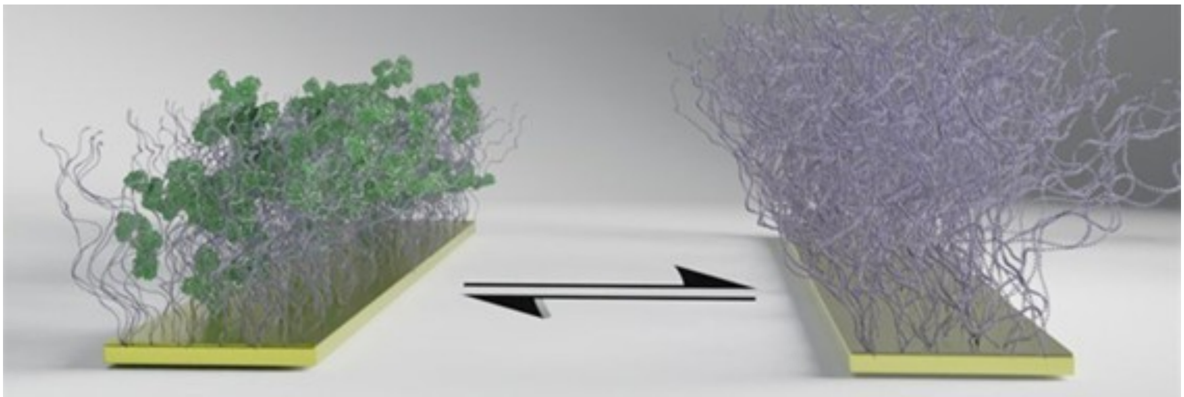

O12 - Surface analysis of PEGylated liposomes for nanomedicine applications.

2. BIO – Bio-interfaces, Biomaterials and Life science

Francesco Fumagalli[1]
Alexander Welle[2], Guillaume Bucher[1], Giacomo Ceccone[1], Dora Mehn[1]
[1] European Commission, Joint Research Centre, Ispra, Italy
[2] Karlsruhe Nano Micro Facility (KNMF), Karlsruhe Institute of Technology (KIT), 76344 Eggenstein-Leopoldshafen, Germany

Liposomes are spheroidal, phospholipid-based bilayer structures with an encapsulated aqueous phase. Due to their size, amphiphilic character, biocompatibility and biodegradability, liposomes emerged as novel systems for drug delivery and many other applications in health and food technology. Liposomes modified with surface-grafted polyethylene glycol(PEG) corona exhibit increased hydrophilicity, stability and antifouling character of their surface. In nanotherapeutics applications, these properties decrease proteins binding thus improving the possibility to escape recognition by the immuno-system and increase the drug's half-life in circulation. Many of such formulations are, since decades, authorized in the EU market but despite their successful implementations, knowledge gaps in the *in-vivo* behaviour still exist. In addition, the understanding of such systems is complicated due to the lack of harmonized methodologies for assessing their surface properties. Accurate physical-chemical characterization of liposome surface coatings and a connection between surface properties and synthesis parameters is a necessary step to build an understanding of critical factors determining their antifouling properties that affect complex biochemical interactions occurring *in-vivo*.

Cryo-XPS provides a suitable technique to asses semi-quantitatively the concentrations of surface coating functionalities while preserving a realistic, hydrated-state relevant organization of layers in such "soft" nanoparticles.(1-2) Moreover, ToF-SIMS on cryogenic samples can be used in parallel to obtaining deeper insights on the nanoparticles surface chemistry.(3) ToF-SIMS is capable of label-free analysis of biomolecules, specifically lipids, with high sensitivity. To detect the abundance of different lipid species, it is possible to measure their unique molecular ion fragmentation patterns and to analyse intensity variations of low mass fragments using a multi-variate analysis approach.

In this work, by analysing liposomes produced by varying specific synthesis parameters, the observed differences in the surface chemistry compositions (XPS,SIMS) are related to measurements of bulk physical-chemical properties (sizing via DLS, lipid content via HPLC and Raman) with the aim of linking back to the nominal formulation compositions. With this approach we aim to consolidate the operational details of surface-analysis characterization methodology for PEG-coated liposomes; semi-quantitatively characterize non-trivial liposomal surface properties (grafted PEG chain surface density) and improve the understanding of coated liposome surface chemistry by establishing a correlation between external synthesis parameters (e.g. components mixing ratio and total flow rate) and internal variables (PEGylated phospholipids excess and liposomes size distribution).

Robust characterization methods for liposome coatings will enable more advanced drug designs where PEG surface density will be traded-off between surface antifouling properties and the possibility to bind protein labels for tracing studies.

Selected references

(1) A. Shchukarev, et al. Applied Surface Science 526 (2020) 146538

(2) D. cant et al., J. Phys. Chem. A 2023, 127, 39, 8220–8227

(3) I. Lanekoff, M. E. Kurczy, R. Hill, J. S. Fletcher, J. C. Vickerman, N. Winograd, P. Sjövall, A. G. Ewing, Anal. Chem. 2010, 82, 6652.

O13 - Surface treatment and functionalization of 2D and 3D titanium alloys for biomedical applications

2. BIO – Bio-interfaces, Biomaterials and Life Science

Samantha Soulé[1]
Malobi Seth[1, 2], Laurent Weiss[2], Liang Liu[1], Marius Colin[3], Halima Kerdjoudj[3]
[1] LCPME UMR 7564, CNRS, Université de Lorraine, Villers-Lès-Nancy, 54600, France.
[2] LEM3 UMR CNRS 7239, CNRS, Université de Lorraine, Metz, 57073, France.
[3] BIOS EA 4691, Université de Reims Champagne Ardenne, Reims, 51100 France.

Titanium alloys are widely used as orthopaedic implant materials due to their mechanical properties, corrosion resistance and biocompatibility. Despite these benefits, common problems such as weak bonding to bone tissue after implantation and poor antimicrobial properties remained[1].
In this context, the progress in additive manufacturing has opened up new perspectives with the possibility of designing scaffolds used as bone substitutes. Among the different technologies developed, selective laser melting (SLM) has recently drawn attention for the fabrication of porous implants with complex geometries and customized features. Nevertheless, the development of surface modifications is required to further improve the mechanical and biological properties and finally obtain biomedical materials that meet medical requirements[2].

Firstly, we have explored the potential of the Surface Mechanical Attrition Treatment (SMAT) for improving the mechanical and surface properties of 2D Ti-6Al-4V (TA6V) substrates. While the ultrasonic shot peening surface treatment was effective in increasing the hardness and fatigue resistance of the parts and enhancing the roughness, our study focused specifically on surface chemical modifications. X-ray Photoelectron Spectroscopy revealed that (1) the SMAT treatment caused cross-pollution between the TA6V surface and the 100C6 balls and (2) the wear of the balls affected significantly the resultant surface chemistry. Surface pollution decreases corrosion resistance particularly when worn balls are used for the SMAT. Further, the bacterial adhesion decreased as the surface roughness was improved.

Secondly, we have developed the elaboration of an antibacterial coating on 3D lattices of TA6V. For this purpose, the method was first optimised on 2D substrates and then transposed on 3D ones. Whereas the unmelted powder particles resulting from the SLM process were effectively removed by acid etching on the 2D substrates leading to a smoother surface, heterogeneities subsisted in the 3D lattices. The following coating involved the deposition of ZnO nanoparticles as seed by dip coating for the subsequent growth of nanowires by hydrothermal method[3]. Several parameters such as precursor composition, deposition/ growth time, and temperature were adjusted to obtain optimized coating. Scanning Electron Microscopy characterization showed that the nanowires have grown perpendicularly from the surface and the formation of ZnO was confirmed by Raman spectroscopy and X-Ray Diffraction. On the 3D lattices, most of the surface is covered with the ZnO nanowires.

Finally, the antibacterial activity evaluated on the 2D substrates was demonstrated and involves both mechanical and chemical effects. The combined actions could be effective in combatting bacterial contamination of biomedical implants.

Selected references

1. Han, X.; Ma, J.; Tian, A.; Wang, Y.; Li, Y.; Dong, B.; Tong, X.; Ma, X. Surface Modification Techniques of Titanium and Titanium Alloys for Biomedical Orthopaedics Applications: A Review. *Colloids and Surfaces B: Biointerfaces* **2023**, *227*, 113339.
2. Chowdhury, S.; Arunachalam, N. Surface Functionalization of Additively Manufactured Titanium Alloy for Orthopaedic Implant Applications. *Journal of Manufacturing Processes* **2023**, *102*, 387–405.
3. Greene, L. E.; Law, M.; Tan, D. H.; Montano, M.; Goldberger, J.; Somorjai, G.; Yang, P. General Route to Vertical ZnO Nanowire Arrays Using Textured ZnO Seeds. *Nano Lett.* **2005**, *5* (7), 1231–1236.

3. CAT – Catalysis and Surface Functionalization

O14 - A guided tour around LEIS spectra

3. CAT – Catalysis and Surface Functionalization

Stanislav Průša[1, 2]
Elena Vaníčková[2], Pavel Bábík[2], Tomáš Šikola[1, 2]
[1] Faculty of Mechanical Engineering, Brno University of Technology, Brno 616 69, Czech Republic
[2] Central European Institute of Technology - CEITEC, BUT, Brno 612 00, Czech Republic

This contribution is aimed at surface scientists who may not be active users of Low Energy Ion Scattering (LEIS) but come across its results in publications relevant to their research. The guided tour could be helpful in planning experiments where the surface or interface composition plays a crucial role, demonstrating the potential and challenges of the LEIS technique.

The Low Energy Ion Scattering technique benefits from simple theory and extraordinary surface sensitivity. The theory of elastic collision and binary collision approximation can effectively explain the position of the measured signals (peaks) in the spectra. Therefore, the qualitative interpretation of the results is straightforward in most cases. However, the quantitative analysis of data requires a comprehensive understanding of charge exchange processes, as well as the use of well-defined reference samples. Several important technical realisations are used in LEIS experiments. Our team has practical experience with noble gas ion scattering and analysis by electrostatic energy analyzers (used in the dedicated LEIS instrument Qtac100). The spectra presented in our study were obtained at a scattering angle of 145°, but they can still be representative of other typical scattering geometries to some degree.

The contribution provides a range of results obtained from various materials and surfaces. It explains how the physics behind Low Energy Ion Scattering can be observed in the spectra. This helps the audience, for example, understand why the spectrum for He^+ scattering (3.0 keV, 145°) on a pure Cu foil differs significantly from that collected on a Ca surface, as demonstrated in the figure. The intensities of peaks and backgrounds are very different and reflect the charge transfer between the He^+ projectiles and surface atoms.

Scientists with a critical understanding of scattering principles can effectively plan their research projects where the LEIS technique could complement established techniques such as XPS and STM.

Selected references

[1] S. Průša, M.R. Linford, E. Vaníčková, P. Bábík, J.W. Pinder, T. Šikola, H.H. Brongersma, A practical guide to interpreting low energy ion scattering (LEIS) spectra, Applied Surface Science 657 (2024), 158793, https://doi.org/10.1016/j.apsusc.2023.158793.
[2] H.H. Brongersma, M. Draxler, M. de Ridder, P. Bauer, Surface composition analysis by low-energy ion scattering. Surface Science Reports 2007, 62 (3), 63-109. DOI: https://doi.org/10.1016/j.surfrep.2006.12.002.

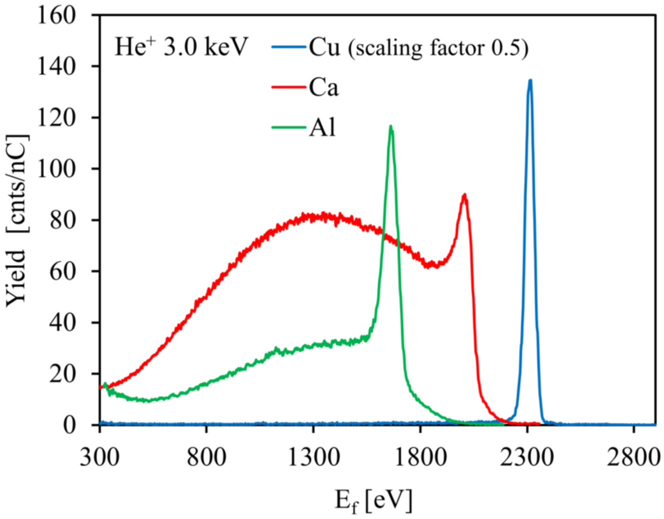
He+ 3.0 keV
Cu (scaling factor 0.5)
Ca
Al
Yield [cnts/nC]
160
140
120
100
80
60
40
20
0
300
800
1300
1800
2300
2800
E_f [eV]

O15 - A synergy of light and water: unveiling the self-breakdown of organophosphonic acid grafted titanium dioxide

3. CAT – Catalysis and Surface Functionalization

Nick Gys[1, 2, 3, 4]
Bram Pawlak[5], Kristof Marcoen[1], Gunter Reekmans[5], Leticia Fernandez Velasco[6], Rui An[3], Kenny Wyns[4], Kitty Baert[1], Kaimin Zhang[3], Léon Luntadila Lufungula[7], Alessandra Piras[5, 8], Laurens Siemons[7], Bart Michielsen[4], Sabine Van Doorslaer[9], Frank Blockhuys[7], Tom Hauffman[1], Peter Adriaensens[5], Steven Mullens[4], Vera Meynen[3, 4]
[1] Vrije Universiteit Brussel, SUME, SURF group, Belgium
[2] KU Leuven, Department of Microbial and Molecular Systems, Ameloot group, Belgium
[3] University of Antwerp, Department of Chemistry, Laboratory of Adsorption and Catalysis, Belgium
[4] Flemish Institute for Technological Research (VITO NV), Belgium
[5] Hasselt University, MATCHEM, Analytical and Circular Chemistry (ACC), Belgium
[6] Royal Military Academy (RMA), Belgium
[7] University of Antwerp, Department of Chemistry, Structural Chemistry Group, Belgium
[8] Namur University, Unit of Nanomaterials Chemistry, Belgium
[9] University of Antwerp, Laboratory of Biophysics and BioMedical Physics, Belgium

The introduction of organic molecules onto the surface of metal oxides through surface grafting provides the ability to tailor the surface properties towards an increased specificity and control of interactions. In the field of hybrid organic-inorganic materials, organophosphonic acid (PA) grafted metal oxides are becoming increasingly more prominent given their versatility in surface tuning and their specific merits in applications ranging from supported metal catalysis(*1*), hybrid (photo)-electric devices(*2*), biosensing(*3*) and sorption and separation processes.(*4*) While synthesis-properties-performance correlations are being studied for organophosphonic acid grafted TiO_2, their stability and the impact of exposure conditions on possible changes in the interfacial surface chemistry remain unexplored. In addition, a differentiation in the stability of the organic group (carbon chain) and the M-O-P bonds is missing. In this study(*5*), the impact of different ageing conditions on the evolution of the surface properties of propyl- and 3-aminopropylphosphonic acid grafted mesoporous TiO_2 over a period of 2 years is reported, using solid-state ^{31}P and ^{13}C NMR, ToF-SIMS, EPR and XPS as main techniques. In humid conditions under ambient light exposure, PA-grafted TiO_2 surfaces initiate and facilitate photo-induced oxidative reactions, resulting in the formation of phosphate species and degradation of the grafted organic group with a loss of carbon content ranging from 40 to 60 wt%. However, the Ti-O-P bonds remain unaffected, confirming its reported high hydrolytic stability. Since exposure under dry air does not result in ageing phenomena, humidity and more specifically, the interactions of adsorbed water with the grafted surface, play a fundamental role in the ageing process. By revealing the underlying ageing mechanism, solutions were provided to prevent degradation. This work creates critical awareness in the research community working on hybrid titania materials and other possible photo-active materials to evaluate changes in photo-activity and stability after surface grafting.

Selected references

1. F. Forato *et al.*, *Chem. - A Eur. J.* **24**, 2457–2465 (2018).
2. H. Chen, W. Zhang, M. Li, G. He, X. Guo, *Chem. Rev.* **120**, 2879–2949 (2020).
3. N. Riboni *et al.*, *RSC Adv.* **11**, 11256–11265 (2021).

4. G. A. Seisenbaeva *et al.*, *RSC Adv.* **5**, 24575–24585 (2015).
5. N. Gys *et al.*, *Chempluschem*. **88** (2023), doi:10.1002/cplu.202200441.

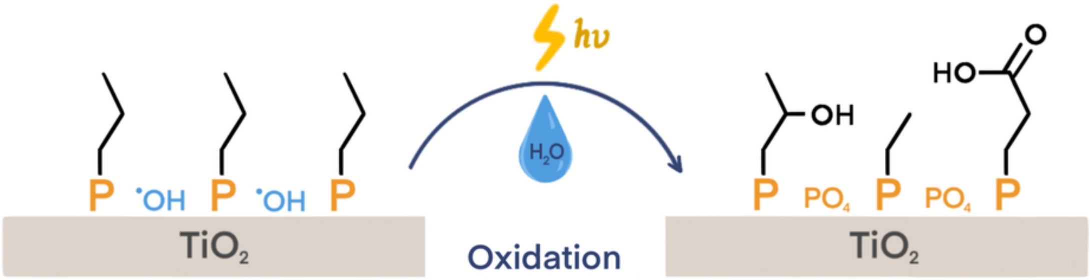

O16 - Advanced photoelectron spectroscopy: A tool to characterise the nature of oxygen defects?!

3. CAT – Catalysis and Surface Functionalization

Martin Hantusch[1]
[1] IFW Dresden, Helmholtzstraße 20, D-01069 Dresden, Germany

Transition-metal oxides, such as TiO2 or ZnO, are widely used in many new applications for environmentally friendly energy conversion e.g. photocatalyticly enhanced synthesis of synthetic fuels or next generation solar cells. A crucial advantage of these materials is that their electronic, optical or chemical properties can be easily tuned by introducing oxygen defects. Since the desired property change or the long time stability of the material depends on the nature of the defect or its origin the careful characterisation of these defect states is necessary to significantly improve the synthesis routes for new functional materials.

Common characterisation methods for defective structures and the subsequent property change in metal oxides like optical spectroscopy, X-ray diffraction or electron spin resonance spectroscopy are bulk sensitive methods. Changes on the surface or the interface are hard to determine and are often overlooked or neglected despite they could have critical influences on the overall performance of the future application. In contrast, Photoelectron spectroscopy (PES) is a surface sensitive method which gives information about the chemical composition and the chemical states. It is used to determine only the presence of oxygen defects by analysing the metal core levels. For some metals (like Zn or In) there are no changes in the metal signal and the defects are overlooked.

In this work, a laboratory PE spectrometre (PHI 5600) is used to investigate the surface of transition metal oxide thin films. Simple additional features, e.g. an external field, visible light illumination during the measurement or a quasi-in-situ surface modification, are introduced to characterise possible oxygen defects and their influence on electronic or chemical properties. The transition metal oxide thin films are modified by annealing, ion sputter etching or plasma etching in order to introduce oxygen defects of different nature.

The correlation between the defect synthesis method and the properties of the materials is evaluated by determining the core level states, the valence states and the work function of each sample. Additionally, the electronic, optical and chemical changes due to the modification is discussed in detail by analysing the behaviour during in-situ measurements.

O17 - Ammonia decomposition over MgFe2O4 and MgFeCoO4 catalysts: An operando soft X-ray spectroscopy study

3. CAT – Catalysis and Surface Functionalization

Lukas Pielsticker[1]
Liqun Kang[1], John Carl Camayang[1], Yves Kayser[1], Serena DeBeer[1]
[1] Max Planck Institute for Chemical Energy Conversion, Muelheim an der Ruhr, Germany

Ammonia is considered a key hydrogen vector for the transport and storage of renewable energy. However, the decomposition of ammonia at the point of use is not yet implemented at industrial scale due to the high cost of the most active Ru catalyst. The development of highly active, cost-effective metal catalysts remains in high demand [1]. Recently, a promising non-noble metal catalyst was developed: layered double hydroxide-derived $MgFeCoO_4$. Its higher activity compared to the mono-metallic $MgFe_2O_4$ counterpart has been attributed to a suppression of Fe nitride formation under reaction conditions [2]. We present here the results of a combined *operando* near-ambient pressure XPS and NEXAFS study on a $MgFeCoO_4$ catalyst under ammonia decomposition reaction conditions. Parallel studies on the less active $MgFe_2O_4$ catalyst were also performed to evaluate the promotional effect of Co. Elemental composition, surface adsorbates, and alloy formation were systematically investigated as a function of reactive gas environment, temperature, and surface coverage. On-line mass spectrometry was used to correlate the catalytic activity of the two different catalysts with the structural changes under different reaction conditions. By combination of *in situ* soft X-ray spectroscopy with mass-spectrometry measurements, a complete temperature-dependent structure-reactivity relationship of ammonia decomposition on Fe and Fe-Co could be revealed. Based on Fe and Co 2p core-level XPS and L-edge NEXAFS spectra, there is a mixture of reduced and oxide phases present under ammonia decomposition reaction conditions. N 1s spectra reveal that the surface of the $MgFeCoO_4$ catalyst contains significantly less iron nitride in the presence of NH_3 compared to $MgFe_2O_4$. By monitoring the gas-phase N_2 peak in the N 1s spectrum in combination with on-line mass-spectrometry, we obtained insights into the correlation between electronic structure, adsorbed surface species, and catalytic activity. Overall, our results strongly support that the introduction of Co to the Fe-based catalyst leads to a reduction of the amount of surface iron nitride species under reaction condition, which is correlated with a higher ammonia decomposition activity (see Fig. 1). The results from this work should be very useful in future efforts to design cheap and efficient ammonia decomposition catalysts.

Selected references

[1] F. Schüth, R. Schlögl, D.S. Su, *Energy Environ. Sci.*, **2012**, *5*, *4*, 6278-6289.
[2] S. Chen, J. Jelic, D. Rein, et al*., Nat. Commun.* **2024***, 1*, *871*

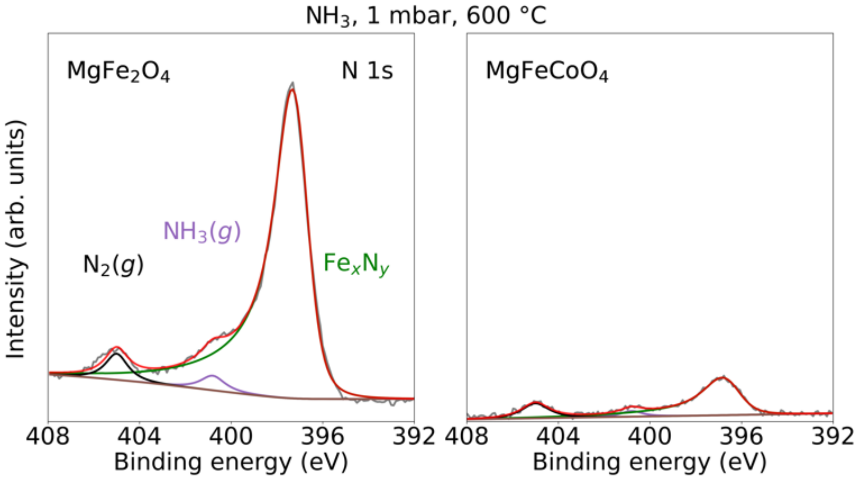

Figure 1. Comparison of adsorbed and gas-phase nitrogen species on Fe and Fe-Co catalysts under ammonia decomposition reaction conditions at 1 mbar.

O18 - Electrocatalytic carbon dioxide reduction on electrodeposited multi-principal element alloy (MPEA) catalysts

3. CAT – Catalysis and Surface Functionalization

Salbin Sediqi[1]
Carsten Prinz[1], Matthias Dimper[1], Julia Witt[1], Özlem Ozcan[1]
[1] Bundesanstalt für Materialforschung und-Prüfung

The aim of this project is to develop novel noble metal-free electrocatalysts that do not rely on critical minerals. We focus on Cu-containing multi-principal element alloys (MPEAs) improve the efficiency and selectivity of the CO_2 reduction reaction. In general, MPEAs consist of more than three elements that form solid solutions without intermetallic phases. The unique chemical composition and atomic level mixing introduces synergetic effects that play a critical role in electrocatalysis, especially in terms of selectivity. The nearly infinite combinations of elements that can be incorporated into MPEAs provide ample opportunities to tailor their functionality for various applications.

This study presents the development of thin films based on CuNiZn MPEAs for CO_2 reduction reaction. The one-step electrodeposition of CuNiZn gradient films was performed on carbon electrodes using a Hull cell under constant current or potential. The influence of pH, additives and current density or potential on the composition and microstructure of the films was characterized by scanning electron microscopy (SEM) and energy dispersive X-ray spectroscopy (EDX). Atomic force microscopy (AFM) was used to study the topography and surface roughness of the CuNiZn films. The results indicate that the addition of ethylenediaminetetraacetic acid (EDTA) and citrate improves the uniformity and adhesion of the thin films.

Electrochemical measurements, including cyclic voltammetry, linear sweep voltammetry, and impedance spectroscopy, were performed to investigate the electrocatalytic activity and corrosion resistance of CuNiZn thin films. The CuNiZn gradient films deposited in the Hull cell allow high throughput screening of the electrocatalytic activity. This approach has identified several compositions with high activity, selectivity and stability. Selected electrodeposited films were further processed to nanoparticles by means of pulsed laser ablation in liquids (PLAL). Further analysis thin film and nanoparticle electrocatalysts was performed with in-line / at line product monitoring using a rotating disk electrode setup coupled to gas chromatography (GC) and high performance liquid chromatography (HPLC). The presentation will summarize the results of our screening study with few deep dives in selected compositions showing superior performance.

O19 - Hard X-ray photoelectron spectroscopy reveals Fe segregation in NiFe electrodes during oxygen evolution reaction

3. CAT – Catalysis and Surface Functionalization

Filippo Longo[1, 2]
Pedro Javier Lloreda-Jurado[3], Jorge Gil-Rostra[3], Agustin R. Gonzalez-Elipe[4], Francisco Yubero[4], Andreas Borgschulte[1, 2]
[1] Laboratory for Advanced Analytical Technologies, Empa, Dübendorf, Switzerland
[2] Department of Chemistry, University of Zurich, Zürich, Switzerland
[3] Nanotechnology on Surfaces Group, Instituto de Ciencia de Materiales de Sevilla (ICMS-US-CSIC), Seville, Spain
[4] Nanotechnology on Surfaces and Plasma, Institute of Materials Science of Seville (CSIC-US), Seville, Spain

Alkaline water electrolysis represents one of the simplest methods employed to perform water splitting reaction [1]. This process is one of the most efficient ways of producing H_2 and O_2 at low cost and high purity [2]. The bottleneck of this reaction stems from the sluggish kinetics of the anodic reaction, i.e., the oxygen evolution reaction (OER), which consists of a four-electron transfer process [3]. The extraordinary performance of NiFe as electrocatalysts for the OER is still a subject of debate [4] . The changes that occur on the electrode surface during electrochemical reactions add another dimension of complexity, which hinders the rational design of electrodes for water splitting. Particularly for binary alloy electrodes, there are various phenomena ranging from the formation of oxides, (oxy)hydroxides and the associated segregation of metal atoms. In this work, we study various NiFe electrodes as model systems for the OER. We have developed the procedure for the quantification of chemical depth-profiling by XPS/HAXPES measurement, showing a marked Fe segregation and dissolution. The results explain the electrochemical performance of NiFe electrodes for OER. All the electrodes studied suffer from segregation of iron and subsequent formation of FeO_x on the surface, with only minor influence from morphology, porosity and total Fe content.

Selected references

[1] S. W. Sharshir et al., International Journal of Hydrogen Energy (**2023**).
[2] Z.-Y. Yu et al., Advanced Materials 33, 2007100 (**2021**).
[3] A. Wang et al., Mater. Chem. Front. 7, 5187 (**2023**).
[4] F. Dionigi and P. Strasser, Advanced Energy Materials 6, 1600621 (**2016**).

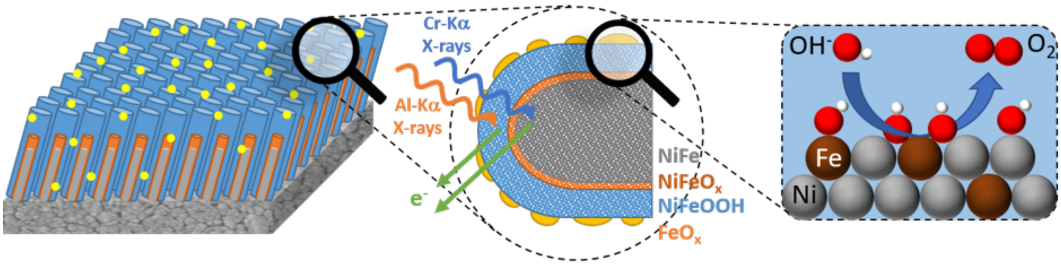

Fig. 1. Schematic representation of the investigated NiFe electrode (left), electronic structure of NiFe investigated by XPS/HAXPES (center) and Oxygen Evolution Reaction taking place at the interface between electrode and electrolyte (right).

O20 - Multi-Technique Characterization of PtNi Nanowires for Enhanced Durability and Efficiency

3. CAT – Catalysis and Surface functionalization

Jennifer Mann[1]
Cesar Saucedo[1], Sarah Zaccarine[1], Kateryna Artyushkova[1]
[1] Physical Electronics

Polymer electrolyte membrane fuel cells (PEMFCs) present a promising avenue for generating sustainable electricity with minimal environmental impact. However, their widespread adoption faces challenges due to concerns about durability and the sluggish kinetics of the oxygen reduction reaction (ORR) at the cathode. Consequently, advancing PEMFCs requires progress in catalyst technologies to overcome these limitations. Previous studies have investigated the synthesis of extended-surface platinum-nickel (PtNi) nanowires (NWs) through atomic layer deposition (ALD) and examined their durability.[1]

In this work, we demonstrate how the composition and chemical states of the nanowires transform after a series of post-synthetic modifications aimed at maximizing their longevity as catalysts. The characteristics of the as synthesized, annealed, acid leached, and reannealed PtNi NWs were investigated using several techniques including X-ray photoelectron spectroscopy (XPS), hard X-ray photoelectron spectroscopy (HAXPES), and Auger electron spectroscopy (AES). Preliminary results indicate that after synthesis, there are multiple surface oxides of Ni present in all samples, with the least amount of oxidation occurring in the acid leached and reannealed samples. Comparison of the XPS and HAXPES results shows there is increased presence of Ni metal below the surface for all the samples. Through the integration of complementary surface analytical techniques, including XPS, HAXPES, and AES, we construct a more comprehensive model of the intricate chemical nature of these catalysts than any individual technique could achieve on its own. This approach accelerates the development of more durable and efficient PEMFC catalysts.

Selected references

[1] Zaccarine, S. F., Alia, S. M., McNeary, W. W., Chattot, R., Dzara, M. J., Martens, I., Mauger, S. A., Weimer, A. W., Drnec, J., Pivovar, B. S., & Pylypenko, S. (2022). Optimization of Extended-Surface PtNi Nanowire Oxygen Reduction Electrocatalysts Produced via Atomic Layer Deposition. ACS Applied Energy Materials, 5(4). https://doi.org/10.1021/acsaem.2c00016

O21 - On the combination of UPS with optical absorption to investigate Cu2O||TiO2 direct Z-schemes with different Cu2O loading

3. CAT – Catalysis and Surface functionalization

Beatriz de la Fuente[1]
Jan Bomnuter[2], Michele del Moro[3], Lien Smeesters[4], Vanina Cristaudo[1], Tom Breugelmans[3], Vera Meynen[2], Pegie Cool[2], Annick Hubin[1], Tom Hauffman[1]
[1] Research Group Sustainable Materials Engineering SUME, Vrije Universiteit Brussel, Pleinlaan 2, 1050 Brussels, Belgium
[2] Laboratory of Adsorption and Catalysis LADCA, University of Antwerp, Universiteitsplein 1, 2610 Antwerpen, Belgium
[3] Applied Electrochemistry and Catalysis ELCAT, University of Antwerp, Universiteitsplein 1, 2610 Antwerpen, Belgium
[4] Brussels Photonics B-PHOT, Department of Applied Physics and Photonics, Vrije Universiteit Brussel, Pleinlaan 2, 1050 Brussels, Belgium

Among the electronic properties, the positions of the electronic band edges and the work function of a photocatalyst are essential parameters for determining its ability to function in a solar conversion system. A novel type of photocatalysts, called direct Z-schemes, possesses many advantages over conventional heterojunctions, which all benefit the catalytic performance under solar light. As oxidation and reduction reactions are greatly affected by the electrical characteristics of the material, ultraviolet photoelectron spectroscopy (UPS) is a powerful tool to determine and quantify important electronic parameters of previously fabricated $Cu_2O \| TiO_2$ junctions. TiO_2 nanotubes modified with Cu_2O nanoparticles exhibit a reduction in the value of the work function (WF = 3.67 ± 0.01 eV) and ionization potential (IP = 6.01 ± 0.04 eV) with respect to the TiO_2 substrate (WF = 4.29 ± 0.02 eV and IP = 7.65 ± 0.05 eV). By varying the electrodeposition time, an optimized amount of deposited Cu_2O nanoparticles was proven to reduce the WF and IP to facilitate the excitation of electrons, which could be correlated to the improved absorbance in the visible wavelength range. This work proposes a valuable methodology for band diagram tracing from UPS spectra and provides new insights in the relationship between synthesis, electronic properties and visible light absorption of titania-based Z-schemes for photocatalytic applications with a combination of surface sensitive techniques and optical absorption studies.

Selected references

[1] Q. Xu et al., “Direct Z-scheme photocatalysts: Principles, synthesis, and applications,” *Materials Today*, vol. 21, no. 10. Elsevier B.V., pp. 1042–1063, Dec. 01, 2018. doi: 10.1016/j.mattod.2018.04.008.
[2] T. Schultz et al., “Reliable Work Function Determination of Multicomponent Surfaces and Interfaces: The Role of Electrostatic Potentials in Ultraviolet Photoelectron Spectroscopy,” *Adv Mater Interfaces*, vol. 4, no. 19, Oct. 2017, doi: 10.1002/admi.201700324.
[3] J. W. Kim et al., “Absolute work function measurement by using photoelectron spectroscopy,” *Current Applied Physics*, vol. 31. 2021. doi: 10.1016/j.cap.2021.07.018.
[4] J. E. Whitten, “Ultraviolet photoelectron spectroscopy: Practical aspects and best practices,” *Applied Surface Science Advances*, vol. 13, Feb. 2023, doi: 10.1016/j.apsadv.2023.100384.
[5] B. de la Fuente et al., “On the combination of ultraviolet photoelectron spectroscopy with optical absorption studies to investigate $Cu_2O||TiO_2$ direct Z-scheme junctions with different Cu_2O loading,” *Applied Surface Science,* Feb. 2024, Accepted.

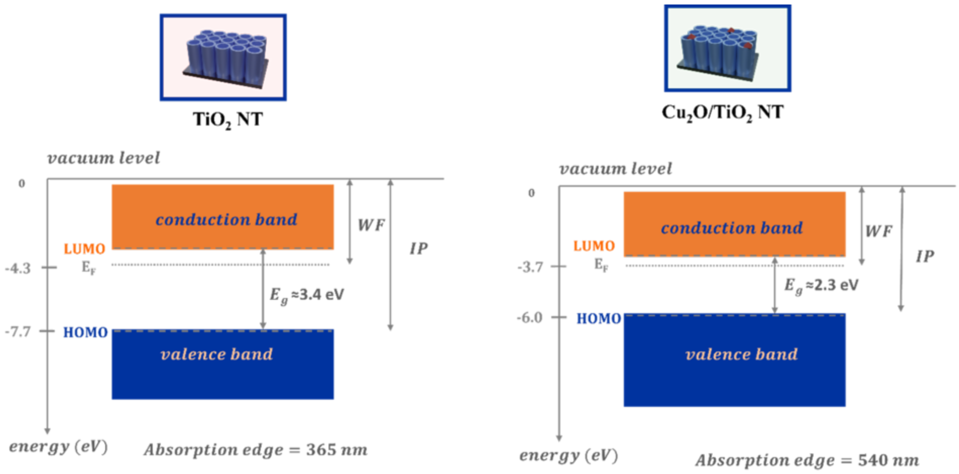

Figure 1: Band diagram of the TiO_2 substrate (left) and of the optimized Cu_2O/TiO_2 junction (right).

O22 - Reliable measurements of the chemical composition of graphene-related 2D materials with X-ray photoelectron spectroscopy

3. CAT – Catalysis and Surface Functionalization

Jörg Radnik[1]
Giovanni Chemello[1], Benjamen P. Reed[2], Sofia Marchesini[2], Andrew J. Pollard[2], Charles A. Clifford[2]
[1] Bundesanstalt für Materialforschung und -prüfung (BAM), Berlin, Germany
[2] National Physical Laboratory (NPL), Teddington, United Kingdom

Graphene and related 2D materials (GR2Ms) are now entering an exciting phase of commercialization and use in products. Graphene nanoplatelets (GNPs) can be obtained in rather large quantities, but the properties of these industrially produced powders can vary depending on the production method, and even from batch to batch. Understanding and optimizing the surface chemistry of GNPs, modified through chemical functionalization processes is crucial, because it affects their dispersibility in solvents and matrices for the purpose of embedding them into real-world products. Therefore, reliable and repeatable measurements of the surface chemistry of functionalized GNPs are an important issue for suppliers as well as users of these materials. To address these concerns, international documentary ISO standards for measurement methodologies are under development which incorporate protocols that are becoming widely accepted in the community.

Recently, it was shown that pelletizing led to lower average O/C atomic ratios than those measured for powders [1]. In another study, the influence of the morphology on the degree of functionalization was shown [2]. As expected, a higher degree of functionalization was detected for smaller GNPs. The functionalization was located at the outermost surfaces of the GNPs by comparing experiments using photoelectron with soft (Al Kα, 1.486 keV) and hard X-rays (Cr Kα, 5.405 keV). Therefore, it is important for those using GNPs to understand both the physical and chemical properties of these particles, when considering their use in different applications.

The next step for reliable characterization protocols was the realization of an interlaboratory comparison under the auspices of VAMAS (Versailles Project on Advanced Materials and Standards) with 22 participating laboratories from all over the world. Samples of oxygen-, nitrogen-, and fluorine- functionalized GNPs were provided to the participants along with a measurement protocol. Participants were asked to prepare the samples as powders on a tape, powders in a sample holder recess, or as pellets. The lower measured O/C ratio reported for pelletized samples [1] was confirmed. The lowest scattering of the results was observed for the powders measured in the recess (Fig. 1). Furthermore, an influence of the humidity on the results was observed.

Acknowledgement

We acknowledge all participants of the VAMAS interlaboratory comparison for their contribution, Haydale Ltd. for providing the samples, and financial funding from the EMPIR programme for the project ISO-G-Scope (Grant agreement no. 19NRM04)

Selected references

[1] B.P. Reed, S. Marchesini, G. Chemello et al., *Carbon* **211** (2023) 118054
[2] G. Chemello, X. Knigge, D. Ciornii et al., *Adv. Mater. Interfaces* **10** (2023) 2300166

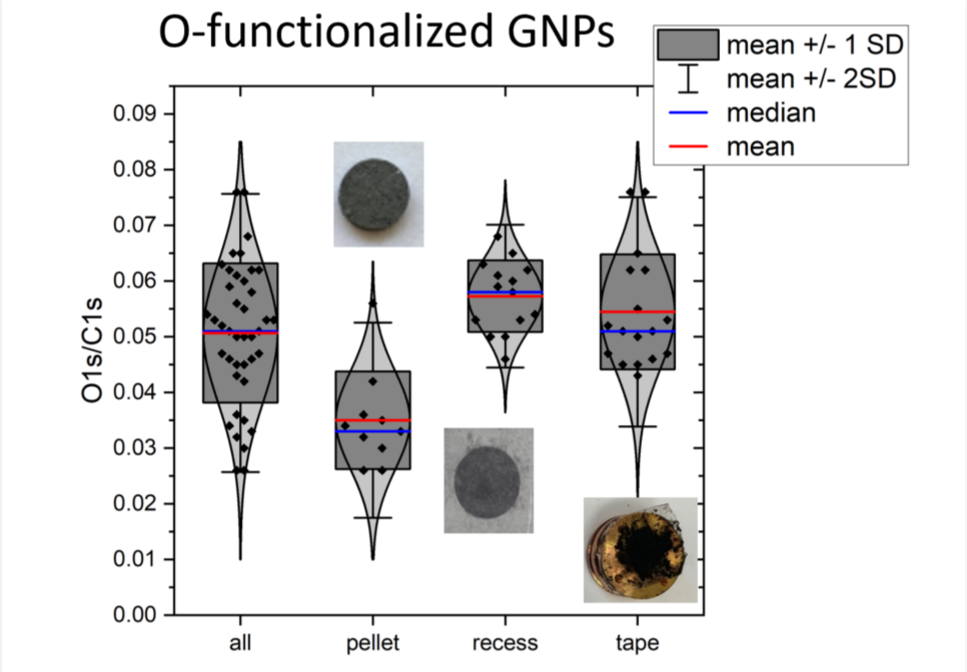

Fig. 1: Differences in the O/C ratio for oxygen-funtionalized grahphene depending on different sample preparation methods.

O23 - Steel surface engineering by non-oxidising wet quenching

3. CAT – Catalysis and Surface Functionalization

Erdni Batyrev[1]
Peter Beentjes[1], Cornelia Ionescu[1], Sebastien Lemaire[2], Xavier Cluzel[2]
[1] Tata Steel Europe
[2] Fives Stein

The effect of 4% formic acid solution treatment on the steel surface after the annealing prior to dipping into the Zn bath, according to the wet quenching concept proposed by Fives Stein, was accessed experimentally. The experiments were done on an ultra-low carbon steel to better understand the reaction of steel with the solution prior to continue with ultra-high strength steel of highly alloyed compositions as an ultimate goal.

A thin native Fe_2O_3 oxide layer is reduced to metallic in the range of 430-450 °C in UHV of 10^{-8} mbar (required strip temperature before entering the Zn bath) while Mn is diffusing outwards where it is also taking part in reducing Fe_2O_3 since its higher affinity to oxygen.

The metallic iron surface reacts with acid first at 23 °C to form a formate film that apparently prevents growth of oxide thickness since metallic iron dominates in XPS spectrum of Fe 2p while a limited iron oxidation is taking place confirmed by smaller Fe_2O_3 contribution. Another, beneficial to Zn wetting, effect of acid treatment is that the formed MnO is reasonably fast (within 1 min) dissolved in the acid and therefore effectively removed from the steel surface.

Interestingly that the wet quenching with 4% formic acid solution at higher surface temperature (>150 °C) leaves only metallic iron, which might be explained by a complete coverage of the steel surface by the formate layer thanks to higher rate of acid-iron reaction at 150 °C than at 23 °C. Moreover there is less formate left on the steel surface as compared to 23 °C confirmed by XPS in O 1s and C 1s spectra. This is a clear indication that only the formic acid molecules that reacted with iron are left on the surface (as formate) due to the stronger bonding while the weakly bonded groups are already desorbed at this temperature.

The Leidenfrost effect at elevated temperatures facilitates the reaction of acid molecules with the steel surface prior to the reaction of water with steel.

Another advantage of having the formate layer instead of the oxides is that it is already removed by heating above 150 °C prior to the galvanising in diluted $5\%H_2/N_2$ atmosphere of the pre-heating oven, the strip temperature is set to 450 °C since the strip needs to be at this temperature before entering the Zn bath.

O24 - Surface Modification of Aged CuO Nanopowders as guided by XPS

3. CAT – Catalysis and Surface Functionalization

Anastasia Batenkova[1, 2]
Bastian Rheingans[1], Maksym Kovalenko[2, 3], Lars P.H. Jeurgens[1]
[1] Empa, Laboratory for Joining Technologies and Corrosion, Switzerland
[2] ETH Zürich, Department of Chemistry and Applied Biosciences, Switzerland
[3] Empa, Laboratory for Thin Films and Photovoltaics, Switzerland

CuO nanoparticles (NPs) possess large potential for diverse applications, including heterogeneous catalysis, energy conversion, magnetic storage, printable electronics, gas sensors, nano-joining, and reactive joining. However, due to the high reactivity of the CuO NPs surface with the surrounding atmosphere, the chemical surface state during storage can be severely altered. This means that CuO nanopowders exhibit continuous and non-uniform changes of their surface chemistry during aging, which can cause unpredictable and irreproducible functional surface properties upon processing (e.g. dispersing or sintering). To study these changes, in a first step, the changes in the chemical surface states of commercial CuO nanopowders during aging under inert and ambient conditions were investigated by detailed XPS analysis of the C 1s, O 1s and Cu 2p photoelectron spectra (see Fig. 1). Next, various mild surface treatments, including washing, synthetic air-annealing at different temperatures and ozone exposure, were performed in an attempt to restore the surface chemistry of the aged CuO nanopowders, independent of their aging conditions. These surface treatments allow targeted modifications of the surface coverage by different types of surface species (e.g. C-OH, C-O-C, C-O, O-C=O), as well as of the CuO surface stoichiometry. Practical guidelines are provided to restore or modify the initial chemical surface state of aged CuO nanopowders for specific applications based on well-defined surface treatments.

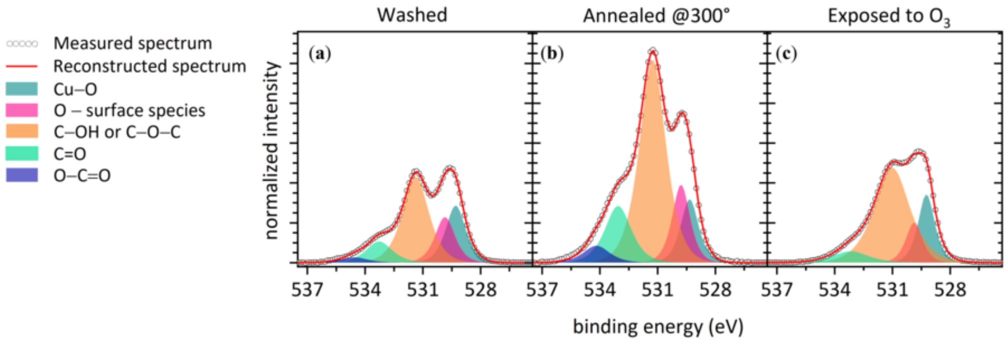

Fig. 1. Measured O 1s XPS spectra of treated CuO NPs (Sigma Aldrich): (a) washed with miliQ water and ethanol; (b) washed, aged in air, and an-nealed at 300 °C; (c) washed, aged in air, and exposed to ozone. The XPS analysis indicates a change mainly in the carbon species on the CuO sur-face after applying different treatments.

O25 - Surface reactivity of cerium oxides thin films

3. CAT – Catalysis and Surface Functionalization

Clémence Thomas[1, 2]
Thomas Gouder[3], Olivier Politano[2], Lionel Jolly[1], Brice Ravat[1], Ioana Popa[2]
[1] CEA - Centre de Valduc, 21120 Is sur Tille, France
[2] ICB UMR 6303 CNRS University of Bourgogne, 9 avenue Savary, 21078 Dijon cedex, France
[3] JRC, European Commission, Eggenstein-Leopoldshafen, 76344, Germany

The purpose of this work is to study the surface reactivity of cerium oxides (CeO_2, CeO_{2-x} and Ce_2O_3) by using experimental and theoretical approaches. Experimentally, homogeneous thin films of both oxides were prepared and analyzed *in-situ* at the so-called «LabStation» at JRC Karlsruhe.

A technique of PVD was used to create surfaces of interest by applying an ECR (Electron Cyclotron Resonance) plasma source under fixed O_2 pressure. Polycrystalline surfaces were produced. The Ce^{3+}/Ce^{4+} ratio in the thin film and at the surface was checked by XPS. The as-prepared surfaces are exposed to H_2O and H_2 and their plasma (increasing the reactivity of species thanks to the production of $OH^{\cdot}$, OH^-, $H^{\cdot}$, H^-, H_2O_2), at different temperatures: from -150°C to 200°C. The nature of the surface, as Ce oxidation state and chemisorbed species are characterized using UPS.

Results show clearly the effect of surface defects on the reactivity of CeO_2 under H_2O, H_2 molecular and plasma. Adsoprtion and/or formation of H_2O and OH^- on perfect CeO_2 surface is extremely lower than on CeO_2 showing top surface defects. This difference of reactivity is observed even during hydrogen plasma exposures at given pressure and temperature. Moreover, a technic to create Ce_2O_3 thin films and the reactivity of this surface will be presented.

To better understand reactivity mechanisms, this experimental study is coupled with Molecular Dynamics (MD) simulations. (111), (110) and (100) CeO_2 and Ce_2O_3 surfaces were modelled and exposed to H_2O and H_2 molecules. The surfaces are perfect or include oxygen vacancies. The results have highlighted different mechanisms of adsorption, dissociation and recombination of these species.

The experimental data used in this research were generated through access to the ActUsLab/PAMEC under the Framework of access to the Joint Research Centre Physical Research Infrastructures of the European Commission (CESAR, Research Infrastructure Access Agreement N°36619/03).

O26 - The competition of CO oxy-chlorination and oxidation

3. CAT – Catalysis and Surface Functionalization

Shaoliang Guan[1]
Philip R Davies[2], David J Morgan[2], David J Willock[2], David Lennon[3], Giovanni E Rossi[3]
[1] University of Cambridge
[2] Cardiff University
[3] University of Glasgow

Introduction

With the rapidly increasing demand for polyurethanes and polycarbonates, more elemental chlorine (Cl_2) or phosgene ($COCl_2$) is consumed.[1] This results in substantial quantities of a hydrogen chloride (HCl) waste stream. The Deacon process is a sustainable way to recover chlorine by oxidizing HCl with molecular oxygen.[2] However, at present, the main industrial Cl_2 production method is still the electrolysis of aqueous solution of sodium chloride. The oxy-chlorination of CO using copper catalysts, which involves the Deacon process, to produce phosgene provides the opportunity for the expanding isocyanate manufacturing industry to minimise the large quantities of HCl waste stream currently generated.[3,4]

Outline

When CO reacted with the $CuCl_2$ catalyst as-received from industry, only CO_2 was formed. However, after pre-treating the $CuCl_2$ catalyst with Cl_2, $COCl_2$ was discovered with FT-IR. Meanwhile, the yield of CO_2 decreased. Both CO_2 and $COCl_2$ formation were observed decreasing with time, indicating the deactivation of the catalyst. XAFS of copper K edge shows the transformation from Cu^{2+} to Cu^{+}. However, this technique couldn't provide precise information of the surface change of the catalyst. XPS plays a key role in this reaction and proves that the surface Cu species is totally transformed to Cu^{+}, which is catalytically inactive.[5]

Figure 1 shows a series of XPS spectra of a type of $CuCl_2$ industrial catalyst undergoing temperature ramping and reacting with CO. The transformation from Cu^{2+} to Cu^{+} indicates complete reduction of copper species on the surface of the catalyst. This proves the deactivation of the catalyst seen in an oxy-chlorination process of CO catalysed by $CuCl_2$ catalyst.[5]

It was discovered that there's a competition between CO_2 and $COCl_2$ formation. And the pre-treatment will help increase the latter one whilst suppress the former one.

Selected references

1. T.A. Ryan et. al., Phosgene and Related Carbonyl Halides, Elsevier, Amsterdam, 1996.
2. H. Deacon, US Patent 016802, 1875.
3. C. Lamberti et.al., Angew. Chem., 2002, **114**, 2447.
4. S. Guan et.al., Faraday Discussions, 2018, **208**, 67.
5. 5. S. Guan et.al., Faraday Discussions, 2021, **229**, 318.

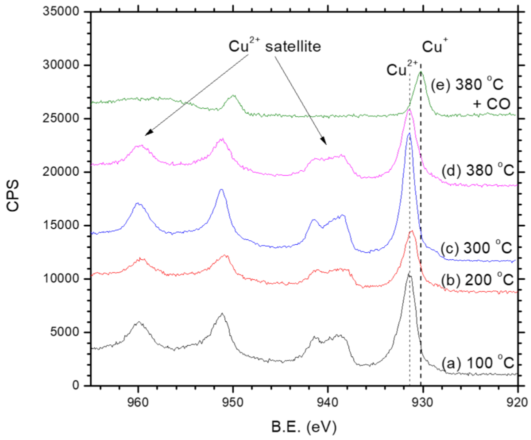

Fig.1 XPS spectra of CuCl2 at different

temperatures before and after reacting with CO

O27 - The use of surface characterization techniques in phosphor materials

3. CAT – Catalysis and Surface Functionalization

Hendrik C Swart[1]
Elizabeth Coetsee-Hugo[1], JJ Terblans[1]
[1] University of the Free State

Surface characterization and optical characterization techniques play a vital role in the complete understanding of the luminescent properties of phosphor nanomaterials. Auger electron spectroscopy (AES), X-ray photo electron spectroscopy (XPS), time of flight scanning ion mass spectrometry (TOF SIMS), Photoluminescence (PL) and cathodoluminescence (CL) are used to characterize different phosphor materials. The crystal field that is determined by the environment in the host material in combination with the various dopant ions with the correct valence state can be used to obtain emissions from the Ultraviolet (UV) to the infra-red (IR) wavelength ranges. Phosphor materials have been successfully used to improve the efficiency of various applications. Nanoparticles both undoped and doped with different rare earth elements were synthesized by several synthesized techniques. The defects incorporated into the bulk material play an important role in the emission efficiency and colour scheme. XPS in combination with PL can be used to identify some of these defects in the material. Degradation of the different phosphors during prolonged electron/photon bombardment also played a vital role in their possible applications. The combination of CL, PL, AES and XPS techniques helps to determine the mechanisms behind the degradation. A small number of impurities in the chemicals used during synthesis can play a large role in the final emission intensity and colour of the phosphor materials. TOF SIMS can point out these impurities. Examples of different phosphor materials with different applications such as Solid-State Lighting will be shown.

Keywords: Surface characterization, phosphors, luminescence materials, degradation, defects

Acknowledgement
The author is highly thankful for the support provided by the South Africa Research Chair Initiative of the Department of Science and Technology (No. 84415), extending financial support from the University of the Free State to carry out the research work.

O28 - Ultrafast surface hydrophilicity transition in TiO2/Si, ZnO/Si, and multilayer heterojunctions

3. CAT – Catalysis and Surface functionalization

Rucha Deshpande[1]
Jesper Navne[2], Rafael Taboryski[1]
[1] DTU Nanolab, Denmark Technical University2, Kgs. Lyngby, 2800 Denmark
[2] ATLANT 3D

Abstract: Active photocatalytic switching is desired in many applications like photocatalytic water-splitting and fuel cells. They rely on metal oxide (MO_x) wide bandgap materials that can generate electron-hole pairs by absorbing light of frequencies corresponding to UV-visible light. These charge carries can be controlled by the thickness, and substrate of the MO_x film, for which we propose a simple model by testing hydrophobic to hydrophilic wettability switching. [1] We use LEDs based latest light sources that provide pure light compared with traditional Xe lamps and in wide range from UV 365 nm to deep-UV 275 nm. A complete study is carried out considering factors like substrate resistivity, interface layer composition, and crystallinity of the MO_x heterostructure stack.

<u>*Figure:*</u> Study schematic of photoinduced hydrophilicity in MO_x heterostructures. (a) Bandgap analysis of TiO_2/Si heterojunction. (b) Thin films deposited using Atomic Layer Deposition (ALD). (c) Experimental testing of UV-DUV light induced hydrophilicity using Goniometer to record contact angle hysteresis. (d) Reversibility of the photoinduced switching tested for one sample. (e) Example of channel induced switching using mask for application in fluid-based devices. (f) Introduction of multiple interface layers to study the optimal criteria for faster switching. The interface is composed of high bandgap materials SiO_2 and Al_2O_3 of thin (<10 nm) and thick (100 nm) layers. The substrate used is standard Si wafer of resistivity 1-5 and 5-10 Ωcm.

<u>*Results and conclusions:*</u> The study shows that deep-UV light alone makes a 10-fold increase in switching rate from hydrophobic to hydrophilic contact angle in all heterojunctions. The distinct light sources provided by LEDs and availability of precise thickness of thin films, allow for systematic study of diffusion of e-h pairs and its concentrations, which can be verified using photoinduced switching model based on computed physical properties. Based on the model, better interface layering, and crystallinity are verified for enhancement in photoinduced switching. Major implications for MO_x based fluidic applications are foreseen.

<u>*Acknowledgements and funding:*</u> This work was supported by National Grant no. 40692 and 5147 from Villum Foundation schemes Villum Experiment and Villum International Postdoc.

Selected references

[1] R. A. Deshpande, J. Navne, M. V. Adelmark, E. Shkondin, A. Crovetto, O. Hansen, J. Bachmann, and R. Taboryski*, Nature Communications*, **15**, 124 (2024).

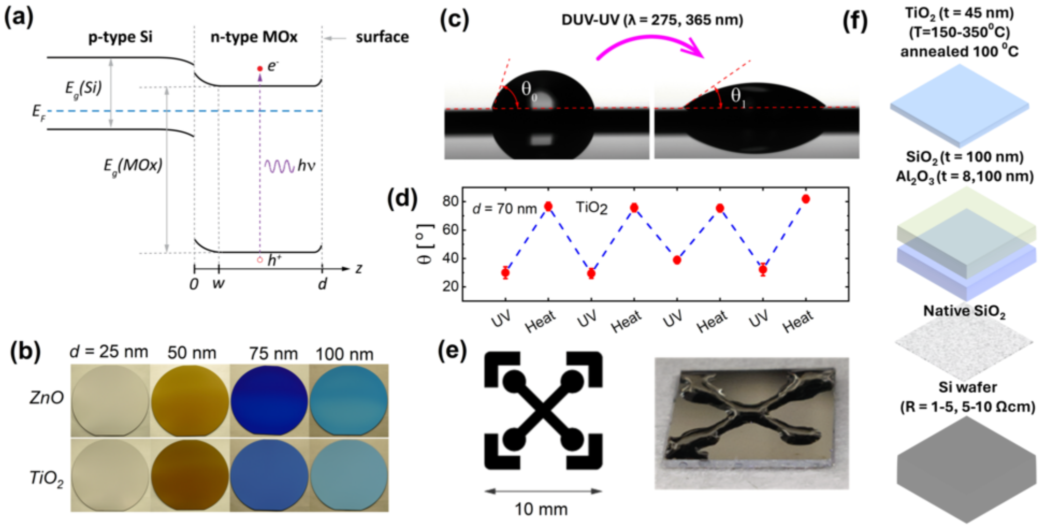
(a)
p-type Si
n-type MOx
surface
$E_g(Si)$
E_F
$E_g(MOx)$
e^-
$h\nu$
h^+
0
w
d
z
(b)
d = 25 nm
50 nm
75 nm
100 nm
ZnO
TiO_2
(c)
DUV-UV (λ = 275, 365 nm)
θ_0
θ_1
(d)
d = 70 nm
TiO2
θ [°]
80
60
40
20
UV
Heat
UV
Heat
UV
Heat
UV
Heat
(e)
10 mm
(f)
TiO_2 (t = 45 nm)
(T=150-350°C)
annealed 100 °C
SiO_2 (t = 100 nm)
Al_2O_3 (t = 8,100 nm)
Native SiO_2
Si wafer
(R = 1-5, 5-10 Ωcm)

O29 - Understanding the enhanced activity of Pd/CeO2 thin films in hydrogen oxidation reaction in alkaline media

3. CAT – Catalysis and Surface Functionalization

Mathilde Luneau[1, 2]
Linnéa Strandberg[2, 3], Gerard Montserrat-Sisó[2, 3], Victor Shokhen[2, 3], Henrik Grönbeck[2, 3], Björn Wickman[2, 3]
[1] Department of Chemistry and Chemical Engineering, Chalmers University of Technology, Gothenburg, SE 41296 (Sweden)
[2] Competence Centre for Catalysis, Chalmers University of Technology, Gothenburg, SE 41296 (Sweden)
[3] Department of Physics, Chalmers University of Technology, Gothenburg, SE 41296 (Sweden)

Introduction

Palladium supported on ceria (Pd/CeO_2) has recently raised strong interest as an alternative catalyst to platinum on the anode electrode in anion exchange membrane fuel cells[1,2]. The enhanced activity of Pd/CeO_2 catalysts for hydrogen oxidation reaction (HOR) activity in alkaline media has notably been attributed to strong metal-support interactions, but the exact mechanism is still under debate. Further understanding is needed to elucidate the role of CeO_2.

In this work, we investigate Pd/CeO_2 thin films with well-defined compositions and structures to gain fundamental understanding of the metal-support interface and its influence on HOR activity in alkaline media. Model thin films have not yet been employed for HOR on Pd/CeO_2 in alkaline media. We develop an approach combining *in situ* electrochemical quartz crystal microbalance (E-QCM), *ex situ* microscopy and spectroscopy, and theoretical calculations to describe the surface interactions between Pd and CeO_2.

Materials and Methods

Pd and Pd/CeO_2 thin films were synthesized via electron-beam physical vapor deposition on quartz crystals (Fig. 1a). Electrochemical activity was studied using cyclic voltammetry (CV) in a standard three-electrode electrochemical cell. Mass changes related to adsorption, absorption, physisorption or desorption phenomena were evaluated *in situ* with E-QCM. The structure and composition of the thin films were probed using scanning electron microscopy (SEM), high-resolution transmission electron microscopy (HRTEM) and x-ray photoelectron spectroscopy (XPS). Density functional theory (DFT) calculations were performed to gain insight into the oxidation state and structure of Pd on prepared Pd/CeO_2 thin films.

Results and Discussion

Pd/CeO_2 leads to expected enhancement of HOR in alkaline media compared to pure Pd (Fig 1b). Using E-QCM, we provide new fundamental understanding of the adsorption, absorption, physisorption and desorption phenomena occurring during HOR. We show that on pure Pd thin films, *absorption* of hydrogen dominates while on Pd/CeO_2 the oxidation/reduction of ceria and *adsorption* of hydroxyl groups are the dominating phenomena (Fig. 1b)[3].

One of the hypotheses for enhanced reactivity of Pd/CeO_2 in HOR is that CeO_2 – at the interface with Pd - serves as a source of OH groups which react with adsorbed H to form water[4]. In this study, we provide new quantitative evidence that this hypothesis is valid. Strong metal-support interactions are also confirmed by TEM, XPS and DFT calculations.

Finally, an important finding is that Pd atoms embedded in CeO_2 are present on the prepared thin films and active for hydrogen activation but are not able to bind CO during CO-stripping characterization.

Selected references

1. K. Singh, E. S. Davydova, J. Douglin, A. O. Godoy, H. Tan, M. Bellini, B. J. Allen, J. Jankovic, H. A. Miller, A. C. Alba-Rubio and D. R. Dekel, *Adv. Funct. Mater.*, 2020, **30**, 2002087.
2. Bellini, M. V. Pagliaro, A. Lenarda, P. Fornasiero, M. Marelli, C. Evangelisti, M. Innocenti, Q. Jia, S. Mukerjee, J. Jankovic, L. Wang, J. R. Varcoe, C. B. Krishnamurthy, I. Grinberg, E. Davydova, D. R. Dekel, H. A. Miller and F. Vizza, *ACS Appl. Energy Mater.*, 2019, **2**, 4999-5008.
3. Luneau, L. Strandberg, G. Montserrat-Sisó, V. Shokhen. R. Mohan, H. Grönbeck, B. Wickman. *J. Mater. Chem. A*, 2023,11, 16370-16382
4. D. Speck, F. S. M. Ali, M. T. Y. Paul, R. K. Singh, T. Böhm, A. Hofer, O. Kasian, S. Thiele, J. Bachmann, D. R. Dekel, T. Kallio and S. Cherevko, *Chem. Mater.*, 2020, 32, 7716-7724.

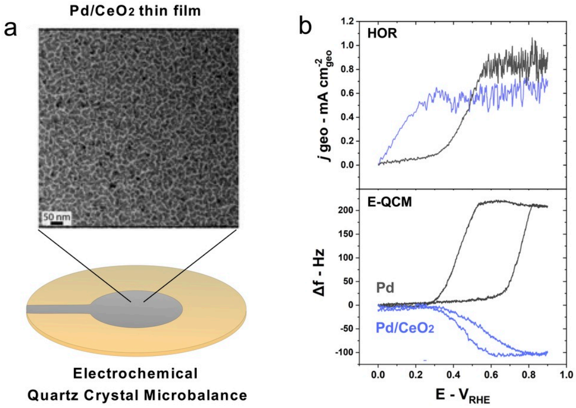

Figure 1. a. Schematic showing the quartz crystal used for in situ electrochemical characterization of thin films using E-QCM and corresponding TEM image of the Pd/CeO_2 thin film. b. E-QCM reveals fundamental differences during HOR on Pd and Pd/CeO_2 as shown by the measured current density during CV (top figure) and simultaneous E-QCM measurements (bottom figure). Reaction conditions: 5 mV.s^{-1} scan rate, H_2-saturated 0.1 M KOH solution.

4. CER – Ceramics; Glass; Oxides

O30 - Barrier heights from XPS without "busting the bank": In-chamber metal deposition on solution-processed zinc-tin oxide

4. CER – Ceramics; Glass; Oxides

Jonas Deuermeier[1]
Carlos Silva[1], Raquel Martins[1], António Dias[1], Afonso Cavaco[1], Rodrigo Martins[1], Asal Kiazadeh[1], Emanuel Carlos[1]
[1] CENIMAT|i3N, Department of Materials Science, School of Science and Technology, NOVA University Lisbon and CEMOP/UNINOVA, 2829-516, Caparica, Portugal

Electronic devices made with amorphous oxide semiconductors (AOS) like indium-gallium-zinc oxide (IGZO) have come a long way. Outperforming silicon in driver transistors of active-matrix displays, they have become a commercial success in flat-screen TVs. To decrease the environmental impact of AOS technology, non-critical raw materials and additive manufacturing are being explored. Sustainable AOS like zinc-tin oxide, printed directly from solution, can be applied in a wide range of electronic devices, from thin-film transistors[1] to diodes and memristors.[2,3]

The electrical performance of Schottky diodes critically depends on the interface properties, which directly influence the barrier height. Usually, in situ metal deposition with precise thickness control is achieved only via costly UHV transfer chambers, connecting the XPS to adequate deposition equipment. An alternative is the use of a common argon sputter gun and a small metal target mounted inside the analysis chamber (see Figure).[4] This contribution shows the applicability of the approach to barrier height measurements and discusses its advantages and shortcomings. The case of solution-processed zinc-tin oxide (ZTO) is examined and compared with electrical data from corresponding diodes.

Selected references

1. Fernandes, C. *et al.* A Sustainable Approach to Flexible Electronics with Zinc-Tin Oxide Thin-Film Transistors. *Adv Electron Mater* **4**, 1800032 (2018).
2. Carlos, E., Branquinho, R., Martins, R., Kiazadeh, A. & Fortunato, E. Recent Progress in Solution-Based Metal Oxide Resistive Switching Devices. *Advanced Materials* **33**, 2004328 (2021).
3. Silva, C. *et al.* Perspective: Zinc-Tin Oxide Based Memristors for Sustainable and Flexible In-Memory Computing Edge Devices. *Adv Electron Mater* **9**, 2300286 (2023).
4. Wenzel, S., Leichtweiss, T., Krüger, D., Sann, J. & Janek, J. Interphase formation on lithium solid electrolytes - An in situ approach to study interfacial reactions by photoelectron spectroscopy. *Solid State Ion* **278**, 98–105 (2015).

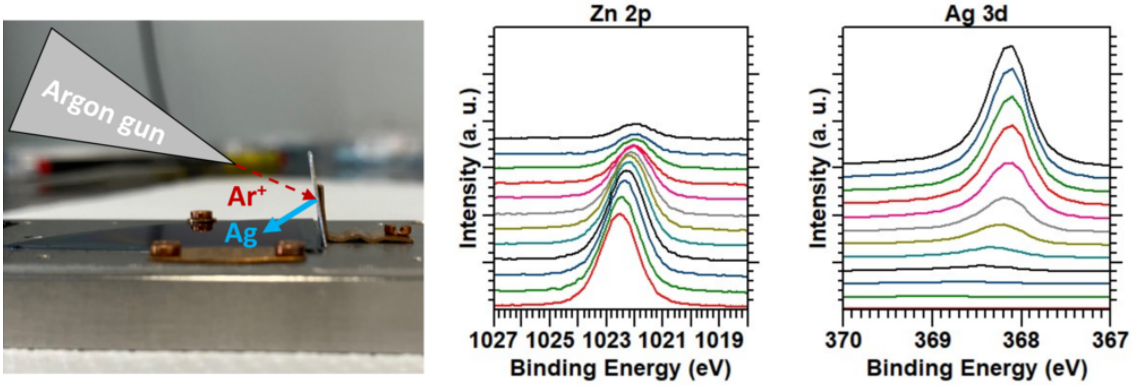
Argon gun
Ar+
Ag
Zn 2p
Intensity (a. u.)
1027 1025 1023 1021 1019
Binding Energy (eV)
Ag 3d
Intensity (a. u.)
370 369 368 367
Binding Energy (eV)

O31 - Influence of dopant ion size and valence on CeO2 properties

4. CER – Ceramics; Glass; Oxides

Tamara Petkova[1]
Elefteria Lefterova[1], Nevena Bozhanova[1], Vania Ilcheva[1], Victor Boev[1], Kolyo Kolev[1], Denitsa Nicheva[1]
[1] Institute of Electrochemistry and Energy Systems, Bulgarian Academy of Sciences, Acad. G. Bonchev str., bl.10, Sofia, Bulgaria

The effect of adding rare earth elements such as samarium and gadolinium on the structure of cerium dioxide has been a subject of scientific inquiry due to the potential applications of these materials in various fields, including catalysis, solid oxide fuel cells, and hydrogen storage.

Studies have shown that incorporating Sm and Gd into the CeO2 lattice can lead to modifications in its structural and chemical properties. One significant impact is the stabilization of the fluorite structure of CeO2. The addition of Sm and Gd ions can suppress the phase transition from the fluorite structure to other phases, such as the monoclinic or tetragonal phases, thus enhancing the thermal stability of CeO_2.

The ionic radius plays a significant role in determining the solid solutions CeO2 and gadolinium and samarium. In the case of CeO2 solid solutions with Gd and Sm, the ionic radii of the substituting ions (Gd3+ and Sm3+) should closely match the ionic radius of the Ce^{4+} ions in the CeO2 lattice to maintain structural integrity. If the ionic radius of the substituting ion deviates too much from that of Ce^{4+}, it can lead to lattice distortion, defects, or even phase separation, affecting the properties of the solid solution.

Furthermore, the presence of Sm and Gd dopants can influence the oxygen vacancy formation and migration properties in CeO2. These dopants can act as charge compensators for oxygen vacancies, affecting the oxygen storage capacity and oxygen ion conductivity of the material. This phenomenon has implications for applications such as oxygen sensors and solid oxide fuel cells, where oxygen transport properties are crucial.

Additionally, Sm and Gd doping can alter the surface properties of CeO2, affecting its interaction with other materials in catalytic processes. The presence of these dopants can modify the surface chemistry and create active sites for catalytic reactions, thereby enhancing the catalytic performance of CeO_2-based materials.

The aim of the present work is to understand the mechanisms underlying these effects and to optimize the properties of doped CeO2 materials for specific applications.

Acknowledgements: The authors appreciate the financial support of the Bulgarian National Science Fund under contract КП 06-H59/13. The study has been carried out using facilities of ESHER funded by the Ministry of Education and Science.

O32 - Thin film deposition of tin and zinc oxide for positional photodetectors

4. CER – Ceramics; Glass; Oxides

Plamen Petkov[1]
Tamara Petkova[2], Veselin Zhelev[2], Pavlina Bancheva[1]
[1] Department of Physics, University of Chemical Technology and Metallurgy, Sofia, Bulgaria
[2] Institute of Electrochemistry and Energy Systems, Bulgarian Academy of Sciences, Sofia, Bulgaria

Metal oxides such as SnO2 and ZnO exhibit n-type semiconductor characteristics, boasting unique properties including high transmission within the visible spectrum, notable reflectance in the infrared range, and elevated electrical conductivity. These properties are significantly influenced by factors such as stoichiometry deviation, oxygen deficiency, and impurity nature. Transparent conducting thin films composed of tin oxide find widespread utility across various applications, serving as transparent electrodes in solar cells, photovoltaic devices, IR windows, and sensors.

The primary objective of this study was to fabricate thin films of tin oxide and zinc oxide through spray pyrolysis and investigate the impact of technological parameters and dopants on their electrical and optical properties. The aim was to assess the feasibility of employing these films in position-sensitive photodetectors.

Characterization of the films was conducted to elucidate their structural properties using techniques such as X-ray diffraction (XRD) and X-ray photoelectron spectroscopy (XPS). Additionally, the microstructure was analyzed via atomic force microscopy (AFM), while surface morphology was examined using scanning electron microscopy (SEM).

The behavior of the films was explored to gauge their suitability for various applications. Optical transmission and reflection properties were investigated using UV-VIS spectroscopy, while Hall Effect measurements were employed to assess electrical properties. Furthermore, the electronic structure of the layers was probed via photoluminescence spectroscopy. Samples with varying thicknesses were utilized to delineate the influence of layer thickness on their structure and properties.

Finally, the sandwich structure fabricated from the studied layers was evaluated for its potential application in position-sensitive configurations.

Acknowledgements: This study is funded by the European Union- Next Generation EU, through the National Recovery and Resilience Plan of the Republic of Bulgaria, project № BG-RRP-2.004-0002,"BiOrgaMCT"

5. COR – Corrosion

O33 - Contribution of imaging X-ray photoelectron spectroscopy (XPS) to characterize corrosion mechanism of chrome free layer

5. COR – Corrosion

Vincent Fernandez[1]
Eva Ros[1], Neal Fairley[2], Bernard Humbert[1], Maria Caldes[1]
[1] Nantes Université, CNRS, Institut des Matériaux de Nantes Jean Rouxel, IMN, F-44000 Nantes, France
[2] Casa Software Ltd, Bay House, 5 Grosvenor Terrace, Teignmouth, Devon TQ14 8NE, United Kingdom

To protect metal from corrosion, passivation layer are widely used in food-packaging industry. Those nanometric protections create a thin oxide nanolayer on the tinplate surface, making it less oxidisable. Common passivation are composed by chromium oxide[1] , using hexavalent chromium as a reagent and reducing it. However, because of the toxicity of Cr(VI), European Union is gradually forbidding its use.

Chromium Free Passivation Alternative is based on transition metal oxides (Sn, Ti, Zr, Mn) and polymers. Passivated tinplate presents some roughness in a few microns range as it has been observed by Atomic Force Microscopy. Corrosion-inducing experimenthave been performed, using acidic (acetic acid), salted (NaCl) and sulfured ($Na_2S_2O_5$) aqueous-based solution.

After pull-off test on coated passivated tinplate, XPS Imaging[2] [3], [4] was performed on the coating (polymer) side at different binding energies, allowing extraction of spectrum in each pixel over six XPS core level process (O 1s, Sn 3d, Ti 2p, N 1s, C 1s and S 2s). In this study it was possible to measure in XPS imagering different chemicals state of carbone and sulphur using CasaXPS. Moreover, this study shows an anti-correlation between atomic concentration of Tin and Sulphate Fig(1).Finally, quantification of 2 sulphur chemical state was possible with an average amountbellow 1 per thousand. These results bring useful informations to understand corrosion mecanisms.

Selected references

[1] R. Sandenbergh, M. Biermann, and T. von Moltke, ‘Surface Analytical Characterization of Chromium Passivation on Tinplate’, in *Passivation of Metals and Semiconductors, and Properties of Thin Oxide Layers*, P. Marcus and V. Maurice, Eds., Amsterdam: Elsevier Science, 2006, pp. 143–148. doi: 10.1016/B978-044452224-5/50024-X.
[2] J. Walton and N. Fairley, ‘Characterisation of the Kratos Axis Ultra with spherical mirror analyser for XPS imaging’, *Surface and Interface Analysis*, vol. 38, no. 8, pp. 1230–1235, Aug. 2006, doi: 10.1002/sia.2381.
[3] R. Ettouri *et al.*, ‘Combined analysis methods for investigating titanium and nickel surface contamination after plasma deep etching’, *Surface and Interface Analysis*, vol. 54, no. 2, pp. 134–147, Feb. 2022, doi: 10.1002/sia.7030.
[4] W. E. S. Unger *et al.*, ‘Summary of ISO/TC 201 International Standard ISO 18516:2019 Surface chemical analysis—Determination of lateral resolution and sharpness in beam-based methods with a range from nanometres to micrometres and its implementation for imaging laboratory X-ray photoelectron spectrometers (XPS)’, *Surface and Interface Analysis*, vol. 54, no. 4, pp. 320–327, Apr. 2022, doi: 10.1002/sia.7025.

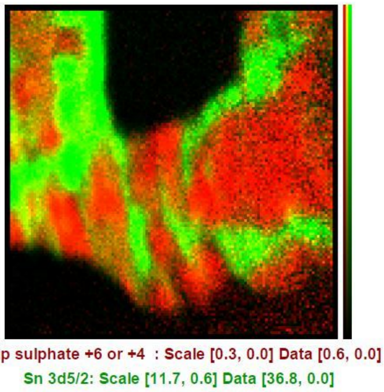

Figure 1. Overlay of Sn 3d and S 2p Sulphate +6 and or + 4 atomic concentration. The concentration of Tin is in red is between 0 and 36.8 percent and 0.6 represent 20% low concentration and 11.7 represent 80% high concentration and the atomic concentration of S Sulphate in red green is between 0 and 0.6 percent with an 20% 80% of 0.0 – 0.3

O34 - Full energy range examination of NiCrFeVCuTi high entropy oxide using XPS, HAXPES and UPS-LEIPS

5. COR – Corrosion

Hsun-Yun Chang[1]
Chia-Jou Lin[2], Wei-Chun Lin[2], Shin-ichi Iida[1]
[1] ULVAC-PHI, Inc., Japan
[2] Department of Photonics, National Sun Yat-sen University, Taiwan

High entropy materials are known to be composed of five or more elements with concentration commonly in equal or near-equal atomic percent. It has been reported that high entropy materials have the properties of greater fracture resistance, tensile strength and corrosion resistance than conventional alloys. High entropy materials with various components are developed aiming to strengthen the desirable mechanical or other properties for industrial applications. For instance, the ZrTaTiNbSi high entropy material was reported to have remarkable glass-forming ability because it can maintain its amorphous structure even after annealing at 1173 K. The face-centered cubic phase of AlCoCrFeNi was reported to have noble corrosion potential than the body-centered cubic phase one. Enhancing the corrosion resistance of high entropy materials is always considered a top priority. Research has shown that as the entropy increases due to the incorporation of a greater number of elements in the alloy composition, high entropy materials exhibit a stable solid solution phase, devoid of intermetallic phases. The random arrangement of multiple elements results in a particular locally disordered chemical environment, which leads to unique corrosion resistance properties. The information of surface variation during corrosion is the key to studying the mechanism of high entropy materials against corrosion. In this work, surface techniques, XPS, HAXPES and UPS-LEIPS, are utilized to examine the surface of NiCrFeVCuTi high entropy materials. XPS provides the chemical state composition of the outmost surface up to approximately 10 nm, while non-destructive HAXPES enables the investigation of deeper depths, reaching around 30 nm. Moreover, HAXPES provides more information regarding core level photoelectron compared to the XPS. In addition, the energy band diagram from UPS-LEIPS analysis provides insight into surface electronic properties. By leveraging the comprehensive energy range, from the conduction band with LEIPS to the core level excitation with HAXPES, the surface analysis of NiCrFeVCuTi before and after sulfuric acid treatment enables the examination of corrosion behaviors in high entropy materials.

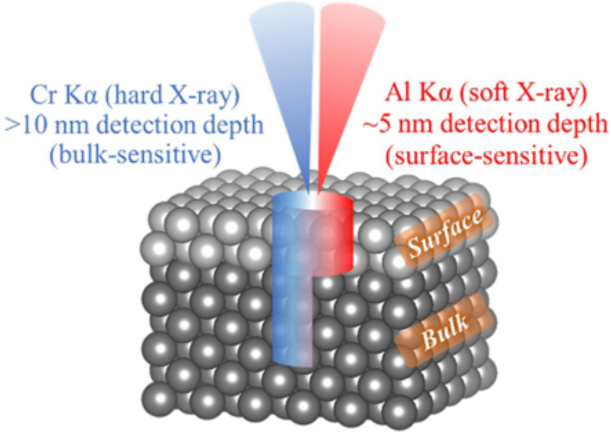

O35 - The interplay of transpassive dissolution and oxygen evolution on multi-principal element alloys (MPEAs)

5. COR – Corrosion

Annica Wetzel[1]
Yasemin Yesilcicek[1], Julia Witt[1], **Özlem Özcan Sandikcioglu**[1]
[1] Federal Institute for Materials Research and Testing (BAM)

Multi-principal element alloys (MPEAs) are of great academic and industrial interest as emerging materials for engineering applications as well as potential electrode materials in energy conversion and storage. Several MPEAs have been studied for their general corrosion behavior, but studies on their dissolution in the high anodic "transpassive" potentials relevant for oxygen evolution reaction (OER) and local corrosion behavior remained scarce.

In this project we have investigated CrMnFeCoNi, FeCrNi and CrCoNi MPEAs in terms of their transpassive behavior in NaCl electrolytes and artificial seawater [1, 2]. We introduced a characterization procedure to distinguish the individual contributions of oxygen evolution reaction (OER) and alloy dissolution [2]. This scheme utilizes scanning electrochemical microscopy (SECM) for detecting the onset of OER and employs quantitative chemical analysis methods, namely inductively coupled mass spectrometry (ICP-MS) and ultraviolet-visible light (UV-Vis) spectroscopy, to elucidate the processes of metal dissolution. In-situ atomic force microscopy (AFM) and scanning Kelvin probe force microscopy (SKPFM) were used to analyze the corrosion morphology and surface potentials before, during, and after passivity breakdown.

Our results clearly demonstrate the superior corrosion behavior of CrCoNi and FeCrNi MPEAs in comparison to the CrFeMnCoNi HEA, as well as AISI 304 stainless steel. We have observed that significant OER occurs in parallel with metal dissolution on the CrCoNi and FeCrNi MPEA surfaces during anodic polarization at potentials relevant to water electrolysis. Most importantly, our findings underscore the necessity of analyzing metal ions dissolved into the electrolyte to accurately assess the Faradaic efficiencies of non-noble metal OER electrocatalysts. The presentation will summarize our characterization procedure and give an overview on the key properties of the studied MPEAs.

Selected references

[1] A. Wetzel, M. von der Au, P.M. Dietrich, J. Radnik, O. Ozcan, J. Witt, The comparison of the corrosion behavior of the CrCoNi medium entropy alloy and CrMnFeCoNi high entropy alloy, Appl. Surf. Sci., 601 (2022) 154171.
[2] A. Wetzel, D. Morell, M. von der Au, G. Wittstock, O. Ozcan, J. Witt, Transpassive Metal Dissolution vs. Oxygen Evolution Reaction: Implication for Alloy Stability and Electrocatalysis, Angew. Chem. Int. Ed. Engl. (2024) e202317058.

6. DAT – Data analysis and Metrology

O36 - Advanced characterization of GaN-based compounds by XPS: a new process of nitrogen and gallium content extraction

6. DAT – Data analysis and Metrology

Kirène Gaffar[1]
Solène Béchu[1], Romain Jouanneaud[2], Guillaume Monier[2], Christine Robert-Goumet[2], Muriel Bouttemy[1]
[1] Institut Lavoisier de Versailles, UVSQ, Université Paris-Saclay, CNRS, UMR 8180, 45 avenue des Etats-Unis, 78035 Versailles CEDEX, France
[2] Institut Pascal, Université Clermont Auvergne, UMR CNRS 6602, Clermont-Ferrand, France

Thanks to its unique combination of high band gap and high breakdown field, GaN-based high-electron-mobility transistors (HEMT) have become one of the prime candidates for high-frequency and power applications [1]. Despite the remarkable progress in performance, interface traps in HEMT devices are still the origin of undesirable effects such as RF dispersion, gate/drain lag, or low electron confinement [2] which need to be understood to improve the overall electrical response and long-term reliability. To answer this issue, the assessment of the chemistry of the constitutive layers and of interfaces is a key point. In the present case, we focus on the implementation of XPS (X-ray Photoelectron Spectroscopy) with two challenges to overcome: the unfortunate overlap between Ga $L_2M_{4.5}M_{4.5}$ transition (~395 eV) and nitrogen N 1s photopeak (~398 eV) encountered while using the conventional Al k-alpha source and passivation layers or barriers thicknesses which can be thinner than the XPS probed depth (~10 nm) requiring specific analysis and data treatment procedures [3]. Thus, access to an accurate quantification and chemical state analysis of the HEMT structure is not straightforward and can end up with erroneous information. Here, we propose an innovative fitting procedure based on the nonlinear decomposition of gallium-based references to separate the gallium and nitrogen contributions in GaN based-materials by modeling Ga $L_2M_{4.5}M_{4.5}$ and Ga $L_3M_{4.5}M_{4.5}$ X-AES transitions to extract the Nitrogen photopeak. The originality lies in using the higher energy Auger line to fix the right fitting parameters on the lower energy transition where the nitrogen and gallium overlap. As experimental conditions during the sample preparation process could be limited with possible exposure to air resulting in oxidized surfaces, gallium oxide chemical environment has also been considered. To reach buried interfaces, modifications induced by Ar^+ sputtering during depth profile have been studied for developing a strong and universal methodology for processing XPS data of GaN components. The fitting parameters for the N1s-Ga $L_2M_{4.5}M_{4.5}$ region have been processed for each reference sample and combined to have a complete decomposition of an N 1s-Ga $L_3M_{4.5}M_{4.5}$ spectrum. This methodology will be a powerful tool to investigate the in-depth chemistry of HEMTs and especially to perform nano-Auger on device cross-section as the upstream XPS study on reference samples is necessary to calibrate Auger Relative Sensitivity Factors (RSF) for each constitutive layer of HEMT structure for precise quantification.

Selected references

[1] F. Medjdoub et al., "Can InAlN/GaN be an alternative to high power / high temperature AlGaN/GaN devices?" 2006 International Electron Devices Meeting, San Francisco, CA, USA,2006.
[2] Vigneshwara Raja, P., Nallatamby, J.-C., DasGupta, N. & DasGupta, A. Trapping effects on AlGaN/GaN HEMT characteristics. *Solid. State. Electron.* 176, 107929 (2021)
[3] Bourlier, Y. and al. In-depth analysis of InAlN/GaN HEMT heterostructure after annealing using angle-resolved X-ray photoelectron spectroscopy. Surf. Interface Anal. 2020.

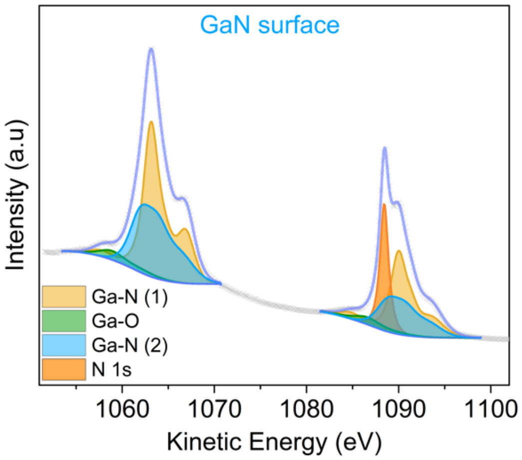

Figure 1. Decomposition of Ga LMM/N 1s region for an accurate quantification of GaN-based materials

O37 - Combination of SIMS and machine learning as a screening technique in an industrial context

6. DAT – Data analysis and Metrology

Danica Heller-Krippendorf[1]
Jan Tröger[1, 2], Elke Tallarek[1], Birgit Hagenhoff[1]
[1] Tascon GmbH, Mendelstr. 17, 48149 Muenster, Germany
[2] University of Muenster, Wilhelm-Klemm-Str. 10, 48149 Muenster

In an industrial context but also e.g. in forensic analysis, samples often have an unknown composition. In the analysis of samples showing “good” and “bad” behaviour, minor variations in surface composition can cause such differences. Consequently, an identification of such compositional differences is required.

In this context, ToF-SIMS is a powerful and well-established screening technique: the surface composition of organic and inorganic molecules can simultaneously be analysed with high sensitivity. In addition, different analysis modes enable a good lateral and/or high depth resolution. Nowadays, ToF-SIMS instruments are highly automated. As a result, complex and meaningful data sets can be easily achieved at short time scales containing Gigabytes of data.

However, the data analysis of such huge data sets can be challenging. As a rule of thumb in an industrial context, one day of data acquisition results in three days of data analysis if performed manually. It therefore does not come as a surprise that multivariate data analysis (MVA) and increasingly machine learning methods techniques (ML) are well sought-after methods to simplify data analysis. Meanwhile many successful studies and applications have been published. It is, however, important to realize that MVA is only a tool for data analysis and does not provide the solution to a tricky analytical problem on its own. The interpretation of the results in the context of the analytical task and the selection of an appropriate model are essential steps to be performed by the analyst. E.g., for samples with an unknown surface composition, it is not sufficient to classify the samples into different groups but it is also necessary to find the differences in chemical composition responsible for the classification, a still challenging task for unsupervised ML approaches.

In this study, different strategies are presented to simplify data interpretation focusing on samples with unknown surface compositions. Samples include, amongst others, SIMS data taken from energy materials. A thorough comparison is performed between manual data analysis and MVA/ML techniques for each sample system. In a next step, both approaches are combined aiming at a comprehensive and efficient interpretation of results from unsupervised ML.

O38 - Combining XPS and HAXPES data to get beneath the surface

6. DAT – Data analysis and Metrology

Benjamen Reed[1]
Alexander Shard[1], Jonathan Counsell[2]
[1] National Physical Laboratory, Hampton Road, Teddington, TW11 0LW, UK
[2] Kratos Analytical Ltd, Trafford Wharf Road, Manchester, M17 1GP, UK

We describe an algorithm to combine X-ray photoelectron spectroscopy data taken from the same sample and elemental line using two different X-ray energies with different sampling depths. The lower energy X-ray data contains information from the surface and the higher energy X-ray data contains the same information plus additional information from the subsurface. Following an appropriate manipulation, we show that it is feasible to extract spectra and compositional information from the subsurface region. The resulting data contains no information from the uppermost atomic layer and is representative of a mean electron escape depth which is the sum of the effective attenuation lengths of electrons from the two sources. The result is largely free from assumptions concerning the sample structure and, unlike angle-resolved analysis, is not influenced by the topography of the sample. To make the best practical use of the algorithm, it is necessary to have homogeneous reference materials that contain the elements of interest in order to determine intensity ratios between the two X-ray sources. The process is simplified if the transmission function of the spectrometer over the full energy range is known and then only one homogeneous reference material, such as silver, can be employed.

We demonstrate the algorithm using Al Kα and Ag Lα radiation using a range of materials and surface layers and show potential applications in reducing the influence of surface contamination for compositional measurements and for mitigating the contribution of ion beam damage after surface cleaning or during depth profiles. The figure illustrates the application of the algorithm to ion-damaged MoS_2 in black using the data acquired from Al Kα (blue) and Ag Lα (red). The signal from the surface damage layer is clearly identifiable and, whilst it contributes the majority of the intensity in the Al Kα data, it is a minor contributor to the extracted subsurface spectrum.

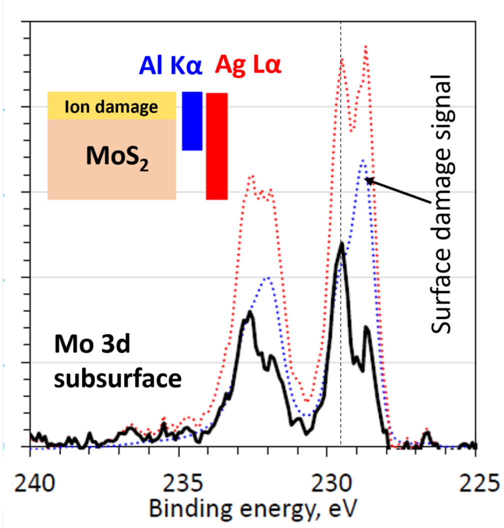

O39 - EnviroMETROS – A novel surface and multilayer thin film analysis tool

6. DAT – Data analysis and Metrology

Paul Dietrich[1]
Francesca Mirabella[1], Andreas Thissen[1]
[1] SPECS Surface Nano Analysis GmbH

The new EnviroMETROS series transforms the realm of surface hybrid metrology by employing the key techniques of parallel detection angle resolved XPS (PARXPS) and multi-wavelength excitation. This method utilizes variable photon energies and emission angles operating under diverse environmental conditions for conducting chemical analyses of thin films and bulk materials. LEIS facilitates high surface sensitivity, while electronic characterization can be enhanced with UPS, IPES, and REELS. Integrated Raman and/or IR spectroscopy provide structural information, whereas XPS mapping and SEM/SAM contribute to elemental surface maps correlated with morphology.

The relevance of ultrathin films and 2D materials in modern devices is continuously increasing, prompting a growing interest in the chemical analysis of these multilayer systems and their surfaces. A thorough characterization of stoichiometries, composition, and depth distribution of elements is crucial. The EnviroMETROS series novel serves as an ideal tool for routine analysis in this research and development field. It combines large sample and wafer handling with a photoelectron spectrometer offering variable information depth. When combined with optical and other analytical techniques, it enables depth-dependent composition analysis with unparalleled precision, reliability, and repeatability.

O40 - In situ determination of indium content in InxGa1-x droplets on GaAs(111)A based on the REELS/XPS complementarity

6. DAT – Data analysis and Metrology

Romain JOUANNEAUD[1]
Guillaume MONIER[1], Luc BIDEUX[1], Philip HOGGAN[1], Christine ROBERT-GOUMET[1]
[1] Université Clermont Auvergne, Clermont Auvergne INP, CNRS, Institut Pascal, F-63000 Clermont-Ferrand, France

Ternary semiconductor nanostructures such as $In_xGa_{1-x}N$ quantum dots are promising materials for a large range of optoelectronic applications such as tuneable wavelength LED, laser diodes and photovoltaic cells or even single-photon emitters. The most relevant challenge for $In_xGa_{1-x}N$ is to vary the indium/gallium content by conserving good crystalline properties and both size and composition homogeneity for the previously quoted applications.

III-V semiconductor quantum dots were firstly grown by a Stranski-Krastanov growth mode based on the lattice mismatch between the epitaxial layer and the substrate. Recently, droplet epitaxy (DE) has emerged as an interesting growth process providing a better control and homogeneity of density, size and composition of quantum dots. First step of the DE is the deposition of group III metallic droplets (Ga, In) on the substrate, followed by the supply of V element (N). Understanding the first stage of droplet epitaxy – the deposition of self-assembled In_xGa_{1-x} droplets – is then an important step for the future growth of $In_xGa_{1-x}N$ quantum dots. For this, a relevant tool to control the composition and the organisation of the deposited atoms is mandatory.

We provide in this talk the complementary use of X-ray Photoelectron Spectroscopy (XPS) and Reflection Electron Energy Loss Spectroscopy (REELS) for the determination *in-situ* of indium/gallium content in self-assembled In_xGa_{1-x} droplets on GaAs(111)A substrate. An XPS intensity model allows to estimate indium/gallium deposited content based on the intensities of Ga3d and In4d core-levels. On the other hand, in REELS, a brand new method of decomposition of the loss probabilities curve obtained from raw experimental spectra is firstly required. Then, based on decomposition for reference spectra (In, Ga) and the development of an envelope method for the substrate, we achieve the resolution of the loss probabilities curve from droplets deposited on semiconducting substrate. Finally, by developing a semi-empirical model of the bulk plasmon energy shift, we can deduct from REELS the indium/gallium content. Comparison of indium/gallium content determined by both XPS and REELS electronic spectroscopies allows to discuss about the In/Ga mixing in the binary droplets for different compositions, leading to promising results for $In_xGa_{1-x}N$ quantum dots grown by droplet epitaxy.

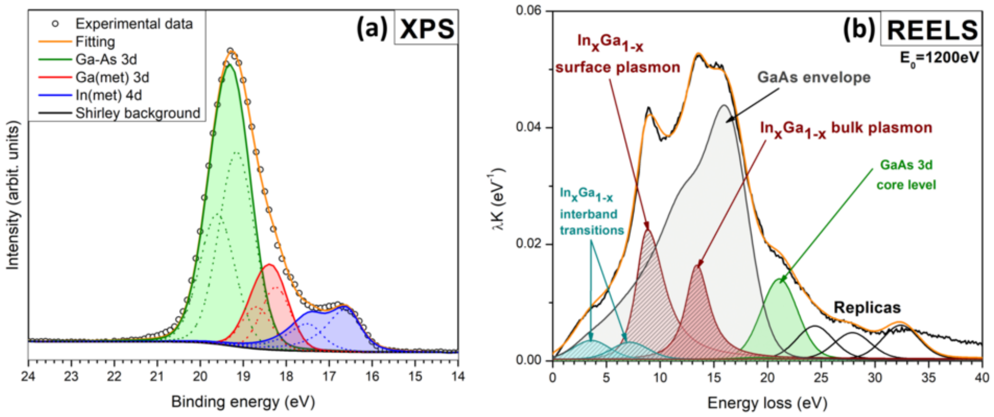

Decomposition of **(a)** XPS spectra and **(b)** REELS loss probabilities curve (E_0=1200eV) for self-assembled In_xGa_{1-x} droplets on GaAs(111)A with unknown x content to be determined. Dashed lines in XPS show the two contributions of spin-orbit splitting.

O41 - New insights into the reduction of ceria morphologies in X-ray photoelectron spectroscopy

6. DAT – Data analysis and Metrology

David Morgan[1, 2]
[1] Cardiff Catalysis Institute, Cardiff University, UK
[2] Harwell XPS Research Complex at Harwell, UK

Given its excellent redox abilities, the use of cerium dioxide (CeO_2, ceria) and related materials in catalysis is widespread[1]. The Ce^{3+}/Ce^{4+} redox shuffle allows for great catalytic ability which can be correlated to the ceria oxidation state[2–4]. Given that catalysis is a surface mediated process, XPS is critical in the analysis of pre- and post-mortem materials.

However, there has been considerable debate on the degree of reduction of CeO_2 caused by XPS analysis. Therefore, in continuation of our work on understanding the reduction of materials,[5] we have investigated different cerium oxide preparations. Through a combination of principal component analysis (PCA), linear algebraic manipulation of spectra (LAMS), and linear least squares (LLS) optimization, it is shown that the degree of reduction and surface speciation is intrinsically linked to the morphology of the ceria which may, at least in part, account for the discrepancies noted in the literature.

Additional evidence to support the incorrect assignment of an O1s peak in the region of 531 – 532 eV as an oxygen vacancy is also given.[6]

Selected references

[1] *Catalysis by Ceria and Related Materials*, 2nd Edition.; Trovarelli, A., Fornasiero, P., Eds.; Imperial College Press: London, 2013.
[2] Smith, L. R.; Sainna, M. A.; Douthwaite, M.; Davies, T. E.; Dummer, N. F.; Willock, D. J.; Knight, D. W.; Catlow, C. R. A.; Taylor, S. H.; Hutchings, G. J. "Gas Phase Glycerol Valorization over Ceria Nanostructures with Well-Defined Morphologies". *ACS Catal*, **2021**, *11* (8), 4893–4907.
[3] Qiao, Z.-A.; Wu, Z.; Dai, S. "Shape-Controlled Ceria-Based Nanostructures for Catalysis Applications". *ChemSusChem*, **2013**, *6* (10), 1821–1833.
[4] Ziemba, M.; Schilling, C.; Ganduglia-Pirovano, M. V.; Hess, C. "Toward an Atomic-Level Understanding of Ceria-Based Catalysts: When Experiment and Theory Go Hand in Hand". *Acc Chem Res*, **2021**, *54* (13), 2884–2893.
[5] Morgan, D. J. "XPS Insights: Sample Degradation in X-ray Photoelectron Spectroscopy". *Surf. Interface Anal.*, **2023**, *55* (5), 331-335.
[6] Morgan, D. J. "Photoelectron Spectroscopy of Ceria: Reduction, Quantification and the Myth of the Vacancy Peak in XPS Analysis". *Surf. Interface Anal.*, **2023**, *55* (11), 845-850.

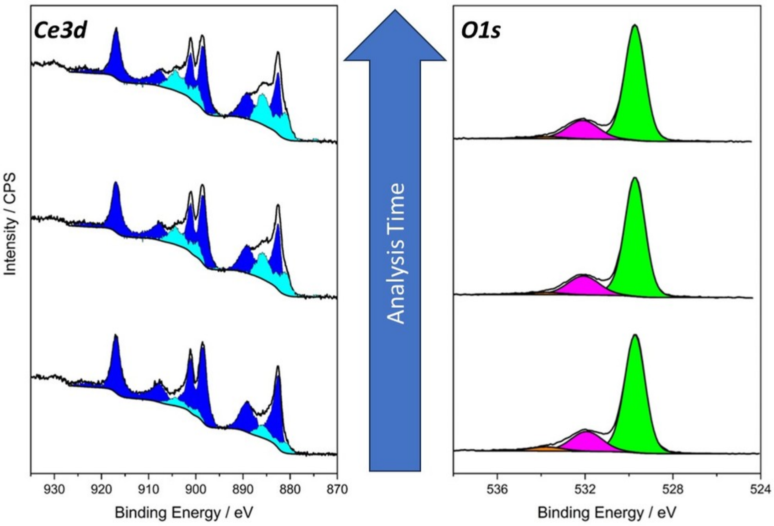
Ce3d
O1s
Intensity / CPS
Analysis Time
930
920
910
900
890
880
870
Binding Energy / eV
536
532
528
524
Binding Energy / eV

O42 - Non-destructive characterization of multi-layered thin films using XPS, HAXPES and structure modeling in StrataPHI

6. DAT – Data analysis and Metrology

Kateryna Artyushkova[1]
Norbert Biderman[1], Jenny Mann[1]
[1] Physical Electronics

X-ray photoelectron spectroscopy (XPS) is a well-established technique for non-destructive analysis of the chemical composition of thin layers and interfaces. Angle-resolved XPS (AR-XPS) has been used to determine the composition of depth profiles and layer thicknesses, traditionally with Al Kα (1486.6 eV) X-ray beams for depths up to 5-10 nm below the surface. In recent years, new AR-XPS capabilities have been added to Physical Electronics XPS scanning microprobe instruments including Cr Kα (5414.8 eV) hard X-ray photoelectron spectroscopy (HAXPES) that can probe buried interfaces up to 15-30 nm below the surface. Coinciding with the HAXPES development, the *Strata*PHI analysis software was developed to reconstruct quantitative, non-destructive XPS/HAXPES depth profiles from angle-dependent and single-angle photoelectron spectra.

In this talk, we will show that the *Strata*PHI software has been further developed to combine Al Kα and Cr Kα XPS and HAXPES data within a single depth profile to enhance extracted analytical information from various depths below the surface. We will explore the method of the combined technique as well as its application to multilayered thin film samples. The updated *Strata*PHI software also includes a fractional coverage analysis mode, relevant in situations where ultra-thin films exist as discrete islands – commonly observed in early thin-film deposition stages on the substrate rather than as a continuous, uniform film. A model system of discrete molybdenum sulfide (MoS_2) monolayer triangles deposited on SiO_2/Si substrate will be discussed.

Such added *Strata*PHI capabilities allow for scientists and engineers in metrology and research & development to analyze multi-layered thin films and ultra-thin films rapidly and non-destructively without potentially damaging ion beam sputtering that might otherwise be required to depth-profile or sputter-clean adventitious contamination off the surface.

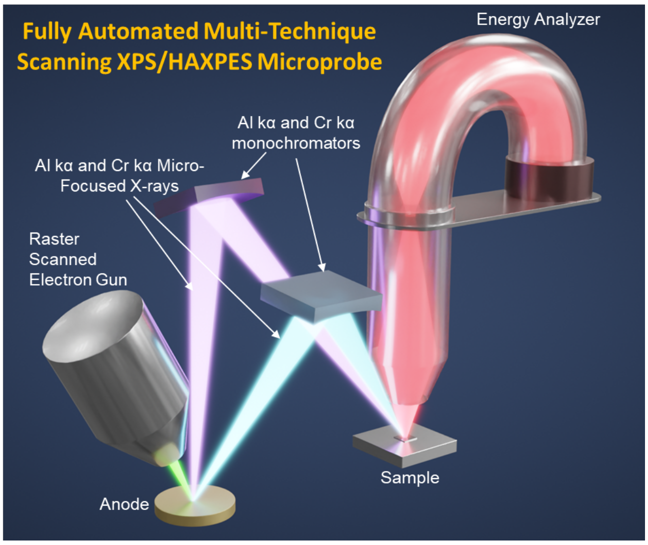

O43 - NXmpes: a unified data transfer standard for photoemission spectroscopy

6. DAT – Data analysis and Metrology

Lukas Pielsticker[1]
Florian Dobener[2], Laurenz Rettig[3], Walid Hetaba[1], Sandor Brockhauser[2]
[1] Max Planck Institute for Chemical Energy Conversion, Muelheim an der Ruhr, Germany
[2] Physics Department and CSMB, Humboldt-Universität zu Berlin, Germany
[3] Fritz Haber Institute of the Max Planck Society, Berlin, Germany

In recent years, there has been a push within experimental science to conform to FAIR (Findable, Accessible, Interoperable, and Reusable) data principles. However, in the field of photoemission spectroscopy (PES), there has been a distinct lack of such efforts. While there exists a widely adopted ISO standard for data transfer in surface chemical analysis [1], it does not fully cover all of the information that is obtained in modern photoemission experiments. Within the FAIRmat project of the German National Research Data Infrastructure (NFDI), we are developing an extensive and elaborated standard (called NXmpes [2]) for harmonizing PES data using NeXus, a community-driven data-modeling framework for experiments [3]. Our NeXus application definition, NXmpes, is set to transition into a fully recognized standard following a one-year incubation period, with the expectation of being officially endorsed by the NeXus International Advisory Committee (NIAC) as the preferred format for data interchange and interoperability in PES by September 2024. Here, we will show how FAIR research data in PES can be organized and how we intend to create benefits for the scientists who adapt the new standard. Comprehensive guidance on how to establish a FAIR data pipeline within a laboratory using NXmpes will be given. Finally, we present our strategy to collaborate with leading manufacturers of PES equipment to foster interoperability of NXmpes with their software solutions.

Selected references

[1] Dench, W.A., Hazell, L.B. and Seah, M.P., VAMAS Surface Chemical Analysis Standard Data Transfer Format, *Surf. Interface Anal.* **1988**, *12*, 161-163.
[2] https://fairmat-nfdi.github.io/nexus_definitions/classes/contributed_definitions/NXmpes.html
[3] Könnecke, M., et al., The NeXus data format, *J. Appl. Crystallogr.* **2015**, *48*, *1*, 301-305.

O44 - Obstacles and how to approach them – three examples in X-ray photoelectron spectroscopy measurement and analysis

6. DAT – Data analysis and Metrology

Andreas Schaefer[1]
Alexander Nellessen[1], Mariavittoria Craighero[1], Johan Gustafson[2], Per-Anders Carlsson[1]
[1] Department of Chemistry and Chemical Engineering, Chalmers University of Technology
[2] Division of Synchrotron Radiation Research, Lund University

X-ray photoelectron spectroscopy (XPS) measurements often come with a variety of challanges ranging from sample mounting, charge compensation, and binding energy referencing to quantification and peak fitting including background subtraction.

In this presentation three cases and the approach used to solve different research questions are going to be discussed. The first deals with an ex-situ mesurement of Vanadium oxide supported on titania. VO_x/TiO_2 is a well studied catalyst system for the selective catalytic reduction (SCR) of NO_x with ammonia. The challenge in the study presented was X-ray beam induced reduction of the vanadium oxide and peak fitting of the V 2*p* region for low concentrations of vanadia. An approach on how to obtain meaningful data despite the experimental obstacles will be presented.[1] The second case discusses an AP-XPS measurement of CeO_2 islands on a rhodium support during thermal reduction and exposure to CO_2. The challenge of the experiment and data analysis was to extract the oxidation state of the ceria as function of CO_2 exposure while only the Ce 4*d* level was experimentally accessible. The last experiment mainly deals with peak fitting a sulfur 2*p* spectrum of a doped conductive polymer. The question in this example was whether the doping level can be determined by XPS measurements. This case exemplifies the importance of constraining parameters to known characteristics when peak fitting complex spectra. Some general points on peak fitting will be addressed.

Selected references

[1] A. Nellessen et al., JPCC 128 (2024) 2894
[2] A. Schaefer et al., PCCP 20 (2018) 19447

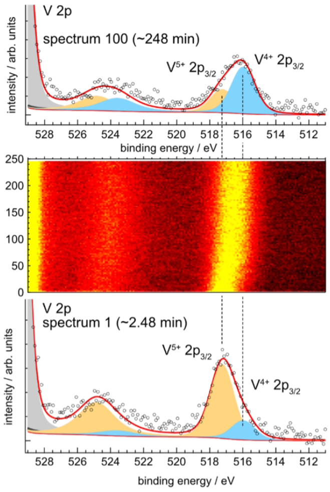

Figure 1: Long time exposure of a VO_x/TiO_2 test sample to the X-ray beam. The first and last spectrum of a measurement series are shown as well as a two dimensional representation of the signal intensity of the intermediate spectra.

O45 - Reliability of XPS analyses of perovskites: evolution of chemical and optoelectronic properties during X-ray irradiation

6. DAT – Data analysis and Metrology

Muriel BOUTTEMY[1, 2]
Pia DALLY[1, 2], Mirella AL KATRIB[1, 2], Guillaume VIDON[3], Daniel ORY[2, 4], Minjin KIM[3], Etienne SORET[3], Eva RANGAYEN[2], Marie LEGRAND[2, 3, 4], Alexandre BLAIZOT[2], Philip SCHULZ[3], Jean-Baptiste PUEL[2, 4], Daniel SUCHET[3], Jean-François GUILLEMOLES[3], Stéfania CACOVICH[3], Arnaud ETCHEBERRY[1]
[1] Institut Lavoisier de Versailles (ILV), Université de Versailles Saint-Quentin-en-Yvelines, Université Paris-Saclay, CNRS, UMR 8180, 45 avenue des Etats-Unis, 78035 Versailles Cedex, France
[2] Institut Photovoltaïque d'Île de France (IPVF), 18 boulevard Thomas Gobert, 91120, Palaiseau, France
[3] CNRS, Institut Photovoltaïque d'Île de France (IPVF), UMR 9006, 18 boulevard Thomas Gobert, 91120, Palaiseau, France
[4] Electricité de France (EDF) R&D, 18 Boulevard Thomas Gobert, Palaiseau 91120, France

Perovskite materials have proven to be emerging class materials in many domains, in particular, optoelectronic and photovoltaic. Metal hybrid perovskites, composed of organic and inorganic subunits, are very promising for solar devices applications due to their large carrier mobility, better photon absorption, high defaults tolerance, bandgap adjustability and low fabrication cost [1]. Despite these advantages, this material suffers from instability issues (water, oxygen, light, …), that are of concern of many research groups at present, working to enhance the long-term reliability of photovoltaic devices. XPS (X-ray photoelectron Spectroscopy) is a choice technique to investigate the chemistry of the hybrid perovskites active layer but artefacts linked to UHV and X-ray operating conditions, have been reported, raising the question of the reliability of such analyses [2], and by consequence, of all X-rays based techniques especially when synchrotron sources are considered [3] (high fluences).

This study apprehends this topic for moderate fluences, enabling to get more insights, at relatively short timescale, on the degradation mechanisms of a metal halide perovskites layer during soft X-ray exposure. A metrological approach employing XPS and Photoluminescence (PL) to concomitantly track the evolution of the chemical and optical properties was employed. This approach, already used to determine the impact of Ar^+ sputtering during XPS profiling [3], has proven to be a real added value for a better chemistry understanding from surface to bulk. In this study, the XPS spectrometer serves both as the irradiation source (Al k-alpha source) and analysis tool. Half-cells constituted of Glass /FTO/c-TiO_2/($Cs_{0.05}(MA_{0.14}, FA_{0.86})_{0.95}$ Pb$(I_{0.84}, Br_{0.16})_3$) have been exposed to irradiation from 1h to 16h. The spot area of 400 µm x 650 µm was scrutinized using temporally and spatially resolved PL imaging and spatially resolved XPS. For XPS, a novel approach was employed, by implementing a series of analysis points of 50µm distributed along horizontal and vertical lines from side to side of the 400 µm spot area. Two processes could be identified. For irradiation duration < 1h (10^{13} ph.cm^{-2}), bulk defects are formed without significant change of the surface chemistry. By increasing the fluence for longer irradiation exposure until 8h (>10^{14}ph.cm^{-2}), we notice the degradation of the organic part (N loss) but also the formation of Pb^0 and an increase of the I/Br ratio yielding to an increase of both bulk and surface defects. In addition, a new phase was evidenced with advanced optical imaging, attributed to I-poor perovskite[4].

Selected references

[1] L. Schmidt-Mende, J. Weickert. Organic and Hybrid Solar Cells, An Introduction. 1st ed. Berlin ; Boston: De Gruyter, 2016.

[2] Maryline Ralaiarisoa et al., *Small Methods* **2023**, 2300458.

[2] S. Svanstrom et al., Phys. Chem. Chem. Phys. 2021, 23, 12479.

[3] Stefania Cacovich et al., *ACS Appl. Mater. Interfaces* 2022, 14, 34228−34237.

[4] G.Vidon et al., Adv. Funct. Mater. 2023, 2304730.

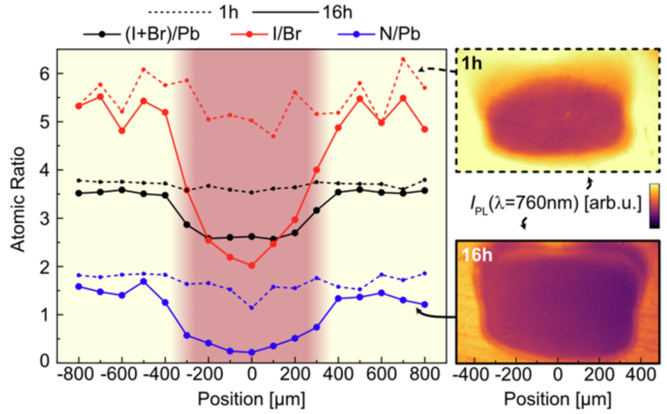

Spatially resolved XPS measurements (50µm spot size) and corresponding continuous wave PL maps at 760 nm after 1h and 16h of X-rays exposure,

O46 - ToF-SIMS depth profiling and quantitative analysis of metals and alloys in a UHV, oxygen, and hydrogen Atmosphere

6. DAT – Data analysis and Metrology

Jernej Ekar[1, 2]
Janez Kovač[1]
[1] Jožef Stefan Institute, Jamova cesta 39, SI-1000 Ljubljana, Slovenia
[2] Jožef Stefan International Postgraduate School, Jamova cesta 39, SI-1000 Ljubljana, Slovenia

Secondary ion mass spectrometry (SIMS) is a versatile method used in the fields of surface analysis, depth profiling, and elemental and molecular mapping. However, it has its limitations that require further improvements and optimizations. The matrix effect, which influences the ionization yield of secondary ions with respect to the substrate from which the analyzed compounds originate, presents a significant drawback for the SIMS technique. It limits the quantification capabilities of the method, influences detection limits, and negatively affects depth profiling, especially concerning layer identification and interface determination. There are several approaches to the reduction of the matrix effect. Our work was mainly done in the field of application of reactive gas atmospheres. We previously showed that H_2 flooding improves the results of the SIMS depth profiling of thin film and multilayered samples composed of metals, metal oxides, and alloys. [1] Furthermore, the H_2 atmosphere reduces surface roughening caused by the intense ion sputtering needed during depth profiling analyses. [2] In our recent work, we have further investigated the possibilities of the ToF-SIMS method for the quantification of selected metals and alloys containing these metals in different ratios by reducing the matrix effect in the presence of H_2 and also O_2. As a means of comparison, the measurements were performed in the ultra-high vacuum (UHV) environment as well. H_2 flooding shows the most significant improvements compared to the UHV analysis, while O_2 is also promising but has some limitations. Improvements are most evident for the transition metals Ti, Cr, Fe, Co, and Ni employed in our study. The p-block elements Al and Si were analyzed as well but changes for these two elements are not as prominent. The deviations from the true atomic ratios of Ti, Cr, Fe, Co, and Ni in different alloys reach a maximum of only 46% when analyzed in the H_2 atmosphere. In contrast, these values are 66 and 228% for the O_2 atmosphere and UHV environment, respectively. Our results suggest that gas adsorption and consequent formation of a new matrix on the surface, especially in the case of hydrogen, reduces the differences between the different chemical environments and electronic structures of the surface. In this way, the quantitative aspects of the SIMS method can be improved.

Selected references

[1] J. Ekar, P. Panjan, S. Drev, J. Kovač. ToF-SIMS Depth Profiling of Metal, Metal Oxide, and Alloy Multilayers in Atmospheres of H_2, C_2H_2, CO, and O_2. *J. Am. Soc. Mass Spectrom.* **2022**, *33*, 31– 44. 10.1021/jasms.1c00218.
[2] J. Ekar, J. Kovač. AFM Study of Roughness Development during ToF-SIMS Depth Profiling of Multilayers with a Cs^+ Ion Beam in a H_2 Atmosphere. *Langmuir* **2022**, *38*, 12871–12880. 10.1021/acs.langmuir.2c01837.

O47 - Understanding the fundamentals for A.I. interpretation of X-ray photoelectron spectra

6. DAT – Data Analysis and Metrology

Simon Hutton[1]
Liam Soomary[1], Kevin Good[1], Karol Macak[1]
[1] Kratos Analytical Ltd

Ensuring robust peak identification is pivotal for precise sample analysis by X-ray photoemission spectroscopy (XPS). The automation of peak identification significantly improves this process by reducing User error and bias. Modern acquisition software offers enhanced computer-driven peak identification for unknown samples, instilling confidence in element identification. This advancement forms the foundation for an automated sample analysis workflow known as data-dependent analysis (DDA). DDA entails identifying peaks in a survey spectrum and subsequently acquiring high-resolution spectra from major components. Recent User surveys indicate most users rely on the large area survey acquisition mode as the initial step in analysis.

To define confidence in the DDA process, existing spectral analysis data, containing element composition information, is utilized to generate reference spectra for testing. These reference spectra serve as the foundational dataset against which the performance of automated analysis algorithms can be evaluated. By comparing algorithm results with reference spectra, statistical parameters are calculated to assess precision, sensitivity, specificity, and accuracy in identifying elements within unknown spectra. For experienced analysts, DDA represents a time-saving acquisition method, while for inexperienced analysts, it provides assurance in accurate peak identification and appropriate high-resolution spectral acquisition.

The application of artificial intelligence and machine learning is a growing area within analytical instrumentation. This discussion highlights the current state of automated XPS data acquisition. We highlight the difference between the *goal driven* 'expert system' paradigm championed in the early 2000s [1,2] and the novel concept of an '*A.I. assisted analysis'* system.

Selected references

[1] J. E. Castle, J. Vac. Sci. Technol. A 2007, 25, 1.
[2] A. S. Lea, K. R. Swanson, J. N. Haack, J. E. Castle, S. Tougaard, and D. R. Baer. Surf. Interface Anal. 2010, 42, 1061–1065

O48 - Impact of powder properties and powder reuse on additive manufacturing of copper

6. DAT – Data Analysis and Metrology

Eduard Hryha[1]
Sofia Kazi[1], Ahmad Raza[1], Phillip Mahoney[2], Katri Kakko[3]
[1] Department of Industrial and Materials Science, Chalmers University of Technology, Rännvägen 2A, 41296 Göteborg, Sweden
[2] GE Additive Arcam EBM, Designvägen 2, 43533, Mölnlycke, Sweden
[3] Electro Optical Systems Finland Oy, Lemminkäisenkatu 36, FI-20520 Turku, Finland

Significant growth of electrification and increasing complexity of energy harvesting and distribution systems requires components with complex geometries and high electrical and thermal conductivity. This creates a breeding ground for additive manufacturing of copper, especially utilizing powder bed fusion technologies as powder bed fusion – laser beam (PBF-LB) and powder bed fusion – electron beam (PBF-EB), allowing to produce copper components with complex geometries, full density and high conductivity. However, even though copper is characterized by low thermodynamic stability of its oxide, copper powder is very sensitive to handling and pick-up of trace elements, that is especially crucial for electrical conductivity.

Initial state of the powder surface chemistry and its changes during number of reuse cycles as well as impact of processing conditions are studied by means of scanning electron microscopy, X-ray photoelectron spectroscopy and Auger electron spectroscopy. Results indicate that even though there are a lot of similarities between the two powder bed fusion processes, there is significant different in powder reuse and degradation during PBF-LB and PBF-EB. Generic model of the powder degradation in dependance on initial powder properties and AM process characteristics is elaborated. Effect of the reused powder on the defect formation during AM processing and its impact on material properties is discussed.

O49 - Using X-ray induced Auger electron spectroscopy transitions to explore the surface reactivity of CIGS

6. DAT – Data analysis and metrology

Anna GAGLIARDI[1]
Neal FAIRLEY[2], **Solene BECHU**[1]
[1] Institut Lavoisier de Versailles (ILV), Université de Versailles Saint-Quentin-en-Yvelines, Université Paris-Saclay, CNRS, UMR 8180, 45 avenue des Etats-Unis, 78035 Versailles Cedex, France.
[2] Casa Software Ltd, Bay House, 5 Grosvenor Terrace, Teignmouth, Devon TQ14 8NE, United Kingdom.

With the exception of the modified Auger parameter, X-ray induced Auger electron (X-AES) transitions aren't exploited to their full potential. Indeed, they can provide as much information (oxidation degree, chemical environment, atomic composition) as the classic photopeaks used in XPS, but their shapes' complexities limit their decompositions.

We offer here to compare two methods of decomposition, the non-linear least square (NLLS) [1] and the linear least square (LLS) [2] analyses for Ga $L_3M_{4,5}M_{4,5}$ and In $M_{4,5}N_{4,5}N_{4,5}$ X-AES lines of $Cu(In_xGa_{1-x})Se_2$ (CIGS) material. CIGS is a p-type absorber used in solar cells which presents some progressive oxidation when exposed to relative humidity.[3] Thus, by combining non-linear and linear fitting procedures, PCA and vectorial method [4], a tracking of the surface oxidation with time was performed on the CIGS material. The growth of oxide phases (Ga_2O_3 and In_2O_3, determined by PCA, vectorial method and by comparison with reference spectra) was monitored on the X-AES lines with NNLS and LLS decompositions, showing an excellent coherence between both, as illustrated in Figure 1 for the Ga $L_3M_{4,5}M_{4,5}$ X-AES transition of CIGS.

However, there are two main differences existing between the NLSS and LSS decompositions. The first one is related to the difficulty of the decomposition. The NLLS method requires multiple photopeaks (up to 15 for In $M_{4,5}N_{4,5}N_{4,5}$ for example) to simulate the decomposition, which increases the possibility of human error. In contrast, the LLS method uses one photopeak to represent one chemical environment, which limits the decomposition error. The second difference is related to the evolution of the X-AES lines. When studying a series of X-AES transitions, one may encounter slight modifications in terms of position or FWHM values. These parameters can be updated using the NLLS method, but not the LSS method. Each method has thus its advantages and disadvantages, and their implementation on X-AES lines will be discussed accordingly to the element studied.

Selected references

[1] J.J. Moré, Numer. Anal. **630**, 105 (1978).
[2] G.H. Golub and C. Reinsch, Linear Algebr. **420**, 403 (1971).
[3] S. Béchu *et al.*, Appl. Surf. Sci. **576**,151898 (2022).
[4] S. Béchu and N. Fairley, J. Vac. Sci. Technol. A **42**, 013202 (2024).

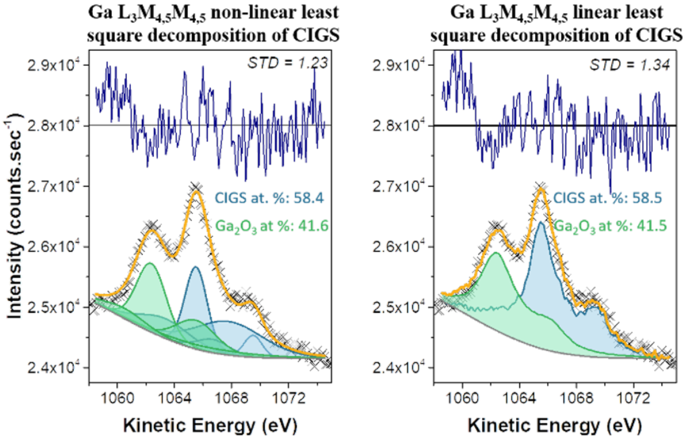

Figure 1. Curves to fitted data of an aged CIGS using non-linear (left) and linear (right) approaches.

O50 - XPS characterisation of brasses

6. DAT – Data analysis and Metrology

Eric Tam[1]

[1] Division of Materials and Manufacture, Department of Industrial and Materials Science, Chalmers University of Technology

A comparative study on the X-ray photoelectron spectra (XPS) among three brasses (i.e. alpha brass(α), machining brass (α+β) and lead-free brass(α-κ)) is made together with its alloying elements, i.e. copper (Cu) and zinc (Zn). Most of the characteristic features in the core level peaks (2p, 3p) and the XPS Auger lines from the two major elements are found to be very close. The alloying of brass causes positive shifts to all the copper-related peaks, and negative shifts to those zinc-related, implying the sharing of valence electron is more dominated by the former element. The derivative of valence bands among the samples do show that all measurements have a common Fermi level. The highest conductivity is copper, in descending order comes with the duplex brasses, alpha brass and then zinc. The binding energy position of the Cu3d has a role here.

Selected references

Figure 1. Derivative of the XPS spectra near the Fermi Level of three different brasses together with pure copper and pure zinc pieces after native oxide removal by sputter cleaning.

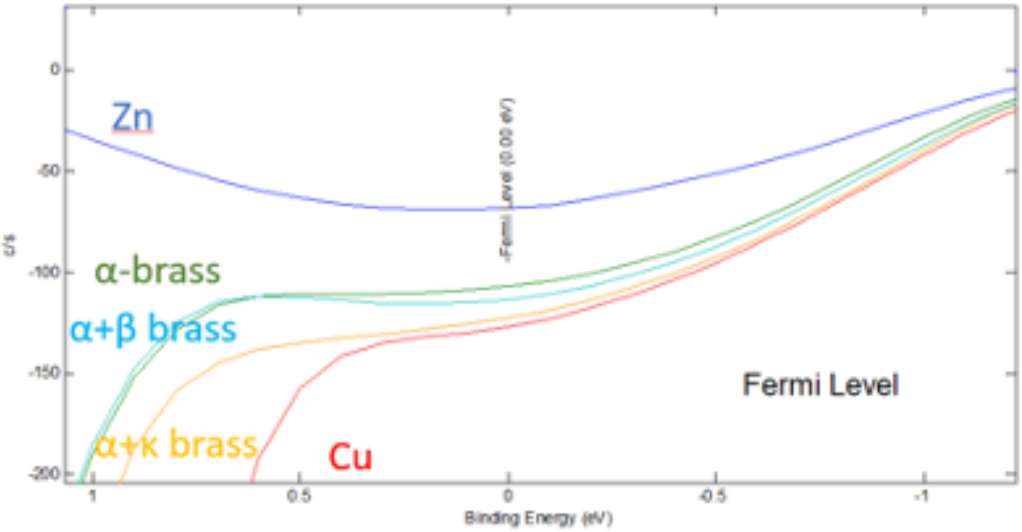

7. DPR – Thin films, Coatings and Depth Profiling

O51 - Integration of 2D Nanolayers in opto-electronic and photonic devices

7. DPR – Thin films, Coatings and Depth Profiling

Vera Marinova[1]
Nikolay Minev[1], Blagovest Napoleonov[1], Dimitre Dimtrov[1, 2]
[1] Institute of Optical Materials and Technologies, Bulgarian Academy of Sciences, Sofia, Bulgaria
[2] Institute of Solid-State Physics, Bulgarian Academy of Sciences, Sofia, Bulgaria

2D layered materials have attracted outstanding attention due to their strong in-plane covalent bonds and weak van der Waals bonds joining adjacent layers which provide extraordinary electron mobility, band gap dependence on the number of layers and extremely high anisotropic optical response.

Here, we report the detailed study of controlled synthesis and characterization of graphene and transition metal dichalcogenides (TMDC) and their intergation in optoelectronic and photonic devices. As example, the application of graphene and PtSe2 as transparent conductive electrode in display devices is demostrated. In addition, surface anchoring energy and pre-tilt angle value were determined to characterize the interfaces. Besides the excellent phase modulation repeatability over the large-scale area, graphene exhibits great potential for future ITO-free integrated photonic devices and bio-oriented technologies.

Next, we focus on synthesis details of MoS_2 nanolayers via close proximity re-evaporation of MoS2. AFM determined the synthesis of triangular nano flakes with lateral dimensions of over 10 mm and flakes' height of 1.3 nm, approving bi-layer MoS_2. Polarization dependence of MoS_2-based photoresist under illumination with 405 nm LED is demonstrated

Acknowledgement: This research was funded by Bulgarian Science Fund under the project numbers FNI КП-06-ДО 02/2 and КП-06-ДО 02/3 in the frame of M-ERA program "Functional 2D materials and heterostructures for hybrid spintronic-memristive devices". We acknowledge the financial support by European Regional Development Fund within the Operational Programme 'Science and Education for Smart Growth 2014–2020' under the Project CoE 'National Center of Mechatronics and Clean Technologies' BG05M2OP001-1.001-0008-C01. Research equipment of distributed research infrastructure INFRAMAT (part of Bulgarian National roadmap for research infrastructures) supported by Bulgarian Ministry of Education and Science is also acknowledged.

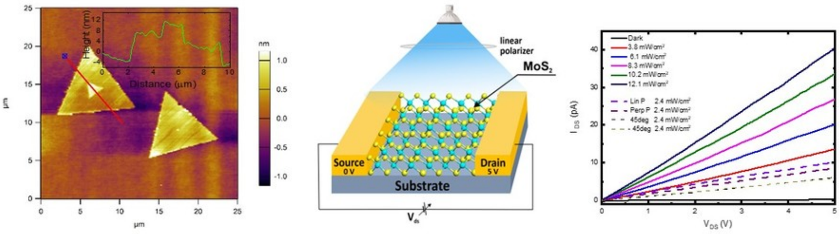

MoS_2-based photoresist and photocurrent dependence under illumination with 405 nm LED (polarization dependence)

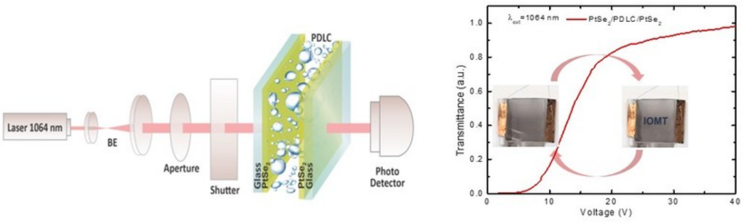

Schematic set-up and "off "and "on" states of $PtSe_2$-based PDLC device

O52 - Uptake of water and ions in organic coatings on metals: an in situ spectro-electrochemical approach

7. DPR – Thin films, Coatings and Depth Profiling

Tom Hauffman[1]
Negin Madelat[1], Benny Wouters[1], Mats Meeusen[1], Annick Hubin[1], Herman Terryn[1]
[1] Research group Sustainable Materials Engineering, Lab of Electrochemical and Surface Engineering

Many metal structures are protected from corrosion by the application of organic coatings. The protection scheme of such hybrid structures is two-fold: a barrier against the ingress of water and ionic species and a durable bonding at the interface between the metal and the coating.

In order to analyze the influence of relevant technical environments on coated metal structures, we used Odd Random Phase Multisine Electrochemical Impedance Spectrocopy combined with Infrared Spectroscopy in the Kretschmann configuration. This approach enabled us the simultaneously analyze the dynamic electrochemical response of the hybrid systems, while correlating it with hybrid interactions at the buried interface.

In the presented work, we focus on the influence of the composition of coatings and pretreatments of aluminium substrates on the uptake of electrolyte species and durability of the complete structure. In a first instance, an electrical equivalent circuit was established to identify the individual contribution of ions and water in the impedance spectra. The EIS data treatment was validated by analyzing series of poly-ethylene glycol diacrylate coatings with varying photo-initiator concentration[1,2]. Furthermore, the contribution of the inert pigment concentration on the coating barrier properties to ion uptake was evaluated[3].

Next, the surface of aluminium 2024 was varied by a pickling or pickling and anodizing procedure. The influence of the changing hybrid interface on the overall electrochemical behavior of the hybrid systems and specific contribution to the phenomena observed in the EIS spectra was evaluated[4].

Based on this work, we are able to provide a fast evaluation tool for the barrier properties of both coatings as well as buried hybrid interfaces in a wide variety of exposure conditions. Furthermore, the mechanistic insights as well as derived parameters (such as diffusion coefficient, ion ingress front position and velocity) serve as a basis for the ongoing development of electrochemical models for the long-term evaluation of hybrid systems[5.]

Selected references

1. Wouters B. et al., Corrosion Science 190 (2021).
2. Madelat N. et al., Corrosion Science 212 (2022).
3. Madelat N. et al., Corrosion Science 227 (2023).
4. Madelat N. et al., Electrochimica Acta 455 (2023).
5. Meeusen M. et al., Progress in Organic Coatings 182 (2023).

O53 - 3D ToF-SIMS analysis of drug distribution and Mg stearate coating on lactose carrier particles

7. DPR – Thin Films, Coatings and Depth Profiling

Peter Sjövall[1]
Marie Ernstsson[2], Denny Mahlin[3], Kyrre Thalberg[4]
[1] RISE Research Institutes of Sweden, PO Box 857, SE-501 15 Borås, Sweden
[2] RISE Research Institutes of Sweden, Malvinas väg 3, SE-114 28 Stockholm, Sweden
[3] RISE Research Institutes of Sweden, Forskargatan 18, SE-151 36 Södertälje, Sweden
[4] Emmace Consulting AB, Scheelevägen 22, SE-223 63 Lund, Sweden

A common type of inhalation medicine uses a dry powder formulation where the active pharmaceutical ingredient (API) is attached on the surface of carrier particles, often in combination with additional components. The spatial distribution of the API on the carrier particle is critical for the exposure to the intended target in the body and thus for the efficacy of the drug. In this work, we use ToF-SIMS imaging in combination with argon gas cluster sputtering to determine the 3D distributions of budesonide (the API) and magnesium stearate (MgSt) on the surface of lactose particles. The sample is a so-called adhesive mixture and was prepared by mixing 2 % micronized budesonide (particle size < 5 µm) in a high shear mixer with a lactose carrier (approximately 100 µm in diameter) coated with 1 % MgSt. The 3D data was acquired by alternating cycles of 2D ToF-SIMS imaging measurements and sputter erosion, in a M6 instrument (IONTOF GmbH) using 30 keV Bi_3^+ primary ions and 10 keV Ar_{2000}^+ ions for sputtering. The results show that the drug carrier particles are initially largely covered by MgSt, with only small spots showing exposed lactose or budesonide. Upon sputtering, MgSt is rapidly removed to expose flat regions of lactose as well as discrete budesonide particles distributed over the lactose surface (Fig. 1a). Depth profiles show that the budesonide signal increases upon initial sputtering to reach a maximum value, after which it gradually decreases with additional sputtering (Fig. 1b). These results provide clear evidence that budesonide to a large extent is covered with MgSt on the surface of the drug particles. Furthermore, if we assume a sputter yield of 40 nm^3 (as previously reported for polymers like polystyrene and polymethylmethacrylate (1)), the thickness of the MgSt coating on the lactose surface can be estimated to 10-20 nm. The results are compared with XPS data for the same sample.

Selected references

(1) M. P. Seah, Argon cluster size-dependence of sputtering yields of polymers: molecular weights and the universal equation, Surf. Interface Anal. 2015, 47, 169–172

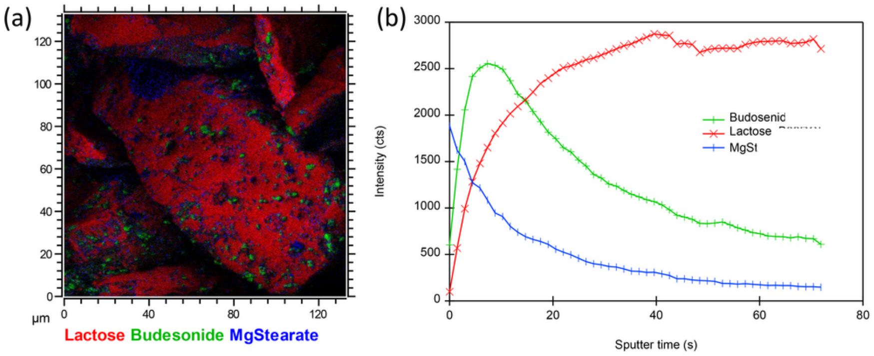

Figure 1 (a) Overlay ion image of drug carrier particles after partial sputtering (30-44 s) showing lactose in red, budesonide in green and MgSt in blue. (b) Depth profiles of lactose (red), budesonide (green) and MgSt (blue) from region of interest (ROI) corresponding to flat lactose regions in (a). Assuming a sputter yield of 40 nm^3, the erosion rate is approximately 5 nm/s.

O54 - Air-stable PdSe2 crystal growth and characterization

7. DPR – Thin films, Coatings and Depth Profiling

Dimitre Dimitrov[1, 2]
Vera Marinova[2], Nikolay Minev[2], Valentina Mussi[3], Peter Rafailov[1], Walter Fuscaldo[3], Dimitrios Zografopoulos[3]
[1] Institute of Solid State Physics, Bulgarian Academy of Sciences, 1784 Sofia, Bulgaria
[2] Institute of Optical Materials and Technologies, Bulgarian Academy of Sciences, 1113 Sofia, Bulgaria
[3] Consiglio Nazionale delle Ricerche, Istituto per la Microelettronica e Microsistemi, 00133 Rome, Italy

Palladium diselenide (PdSe2) is an air-stable 2D layered material with high carrier mobility, a high on/off ratio, as well as a widely tunable band gap, making it promising for electronics and photonic applications [1]. Although PdSe2 has demonstrated potential for many applications and exfoliated flakes have been successfully applied in various optoelectronic devices, the availability of high-quality large-area PdSe2 crystals and nanolayers remains a challenging issue. Here, we report the growth process details of large-area single-crystal PdSe2 using the self-flux method. The crystals were characterized by scanning electron microscopy (SEM), energy-dispersive X-ray spectroscopy (EDS), X-ray diffraction (XRD), X-ray photoelectron spectroscopy (XPS), and transmission electron microscopy (TEM) to confirm the crystal quality, phase, and composition. High-quality large-area PdSe2 single crystals are successfully grown by the self-flux method. The crystal structure and quality are confirmed by XRD, TEM, and XPS. The performed polarization Raman spectroscopy reveals a 2D layered structure mode with anisotropic properties. The control of the crystal growth process opens the potential use of PdSe2 for integrated electro-optical applications, field-effect transistors, and broadband polarization-sensitive photodetectors and sensors

Acknowledgment: We acknowledge the support of the Bulgarian Science Fund under the project numbers FNI КП-06-ДО 02/2 and КП-06-ДО 02/3 in the frames of M-ERA program project “Functional 2D materials and heterostructures for hybrid spintronic-memristive devices”. D. Z. and V. M. acknowledge the bilateral project between the Consiglio Nazionale delle Ricerche and the Bulgarian Academy of Sciences “Two-dimensional nanomaterials toward terahertz optoelectronic applications” (B83C23000610005).

Selected references

[1] Ryan A. Nelson et al., Mater. Horiz., 2023, 10, 3740

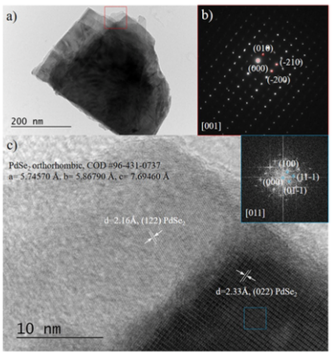

Fig.1. (a) Bright Field TEM image, (b) the corresponding SAED pattern and (c) HRTEM image and the Fast Furrier Transform pattern from the blue square area (inset) of $PdSe_2$ crystal

O55 - Angle resolved XPS depth profiling for extreme ultraviolet lithography optics research- monoatomic vs cluster ion source

7. DPR – Thin Films, Coatings and Depth Profiling

Shriparna Mukherjee[1]
Véronique de Rooij-Lohmann[1], Chien-Ching Wu[1], Jonathan Counsell[2], Frank Driessen[1]
[1] Department of Nano Instrumentation, TNO, the Netherlands Organisation for Applied Scientific Research, The Netherlands
[2] Kratos Analytical Ltd., United Kingdom

Within the Nano Instrumentation department of TNO, X-ray photoelectron spectroscopy (XPS) analysis is used for characterization of optical surfaces (mirrors). This is related to development in optics life-time research for extreme ultraviolet (EUV) lithography.

In this work, we focus on understanding the sensitivity of XPS depth profiling to multilayer mirrors which are similar to the EUV mirrors. Traditional XPS depth profiling using the Ar ion-gun is performed on a commercial Ru-capped Mo/Si multilayer mirror before and after annealing in vacuum at 330 °C for 48 hours. Annealing of the mirror was performed to induce intermixing of the multilayers. However, traditional XPS depth profiling results in artefacts due to preferential sputtering of light elements, and the ion-induced intermixing severely reduces the contrast between the layers. Development of sputtering methods that reduce those artefacts is therefore of importance. In this respect, a Gas Cluster Ion Source (GCIS), where large ion clusters are used instead of single ions might be of interest. Due to larger ion clusters, the energy-to-mass ratio of the impact and its effect on the sub-surface is reduced tremendously. Gas Cluster Ion Sources are gaining momentum in the field of XPS and are in a fast transit from high-end, academic research towards semi-standard add-on for modern instruments. However, since sputtering is material-dependent, the usefulness of a GCIS needs to be tested on samples relevant for our field, i.e. EUV mirrors. Secondly, because the thickness of the layers in EUV mirrors is smaller than the XPS information depth, we investigated the benefit of combining sputter depth profiling with angle-resolved (AR) XPS to enhance the surface sensitivity (shown in Figure (a) and (b)). Results obtained from the comparative study of traditional XPS depth profiling and GCIS will be presented here. Based on these results, further development on the analysis of the EUV mirrors and their degradation mechanisms will be sought for.

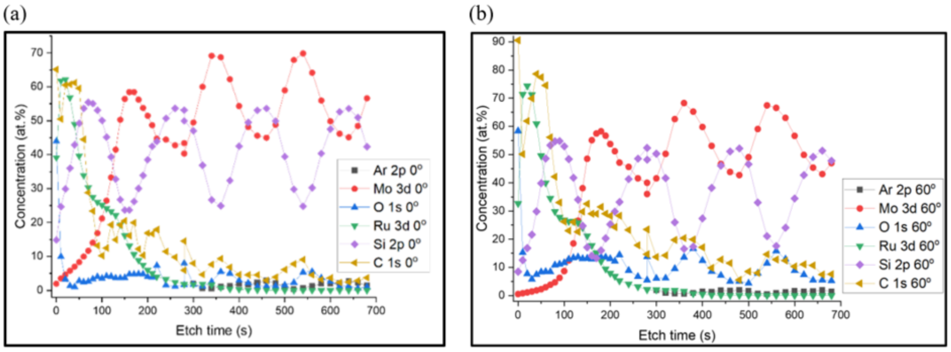

Figure: Concentration variation of the multilayers in a fresh mirror (not annealed) obtained using traditional Ar-ion gun etching (a) at 0° take-off angle and (b) at 60° take-off angle; combining sputter depth profiling with AR-XPS to enhance the surface sensitivity.

O56 - Carbide-rich nano-layers produced by ion beam mixing

7. DPR – Thin Films, Coatings and Depth Profiling

Adel Sarolta Racz[1]
Zsolt Fogarassy[1], Zsolt Kerner[1], Ulrich Kentsch[2], Matjaz Panjan[3], Miklos Menyhard[1]
[1] HUN-REN Centre for Energy Research, Konkoly Thege M. út 29-33, 1121 Budapest, Hungary
[2] Helmholtz-Zentrum Dresden-Rossendorf, Bautzner Landstraße 400, 01328 Dresden, Germany
[3] Jožef Stefan Institute, Jamova 39, 1000 Ljubljana, Slovenia

Carbides have many attractive properties like corrosion resistance, mechanical durability, high heat resistance and some of them possess catalytic activity, as well. Therefore, their application ranges from protective coatings in harsh environments, through structural materials to electrocatalysts. The production of certain carbides needs high temperature and high pressure, many substrates can not tolerate such conditions, however. In these cases, the stable material might be produced by far from equilibrium conditions methods. By applying ion irradiation, it is possible to produce various materials at room temperature for which generally high temperatures are needed. If we irradiate a layer structure at the interfaces, atomic mixing or ion mixing happens. Herein, the results are shown for the production of W_2C and Mo_2C nano-layers. C/W and C/Mo multilayer structures - with individual thicknesses of 10-20 nm - are irradiated by xenon and argon atoms. The irradiation conditions are chosen with the help of simulation programs (TRIDYN, SRIM). The layer thickness and the in-depth distribution of the formed carbides is investigated by Auger electron spectroscopy and XPS depth profiling. [1] We show that the thickness of the carbide-rich region can be tailored by changing the ion irradiation conditions and the layer structure. It is shown that the corrosion (potentiodynamic corrosion test in 3.5 wt% NaCl) and mechanical resistance (scratch test) of the W_2C layers is better than a commercially available WC-Co cermet. [2]

Acknowledgements
HZDR-Dresden and project funding of Centre for Energy Research is highly acknowledged.

Selected references

[1] Z. Fogarassy, U. Kentsch, P. Panjan, A.S Racz Experimental and Theoretical Study on the Production of Carbide-Rich Composite Nano-Coatings *Surf. Interfaces*, 38, **2023**, 102773
[2] A.S. Racz, P. Kun, Z. Kerner, Z. Fogarassy, M. Menyhard, Tungsten Carbide Nanolayer Formation by Ion Beam Mixing with Argon and Xenon Ions for Applications as Protective Coatings, *ACS Appl. Nano Mater.* 6, **2023**

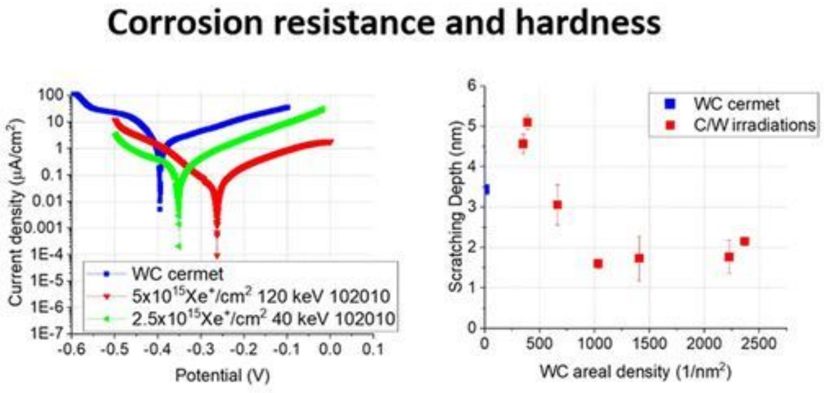

Figure 1. Results of corrosion and scratch test for W_2C-rich samples.

O57 - Chemical state analysis of differently miscible interfaces in metallic multilayers

7. DPR – Thin films, Coatings and Depth Profiling

Claudia Cancellieri[1]
Giacomo Lorenzin[1], Manura Lyanage[2], Vladyslav Turlo[3], Lars Jeurgens[1]
[1] Empa, Swiss Federal Laboratories for Materials Science and Technology, Laboratory for Joining Technologies and Corrosion, Dübendorf, Switzerland.
[2] National Centre for Computational Design and Discovery of Novel Materials MARVEL, EPFL, Lausanne, Switzerland.
[3] Empa, Swiss Federal Laboratories for Materials Science and Technology, Laboratory for Advanced Materials Processing, Thun, Switzerland.

Hard X-ray photoemission spectroscopy, in particular chemical state analysis on the basis of the Auger parameter, are used to study the interface chemistry of magnetron-sputtered metallic multilayers. Charge transfer and electronic redistribution may occur for metallic materials when put in contact and forming an interface. By performing in situ X-ray photoemission analysis, the Auger parameter of W in contact with different metals (Cr, Cu and Mo) in a multilayer structure was derived. The different degree of metal miscibility and intermixing at the interface were found to affect the Auger parameter, as attributed to the electronic charge redistribution taking place at the multilayer interfaces. The experimental data are supported by *ab initio* calculations of the charge transfer at the metal interfaces. Assessing at the atomic level charge transfer/redistribution at metallic interfaces will help in understanding crystal structure variation, order and disorder phenomena and their effect on properties like electronic/thermal conductivity when intermixing occurs.

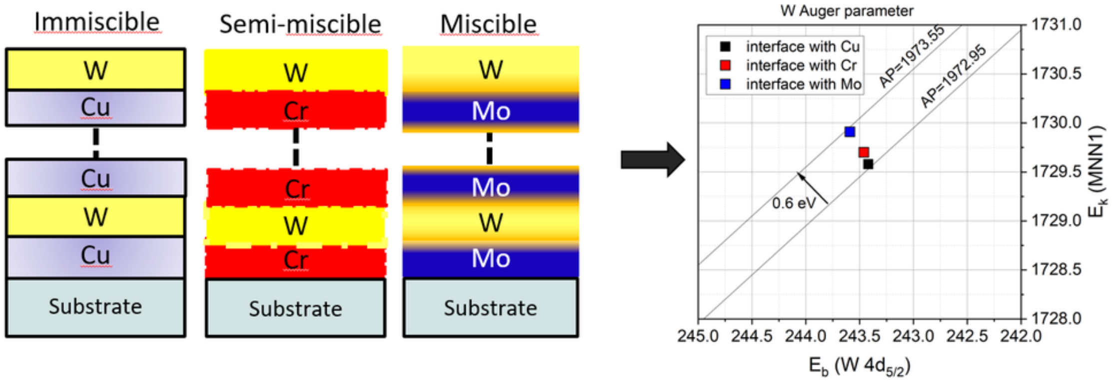

O58 - Combined XPS/ToF-SIMS investigation of the adsorption of an amine curing agent on converted HDG steel

7. DPR – Thin Films, Coatings and Depth Profiling

Vanina Cristaudo[1]
Zahra Jiryaeisharahi[1], Kitty Baert[1], Priya Laha[1], Lee Steely[2], Daniel Clingerman[2], Elizabeth Brown-Tseng[2], Herman Terryn[1], Tom Hauffman[1]
[1] Department of Materials and Chemistry, Research Group Electrochemical and Surface Engineering (SURF), Vrije Universiteit Brussel, Pleinlaan 2, 1050 Brussels, Belgium
[2] Coatings Innovation Center, PPG, Allison Park, PA 15101, Unites States

In the automotive industry, the corrosion protection of hot-dip galvanized (HDG) steel is of pivotal importance. To this purpose, a Zr oxide-based conversion pre-treatment of the metal surface for passivation and improved adhesion [1], in combination with the application of a polymeric coating is here performed. The efficiency and durability of a such hybrid (hydr)oxide-polymer system depend on the formation and degradation of the chemical bonds at the buried interface, and this deserves a fundamental understanding at the molecular level.

This work aims first at the elucidation of the deposition mechanism of the Zr-based conversion of the surface of HDG steel, in presence and absence of a Cu(II) accelerator, that represents the substrate for the application of an epoxy-based coating. It is found that the conversion inorganic film has a multi-metal and heterogeneous nature, the latter being both laterally and in-depth [2]. Then, the interfacial interactions established between this very complex converted metal substrate and an amine-functionalized curing agent commonly used in the epoxy-based coatings are investigated. The model amine molecule – diethylenetriamine (DETA) – is therefore adsorbed and used as an indicator of the acid-base properties of the multi-metal oxide surface [3]. Owing to the high complexity of the multi-metal oxide substrate, derivative and simpler systems – namely, pure Zn, Zr, and Cu – are employed for a more fundamental understanding of the chemisorption process. The resulting DETA-adsorbed model and multi-metal surfaces are investigated by X-ray photo-electron spectroscopy (XPS), and by examination of the N 1s peak, the interfacial bond densities are determined. Time-of-flight secondary ion mass spectrometry (ToF-SIMS) analysis is conducted to complement/confirm the findings of the XPS investigation.

Selected references

[1] I. Milošev, *et al.* Conversion coatings based on zirconium and/or titanium. J. Electrochem. Soc. (2018), 165, p.C127.
[2] V. Cristaudo, *et al.* A combined XPS/ToF-SIMS approach for the 3D compositional characterization of Zr-based conversion of galvanized steel. Appl. Surf. Sci. (2021), p.150166.
[3] V. Cristaudo, *et al.* Unravelling the chemisorption mechanism of epoxy-amine coatings on Zr-based converted galvanized steel by combined static XPS/ToF-SIMS approach. Appl. Surf. Sci. (2022), 599, p.153798.

O59 - Comparative study on advanced preparation techniques for internal structure analysis of organic coatings

7. DPR – Thin Films, Coatings and Depth Profiling

Daniel Leidlmair[1, 2]
Jiří Duchoslav[1], Georg Mayr[3], Heiko Groiss[4], Bernhard Strauß[3], Gernot M. Wallner[2], David Stifter[1]
[1] Center for Surface and Nanoanalytics (ZONA), Johannes Kepler University Linz, Austria
[2] Christian Doppler Laboratory for Superimposed Mechnical-Environmental Ageing of Polymeric Hybrid Laminates, Institute of Polymeric Materials and Testing (IPMT), Johannes Kepler University Linz, Austria
[3] Voestalpine Stahl GmbH, Linz, Austria
[4] Christian Doppler Laboratory for Nanoscale Phase Transformations, Center for Surface and Nanoanalytics (ZONA), Johannes Kepler University Linz, Austria

Organic coatings are representing a valuable enhancement of final products in many aspects, typically linked to corrosion inhibitive and aesthetic purposes. For gaining deeper understanding of, *e.g.*, the formation of chemical gradients or degradation processes, depth-resolved analysis delivers crucial information of the interior coating structure [1]. However, in order to assess the complex internal composition of high-end paint systems, careful selection of suitable depth profiling methods is required.

In this work, a comparative examination of state-of-the art preparation techniques for depth-resolved analysis, exemplified on a high-build polyester-polyurethane coating system applied on galvanized steel, is reported. The fabrication of wedge-shaped tapers by applying cryo-ultra-low-angle microtomy (cryo-ULAM), a standardized paint borer and Ar^+-ion flat milling was comprehensively evaluated using advanced surface analysis techniques. Scanning electron microscopy (SEM) and energy-dispersive X-ray spectroscopy (EDX) were employed to examine the resulting surface morphology of extended sections down to the steel substrate and to determine cutting artefacts, smearing and structural deformation (Fig. 1). Qualitative and quantitative elemental and chemical depth analysis was achieved by X-ray photoelectron spectroscopy (XPS), Fourier-transform infrared (FTIR) spectroscopy and sputter depth profiles recorded by Auger electron spectroscopy (AES).

Consequently, thorough correlative investigation allowed to determine the impact of the respective preparation process on the accuracy of depth profiling results with regard to gaining profound understanding of high-end organic coated material systems. All methods consistently showed that cryo-ULAM is preferably used to fabricate extended sections for depth-resolved investigations of organic coatings.

Selected references

[1] D. Leidlmair, J. Duchoslav, G. Mayr, M. Arndt, H. Gsaller, B. Strauß, D. Stifter, Elemental and chemical depth profiling of high-build single-component (1K) polyester-polyurethane coil coatings, Progress in Organic Coatings 179 (2023) 107490, doi: https://doi.org/10.1016/j.porgcoat.2023.107490.

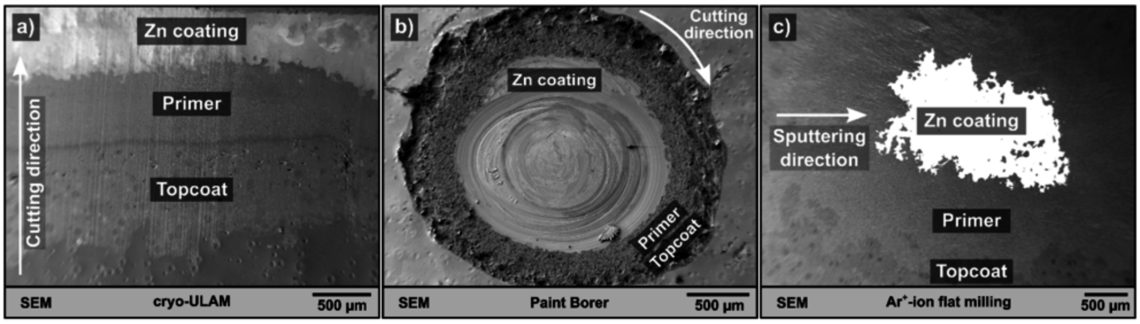

Figure 1: SEM images of fabricated extended sections through organic-coated steel prepared by a) cryo-ULAM, b) a standardised paint borer and c) Ar^+-ion flat milling.

O60 - Effect of hydrogen on the chemical state of amorphous alumina films grown by thermal atomic layer deposition

7. DPR – Thin Films, Coatings and Depth Profiling

Lars P.H. Jeurgens[1]
Simon Gramatte[1, 2, 3], Olivier Politano[4], Ivo Utke[3], Vladyslav Turlo[2], Claudia Cancellieri[1]
[1] Laboratory for Joining Technologies& Corrosion, Empa, Swiss Federal Laboratories for Materials Science and Technology, Dübendorf, Switzerland
[2] Laboratory for Advanced Materials Processing, Empa, Swiss Federal Laboratories for Materials Science and Technology, Thun, Switzerland
[3] Laboratory for Mechanics of Materials and Nanostructures, Empa, Swiss Federal Laboratories for Materials Science and Technology, Thun, Switzerland
[4] Laboratoire Interdisciplinaire Carnot de Bourgogne, UMR 6303 CNRS-Université Bourgogne Franche-Comté, Dijon Cedex, France

Thermal atomic layer deposition (ALD) is widely applied to produce ultra-thin amorphous barrier oxide films for e.g. microelectronic, photovoltaic and sensing devices. The density, stoichiometry and H-impurity content of such amorphous oxide films are known to vary depending on e.g. the precursor species and the temperature of the ALD process [1, 2]. As shown in this work, chemical state analysis by lab-based XPS/HAXPES (i.e. applying Al-Kα and Cr-Kα X-ray sources [3]) can disclose the effect of H incorporation during the ALD process on the local chemical states of Al and O in amorphous Al_2O_3 ALD films. Incorporated H originates from unreacted covalent –OH hydroxyl bonds in the nearest-neighbour coordination sphere of the interstitial Al cations [2], thereby affecting the final-state electronic screening of core-ionized Al cations during the photoemission and Auger processes [1]. The experimental findings are compared with those of well-defined crystalline anhydrous α-Al_2O_3 (sapphire) and hydroxide α-$Al(OH)_3$ (bayerite) reference phases. Molecular dynamics simulations were performed to correlate the measured Auger parameter shifts to the change in the O ligand polarizability due to the formation of covalent –OH hydroxyl bonds in the local chemical environment of Al: see Fig. 1.

Selected references

[1] C. Cancellieri, S. Gramatte, O. Politano, L. Lapeyre, F. Klimashin, K. Mackosz, I. Utke, Z. Novotny, A. M. Müller, C. Vockenhuber, V. Turlo, L. P. H. Jeurgens, *Effect of Hydrogen on the Chemical State, Stoichiometry and Density of Amorphous Al_2O_3 Films Grown by Thermal Atomic Layer Deposition*, **Surface and Interface Analysis** (2024) 1–12.

[2] C. Guerra-Nuñez, M. Döbeli, J. Michler, I. Utke, *Reaction and Growth Mechanisms in Al_2O_3 deposited via Atomic Layer Deposition: Elucidating the Hydrogen Source*, **Chemistry of Materials** 29 (2017) 8690–8703.

[3] S. Siol, J. Mann, J. Newman, T. Miyayama, K. Watanabe, P. Schmutz, C. Cancellieri, L.P.H. Jeurgens, *Concepts for chemical state analysis at constant probing depth by lab-based XPS/HAXPES combining soft and hard X-ray sources*, **Surface & Interface Analysis** 52 (2020) 802–810.

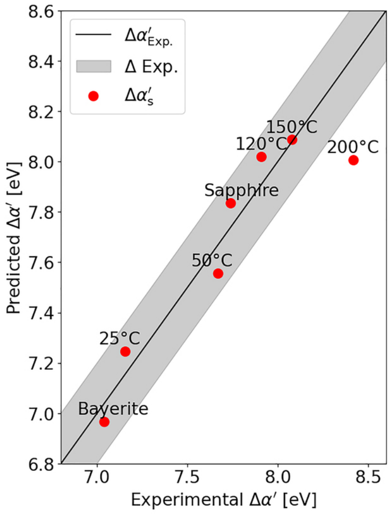

Fig. 1. Predicted versus calculated shift of the Al Auger parameter in amorphous Al_2O_3 film grown by ALD at various temperatures in the range of 25 – 200 °C. Corresponding values for the sapphire and bayerite reference phases are also shown.

O61 - Exploiting the anion exchange properties of layered double hydroxide films for the design of functional coatings

7. DPR – Thin Films, Coatings and Depth Profiling

Samantha Soulé[1]
Pierrick Durand[2], Sofiane El-Kirat-Chatel[1], Fabienne Quilès[1], Cédric Carteret[1]
[1] LCPME UMR 7564, CNRS, Université de Lorraine, Villers-Lès-Nancy, 54600, France.
[2] CRM2 UMR 7036, CNRS, Université de Lorraine, Vandoeuvre-Lès-Nancy, 54500, France.

Layered double hydroxides (LDH) consist of a stack of positively charged brucite-like layers and charged-compensating anions. The general formula of LDH is given by $[M^{II}_{1-x}\,M^{III}_{x}\,(OH)_2]^{x+}[(A^{n-}_{x/n}).\ M\ H_2O]^{x-}$ where M^{II} and M^{III} are metal cations, A^{n-} the interlayer anion and x defines the charge density of the layers. For some applications in practical devices or functional coatings, LDH must be fabricated into supported films to maximize their functionalities while controlling the surface properties. This step can be very challenging as the synthesis methods developed for powder LDH samples to control the material composition are not always transposable to the films.

In this work, ZnAl–NO_3 LDH films were first grown *in situ* onto Al-based substrates and the morphology of the coating was controlled by varying the thickness of the Al-precursor layer. The anion exchange properties were then specifically investigated depending on the film morphology following the exchange dynamics and the structural, morphological and chemical modifications by Scanning Electron Microscopy, X-Ray Diffraction and vibrational spectroscopies. Different organic anions were studied regarding their size and potential functionalities[1].

The initial LDH film morphology and structure were demonstrated to impact significantly the intercalation of anions by constraining the expansion of the interlayer space. Indeed, whereas the intercalation of benzoates was successfully achieved in 1.9 µm-thick films, the anion exchange in a denser 2.4 µm- thick film resulted in the detachment of the LDH particles from the surface as a result of mechanical stress. After optimizing the starting film morphology, the intercalation of functional anions with potential antimicrobial properties was successfully achieved with the possibility to expand the interlayer space up to 150 % while holding the film integrity.
The stability of the coatings was then addressed in saline solution following the anion release kinetics. The rapid release (from minutes to hours) of the intercalated anions would need to be improved. The regeneration capacity of the film was demonstrated as it could be key for practical applications.

This experimental work provides a fundamental understanding of the structural and dynamic behaviour of the interlayer space of LDH coatings which would largely open the possibilities of applications. Additional work is ongoing to demonstrate the functionality of the loaded and released anions. Antimicrobial, antiadhesive or antifouling properties could be obtained with these surfaces which would be of great interest either as a release/uptake system or active coating for food packaging, self-disinfecting surfaces in medicine, waste-water treatment or marine environments.

Selected references

1. S. Soulé, P. Durand, S. El-Kirat-Chatel, F. Quilès, C. Carteret, Materials Today Chemistry, Volume 35, 2024, 101897.

O62 - Fabrication of multilayered biofilms using gas cluster ion beam assisted deposition

7. DPR – Thin Films, Coatings and Depth Profiling

Benjamin Tomasetti[1]
Mehdi Lakhdar[1], Christine Dupont[1], Clément Lauzin[1], Arnaud Delcorte[1]
[1] UClouvain (Louvain-La-Neuve, Belgium)

Gas Cluster Ion Beam (GCIB) assisted deposition is used to build multilayered protein biofilms. In this process, $Ar_{3000\text{-}5000}^+$ clusters bombard and sputter molecules from a reservoir (target) to a collector, an operation that can be sequentially repeated with multiple targets. The process occurs under vacuum, making it adequate for further sample conservation in the dry state, since many proteins do not have long-term storage stability in the aqueous state. An important advantage of the method is that the thickness and the bioactivity of the deposited protein layers are both proportional to the argon ion dose (number of Ar_n^+ clusters), a parameter meticulously regulated. The impact of large clusters composed of a few thousands of atoms is sufficiently soft to transfer large molecules. Indeed, the internal energy of the desorbed molecules is low enough to avoid fragmentation. The detection of large intact proteins by SDS-page gel electrophoresis and bioassay (trypsin at ≈25 kDa and glucose oxidase at ≈80 kDa) after their deposition on a collector was recently demonstrated, in agreement with the predictions of molecular dynamics (MD) simulations. [1] In turn, multilayered biofilms can be fabricated by successive transfers (Figure 1). These multilayers remain separate and can be built on any substrate, as shown by ToF-SIMS measurements. As an example, glucose oxidase (GOx) and horseradish peroxidase (HRP), two proteins involved in the same enzymatic cascade, were successively deposited on β-D-glucose to build an on-demand delivery system. On-demand means that the enzymes and the substrate (β-D-glucose) are combined in a trilayer, and the reaction occurs only upon reintroduction into solution.

Selected references

[1] S. Bertolini, A. Delcorte, J. Phys. Chem. B 127 (2023) 9074–9081.

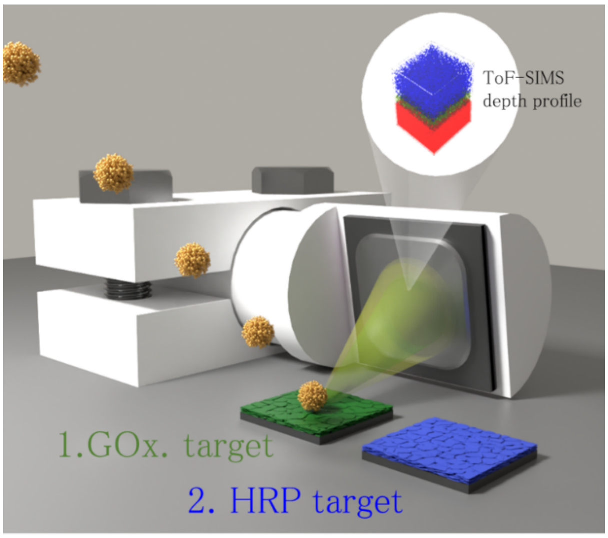

O63 - Femtosecond laser ablation (fs-LA) XPS depth profiling of lead halide perovskite thin film solar cells

7. DPR – Thin films, Coatings and Depth Profiling

Charlie Chandler[1]
Simon Bacon[2], Steven Hinder[1], Dhilan Devadasan[2], Jae Yun[3], Helen Park[4], Mark Baker[1]
[1] The Surface Analysis Laboratory, School of Mechanical Engineering Sciences, University of Surrey, Guildford, Surrey, GU2 7XH, UK
[2] Thermo Fisher Scientific, 1 The Feldbridge Centre, Imberhorne Lane, East Grinstead, West Sussex, RH19 1XP, UK
[3] Advanced Technology Institute, University of Surrey, Guildford, Surrey, GU2 7XH, UK
[4] Advanced Materials Division, Korea Research Institute of Chemical Technology (KRICT) ,Daejeon 34114, South Korea

Perovskites are finding strong interest as thin film solar cell materials for space applications. XPS depth profiling of a spin-coated formamidimium lead Iodide ($CH_5N_2PbI_3$) perovskite based thin film solar cell, both as-deposited and following environmental testing has been performed. Profiles have been recorded using traditional monatomic and cluster ion beam bombardment and compared to those recorded using a new femtosecond laser ablation (fs-LA) approach. The femtosecond laser employed has a 1030 nm peak wavelength and pulse length of 160 fs. Monatomic and cluster ion sputter depth profiling of the perovskite results in preferential sputtering of C, N, and I whilst fs-LA retains the original composition and chemical state information with no observed damage. The fs-LA XPS depth profiles highlight important changes in the perovskite chemical composition following environmental testing affecting the device performance.

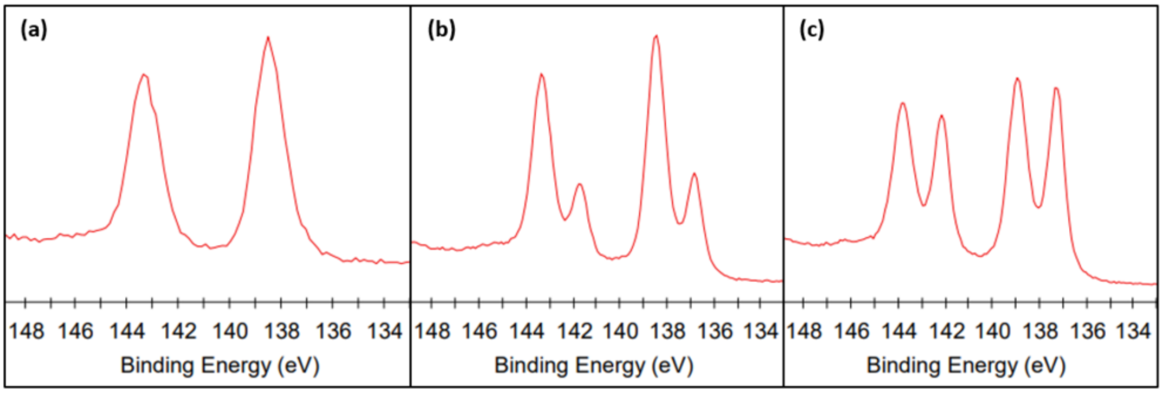

Figure 1: *XPS Pb 4f spectra: (a) fs-LA; (b) 500 eV Ar^+; (c) 8 keV Ar_{150}^+*

O64 - Femtosecond laser ablation (fs-LA) – A new approach to XPS depth profiling

7. DPR – Thin Films, Coatings and Depth Profiling

Mark Baker[1]
Simon Bacon[2], Stephen Sweeney[3], Steve Hinder[1], Adam Bushell[2], Tim Nunney[2], Richard White[2]
[1] School of Mechanical Engineering Sciences, University of Surrey, Guildford, Surrey, UK
[2] Thermo Fisher Scientific, 1 The Feldbridge Centre, Imberhorne Lane, East Grinstead, West Sussex, UK
[3] James Watt School of Engineering, College of Science and Engineering, University of Glasgow, UK

XPS depth profiling is a widely employed analytical technique to determine the chemical composition of thin films, coatings and multi-layered structures, due to its ease of quantification, good sensitivity and chemical state information. Since the introduction of XPS as a surface analytical technique more than 50 years ago, depth profiles have been performed using ion beam sputtering. However, many organic and inorganic materials suffer from ion beam damage, resulting in incorrect chemical compositions to be recorded during the depth profile. This problem has been resolved for most polymers through the use of argon gas cluster ion beams (GCIBs), but the use of GCIBs does not solve the issue for inorganics. A prototype XPS depth profiling instrument has been constructed which employs a femtosecond laser rather than an ion beam for XPS depth profiling purposes. This novel technique has shown the capability of eradicating chemical damage during XPS depth profiling for all initial inorganic, compound semiconductor and organic materials examined. The technique is also capable of profiling to much greater depths (several 10s microns) and is much faster than sputter XPS sputter depth profiling. fs-LA XPS depth profiles results will be shown for selected thin films, coatings, multilayers and oxidised surfaces and the outlook for this new technique discussed.

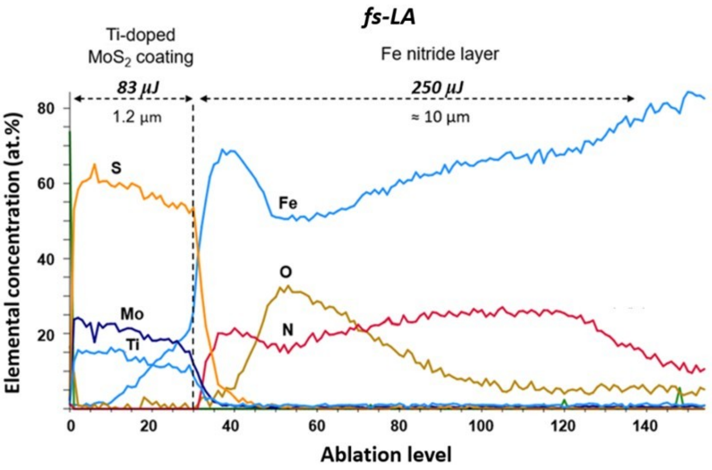

***Figure 1**: fs-LA XPS depth profile of a EN31CrMoV9 steel subjected to a duplex gas nitriding surface treatment followed by PVD deposition of a titanium-doped molybdenum disulfide (MoS_2:Ti) coating*

O65 - Highly transparent, stable, and superhydrophobic coatings for glass and PV panels

7. DPR – Thin Films, Coatings and Depth Profiling

Zineb Matouk[1]
[1] Technology Innovation Institute , Abu Dhabi, UAE

Superhydrophobic coating As advancements in material engineering and coating industries progress, the interest in superhydrophobic coatings with exceptional water repellent properties has intensified among researchers. A superhydrophobic surface is typically characterised by a water droplet contact angle (CA) exceeding 150°, and when the surface is gently tilted at an angle of 5° or less, the droplet tends to roll off or slide away.

Superhydrophobic coatings offer versatile performance across various sectors. They find applications in self-cleaning for automotive windshields and solar photovoltaic (PV) panels in the solar power industry, corrosion resistance for maritime infrastructures and vessels in the marine sector, and anti-icing properties for airfoils and empennage in the aircraft field, among others.

This study emphasizes the development of dust-repellent coatings specifically tailored for PV panels used in the UAE region, known for its challenging environmental conditions. Transparency emerges as a critical attribute of superhydrophobic coatings, particularly for optical surfaces like car windshields, PV panels, and solar collectors. These panels utilize sunlight for heat and electricity generation, necessitating optimal light transmission. Superhydrophobic coatings possess anti-reflective properties that minimize solar energy loss due to sunlight reflection, thereby enhancing photoelectric and photothermal conversion efficiency.

The results presented herein outline a dip coating method for creating transparent superhydrophobic films, incorporating functionalized nanoparticles within a binder matrix. By adjusting nanoparticle concentration within the thin film, surface roughness and chemistry can be finely tuned to achieve superhydrophobic properties while maintaining transparency.

The dip-coated films exhibit a significant increase in contact angle (WCA) as nanoparticle concentration increases. The WCA drastically increases from 80° for the reference sample (without nanoparticles) to up to 155° for the nanoparticle-incorporated films. It is demonstrated that the superhydrophobicity of the films mainly depends on surface roughness and/or chemical composition. Scanning electron microscopy (SEM) measurements indicate that roughness increases with nanoparticle incorporation. Additionally, XPS measurements show an increase in silanol group (Si-OH) density at the surface, contributing to higher hydrophobicity of the films. Moreover, the transmittance of the deposited film is enhanced with the addition of nanoparticles.

XPS Versa Probe III equipped with a Hot/cold stage providing temperatures from -140°C to +600°C, was used to conduct temperature-dependent analysis to assess the durability of the films under varied temperature conditions.

O66 - Interactions of a latent curing agent and metal oxides – relation of pH of the varnish and isoelectric point of surfaces

7. DPR – Thin Films, Coatings and Depth Profiling

Gary Säckl[1, 2]
Gernot Wallner[1, 3], Jiri Duchoslav[2], Cornelia Marchfelder[1, 3], David Stifter[2]
[1] Christian Doppler Laboratory for Superimposed Mechanical-Environmental Ageing of Polymeric Hybrid Laminates (CDL-AgePol), Johannes Kepler University Linz, Altenberger Str. 69, 4040 Linz
[2] Center for Surface and Nanoanalytics (ZONA), Johannes Kepler University Linz, Altenberger Str. 69, 4040 Linz, Austria
[3] Institute of Polymeric Materials and Testing (IPMT), Johannes Kepler University Linz, Altenberger Str. 69, 4040 Linz, Austria

Epoxy coatings are found in several industrial applications. A special trend are water-borne epoxies which allow for rather thin coating layers. For delayed crosslinking of epoxy varnishes, dicyandiamide (DICY) is established as latent curing agent. The amine-based hardener of the coating formulation is highly reactive. In a previous study, chemical interactions of DICY with metal surfaces were ascertained. The main focus of this work is a more comprehensive and systematic assessment considering various metal substrates differing in the isoelectric point (IEP) of the metal oxide. Six metal (oxides) with IEPs ranging from 3 to 12 were examined. First, immersion tests of the metal substrates in a boiling solution of DICY in pure water were performed. The products of the reaction were characterized by X-ray photoelectron spectroscopy (XPS). It was confirmed that an isoelectric point of the metal oxide below, above or close the pH of the used solution results in different chemical interactions. While a low IEP caused the amine groups to protonate, a higher IEP increased the peak intensity of the imine group. Less pronounced interactions were confirmed when the IEP was similar to the pH values. Under certain conditions such as catalytic TiO_2, also nitro groups were detected.

In a next step, epoxy coated metal sheets were evaluated using cryo ultra-low-angle microtomy (cryo-ULAM) and XPS. In agreement with previous work, an enrichment of the hardener at the exposed metal/polymer interface was deduced for some of the substrates. In comparison to the results of the immersion tests, a good agreement of the detectable reaction products and the relationship between IEP of the substrate and the pH of the varnish was ascertained.

O67 - Interferometric NIR optics for liquid analysis

7. DPR – Thin Films, Coatings and Depth Profiling

Javier Lloreda[1]
Jorge Gil-Rostra[1], Agustín R González-Elipe[1], Ramón González[2], **Francisco Yubero**[1]
[1] Instituto de Ciencia de Materiales de Sevilla, CSIC - USE, Sevilla, Spain
[2] Instituto de Ciencias de la Vid y del Vino, CSIC – Univ. La Rioja, Logroño, Spain

Evaluation methods for the monitoring of industrial fluids such biofuel, milk products, oils, soft drinks, or alcoholic beverages are needed to control evolution of liquid phase reactions and quality of the final products. Among the technique's available, high-pressure liquid chromatography or mass spectrometry provide analysis with great precision, however they are not very attractive for automatic label-free monitoring of industrial processes because they are slow, complex and expensive to operate online. An analytical technique capable of overcoming these drawbacks is Near Infrared Spectroscopy (NIRS) [1], which has been extensively used in the pharmaceutical and agri-food industry. In fact, there are several commercial NIRS based apparatus for label-free analysis of liquid samples available on the market. However, they are often designed for static laboratory applications and they are difficult to adapt to for automatic evaluation in an industrial environment.

In this presentation we will introduce a new low cost NIRS based fluid analyzer prototype that allows static (for traceability and quality control) and dynamic (for monitoring transformation processes) liquid analysis. It is based on an optofluidic cell that operates in transflectance mode and a specific interferometric variable NIR band-pass filters that replace expensive NIR monochromators based on diffraction gratings or Fourier Transform optics. The filters consist of Fabry-Perot wedged cavities built up by Si/SiO_2 multilayers fabricated by a magnetron sputtering deposition process. The optical path of the optofluidic cell as well as the filter response are designed to optimize the signals from the overtones and combination bands of O-H and C-H functional groups of the molecular components of liquid samples in the 1500-2000 nm NIR range. We will focus on the description of the multilayer manufacturing procedure and the physico-chemical and optical analysis of the interferometric variable band pass filter, as well as the performance of the device to monitor alcoholic fermentation processes.

Acknowledgement

Financial support provided by the Spanish Ministry of Science and Innovation (grant PDC2021-121379I00) is acknowledged.

Selected references

[1] B.H. Stuart, Infrared Spectroscopy: Fundamentals and Applications, 2004 (10.1002/0470011149).

O68 - Multidimensional Elemental and Molecular Analysis for Surface & Interface studies

7. DPR – Thin Films, Coatings and Depth Profiling

Patrick Chapon[1]
Alice Stankova[1]
[1] HORIBA

Surface and Interface corrosion studies require the use of complementary analytical techniques as each instrumentation provides results based on the interaction of the investigated material with a probing medium [1].

Obtaining elemental and molecular information for different probing size and depth are especially crucial HORIBA offers a Platform with multiple instruments able to tackle these complex analytical challenges.

Glow Discharge Optical Emission (GD) relies on a plasma to sputter a representative area of a material and provides fast elemental depth profile with nanometer resolution [2].

Coupling GD and Raman microscopy allows to obtain molecular information at various depths with micrometer lateral resolution [3,4].

Applying the GD software ideal to follow transient signals to a simultaneous ICP instrument coupled with an electrochemical cell (AESEC technique) offers deep insight on dissolution mechanisms and metallic surfaces performances [5].

We will illustrate the benefit of this Surface Platform for Elemental and Molecular Analysis with selected results on metallic parts for high temperature fuel cells, hard facing materials in Na fast reactors, perovskite solar cells, hydratation of anodic films and DCL coatings on bipolar plates.

Selected references

1) Compendium of Surface & Interface Analysis, Springer
2) Review: What Can Glow Discharge Optical Emission Spectroscopy (GD-OES) Technique Tell Us about Perovskite Solar Cells? Small Methods 2022, 2200633
3) Raman and glow discharge optical emission spectroscopy studies on structure and anion incorporation properties of a hydrated alumina film on aluminum. Applied Surface Science 592 (2022) 153321
4) Advances in RF Glow Discharge Optical Emission Spectrometry Characterization of Intrinsic and Boron-Doped Diamond Coatings. https://doi.org/10.1021/acsami.1c20785
5) Transient stainless-steel dissolution and its consequences on ex-situ bipolar plate testing procedure. International journal of hydrogen energy 45 (2020) 984-995

O69 - Optimal conditions for depth profiling with hard/soft multilayers using small cluster beams of C60, Ar and CO2

7. DPR – Thin Films, Coatings and Depth Profiling

Naoko Sano[1]
Kate McHardy[1], Paul Blenkinsopp[1]
[1] Ionoptika Ltd.

Large cluster ion beams, especially Gas Cluster Ion Beams (GCIBs), are a low-damaging, highly versatile ion source used predominantly for surface analysis of organic and biological samples. Ionised clusters of atoms/molecules accelerated to high energies (keV) are highly efficient at sputtering intact molecules from surfaces with reduced damage, making them suitable for applications from fundamental biology to materials science. Meanwhile, use of smaller-cluster GCIBs has also been reported as an efficient technique to provide chemical information in depth profiling of inorganic and organic hybrid multilayer semiconductor materials such as OLEDs, perovskite solar cells, and nano/micro-structured films. Smaller-cluster GCIBs have the feature of combining the strengths of monoatomic ion beam and large-cluster beams for depth profiles on hybrid materials.

When compared to traditional monoatomic or even C_{60} ion beams, these smaller GCIBs could potentially provide sufficient energy (over 20 eV/atom) to sputter inorganics effectively, whilst maintaining the advantages of larger cluster beams such as reduced inter-laying mixing, lower sub-surface damage and no carbon deposition. However, previous studies have been hindered by the low total beam energy available for analyses.

In this work, we demonstrate the advantages of using smaller GCIBs to hybrid materials including semiconductor devices and TiO coating on polymer film as fast and less preferential sputtering when compared to both monoatomic ion beam and large-cluster beams.

Utilising the 70 keV GCIB on the J105 Cluster SIMS (Ionoptika Ltd, UK) allows the potential for higher total beam energy, offering the ability to study a wide range of cluster parameters including various gas species such as $(Ar)_n^+$ and $(CO_2)_n^+$ and also C_{60}^+ cluster ion beams with a range of beam energies and cluster sizes.

Initial results show that C_{60}@20 kV (333 eV/atom) had the preferential sputtering effect from a TiO/polymer sample, but Ar_{210}@ 70keV (333 eV/atom) did not as shown in the figure below. Included in the results, we will discuss the phenomenon amongst the cluster beams to optimise the best sputter conditions for hybrid materials.

There is no universal condition for depth analysis, however, it is possible to choose a set of conditions that will be more or less optimal depending on the experimental goals, *i.e.* maximising sputter rate, depth resolution, or molecular ion yield with fewer artefacts due to sputtering. These results are valid for XPS, SIMS, and any technique that utilises GCIBs.

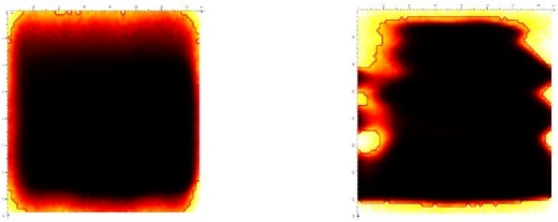

(a) (b)

Figure: Illustrations of preferential sputtering effects by (a) a 70kV Ar$_{210}$ *GCIB (333 eV/atom), and (b) a 20 keV C*$_{60}$ *cluster beam (333 eV/atom) on a 2μm TiO film on polymer substrate*

O70 - P-ARXPS analysis and ion profiling of nanometer-thick polyphosphazene (PPP) films on n-InP

7. DPR – Thin Films, Coatings and Depth Profiling

Gianluca Visagli[1]
Mathieu Fregnaux[1], Arnaud Etcheberry[1], Anne-Marie Gonçalves[1]
[1] Institut Lavoisier de Versailles UMR8180 CNRS_UVSQ

The $NH_{3(liq)}$/n-InP junction allows to perform a passivation by dissolution anodic/precipitation of a polyphosphazene film (PPP). The electrochemical responses allow us to assume the existence of an ultra-thin nitrided passivating film, with high reproducibility of overlap and remarkable post-growth chemical stability. XPS film analysis demonstrates the "phosphazene-like" signature of the film and reinforces the electrochemical hypothesis of an ultra-thin film ($e_{PPP<10nm}$). The passivated surface can be chemically described as a polymer/SC heterojunction: -(NH_2-P=N)-(n-InP). This hypothesis is consistent with the photoemission response. It implies a very particular chemical arrangement on the surface that implicates a double energy distribution for nitrogen as well as for phosphate and a matrix signal attenuated by the overlay. All these points have been established, it remains to work on the spatial organization of the film, known to be perpendicular to the surface. This is what will be presented in this contribution.

To differentiate the spatial arrangement of the film, an angularly resolved XPS response was used. The analysis was performed in a p-ARXPS configuration (Thermo Theta Probe spectrometer) which allows, by angular sectorization of the emission without rotation, to determine the evolution of the different signals.

The angular dependence of the "double" energy bond distribution of the N1s level has been established as well as the correlated dependence of the P2p – 133eV contribution following the previous XPS information. The “buried” nature of the In3d contribution as well as that of P2p-129eV has also been demonstrated by this approach. The work on the angular dependence of the O1s and C1s signals present in the responses showed that these two elements are involved in the outermost part of the film. These points must be considered to describe the contribution of the carbon contamination but also the reactivity of the film on the "external carpet of amine functionalities" at the time of the rupture of the junction and the extraction of the passivated surface. Figure 1 summarizes the spatial arrangement of the film by working together on the angular evolutions of the intensities of the different components of each core level. To complete this study, an XPS profiling was performed, which allowed us to reflect on the "peeling" of the laminated structure as soon as the inorganic polymer skeleton was partially destructured. The confrontation/complementarity between these two approaches will be discussed by way of conclusion.

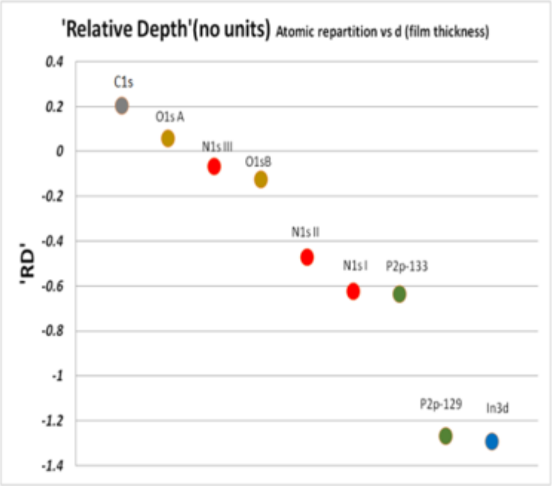

Figure 1. p-ARXPS atomic ripartition in the PPP film

O71 - Polyelectrolyte adsorption on different surfaces evaluated by XPS using two different quantification approaches

7. DPR – Thin Films, Coatings and Depth Profiling

Marie Ernstsson[1]
Per M. Claesson[2]
[1] RISE Research Institutes of Sweden, Material and Surface Design Department, Stockholm, Sweden
[2] KTH Royal Institute of Technology, Division of Surface and Corrosion Science, Stockholm, Sweden

The X-ray photoelectron spectroscopy (XPS) technique was employed to quantify the adsorption of differently charged cationic polyelectrolytes from aqueous solutions of low ionic strength onto negatively charged mica, glass, and silica substrates. Before the adsorption experiments, the silica surfaces were pretreated in two ways, using either base or acid media as the last step (silica-base last or silica-acid last, respectively).

Two quantification approaches to calculate the adsorbed amount, expressed as a surface density (atoms/nm^2 or mg/m^2), will be outlined in the presentation. These approaches are based on using either mica, or the atomic density of the substrate, as calibration standard. Consistent results for the adsorbed amount of polyelectrolyte were obtained independent of the approach chosen. Since only one set of measurement is necessary using the atomic density approach, instead of two when employing the mica calibration method, it is suggested that the atomic density approach is more convenient.

The adsorbed amount for each polyelectrolyte was dependent on the surface and followed the order mica > silica-base last ≈ glass > silica-acid last (see figure below). For each substrate the adsorbed amount increased with decreasing polyelectrolyte charge density of the polyelectrolyte (100% to 1% of segments being charged). In the figure different colors are used for the differently charged polyelectrolytes: 100% (white), 10% (light grey) and 1% (dark grey).

For the low charge density polyelectrolytes the adsorbed amounts were high, but at the same time the number of charged segments per square nanometer was low. The reason for this is that steric repulsion between the polyelectrolyte chains limited the adsorption.

For the highly charged polyelectrolytes the adsorbed amounts were controlled by electrostatic interactions, and the adsorbed amount therefore closely correspond to that needed to neutralize the surface charges on the substrate. The number of charged segments per square nanometer in the adsorbed polyelectrolyte layer thus gives an estimate of the surface charge density for each substrate, decreasing in the following order mica > silica-base last ≈ glass > silica-acid last.

For silica the choice of cleaning method strongly affected the adsorbed amount, indicating that the cleaning process influenced the surface concentration and fraction of different silanol groups. Our results show that a higher density and/or more acidic silanol groups are formed when using base, instead of acid, treatment in the last step.

Selected references

Ernstsson M, Dedinaite A, Rojas OJ, Claesson PM.
Two different approaches to XPS quantitative analysis of polyelectrolyte adsorption layers.
Surf Interface Anal. 2023;55(1):26-40. doi:10.1002/sia.7154

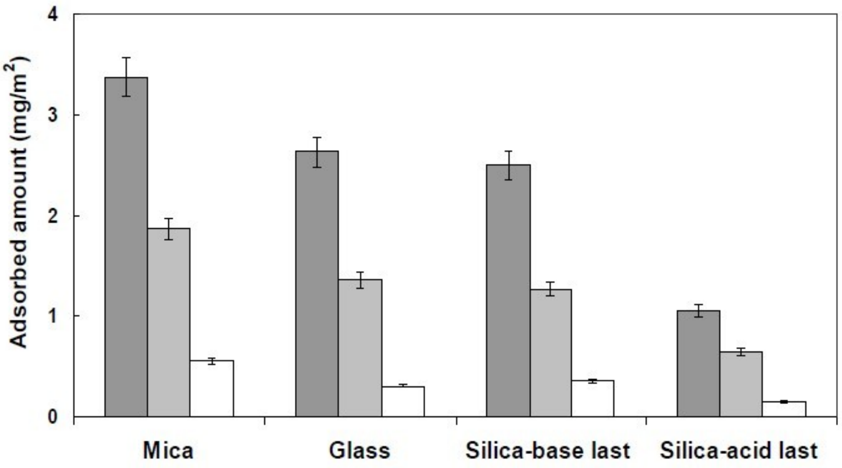

O72 - Stability investigation of atomic layer deposited cerium oxide depending on oxidant choice

7. DPR – Thin Films, Coatings and Depth Profiling

Rudi Tschammer[1]
Yuliia Kosto[1], Carlos Morales[1], Carlos Alvarado[2], Andreas Schubert[2], Karsten Henkel[1], Christian Wenger[2], Jan Ingo Flege[1]
[1] BTU Cottbus-Senftenberg, Applied Physics and Semiconductor Spectroscopy, Germany
[2] IHP – Leibniz Institute for High Performance Electronics, Materials for Micro- and Nanoelectronics, Germany

Atomic layer deposition (ALD) has been used extensively to grow homogeneous films with excellent coverage and atomic-scale thickness control for a variety of applications. However, remaining challenges include unraveling the complex interplay between substrate and deposit as well as the oxide film and potential capping layers, which can cause significant deviations from bulk properties, especially for ultrathin (< 20nm) layers. In this work, we present a detailed investigation of ultrathin cerium oxide films grown using the novel Ce(dpdmg)$_3$ precursor with H_2O, O_2, and O_3 on different substrates. Using in-situ X-ray photoelectron spectroscopy and operando spectroscopic ellipsometry allows us to gain first-hand information on the growth dynamics without exposure to ambient conditions, revealing distinct changes in growth mode, oxide stoichiometry (see Fig. 1a), and residual contamination (see Fig. 1b-c) mediated by the use of different oxidants. Combined with ex-situ characterization by Raman spectroscopy and transmission electron microscopy, we are able to establish the connection between our in-situ observations and the formation of a stable oxide-substrate interface under ambient conditions, which is crucial for use in future applications.

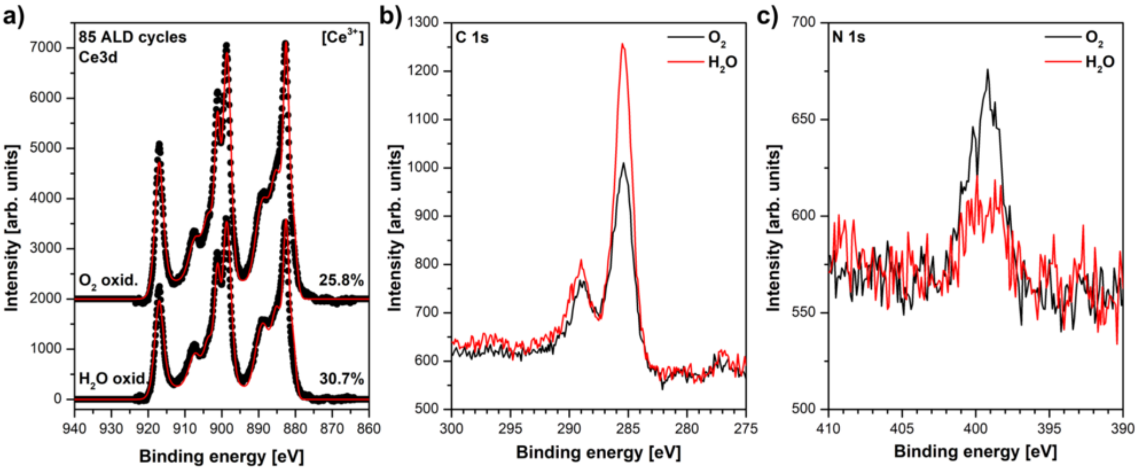

Fig. 1 a) Comparison of Ce3d XPS spectra for 85 ALD cycles of CeO$_x$/Si with different oxidants (black lines) and the respective Ce^{3+}-concentration determined from fitting (red lines), b) C1s XPS spectra and c) N1s XPS spectra for 85 ALD cycles of CeO$_x$/Si with different oxidants

O73 - Surface Analysis of Nanolayers by LEIS, SIMS and XPS

7. DPR – Thin Films, Coatings and Depth Profiling

Birgit Hagenhoff[1]
Jan Tröger[1, 2], Daniel Breitenstein[1], **Danica Heller-Krippendorf**[1]
[1] Tascon GmbH, Mendelstraße 17, 28149 Muenster, Germany
[2] University of Muenster, Wilhelm-Klemm-Str. 10, 48149, Muenster, Germany

Advanced and smart materials nowadays consist of various materials featuring layers and layer systems at the nanoscale. In order to monitor the development process as well as production and customer returns, analytical techniques are required which have an information depth suited for the layered samples.

Starting with information from the outermost atomic layer using Low Energy Ion Scattering (LEIS), adding Time-of-Flight SIMS (ToF-SIMS) for the outermost 3-5 monolayers and ending with X-ray Photoelectron Spectroscopy (XPS) for accessing up to 20 monolayers, a detailed insight can be gained into the composition of layers at the nanoscale. On the other hand, layer systems the structure of which is well known can help to better understand the performance features of the different analytical techniques.

In our ongoing studies we have compared analytical results from LEIS, ToF-SIMS and XPS for various layered systems. We will report on films produced by Atomic Layer Deposition (ALD) as well as core-shell nanoparticles. Amongst the three, XPS is the most often used technique in industry because of its power to obtain quantitative results. Our comparative data will help to put XPS data in a suited information depth perspective.

O74 - Synthesis of ultra-thin advanced MOF-like materials by use of ALD and their characterization

7. DPR – Thin Films, Coatings and Depth Profiling

Jakob Rath[1]
Bernhard Fickl[1], Daniel Matulka[1], Tomas Gregan[1], Nick Parak[1], Laura Aichinger[1], Gerlinde Habler[2], Njomza Isufaj[1], Shaghayegh Naghdi[1], Markus Sauer[3], Florian Fahrnberger[3], Herbert Hutter[3], Annette Foelske[3], Bernhard Christian Bayer[1], Dominik Eder[1]
[1] Institute for Materials Chemistry, TU Wien
[2] Department for Lithosphere Research, Uni Wien
[3] Analytical Instrumentation Center, TU Wien

New strategies for design and implementation of ultrathin coatings of various materials on a multitude of different substrates have been on the rise for the past decades now. At the moment, we experience the opportunity to utilize a vast spectrum of possible methods for both, synthesis and characterization of these new materials. While many established methods for the deposition of thin films (CVD, PVD) offer outstanding properties in terms of speed, scalability and cost-effectiveness, they are somewhat limited in terms of uniformity of coatings on surfaces of complex geometry and often restricted to producing materials of lower complexity, like oxides or nitrides.

Atomic layer deposition (ALD) may be seen as a state-of-the-art thin-film deposition technique capable of bypassing these limitations, since the coating process is self-limited and diffusion-controlled, thus, enabling coating of highly complex substrates with a very uniform layer and allowing for thickness control in the sub-nm region. The large variety of existing – and constantly expanding – precursors, very recently, allowed for coating with intricate matter, like transition-metal dichalcogenides (TMDs) and metal organic frameworks (MOFs). [1,2]

Herein, we report on the first attempt of all-gas-phase ALD synthesis of the MOF Ti-MIL-125 on silicon wafers and silicon nanoparticles followed by alternating layers consisting of Ti-MIL-125 and UiO-66. The ALD films have been characterized by means of STEM-EDX (Fig 1a) and TOFSIMS as well as XPS depth-profiling (Fig 1b). The data confirmed that (i) ALD is suitable for synthesis of ultrathin MOF-films on complex substrates, such as nanoparticles, and (ii) high-quality nano-laminates consisting of various different MOFs can be synthesized.

Since materials produced by ALD often lack crystallinity, structure determination using XRD does not provide sufficient understanding. Anyway, the use of Raman Spectroscopy, ssNMR and EXAFS provides a good explanation of the atomic arrangement in these materials. A set of further characterization techniques, like BET-physisorption measurements, enabling an even deeper understanding on these novel MOF-like materials will be presented.

Selected references

(1) Cai, J.; Han, X.; Wang, X.; Meng, X. Atomic Layer Deposition of Two-Dimensional Layered Materials: Processes, Growth Mechanisms, and Characteristics. *Matter* **2020**, *2* (3), 587–630. https://doi.org/10.1016/j.matt.2019.12.026.
(2) Lausund, K. B.; Nilsen, O. All-Gas-Phase Synthesis of UiO-66 through Modulated Atomic Layer Deposition. *Nat. Commun.* **2016**, *7* (1), 13578. https://doi.org/10.1038/ncomms13578.

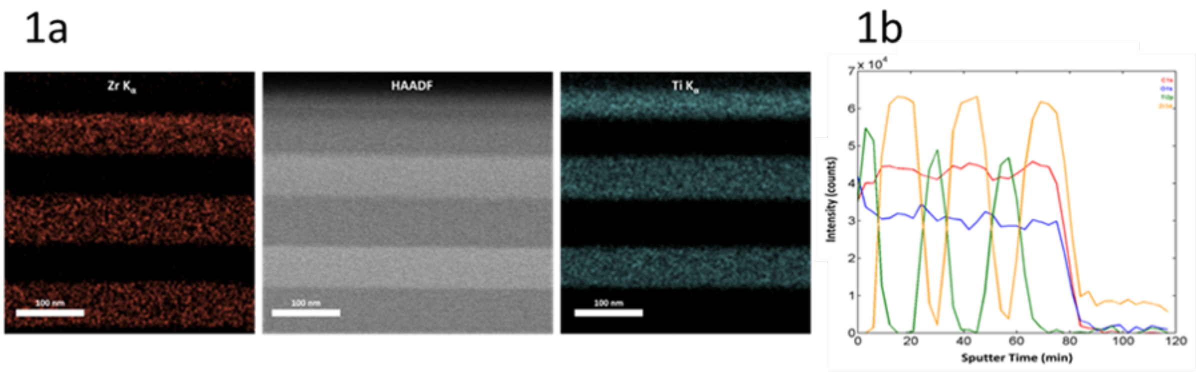

Figure 1: a – STEM-EDX maps of a nanolaminate film consisting of alternating layers of two ALD-synthesized MOF-like materials, b – corresponding XPS-depth profile threw a nanolaminate film consisting of alternating layers of two ALD-synthesized MOF-like materials

O75 - The effects of substrate interaction on the chemical properties of atomic layer deposited ultrathin ceria layers

7. DPR – Thin Films, Coatings and Depth Profiling

Carlos Morales[1]
Rudi Tschammer[1], Julia Kosto[1], Carlos Alvarado-Chavarin[2], Christian Wenger[2], Ignacio Villar-Garcia[3], Virginia Pérez-Dieste[3], Karsten Henkel[1], Jan Ingo Flege[1]
[1] Brandenburg University of Technology, Cottbus, Germany
[2] IHP - Leibniz-Institut für innovative Mikroelektronik, IHP, Frankfurt (Oder), Germany
[3] NAPP Station, CIRCE Beamline, ALBA synchrotron, Cerdanyola del Vallès, Spain

Nowadays, atomic layer deposition (ALD) has gained prominence in the materials and surface science communities owing to its well-controlled layer-by-layer deposition and growth conformity on 3D structures [1], finding multiple uses in various fields. Besides, the ALD technique is also well known to lead to amorphous and defective, non-stoichiometric thin films, resulting in modified material properties that may even preferentially be used in certain applications. For example, the formation, diffusion, and recovery of oxygen vacancies in reducible metal oxides can be favored in disordered films compared to more ordered deposits, whereas interdiffusion processes can critically affect the film/substrate interface region. However, most ALD-based studies deal with relatively thick layers (>10 nm) that neglect film/substrate interaction, which might initially modify the growth reaction mechanism, create complex interfaces, and change the electronic and chemical properties.

These effects have extensively been studied for thin ALD-ceria films grown using the commercial $Ce(thd)_4$ organometallic precursor and O_3/O_2 by combining in-situ and ex-situ characterization techniques in our lab [2] and at synchrotron radiation facilities, focusing on its early stages of growth, the effects of film/substrate interaction on catalytic applications, and its reducibility at low temperatures as a function of different growth parameters. Interestingly, initial in-situ X-ray photoemission spectroscopy (XPS) measurements of ceria ALD-deposits on Al_2O_3/Si, sapphire, and SiO_2 substrates confirm a Ce^{3+}/Ce^{4+} mixture dependent on the substrate interaction, deposit thickness, and morphology. Using near-ambient pressure XPS, we have significantly reduced ultrathin (<10 nm) ALD-ceria films by exposing them to different H_2/O_2 partial pressures at lower temperatures (300 – 525 K) than thicker films grown by physical vapor deposition techniques [3]. Interestingly, these experiments combined with hard-X-ray photoemission spectroscopy (HAXPES) measurements have shown that this reducibility at moderate temperatures critically depends on the film/substrate interaction, inhibited for alumina substrates due to the formation of aluminates at the interface regions, which prevent further oxidation. Furthermore, the comparison with more ordered films grown by other methods indicates a key role of the defective structure of ALD films in Ce^{3+}/Ce^{4+} conversion.

Selected references

[1] V. Cremers, et al., *Appl. Phys. Rev.* **6**, 021302 (2019)
[2] C. Morales et al. *Inorganics* **11** 477 (2023)
[3] K. Suzuki et al. Sens. *Actuators B Chem.* **250** 617 (2017)

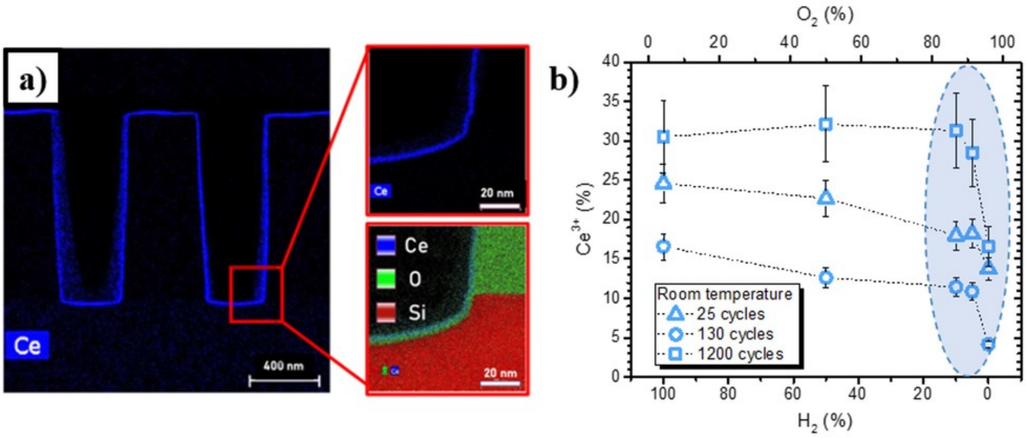

Figure 1. *a) Ce-EDX false color TEM images of CeO_x (150 cycles) deposited on Si-nanostructured substrates; b) percentage of Ce^{3+} states as a function of H_2 content in the H_2/O_2 mixture at room temperature.*

O76 - Towards a high-entropy alloy thin-film reference material

7. DPR – Thin Films, Coatings and Depth Profiling

Elisabeth John[1]
Matthias Weise[1], Mario Sahre[1], Jörg Manfred Stockmann[1], Thorid Lange[1], Jörg Radnik[1], Vasile-Dan Hodoroaba[1]
[1] Bundesanstalt für Materialforschung und -prüfung, Unter den Eichen 87, 12205, Berlin, Germany

Analyzing materials composed of multiple elements with spectroscopic techniques such as X-ray Photoelectron Spectroscopy (XPS), Auger-Electron Spectroscopy (AES) or Electron Probe Microanalysis (EPMA), can be challenging due to spectral overlap. Moreover, each analytical method introduces its own set of challenges, e.g., the strong secondary fluorescence effect for neighbor elements in EPMA, thus, making the accurate elemental quantification in such materials difficult. When the material is available as thin film, additional constraints are inherently present. To provide a reference material for these analytical challenges high entropy alloys (HEAs) are excellent candidates. Currently, there is no thin film reference available containing more than 2 elements.

Unlike traditional alloys, which typically consist of one or two main elements and smaller amounts of secondary elements, HEAs are characterized by the presence of multiple principal elements in almost equal proportions. This unique composition results in a high degree of disorder at the atomic level, leading to exceptional mechanical, physical, and often unexpected properties. HEAs have garnered significant attention in materials science and engineering due to their potential applications in a wide range of industries, from aerospace and automotive to electronics and renewable energy. [1]

For the preparation of a dedicated thin film reference material, we have chosen to prepare HEAs by magnetron sputtering, since it is not associated with elemental segregation that may occur due to the high configurational entropy of HEAs, which promotes atomic rearrangements [2]. Our goal was to prepare films with a homogeneous thickness and defined chemical composition to be analyzed by various methods dedicated to surface analysis.

The material, consisting of titanium, chromium, manganese, iron, and nickel was deposited as film on silicon substrates - to our knowledge the first HEA thin film of this type reported in literature. A set of different thickness of the films was chosen, on the one hand to facilitate the analysis with different techniques, and on the other side to evaluate the limitations of the respective methods. The films morphology was characterized as prepared by SEM followed by the analysis of their 2D compositional homogeneity by EDX, XRF, ToF-SIMS and XPS. in-depth chemical composition was evaluated by ToF-SIMS and AES. The outcomes of analyzing the initial batches of films will be presented.

Selected references

[1] George, E.P., Raabe, D. & Ritchie, R.O. High-entropy alloys. Nat Rev Mater 4, 515–534 (2019). https://doi.org/10.1038/s41578-019-0121-4
[2] Xue Hui Yan, et al., A brief review of high-entropy films, Materials Chemistry and Physics, 210, (2018), 12-19, https://doi.org/10.1016/j.matchemphys.2017.07.078.

O77 - Tuning the surface chemistry and structure of a phosphated zinc coating by hot active plasma

7. DPR – Thin Films, Coatings and Depth Profiling

Jiri Duchoslav[1]
Thomas Stehrer[2], David Stifter[1]
[1] Center for Surface an Nanoanalytics, Johannes Kepler University Linz, Altenberger Straße 69, 4040 Linz, Austria
[2] Fronius International GmbH, Günter-Fronius-Straße 1, 4600 Thalheim/Wels, Austria

The effect of hot active plasma (HAP) on the surface chemistry and structure of phosphated zinc coated steel was investigated in detail by means of electron microscopy and spectroscopy, with x-ray photoelectron (XPS) and scanning Auger electron spectroscopy (AES) used in a complementary way. In order to extend the scope of the methods from the surface down to the bulk of the investigated coatings, Ar^+ ion sputter depth profiling coupled with XPS was utilized. The results confirmed, at first, an assumed relationship between the intensity and the impact of the HAP treatment on the coating chemistry and structure. While a mild surface cleaning effect was observed for weak plasma treatments, with increased intensity the plasma caused already significant chemical and structural changes on the surface as well as down to the bulk of the treated material. Initially, a partial decomposition of zinc orthophosphate ($Zn_3(PO_4)_2$), as the sole surface constituent of the untreated coating, led to a mixed zinc metaphosphate ($Zn(PO_3)_x$) and zinc oxide (ZnO) phase, highly localized in randomly distributed micrometer sized stains on the treated surface. Finally, the most intensive HAP treatment led into a complete transformation of the zinc phosphate material into a porous and rough ZnO layer. Moreover, the heat contribution of the HAP treatment leading to a temperature rise of the treated sample up to 700 ºC as revealed by in-situ temperature measurements induced also remarkable modifications within the bulk of the coating – diffusion of zinc into the steel substrate – an effect mimicking a galvannealing process.

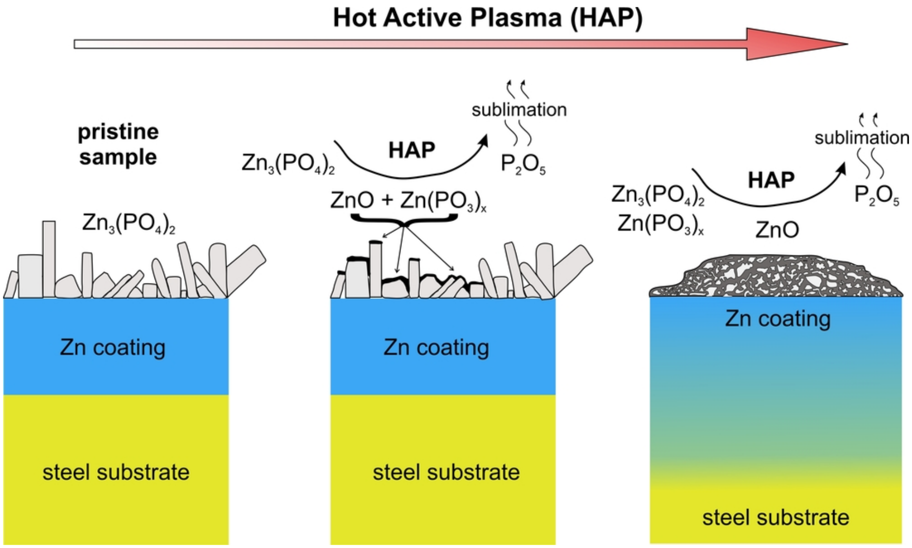

O78 - Unraveling Photostability of Multi-cation Hybrid Perovskites via Surface Analysis Techniques

7. DPR – Thin Films, Coatings and Depth Profiling

Wei-Chun Lin[1]
Jun-Xian Li[1], Yi-Kai Wang[1], Jui-Fu Tang[1]
[1] National Sun Yat-sen University

Recently, the efficiency of the organic/inorganic hybrid perovskite solar cell reached 25.7% in 2023. One of the next challenges is the long-term stability of perovskite crystals for further commercialization. In this study, we conducted a photo-induced degradation on three cationic compositional engineered perovskites, FA0.83MA0.17PbI3, Cs0.05(FA0.83MA0.17)0.95PbI3 and Cs0.05(FA0.83MA0.17)0.95Pb(I0.83Br0.17)3 upon exposure to AM1.5G solar spectra in a controlled environment. X-ray photoelectron spectroscopy (XPS), Auger electron spectroscopy (AES), and time-of-flight secondary ion mass spectrometry (ToF-SIMS) are used to confirm surface chemistry, 2D elemental mapping, and 3D molecular distribution, respectively. Here, it is found that methylammonium (MA) would preferentially escape during photo-degradation, which leads to the structural collapse of the crystal. The Cesium and formamidinium (FA) help to stabilize perovskite crystal with FAI and CsI bonding, which locks iodine down from vaporization. It is further demonstrated that chlorine-related molecules appear under 3 days of illumination, which is proved by the stabilizer MACl in the precursor. Moreover, the bromide doping helps to stabilize perovskite initially but leads to phase separation and material degradation eventually.

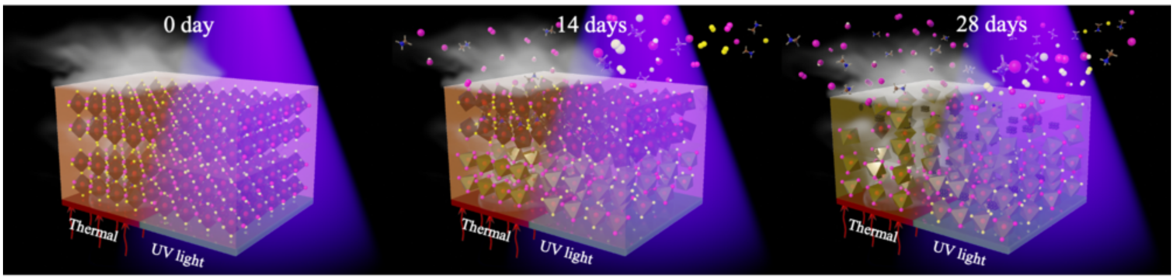

O79 - XPS characterization of thermochemical nitriding MoS2 template sub-layer to prevent AlN delamination during regrowth

7. DPR – Thin Films, Coatings and Depth Profiling

Nicolas Gauthier[1]
Julien Patouillard[1, 2], Rémy Gassilloud[1], Amélie Dussaigne[1], Stéphane Cadot[1], Nicolas Vaxelaire[1], Nicolas Bernier[1], Christine Raynaud[1], Frédéric Gianesello[2], Bérangère Hyot[1]
[1] Univ. Grenoble Alpes, FR-38000 Grenoble, CEA, LETI, Minatec Campus, FR-38054 Grenoble Cedex 9, France.
[2] STMicroelectronics, 850 rue Jean Monnet, F-38926 Crolles, France

AlN-based acoustic filters serve as crucial components in Radio Frequency (RF) communications. The current performances of these devices are limited on silicon substrates because of poor AlN crystal quality. This could be improved using ALD-grown 2D-MoS_2 thin film as a template on silicon. Nevertheless, after deposition of thicker sputtered AlN films (≥ 200 nm), a systematic delamination of the AlN/MoS_2 stack occurs which prohibits the integration of these materials in RF devices [1]. That is why a new elaboration process to grow thick AlN films with an improved crystal quality while avoiding the delamination issue is proposed in this work. This process is based on the chemical conversion of the MoS_2 through a very thin 5 nm AlN seed layer using an ammonia (NH_3) heat treatment [2]. A thorough XPS study was carried out to optimize a trade-off between the AlN thickness and the reactive annealing conditions allowing the diffusion of NH_3 towards the underlaying MoS_2 and its conversion into $Mo(O_x)N_y$. The synthesis and the analysis of molybdenum oxynitride by nitriding a well-controlled uniform molybdenum disulfide (MoS_2) layer via a 700 °C ammonia NH_3 reactive heat treatment without AlN seed layer was previously performed as reference [3,4]. The MoS_2 nitriding reaction has also been demonstrated by in-plane XRD analysis and its progressive conversion has been monitored by *in situ* reflectance measurements. To support the XPS measurements mentioned above, the films were also characterized by combining Raman micro-spectroscopy and TEM (transmission electron microscopy). Moreover, ToF-SIMS analysis highlighted the MoS_2 conversion even after a regrowth of a thick AlN film avoiding any interface (of interest AlN/MoN_x) air exposure. Finally, this new synthesis route allowed to improve the crystal quality of thick AlN layers deposited on low cost silicon substrate.

Acknowledgements

A part of this work, carried out on the Platform for Nanocharacterisation (PFNC), was supported by the “Recherche Technologique de Base” and "France 2030 - ANR-22-PEEL-0014" programs of the French National Research Agency (ANR).

Selected references

[1] Benech, P.; Duchamp, J.-M. Piezoelectric Materials in RF Applications. In *Piezoelectric Materials*; Ogawa, T., Ed.; InTech, 2016. https://doi.org/10.5772/63125.
[2] Patouillard, J. Optimization of Innovative AlN-Based Stacks and Texturing on 2D-MoS2 - Applications to Acoustic Wave Resonators and Power Electronics, Grenoble Alpes, Grenoble, 2023.
[3] Cadot, S.; Renault, O.; Frégnaux, M.; Rouchon, D.; Nolot, E.; Szeto, K.; Thieuleux, C.; Veyre, L.; Okuno, H.; Martin, F.; Quadrelli, E. A. A Novel 2-Step ALD Route to Ultra-Thin MoS_2 Films on SiO_2 through a Surface Organometallic Intermediate. *Nanoscale* **2017**, *9* (2), 538–546. https://doi.org/10.1039/C6NR06021H.

[4] J. Patouillard, R. Gassilloud, F. Mercier, A. Mantoux, R. Boichot, M. Bernard, N. Gauthier, S. Cadot, C. Raynaud, F. Gianesello, E. Blanquet. Chemical conversion of MoS_2 thin films deposited by atomic layer deposition (ALD) into molybdenum nitride monitored by *in situ* reflectance measurements. *J. Vac. Sci. Technol. A* 41, 052201 (2023). https://doi.org/10.1116/6.0002678

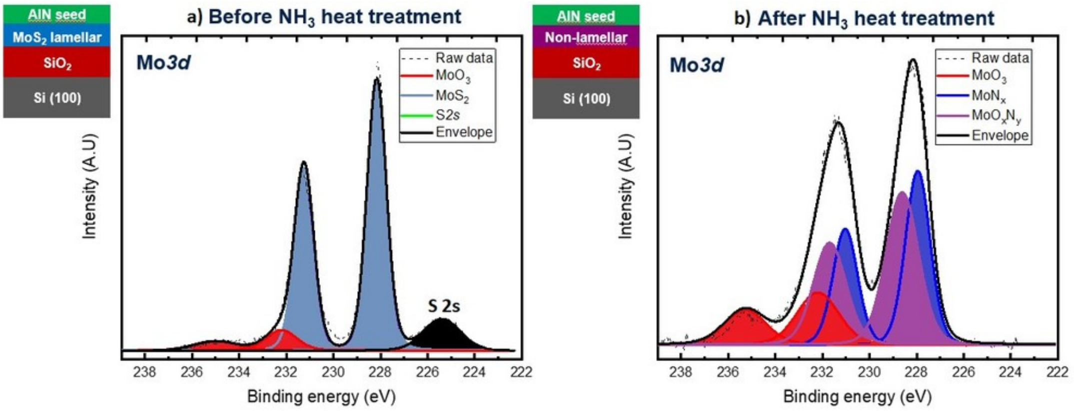

***Figure 1**: Mo3d XPS spectra of MoS_2 before a) and after 1000 °C NH_3 heat treatment b).*

O80 - XPS depth profiling of highly porous black metal films

7. DPR – Thin films, coatings and depth profiling

Matej Micusik[1]
Premysl Fitl[2], Martin Hruska[2], Peter Machata[1], Maria Omastova[1], Midori Kawamura[3]
[1] Polymer Institute SAS, Dúbravská cesta 9, 84541 Bratislava, Slovakia
[2] University of Chemistry and Technology Prague, Department of Physics and Measurements, Technická 5, 16628 Prague, Czech Republic
[3] Kitami Institute of Technology Kitami, Hokkaido, Japan

Black metals (BM) are highly porous nanocrystalline materials with a sponge-like structure with a high surface-to-volume ratio, and the ability to effectively capture incident light. The porous structure of these materials is the result of the presence of impurities during the growth of the metal film, which creates a structure with pores ranging from micron to subatomic sizes. BMs have been used in many applications such as electronics, including optical sensing, enhancement of thermal emitters and electrochemical sensing. Especially recent studies reported surface desorption processes on thin ferrous metal layers [1]. Different properties of BM can be achieved by changing the deposition conditions or by subsequent annealing.

Thin layers of various ferrous metals (Au, Ag, Pd, Al) were prepared and characterized, and their surface properties were characterized using XPS depth profiling and contact angle measurements. Gold BM films were then tested for the detection of hydrogen gas. The films exhibited micro- and nanostructured surfaces with nanoporous columnar morphologies consisting of gold grains and nanoparticles. The sensing mechanism was found to be primarily related to the interaction between hydrogen molecules and the nanoporous surface rather than hydrogen absorption in the gold lattice. Even after interacting with hydrogen, gold remained in a metallic state. The results showed a linear response in the hydrogen concentration range from 0.4% to 1.0% [2].

Acknowledgements

This work was supported by the V4-Japan 2021 Joint Call on Advanced Materials under registration number V4-Japan/JRP/2021/96/BLACKSENS and by agency VEGA 2/0006/22 (Slovakia).

Selected references

[1] P. Pokorny, M. Novotny, J. More-Chevalier, Y. Dekhtyar, M. Romanova, M. Davidkova, S. Chertopalov, P. Fitl, M. Hruska, M. Kawamura, T. Kiba, J. Lancok, Surface processes on thin layers of black aluminum in ultra-high vacuum, Vacuum 205 (2022), 111377, https://doi.org/10.1016/j.vacuum.2022.111377.
[2] M. Hruška, J. Kejzlar, J. Otta, P. Fitl, M. Novotný, J. Čížek, O. Melikhova, M. Mičušík, P. Machata, M. Vrňata. Hydrogen sensing capabilities of highly nanoporous black gold films. Applied Surface Science, 647 (2024), 158618, http://doi.org/10.1016/j.apsusc.2023.158618.

8. ELC – Micro-, Opto- and Organic Electronics

O81 - Advanced optimization of C&O species adsorbed on highly reactive surfaces during vacuum transfer step in microelectronic

8. ELC – Micro-, Opto- and Organic Electronics

Bernard Pelissier[1]
Camille Petit-Etienne[1], Mickael Martin[1], Narciso Gambacorti[2], Olivier Joubert[1]
[1] University Grenoble Alpes, CNRS, LTM, Minatec Campus, Grenoble, France
[2] Univ. Grenoble Alpes, CEA, Leti, F-38000 Grenoble

The increasing complexity of the production chain for microelectronics chips manufacturing leads to an increasing number of process steps. In fact, wafer's queue time and storage conditions between them are becoming more and more critical, especially for materials and surfaces sensible to Airborn Molecular Contamination (AMC). For those materials, oxidation, organic contamination, or surface instability when exposed to atmosphere are issues that need to be avoided or accurately controlled.

In addition to this problematic of surface control between process steps, preserving the surface physico-chemical state is also a key point for advanced characterization studies.
In our case, keeping the surface chemical integrity during transfer between a process tool and an advanced characterization tool allows performing so called "quasi in situ" analyses.
This transfer concept, based on keeping a high quality static vacuum inside a specific carrier [1] has been demonstrated to be a key advantage for processes development and associated mechanisms understanding, especially when considering highly air-reactive surfaces [2] [3] [4].

After a brief reminder about the actual capabilities and details of this unique setup, the study focus on AMC contamination inside the carrier on several highly sensitives surfaces. Thus, the influence of the vacuum « nature » inside the carrier is investigated, thanks to the direct transfer chain under vacuum between several industrial 300mm tools (passivation and plasma etch tools) towards a 300mm pARXPS spectrometer.

Based on the monitoring of surface C and O residual "adsorbed" species after a very rigorous protocol including a base line acquisition followed by significant queue times inside the carrier (fig.1), the study takes advantage of the pARXPS acquisitions, systematically considered at grazing angle in order to enhance extreme surface sensitivity. In addition, the high reproducibility level brought thanks to the use of industrial 300mm tools enforce the robustness of the results.

This work has been partially supported by the French CNRS Renatech Network

Selected references

[1]. B. Pelissier & al. Micr. Elec. Eng. 85 151-155 (2008)
[2]. E. Gourvest, & al. J. of the Electrochem. Society, 159 (4) H373-H377 (2012)
[3]. N. Coudurier & al. ECS Trans., 92, 73-83 (2019)
[3]. R. Vallat, & al. J. Vac. Sci. technol. A, 37 (2), art. no. 020918, (2019).

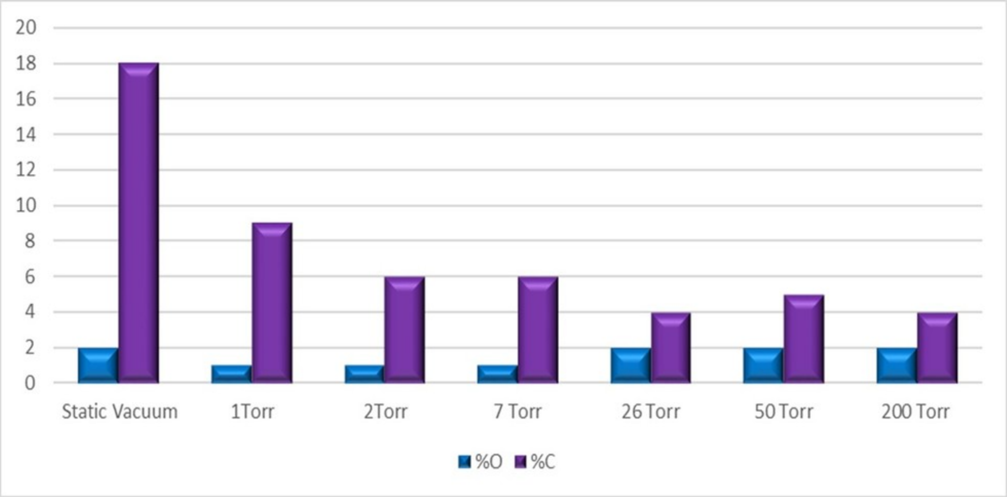

Fig. 1 : C and O pARXPS quantification (considered at 76,25 ° grazing emission angle) after Si Ar etching in a 300mm industrial tool and 30 min queue time, with regards to several N2 pressure in the carrier

O82 - Damage-free depth profiling of organic LEDs: a tool for understanding degradation mechanisms

8. ELC – Micro-, Opto- and Organic Electronics

Olivier Renault[1]
Claire Guyot[1], Jean-Paul Barnes[1], Tony Maindron[1]
[1] CEA-Leti, Univ. Grenoble Alpes, F-38000 Grenoble, France

Organic LEDs (OLEDs) are widedly used in many types of displays, however understanding their degradation mechanisms to help improve electro-optical and lifetime performances remains a challenge. Recently, we developed a correlative analysis protocol that minimises damages related to analysis beams. It uses a shallow angle bevel crater fabricated inside a ToF-SIMS analysis chamber [1]. With this preparation method, the in-depth information is displayed over the surface of the bevel crater. XPS profiles and high-resolution spectra paired with ToF-SIMS images enable an easy identification of the organic layers and complete understanding of their chemistry. Here, we present the results of a study on OLEDs after constant-current electrical ageing, based on this methodology and combining XPS & ToF-SIMS, using the spectra of single layers as reference. The ageing of OLEDs is first characterized by the evolution of the profile and fragmentation of molecular ions analyzed by ToF-SIMS and tandem MS, while XPS brings details in terms of chemical changes and evolution of the energy band diagram. Both emissive and electron-transport layers are degraded the most during ageing, whereas other layers show virtually no changes. In the degraded layers, the observed fragmentation of the characteristic molecules upon ageing would create defect states in the HOMO-LUMO molecular gap and introduce non-radiative traps closely related to the decreased electro-optical performances of the devices.

Acknowledgements: This work, carried out on the Platform for Nanocharacterisation (PFNC), was supported by the “Recherche Technologique de Base” and "France 2030 - ANR-22-PEEL-0014" programs of the French National Research Agency (ANR) ”

Selected references

[1] C. Guyot, J.-P. Barnes, O. Renault, T. Maindron, *Surf. Interface Anal*. 2024; 56:129-135.

9. IMA – Nanomaterials and Imaging

O83 - A new XPS test material for more reliable surface analysis of microstructures

9. IMA – Nanomaterials and Imaging

Jörg M. Stockmann[1]
Jörg Radnik[1], Vasile-Dan Hodoroaba[1], Thomas Weimann[2], Sebastian Bütefisch[2]
[1] Bundesanstalt für Materialforschung und -prüfung (BAM), 6.1 Surface and Thin Film Analysis, Unter den Eichen 87, 12205, Berlin, Germany
[2] Physikalisch-Technische Bundesanstalt (PTB), 5.22 Displacement Interferometry, Bundesallee 100, 38116, Braunschweig, Germany

Small-area XPS analysis is one of the most popular and powerful methods for analysing the surface of features in the micro-range. When measuring microstructures, the question arises whether the measuring point is really located at the point intended to be analysed. Information in a measured spectrum might originate within the field of view (FoV) on the surface of the sample, from outside the FoV, or even from inherent contamination. To ensure that small structures can be measured correctly regardless of user and instrument, certain instrument and sample settings must be known and selected correctly: beam and aperture size as well as the aperture settings and the approximate dimensions of the structure to be analysed. This is the only way to ensure that the information in the spectrum originates only from the FoV on the analysed structure.

To test the performance of the XPS instruments, a dedicated test material was developed that consists of a gold surface on which 8 circles and 8 squares of chrome are incorporated using a masking process, so that the Au substrate and the Cr structure surfaces are in the same surface plane. In order to be able to test as many as possible instruments from different manufacturers, the structures have been designed with a size ranging from 300 µm down to 7 µm. The layout of the test material has been optimised in regard of the handling, see figure 1. The structures are arranged along lines instead of a circumference, marking arrows around the smaller structures (≤ 50 µm) are added, and the lithography mask is optimised regarding edge and diffraction effects. Furthermore, the manufacturing process was changed from electron-beam deposition to mask lithography due to costs reasons. The structures on the test material were measured with a metrological SEM to determine their accurate dimensions and check the repeatability of the manufacturing process. XPS investigations with a Kratos AXIS Ultra DLD and an ULVAC-Phi Quantes demonstrates the suitability of this new test material for measuring the analysed area.

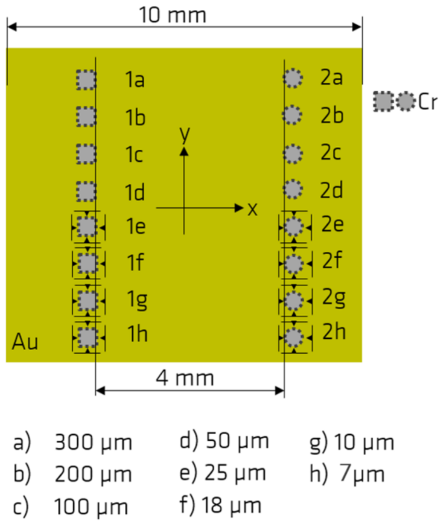

Figure 1: Layout of the new XPS test material.

O84 - Chemical analysis of functionalized graphene along the production process

9. IMA – Nanomaterials and Imaging

Loay Akmal Madbouly[1]
Paul Mrkwitschka[1], Robert Schusterbauer[1, 2], Jörg Manfred Stockmann[1], Elliot Jones[3], Vasile-Dan Hodoroaba[1], Jörg Radnik[1]
[1] Bundesanstalt für Materialforschung und -prüfung (BAM), Germany
[2] Freie Universität Berlin, Germany
[3] HAYDALE Composite Solutions, UK

Graphene has been commercialized for over a decade. It is usually used in the form of suspensions or inks [1]. In this study, we analyze the starting material for commercial functionalized graphene (FG) solutions and inks as well as their starting material (FG powders) using X-ray photoelectron spectroscopy (XPS), scanning electron microscope (SEM), energy-dispersive X-Ray spectroscopy (EDX), time of flight secondary ion mass spectrometry (ToF-SIMS) and Auger electron spectroscopy (AES). Graphene was functionalized with fluorine, oxygen, ammonia, and carboxylic acid.

Our results suggest a significant effect of water and commercial resins on the presence as well as the morphological behavior of graphene and associated functionalized group. For example, XPS analysis shows some significant differences between the solutions and the starting materials (powders). These changes can be explained by the location of the functionalization at the outer most surface as indicated by Chemello et al [2].

Selected references

[1] Zhang, M., Hou, C., Halder, A., Wang, H., & Chi, Q. (2017). Graphene papers: smart architecture and specific functionalization for biomimetics, electrocatalytic sensing and energy storage. Materials Chemistry Frontiers, 1(1), 37–60. https://doi.org/10.1039/C6QM00145A
[2] Chemello, G., Knigge, X., Ciornii, D., Reed, B. P., Pollard, A. J., Clifford, C. A., Howe, T., Vyas, N., Hodoroaba, V., & Radnik, J. (2023). Influence of the Morphology on the Functionalization of Graphene Nanoplatelets Analyzed by Comparative Photoelectron Spectroscopy with Soft and Hard X-Rays. Advanced Materials Interfaces, 10(20). https://doi.org/10.1002/admi.202300116

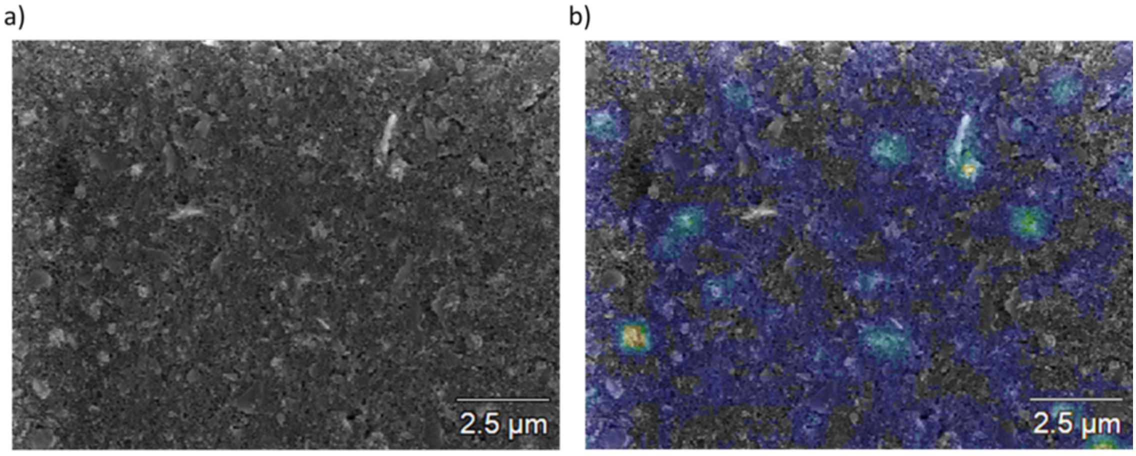

Figure 1. SEM image (a) and corresponding 5 kV EDX elemental map (b) of fluorine for an ink containing fluorine-functionalized -graphene within ink, after deposition of ink on silicon wafer, overlayed on (a)

O85 - Engineering materials at the atomic scale for the development of 3D-printed complex architecture

9. IMA – Nanomaterials and Imaging

Chandra Tiwary[1]
[1] Metallurgical and Materials Engineering, Indian Institute of Technology Kharagpur, India

Since its isolation, a single atomically thin layer of graphite, called graphene, has received a lot of attention from the research community as well as industry. Taking inspiration from graphene, the materials community started atomically exploring materials, which resulted in the development of a two-dimensional (2D) materials family consisting of elemental metals, metal carbides, dichalcogenide, oxide, nitride, and others. Engineering such atomically thin materials is different from conventional materials. In the current talks, the different methods/processes of engineering materials at atomic scale have been summarized. In the first section, the exfoliation of 2D materials from their bulk phase and tuning of their composition, thickness, and other physical, chemical, and optical properties are discussed. Taking inspiration from atomically engineered topological complex architectures have been 3D printed. Such architecture shows superior structural and functional properties. In the last section of the paper, nature-inspired processes have been utilized to build advanced/unique materials using energy-efficient methods. The bio-inspired 3D printed using 2D materials have been utilized in the environment, energy, and health care.

O86 - Growth of high density and crystalline GaN nanostructures on GaAs by droplet epitaxy

9. IMA – Nanomaterials and Imaging
Guy Tsamo[1]
Alla G. Nastovjak[2, 3], Nataliya L. Shwartz[2, 3], Philip Hoggan[1], Emmanuel Gardes[4], Christine Robert-Goumet[1], Alberto Pimpinelli[1], Matthieu Petit[5], Alain Ranguis[5], Mamour Sall[6], Luc Bideux[1],
Guillaume Monier[1]
[1] Université Clermont Auvergne, Clermont Auvergne INP, CNRS, Institut Pascal UMR 6602, F-63000 Clermont-Ferrand, France
[2] A.V. Rzhanov Institute of Semiconductor Physics SB RAS, 13 Lavrentiev aven., Novosibirsk, 630090, Russia
[3] Novosibirsk State Technical University, 20 K. Marx str., Novosibirsk, 630073, Russia
[4] Université Clermont Auvergne, CNRS, IRD, OPGC, Laboratoire Magmas et Volcans, F-63000 Clermont-Ferrand, France
[5] Aix Marseille Université, CNRS, CINaM UMR 7325, 13288, Marseille, France
[6] CIMAP Normandie Univ, CEA, CNRS, ENSICAEN, UNICAEN, 14000 Caen, France

Strain-induced growth techniques, based on the Stranski-Krastanov mechanism, are commonly used to elaborate self-assembled nano-structures. The mechanism of this technique requires lattice-mismatched material systems, which significantly limits the range of materials for nano-structure formation, despite its extensive use. An alternative approach is the droplet epitaxy (DE) technique, first reported in the 1990s [1]. Although much research effort has been devoted to DE since then, it is only recently that DE has gained worldwide attention. DE, which consists of droplet formation and crystallization, enables three-dimensional nanostructure manufacture in both mismatched and lattice-matched material systems, enabling the use of a wide range of material combinations [2, 3]. Among these combinations, the fabrication of III-N/III-V nano-structures by DE could present important assets for optoelectronic applications (such as solar cells, LEDs, photodetectors) and microelectronic (such as bipolar field effect transistors, biomedical sensors) applications [4, 5, 6].

In our work, the deposition of Volmer-Weber-grown Ga droplets on a GaAs substrate was followed by their N2 plasma nitriding to grow self-assembled GaN nanostructures. These two steps were carried out in an ultra-high vacuum environment and studied *in situ* by XPS. Innovating modelling of XPS intensities was developed, taking the spherical cap shape of the droplets into account to monitor surface organization. Scanning electron microscopy (SEM) and atomic force microscopy (AFM) were used to determine the morphologies of the nano-structures, which are highly sensitive to growth parameters. These characterizations were coupled with kinetic Monte Carlo simulations to precisely understand the phenomena occurring during the nitridation and to find the optimum conditions for complete nitridation of gallium droplets. The HRTEM observation showed a cubic crystal structure (zinc blende) of the GaN nanodots for nitriding at 300°C. Increasing the temperature from 100°C to 350°C during droplet nitriding achieved a very high density ($>10^{11}$ cm^{-2}) of GaN nanodots with the zinc blende crystallinity. In addition, varying the materials provided (Ga, In) and the growth parameters make it possible to obtain different cluster shapes on III-V substrates.

Selected references

[1] Koguchi, N., Takahashi, S., & Chikyow, T. *Journal of crystal growth* (1991) *111*(1-4), 688-692.
[2] Mano, T., Kuroda, T., Mitsuishi, K., Noda, T., & Sakoda, K. *Journal of crystal growth* (2009) *311*(7), 1828-1831.

[3] Mano, T., Abbarchi, M., Kuroda, T., McSkimming, B., Ohtake, A., Mitsuishi, K., & Sakoda, K. *Applied physics express* (2010)*3*(6), 065203.
[4] Wu, J., & Wang, Z. M. *Journal of Physics D: Applied Physics* (2014)*47*(17), 173001.
[5] Nemcsics, Á., & Stavrou, V. N. *Nonmagnetic and Magnetic Quantum Dots* (2017) (pp. 43-59). IntechOpen.
[6] Tsamo, G., Monier, G., Hoggan, P., Robert-Goumet, C., Petit, M., Ranguis, A., & Bideux, L. *Journal of Electron Spectroscopy and Related Phenomena* (2022)*261*, 147257.

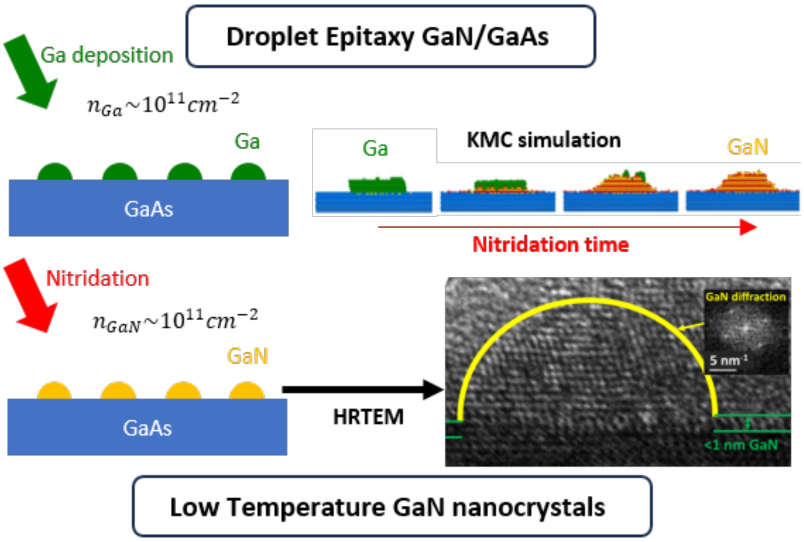

O87 - Modelling method for quantitative analysis of complex responses in piezo-response force microscopy

9. IMA – Nanomaterials and Imaging

Charlie O'Mahony[1]
Ehtsham-Ul Haq[1], Krittish Roy[1], Syed A. M. Tofail[1]
[1] University of Limerick

Piezo-response Force Microscopy (PFM) is a variant of Atomic Force Microscopy (AFM) that enables the imaging of ferroelectric domains, measurement of hysteresis loops, local ferroelectric behaviour and, as the name suggests, the local piezoelectric response of a material. The method involves applying an AC signal of a specified frequency, from tip to sample or vice versa, and measuring the samples inverse piezo-response from stress (or shear strain) induced in the sample, of the same specified frequency due to the electric field. This work looks to expand on previously conducted works in PFM, looking to better quantify and determine the orientation dependencies of piezo-response. [1-2] Along with addressing due scepticism that arises from PFM measurements in piezo- and ferro-electric material determination. [3]

PFM is split into two amplitudes and phases, in terms of Vertical-PFM (VPFM) and Lateral-PFM (LPFM). These arise from the out-of-plane presumed as the d33 + d15 piezo-constants or in-plane presumed as the d34/d15 (though also components such as d22 have effects). This presents, in part, the current difficulties associated with quantification in PFM. The signal measured contains contributions from numerous piezoelectric properties, and this is before we consider the actual orientation on the crystal and all non-piezoelectric effects a sample can undergo during PFM. By dissecting the individual effect of piezo-tensors, in the geometric orientation of the validation samples, we can further determine the inverse piezoelectric effects induced on the AFM cantilever. [4]

Through the use of finite element modelling of the PFM measurements, accompanied by validation, we look to solve the inverse problem that piezo-response signal from PFM gives us. Through these models we can interpret cases such as non-standard conduction paths (allowing measurements agnostic to the orientation and conduction path necessary through the sample), effect of all piezo-response on tip deflection and explore into other variables generally considered as constant in PFM measurements (e.g. temperature and topography).

Selected references

[1] J. O’Donnell, E. U. Haq, C. Silien, T. Soulimane, D. Thompson, and S. A. M. Tofail, ‘A practical approach for standardization of converse piezoelectric constants obtained from piezoresponse force microscopy’, *J. Appl. Phys.*, vol. 129, no. 18, p. 185104, May 2021, doi: 10.1063/5.0037201.
[2] S. V. Kalinin *et al.*, ‘Vector piezoresponse force microscopy.’, *Microsc. Microanal. Off. J. Microsc. Soc. Am. Microbeam Anal. Soc. Microsc. Soc. Can.*, vol. 12, no. 3, pp. 206–220, Jun. 2006, doi: 10.1017/S1431927606060156.
[3] J. F. Scott, ‘Ferroelectrics go bananas’, *J. Phys. Condens. Matter*, vol. 20, no. 2, p. 021001, Dec. 2007, doi: 10.1088/0953-8984/20/02/021001.

[4] S. Lei *et al.*, ‘Origin of piezoelectric response under a biased scanning probe microscopy tip across a 180^\ensuremath\circ ferroelectric domain wall’, *Phys Rev B*, vol. 86, no. 13, p. 134115, Oct. 2012, doi: 10.1103/PhysRevB.86.134115.

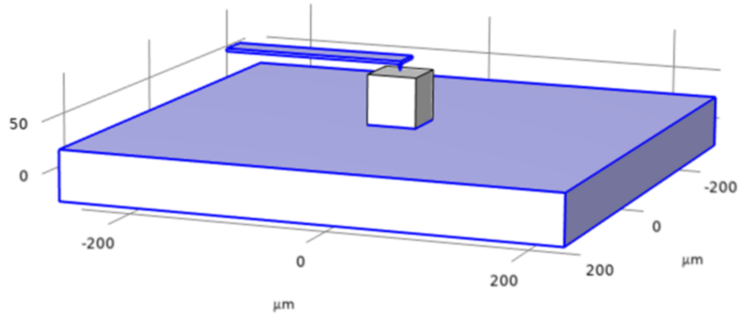

Figure 1: COMSOL model geometry for a simple cube sample, allowing tip angle to be 0°

O88 - New HDR approach for TOF-SIMS data acquisition

9. IMA – Nanomaterials and Imaging

Henrik Arlinghaus[1]
Matthias Kleine-Boymann[2], Julia Zakel[1], Rading Derk[1], Sven Kayser[2], Rudolf Moellers[1]
[1] IONTOF Technologies GmbH, Muenster, Germany
[2] IONTOF GmbH, Muenster, Germany

The generation of secondary ions in a ToF-SIMS experiment depends upon numerous factors. While the operator can optimize the instrument settings to control the secondary ion yield, certain aspects such as ionization probability, variations in species concentrations, and the uniformity of the spatial distribution within the sample are beyond control. Consequently, challenging samples may push the dynamic range of a contemporary SIMS instrument, which spans around five orders of magnitude, to its limits. In such instances, the operator is tasked with finding a balance that mitigates noise in low intensity signals and regions while preventing oversaturation of high intensity signals or regions.

In photography, a technique known as "High Dynamic Range" (HDR) is employed to circumvent similar limitations. This method involves capturing multiple images in quick succession with varying exposure times and subsequently merging them to create a single composite image.
This method was adapted to the TOF-SIMS technology and recently implemented in IONTOFs software for TOF-SIMS instrument operation and data analysis. It effectively reduces noise in low intensity regions and saturation effects in high intensity regions, thereby simplifying data interpretation on challenging samples.

In our prior work, we demonstrated the feasibility of collecting multiple datasets during a single acquisition pseudo simultaneously, each obtained using distinct instrument parameters. This approach minimized the effects of changes in the sample or the environment using multiplexing. In this presentation, we will show application examples utilizing the capability to generate combined profiles and images for substances of interest from a dataset, using our HDR-like algorithm.

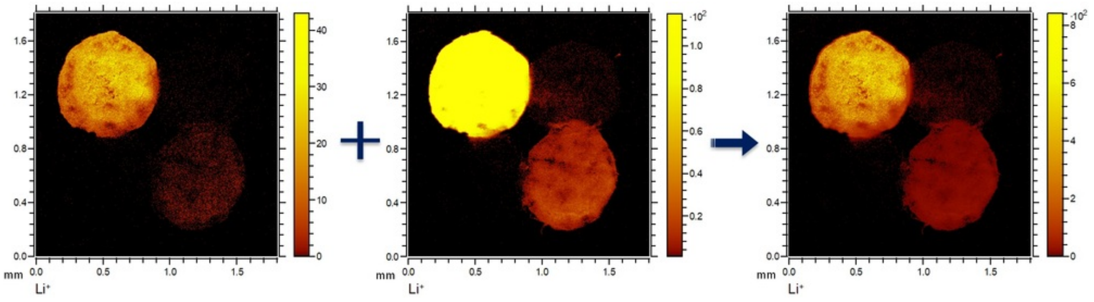

PI current: low

PI current: high

HDR Image

O89 - Sample preparation methods for ToF-SIMS surface analysis of TiO2 nanoparticles: An interlaboratory comparison

9. IMA – Nanomaterials and Imaging

Francesca Bennet[1, 2]
Robert Opitz[1], Narges Ghoreishi[1], Kristina Plate[1], Jean-Paul Barnes[3], Allen Bellew[4], Anna Belu[5], Giacomo Ceccone[6], Eric de Vito[7], Arnaud Delcorte[8], Alexis Franquet[9], Francesco Fumagalli[6], Douglas Gilliland[6], Harald Jungnickel[1], Tae Geol Lee[10], Claude Poleunis[8], Derk Rading[11], Hyun Kyong Shon[10], Valentina Spampinato[9, 12], Jin Gyeong Son[10], Fuyi Wang[13, 14], Yung-Chen (Andrew) Wang[5], Yao Zhao[13], Alexander Roloff[1], Jutta Tentschert[1], Jörg Radnik[2]
[1] Federal Institute for Risk Assessment, Max-Dohrn-Strasse 8-10, Berlin 10589, Germany
[2] Federal Institute for Materials Research and Testing, Unter den Eichen 44-46, Berlin 12203, Germany
[3] Univ. Grenoble Alpes, CEA, Leti, Grenoble F-38000, France
[4] Ionoptika Ltd., Unit B6, Millbrook Close, Chandler’s Ford SO53 4BZ, United Kingdom
[5] Medtronic Corporate Science & Technology, 710 Medtronic Parkway, Mailstop LT240, Minneapolis, Minnesota 55432
[6] European Commission, Joint Research Centre, Via E. Fermi 2749, Ispra (VA) 21027, Italy
[7] Univ. Grenoble Alpes, CEA, Liten, Grenoble F-38000, France
[8] Institute of Condensed Matter and Nanosciences - Bio & Soft Matter, Surface Characterisation, Université catholique de Louvain, Place Louis Pasteur, 1 bte L4.01.10, Louvain-la-Neuve B-1348, Belgium
[9] IMEC, Kapeldreef 75, Leuven 3001, Belgium
[10] Bioimaging Team, Safety Measurement Institute, Korea Research Institute of Standard and Science, 267 Gajeong-ro, Yuseong-gu, Daejeon, 34113, Republic of Korea
[11] IONTOF Technologies GmbH, Heisenbergstr.15, Münster 48149, Germany
[12] Dipartimento di Scienze Chimiche, Università degli Studi di Catania, Viale A. Doria 6, Catania 95125, Italy
[13] Beijing National Laboratory for Molecular Sciences; National Centre for Mass Spectrometry in Beijing; CAS Key Laboratory of Analytical Chemistry for Living Biosystems, Institute of Chemistry, Chinese Academy of Sciences, Beijing 100190, People’s Republic of China
[14] University of Chinese Academy of Sciences, Beijing 100049, People’s Republic of China

Nanomaterials have a wide variety of applications, but may also come with potential hazards to both humans and the environment. To assess these hazards, effective characterisation of their physical and chemical properties is necessary so that relevant structure-property relationships and behaviour can be determined. The development of effective and reliable analytical methods is therefore of key importance for the regulation of nanomaterials.

The high specific surface area of nanoparticles, which is orders of magnitude higher than for bulk materials, has a large influence on the material properties as well as offering high potential for interaction with the surrounding environment. The results of surface analysis can therefore be highly dependent on the history of the particles, particularly regarding sample preparation and storage. Because of the highly surface-sensitive nature of ToF-SIMS analysis, the sample preparation method in particular has a significant potential to influence the measurement results. Hence, various commonly used sample preparation methods should be tested and compared by means of inter-laboratory comparisons (ILC), in order to determine which sample preparation method provides the most intra- and interlaboratory consistency and the least amount of sample contamination.

Here we present results from an ILC undertaken as part of the VAMAS TWA2 (Versailles Project on Advanced Materials and Standards Technical Working Area 2 - Surface Chemical Analysis), which compared three different sample preparation methods (two wet and one dry) for ToF-SIMS surface analysis of nanoparticles. The study used the reference material BAM-P110 (TiO_2 nanoparticles with a mean Feret diameter of 19 nm) provided by the German Federal Institute for Materials Research and Testing (BAM). A total of 11 participants using instruments from three different manufacturers provided ToF-SIMS data.

No sample preparation method stood out as clearly superior, which is a disadvantage for method standardization but has the advantage that suitable methods are available for both wet and dry nanoparticle samples. The results showed that the largest sources of variation within the entire data set were caused by adventitious hydrocarbon contamination or incomplete substrate coverage, with the spin-coating protocol applied in this ILC showing a tendency toward incomplete substrate coverage. Additionally, no single participant stood out in the main sources of variance, which is a positive result for the ToF-SIMS community. This study provides a basis for the development of best-practice methods for the preparation of nanoparticles for surface analysis, which should be developed and monitored in each individual laboratory.

O90 - Surface analysis of graphene oxide films reduced by thermal treatments

9. IMA – Nanomaterials and Imaging

Alessio Mezzi[1]
Saulius Kaciulis[1], Marino Lavorgna[2], Federica Recupido[2], Giuseppe Cesare Lama[2]
[1] Institute for the Study of Nanostructured Materials, ISMN-CNR, PO Box 10, 00015 Monterotondo Stazione, Rome, Italy
[2] Institute of Polymers, Composites and Biomaterials, IPCB-CNR, P.le E. Fermi 1, 80055 Portici (NA), Italy

A series of graphene oxide (GO) films were fabricated starting from chemical oxidation of graphite powder, which was afterwards purified, dispersed in water and used for solution casting to obtain thin solid GO films. Two different methods of thermal GO reduction were performed at temperatures up to 200 °C. The first one was carried out in static oven at room pressure and atmosphere, whereas the second one was done in autoclave by using saturated steam and higher pressure. The chemical composition of obtained conductive films was investigated by X-ray photoelectron spectroscopy (XPS) and Auger electron spectroscopy (AES), whereas the surface morphology was examined by scanning electron microscopy (SEM).

GO films reduced by the hydrothermal autoclave method were characterized by significantly lower values of electrical resistivity and oxidation degree. These promising results indicate the possibility to apply this ecological route for sustainable fabrication of graphene-based conductive materials.

10. MET – Metallic Materials

O91 - Advancing X-ray photoelectron spectroscopy (XPS) methodologies for materials research

10. MET – Metallic Materials

Mark Biesinger[1, 2]
[1] Surface Science Western, Western University, London ON, Canada
[2] Department of Chemistry, Western University, London ON, Canada

Chemical state X-ray photoelectron spectroscopic (XPS) analysis of first row transition metals and their oxides and hydroxides is challenging due to the complexity of the 2p spectra resulting from peak asymmetries, complex multiplet splitting, shake-up and plasmon loss structure, and uncertain, overlapping binding energies. Our work has shown that all the values of the spectral fitting parameters for each specific species, i.e. binding energy (eV), full width at half maximum (FWHM) value (eV) for each pass energy, spin-orbit splitting values and asymmetric peak shape fitting parameters, are not all normally provided in the literature and databases, and are necessary for reproducible, quantitative chemical state analysis.

We have worked toward a consistent, practical, and effective approach to curve fitting based on a combination of 1) standard spectra from quality reference samples, 2) a survey of appropriate literature databases and/or a compilation of literature references, 3) specific literature references where fitting procedures are available and 4) theoretical fittings, where available, of multiplet split reference spectra. The use of well characterized standard samples and fitting of the entire peak shape has been shown to increase our ability to accurately identify and (semi) quantify the various species present in mixed oxide/hydroxide systems [1,2]. Additional chemical information has also been elucidated from Auger parameters and by using Wagner plots for compounds of Ni, Cu, Ga, In, Cd, and Zn. The unique spectral shapes of the LMM Auger peaks for these transition metals, particularly for Cu [3], as well as for Zn, In and Cd, have also been shown to be of use for chemical speciation. These methods have been shown to be effective in a wide variety of applications.

Additionally, a recent assessment [4] of available charge corrections procedures for insulating samples will also be shown including recent work on defining the nature of adventitious carbon and improving its merit for charge correction usage [5].

Selected references

1. M.C. Biesinger, L.W.M. Lau, A.R. Gerson, R.St.C. Smart, Applied Surface Science 257 (2010) 887.
2. M.C. Biesinger, B.P. Payne, A.P. Grosvenor, L.W.M. Lau, A.R. Gerson, R.St.C. Smart, Applied Surface Science 257 (2011) 2717.
3. M.C. Biesinger, Surface and Interface Analysis 49 (2017) 1325.
4. M.C. Biesinger, Applied Surface Science 597 (2022) 15381.
5. L.H. Grey, H.-Y. Nie, M.C. Biesinger, Applied Surface Science 653 (2024) 159319.

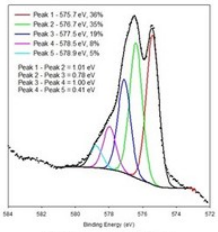

Cr $2p_{3/2}$ peak-fitting parameters for Cr_2O_3

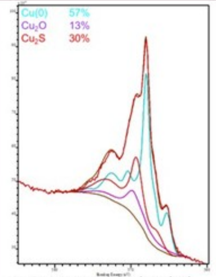

Cu LMM Auger chemical state analysis

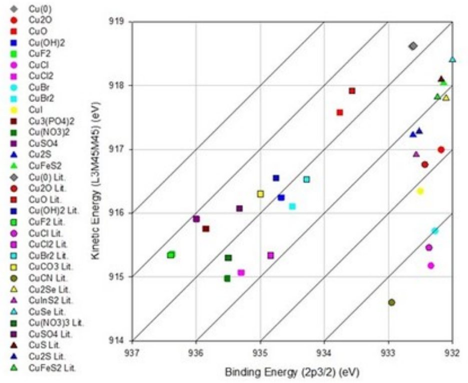

Cu $2p_{3/2}$ - Cu LMM Wagner Plot

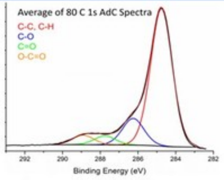

Average AdC C 1*s* Spectrum

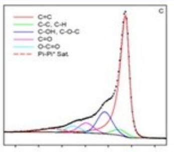

Standardized C 1*s* Fitting for Graphitic or CNT Materials

O92 - Exploring the impact of pure copper powder reuse on surface chemistry during powder bed fusion electron beam

10. MET – Metallic Materials

Sofia Kazi[1]
Phillip Mahoney[2], Eduard Hryha[1]
[1] Chalmers University of Technology, Department of Industrial and Materials Science, Gothenburg, Sweden
[2] GE Additive, Arcam EBM, Gothenburg, Sweden

Powder degradation during additive manufacturing poses a significant challenge to achieving optimal part quality as well as maximal powder feedstock utilization and hence sustainability of the process. Pure copper possesses high optical reflectivity and excellent thermal and electrical conductivity. Powder bed fusion electron-beam is a promising method for fabricating pure copper parts as it can melt materials regardless of their reflectivity and operates under vacuum, preventing oxidation. This study investigates the influence of pure copper powder properties and reuse on the powder surface oxide chemistry and hence processability by PBF-EB. Changes in powder surface chemistry were studied by HR SEM and X-ray Photoelectron Spectroscopy in virgin and reused state. Results indicate that there is evident degradation in powder properties during reuse with increase in oxygen content, connected to increase in surface oxide layer as well as transformation of CuO into Cu_2O and formation of $Cu(OH)_2$ on top surface during handling.

O93 - Fracture surface analysis of LPBF-produced Ti-6Al-4V by XPS and AES

10. MET – Metallic Materials

Yu Cao[1]
Lars Nyborg[1]
[1] Chalmers University of Technology

Additive manufacturing (AM) is the general term for all manufacturing techniques where the component is built by adding material layer by layer from a CAD (computer-aided design) model. Laser beam Powder-Bed-Fusion (LPBF) is a core AM technique in the context of metallic materials. This study aims to establish the correlation of local chemistry with the fatigue fracture in LBPF-produced Ti-6Al-4V. The strain-controlled fatigue test was performed at room temperature with R = 0. Four specimens with two different strain levels ($\Delta\varepsilon = 0.65\%$ and 0.8%) and varied fatigue lives were chosen to be studied.

The fatigue fractured surfaces were investigated using surface analysis techniques - X-ray photoelectron spectroscopy (XPS) and Auger electron spectroscopy (AES). The crack initiation, propagation and final fracture region were identified. Thanks to the small area XPS together with AES having high lateral resolution, the chemistry of the features at different locations on the fracture surface was investigated. The role of some elements or impurities in crack development was examined, especially for crack initiation. A comparison was made between the specimens with low and high fatigue life at two strain levels. This study provides some insight into fatigue life improvement and scatter reduction for LBPF-produced Ti-6Al-4V.

O94 - Preparation and characterization of refractory high-entropy alloys for nuclear fusion reactors

10. MET – Metallic Materials

Miwen Yuan
Xiuyu Wei[1, 2], Ji Yang[1, 2], Xiaokang Hu[1, 2], Zhixiang Li[1, 2], Chongwei Fu[1, 2], Jianguo Wu[1, 2]
[1] CMT Rare Metal Advanced Materials (Hunan) Co. Ltd., Changsha, Hunan 410000, China
[2] State Key Laboratory of Cemented Carbide, Zhuzhou, Hunan 412000, China

Introduction/Purpose

The first wall of a fusion reactor is the material directly facing the extremely high temperature plasma. Hence, the plasma-facing materials (PFM) should stand with high-energy neutron irradiation, high-density plasma irradiation, and high thermal loads [1]. Long time H plasma irradiation could cause PFM hydrogen bubbles, which is detrimental to the material's properties. Therefore, it is critical to improve the plasma irradiation resistance of the PFM. In the past few years, high entropy alloys (HEA) have received much attention due to their excellent radiation resistance and high-temperature properties [2]. It is challenge that how to prepare refractory high-entropy alloys using industrial methods.

Method

A WTaCrVTi refractory high-entropy alloy was fabricated by suspension melting. Then the alloy was solution treated at 1300 ℃ for 2 h. After that, the samples were irradiated with 200 eV H ions at 500 °C. Finally, thermal desorption experiments and positron annihilation experiments were performed.

Results

Mircro-segregation and the oxidation of Ti was found in the as-cast samples. Therefore, solution treatment was performed to homogenize element distribution. SEM and EDS were used to characteristic the microstructure and compostion evolution. Compareing the pure tungsten, WTaCrVTi refractory high-entropy alloy showed a better resistance of H plasma irradiation. In addition, the thermal desorption experiments were performed to examine the H retention, positron annihilation experiments were used to inspect the lattice vacancy defects of the irradiated samples .

Conclusions

It is expected to clarify plasma irradiation resistance of refractory high-entropy alloy fabricated by suspension melting.

Selected references

[1] A. Dubinko, D. Terentyev, C. Yin, et al. Microstructure and Hardening Induced by Neutron Irradiation in Single Crystal, ITER Specification and Cold Rolled Tungsten. International Journal of Refractory Metals and Hard Materials, 2021, Vol 98: 105522.

[2] X. Y. Ding, H. Y. Zheng, P. P. Zhang, et al. Microstructure and Mechanical Properties of WTaVCrTi Refractory High-Entropy Alloy by Vacuum Levitation Melting for Fusion Applications. Journal of Materials Engineering and Performance, 2022, Vol 32 (no. 17): 7869-7878.

O95 - Reduction of iron oxides with in situ hydrogen charging of DP1000 steel in X-ray photoelectron spectroscopy XPS

10. MET – Metallic Materials

Benedikt Wolfsjäger[1]
Jiri Duchoslav[2], Philipp Kürnsteiner[1], Reza Sharif[3], David Stifter[2], Heiko Groiss[1]
[1] Christian Doppler Laboratory for Nanoscale Phase Transformations, Center for Surface and Nanoanalytics, Johannes Kepler University Linz, Altenberger Straße 69, 4040 Linz, Austria
[2] Center for Surface an Nanoanalytics, Johannes Kepler University Linz, Altenberger Straße 69, 4040 Linz, Austria
[3] Voestalpine Stahl GmbH, voestalpine-Straße 3, 4020 Linz, Austria

The applications of advanced high strength steels AHSS in the automotive industry due to their advantages in fuel consumption, passenger safety and material usage underlines their importance in the future. However, they are especially susceptible to hydrogen embrittlement HE calling for a better understanding of the interaction of hydrogen with steel microstructures. Therefore, our work wants to contribute in this field with in situ XPS experiments as an indirect way to detect hydrogen through the reduction of iron oxides in dual phase steel DP1000. With a self-developed liquid in situ cell, hydrogen is introduced via the reaction of perchloric acid with the zinc layer of the galvanized steel samples at the hydrogen entry side of the steel sheet. At the same time, an iterative XPS measurement is performed on the opposite, hydrogen exit side, at which changes in the high-resolution Fe2p peak are detected (see Fig. 1). Iron is reduced from the third to the second oxidation state $Fe^{3+} \rightarrow Fe^{2+}$ leading to a shift of the main Fe2p iron oxide peak towards lower binding energies as well as the disappearance and emergence of the shake-up satellite loss feature of Fe^{3+} and Fe^{2+}, respectively. An adequate fitting procedure was applied to the $Fe2p_{3/2}$ peak with which the percentual amount of converted iron was estimated. An oxide layer with various oxide species is presented, with their respective thicknesses calculated using the modified Strohmeier equation.

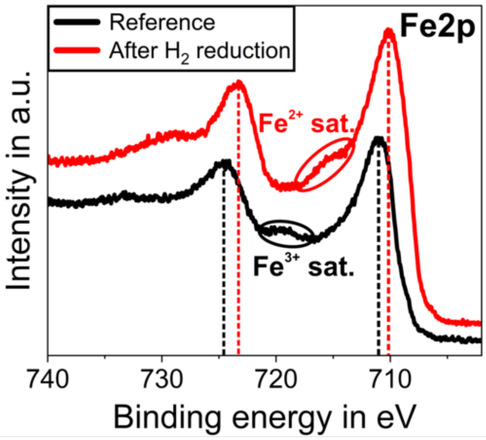

Figure 1. Changes in the high-resolution Fe2p peak after hydrogen reduction

O96 - Surface oxide chemistry of β-titanium Ti-Nb-Ta-Zr alloy powder and its changes during additive manufacturing

10. MET – Metallic Materials

Silja-Katharina Rittinghaus[1]
Gowtham Soundarapandiyan[2], Pui Lam Tam[2], Ivan Zhirnov[1], Bilal Gökce[1], Eduard Hryha[2]
[1] University of Wuppertal, Chair of Materials Science and Additive Manufacturing, Germany
[2] Chalmers University of Technology, Department of Industrial and Materials Science, Sweden

Compared to (α+β) titanium alloys widely used in manifold e.g., aerospace and biomedical applications, β-Ti alloys exhibit a number of unique properties, such as a low modulus of elasticity and high yield strength combined with excellent formability. Among the β-Ti alloys, Ti-Nb-Ta-Zr alloys are especially attractive as structural materials considering high potential of their utilization for metal additive manufacturing (AM). Powder degradation during powder-based metal additive manufacturing, especially in case of such an oxygen- sensitive alloys as Ti-Nb-Ta-Zr, significantly impact powder reusability and hence economic and environmental feasibility of powder-based metal AM of such alloys. Ti-Nb-Ta-Zr is particularly demanding and interesting in this respect, as all alloying elements are very prone to oxidation. At the same time, the oxygen content is very important for the final microstructure and component properties. Thus, X-ray photoelectron spectroscopy (XPS) was used to comparatively analyze the oxidation state of the virgin powder and its changes during powder bed fusion - electron beam (PBF-EB) and powder bed fusion - laser beam (PBF-LB) processing. Auger electron spectroscopy (AES) was additionally used to understand size, chemistry and distribution of the specific particulate phases on the powder surface. Supplementary scanning electron microscopy (SEM) and bulk chemical analysis of powders and printed parts were performed to understand powder morphology and chemistry and draw conclusions about the significance of the observations for component properties.

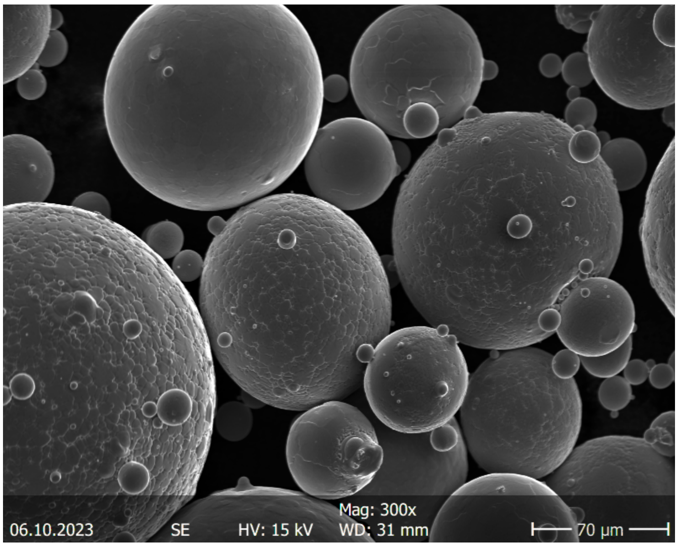

O97 - Wear behavior of an experimental boron-containing advanced high-strength complex-phase steel

10. MET – Metallic Materials

Antonio Salas-Reyes[1]
Rafael González-Parra[2], Miguel Hernandez[2], Arturo Barba[2], Jaime Garcia[1]
[1] 1 Departamento de Ingeniería Metalúrgica, Facultad de Química, UNAM, 04510 Ciudad de México, México
[2] 2 División de Ingeniería Mecánica e Industrial, (DIMEI), CENISA, Facultad de Ingeniería, UNAM, 04510 Ciudad de México, México

Advanced high-strength steels (AHSS) are of great importance in the fabrication of automotive parts due to their outstanding mechanical properties. Since wear can occur between two displacement surfaces that are in contact after ensamble, knowing their wear resistance response becomes very significant during the workpiece metallurgical design, processing and final application. Based on the above, this work explores the effect of boron as microalloying element in the wear behavior of an experimental complex-phase (CP) steel under different microstructural conditions. For this purpose, samples of two CP steels identified as CP-B0 (reference steel) and CP-B60 (steel with 60 ppm of B) were processed separately from the as-cast condition as follows: i) as-cast microstructure + quench and tempering heat treatment (CP-BO-QT and CP-B60-QT), ii) as-cast microstructure + one-step quenching and partitioning heat treatment (CP-BO-Q&P and CP-B60-Q&P), and iii) as-cast microstructure + hot and cold rolling + stress relieve heat treatment (CP-BO-SR and CP-B60-SR). After achieving each desired microstructural condition, samples were obtained for microstructural and wear characterization. Wear testing was carried out by the pin-on-disk method accordingly with the ASTM-G99 standard using a force of 24.5 N, a testing velocity of 0.471 m/s and a total rotating distance of 2.544 km during three hours. Also, a commercial alumina disc was employed as the wearing disk. Results showed that the combination of boron microaddition and the deformed + stress relieve condition (i.e., CP-B60-SR steel) has a beneficial effect on the wear resistance due to the grain refinement, cold working and particle precipitation hardening competing mechanisms instead of the rest material conditions. Thus, CP-B60-SR steel has manifested the highest hardness, less plowing and the least mass removal, and in consequence, less superficial oxidation. However, all the evaluated material conditions present good wear displacement resistance by the fact of presenting wearing rate values between 10^{-8} and 10^{-10}. Finally, fatigue was found to be the primary abrasive wear mechanism acting in all the tested material conditions.

11. NRG – Energy, Environment, geology and heritage

O98 - A Study of the chemistry of Mary-Rose timber hull core samples using XPS and ToF-SIMS

11. NRG – Energy, Environment, Geology and Heritage

Marie-Laure Abel[1]
Eleanor Schofield[2], Alastair Miles[2], Anna Kotowska[3], Darcey Holmes[1], Wiktor Kawala[1], John Farnham Watts[1]
[1] University of Surrey, School of Mechanical Engineering Sciences, Guildford Surrey, GU2 7XH UK
[2] The Mary Rose, Main Street, Portsmouth Historic Dockyard, Portsmouth Hants PO1 3PY UK
[3] University of Nottingham, School of Pharmacy, University Park, Nottingham Nottinghamshire NG7 2RD UK

One of the most important maritime artefacts in the United Kingdom is to be found in Portsmouth. The *Mary Rose*, the favourite warship of Henry VIII, was retrieved from the Solent in 1982 long after it sank while engaged in a battle with the French in 1545. After spending so long in the sea, it was crucial to find a method to conserve the *Mary Rose* following retrieval from the silt of the Solent. Various "washing" methods were used initially, followed by a spray of polyethylene glycol (PEG) of two different molecular weights inspired by the protocol followed for the Vasa [1] in Sweden. While the ship seems to be holding well, we do not have a detailed picture of the depth reached by the PEG or its chemical stability or exactly what impurities are to be found within the wood.

Core samples were taken by the Mary Rose Trust in various locations on the ship and two of those were tested at the Universities of Surrey and Nottingham, using X-ray photoelectron spectroscopy and secondary mass spectrometry (both with ToF and Orbitrap analysers). These core specimens were sectioned at regular intervals to investigate the chemistry of the timber as a function of depth into the hull. Both sides of the specimens were analysed using a specially designed rotating sample holder.

Elements indicative of the wash using tap water (e.g. calcium) and seawater (e.g. chlorine and sodium) were observed. The presence of PEG was demonstrated at a depth of at least 20mm as well as its degradation via cleavage of entire portions of the polymer chain. Its presence is inhomogeneous, this probably due to the inherent structure of the wood as well as the presence of cracks within the material (likely pre and post sampling). In addition, the drop in PEG concentration as a function of depth is concomitant with the uptake in concentration of sodium and chlorine possibly indicating that the initial water wash was not entirely successful for the full thickness of the planks. Several possible sources of the PEG degradation may be identified such as ultra-violet light or the presence of bacteria.

Selected references

[1] Hocker, E., Almkvist, G. & Sahlstedt, M., 2012. The Vasa experience with polyethylene glycol: A conservator's perspective. *Journal of Cultural Heritage*, 13(S), pp. 175-182.

O99 - Charge compensation mechanism in LixNiO2 electrode studied by experimental and theoretical HAXPES

11. NRG – Energy, Environment, Geology and Heritage

Roberto Fantin[1]
Ambroise Van Roekeghem[1], Jean-Pascal Rueff[2], **Anass BENAYAD**[1]
[1] Univ. Grenoble Alpes, CEA, LITEN, 38000 Grenoble, France
[2] Synchrotron SOLEIL, L'Orme des Merisiers, Saint-Aubin, BP 48, 91192 Gif-sur-Yvette Cedex, France

The performances of lithium-ion batteries are set by the electrodes materials capacity to exchange lithium ions and electrons faster and reversibly. Understanding the mechanism behind these processes sets the direction for designing high density cathode materials with good structural and chemical stability upon different cycling regime. Our study focuses on $LiNiO_2$ materials for advanced high-energy positive electrode materials. This material is currently at the center of all expectations to remove cobalt in Li-ion batteries at the industrial scale. However, the link between electronic correlations and the redox mechanism during (de-)lithiation is not well understood. The performances of $LiNiO_2$ based electrodes are strongly linked to their electronic structure which plays a fundamental role in the charge and discharge processes, and therefore in their capacity retention and stability. Since the redox mechanism is at the center of the electrochemical processes, the role of transition metals and oxygen ions in the redox process is yet to be clarified and resolved in-depth from the surface towards the bulk of the electrode. Therefore, a global picture considering the charge compensation mechanism involving both anion and cation is needed but also it must be demonstrated experimentally. Recently, we demonstrated the self-regulation of the charge transfer process between oxygen and cobalt upon delithiation in Li_xCoO_2, an electrode material considered as an archetypical one.[1] To widen this picture, we studied herein the charge transfer process in $LixNiO_2$ by using for the first time a combined laboratory and synchrotron-based XPS/HAXPES supported by dedicated DFT based calculation to resolve the role of nickel and oxygen in the redox process down to 30 nm with a depth resolution of 5 nm[2]. We highlight the negative charge transfer and bond/charge-disproportionation characters of $LiNiO_2$. By combining non-destructive core-level depth profiling coupled to appropriate cluster model simulation, we bring new insights on the overall charge transfer process involving Nickel and oxygen in cooperative way.

Selected references

[1] Self-Regulated Ligand-Metal Charge Transfer upon Lithium-Ion Deintercalation Process from LiCoO2 to CoO2, R. Fantin, A. Van Roekeghem, and A. Benayad, PRX Energy 2023, 2, 043010
[2] Depth-Resolving the Charge Compensation Mechanism from LiNiO2 to NiO2, R. Fantin, T. Jousseaume, R. Ramos, G. Lefevre, A. Van Roekeghem, J.-P. Rueff, A. Benayad, ACS Energy Letters, 2024, 9, 1507-1515

Acknowledgements

This work was supported by the "Recherches Technologiques de Base" program of the French National Research Agency (ANR) and by the CEA FOCUS-Battery Program and was in part carried out at the platform of Nano characterization (PFNC) of CEA Grenoble. We acknowledge the Battery Interface Genome- Materials Acceleration Platform (Big-Map) EU project for providing the LiNiO2 electrodes and materials for electrochemical characterization. The synchrotron HAXPES experiments were carried out within in-house Galaxies beam time at SOLEIL

O100 - Comparison of different deposition procedures of SAMs on their distribution in perovskite solar cells by ToF-SIMS

11. NRG – Energy, Environment, Geology and Heritage

Wolfram Hempel[1]
Tina Wahl[1], Theresa Friedlmeier[1], Erik Ahlswede[1], Jonas Hanisch[1]
[1] Zentrum für Sonnenenergie- und Wasserstoff-Forschung Baden-Württemberg

Perovskite solar cells (PSC) have aroused unprecedented interest in research and industry within the past few years. After their first introduction in 2009, the maximum power conversion efficiency rose quickly up to 26.1 % in 2023[1]. There are two main fields of development. First, the scale up of area from small cells to commercial module sizes. Second, the combination with another solar material as silicon, CIGS or CdTe in tandem cells to reach higher conversion efficiencies.

A typical inverted cell stack consist of a transparent conduction layer (TCO) as front contact, a hole transport layer (HTL), the perovskite absorber, an electron transport layer (ETL) and the back contact. Common materials are ITO as TCO, PEDOT:PSS, PTAA, NiOx or self-assembled monolayers (SAMs) as HTL, PCBM/BCP, C60/BCP or C60/SnO2 as ETL and Ag, Cu or TCO materials as back contact. The quality of the layer interfaces plays a major role to gain high efficiencies and to avoid a large hysteresis of JV-measurements. Therefore, a good coverage of all the subsequent solution-processed wet films is necessary to obtain uniform and homogeneous layers.

The use of some SAM as HTL reveals a bad wetting behavior and can lead to a not fully covered perovskite layer. Usually, we deposit SiO_2 nanoparticles to assist a good wetting of the perovskite on the SAM. In this work, we examine an alternative way by using a mixture of perovskite and SAM as precursor formulation. This saves two process steps while maintaining similarly high power conversion efficiencies. However, fill factor and open circuit voltage decrease. We investigate the SAM distribution in the stack by ToF-SIMS measurements for a better understanding of this effect. We observe a decrease of SAM intensity beyond perovskite for the mixed process compared to the reference process with the sequential deposition of the perovskite and SAM layers. Furthermore, some of the SAM molecules occur also on top of the perovskite layer.

Our investigations thus help to explain the behavior of these perovskite solar cells with SAMs as HTL and pave the way for further improvements in the power conversion efficiency.

Selected references

[1] https://www.nrel.gov/pv/assets/images/cell-pv-eff-emergingpv.jpg

O101 - Correlating electronic structure to material formation, growth, and chemistry in BaZrS3 thin films: from bands to bonds

11. NRG – Energy, Environment, Geology and Heritage

Soham Mukherjee[1]
Stefania Riva[1], Corrado Comparotto[2], Fredrik O. L. Johansson[1], Gabriel J. Man[3], Dibya Phuyal[4], Konstantin A. Simonov[5], Justus Just[3], Konstantin Klementiev[3], Garima Aggarwal[1], Mahmoud A. Hafiez[1], Sergei Butorin[1], Jonathan Scragg[2], Håkan Rensmo[1]
[1] Condensed Matter Physics of Energy Materials, Division of X-ray Photon Science, Department of Physics and Astronomy, Uppsala University, SE-75120 Uppsala, Sweden
[2] Division of Solar Cell Technology, Department of Materials Science and Engineering, Uppsala University, Uppsala 75237, Sweden
[3] MAX IV Laboratory, Lund University, PO Box 118, Lund 221 00, Sweden
[4] Division of Material and Nano Physics, Department of Applied Physics, KTH Royal Institute of Technology, Stockholm 10691, Sweden
[5] Department of Materials and Process Development, Swerim AB, SE-164 07 Kista, Sweden

The Chalcogenide perovskite family have gained strong interest[1],[2] recently as photovoltaic materials, offering a promising lead-free alternative to halide perovskites. While the flexibility of the perovskite structure allows for effective band engineering, its exceptional chemical stability also offers possibilities for large-scale manufacturing, in the quest of finding affordable and sustainable clean energy solutions. Among them, the prototypical chalcogenide perovskite $BaZrS_3$, characterized by its direct band gap, exceptionally strong light-harvesting ability, and good carrier transport properties, meets fundamental prerequisites for a promising photovoltaic material.

This motivated us to synthesize and characterize $BaZrS_3$ thin films[3] using sputtering and rapid thermal processing, aimed at device fabrication for future optoelectronic applications and compare it to $BaZrS_3$ microcrystals as the reference. The films were characterized in terms of their short- and long-range geometric structures, phase distribution, surface, sub- surface and bulk chemical and electronic structures and how they correlate to the optical absorption and band gap data. Combining XRD, XAFS, EDX and PL measurements allowed us to directly link the temperature-evolution of PL to material formation and growth, film crystallinity, down to the atomic-level Zr-S bond variance [4], as annealing induces crystallization and growth of $BaZrS_3$ from an amorphous matrix of Ba, Zr, and S atoms. The depth-profiling information on material chemistry obtained from photoelectron spectroscopy identified minimal surface effects on the valence band edge position. This led us to conclude the semiconductor films to be close to intrinsic in nature, determined from the energy difference between the valence band edge and the Fermi level with respect to the measured optical band gap of $BaZrS_3$. This is of particular interest from a materials fabrication perspective since the surface of the film contributes to the properties of subsequent interfaces in a multilayer device like a solar cell.

Finally, we map the experimental valence band spectra to the theoretically calculated one from DFT+U method, resolving different orbital contributions[5], specifically S 3*p* in the valence band and unoccupied S 3*d* and empty cationic d states (Ba 5*d*, Zr 4*d*) in the conduction band, and how it connects to the distorted orthorhombic structure. Our findings provide a deeper understanding of the electronic structure of $BaZrS_3$ in relation to the fundamental bonding properties of the material, which, in the context of current prospects and challenges, provide vital knowledge for future interfaces development, and consequently, for device integration.

Selected references

[1] Filippone, S.; Zhao, B.; Niu, S.; Koocher, N. Z.; Silevitch, D.; Fina, I.; Rondinelli, J. M.; Ravichandran, J. & Jaramillo, R. Discovery of Highly Polarizable Semiconductors $BaZrS_3$ and $Ba_3Zr_2S_7$. *Phys. Rev. Mater*. **4**, 091601 (2020).

[2] Sun, Y. Y.; Agiorgousis, M. L.; Zhang, P. & Zhang, S. Chalcogenide Perovskites for Photovoltaics. *Nano Lett.* **15**, 581 (2015).

[3] Comparotto, C.; Davydova, A.; Ericson, T.; Riekehr, L.; Moro, M. V.; Kubart, T.; & Scragg, J. Chalcogenide perovskite BaZrS3: thin film growth by sputtering and rapid thermal processing. *ACS Applied Energy Materials*, **3** (3), 2762 (2020).

[4] Mukherjee, S.; Riva, S.; Comparotto, C.; Johansson, F. O.; Man, G. J.; Phuyal, D.; Simonov, K.A.; Just, J.; Klementiev, K.; Butorin, S.M.; Scragg, J & Rensmo, H. (2023). Interplay between Growth Mechanism, Materials Chemistry, and Band Gap Characteristics in Sputtered Thin Films of Chalcogenide Perovskite BaZrS3. *ACS Applied Energy Materials*, **6**, 11642 (2023).

[5] Riva, S.; Mukherjee, S.; Butorin, S. M.; Allan, A. R., Comparotto, C.; Aggarwal, Johannesson, E.; A.-Hafiez, M.; Scragg, J & Rensmo, H. (2024). Electronic structure characterization by photoelectron spectroscopy of BaZrS3 perovskite powder and thin film. https://chemrxiv.org/engage/chemrxiv/article-details/65a15053e9ebbb4db901d416

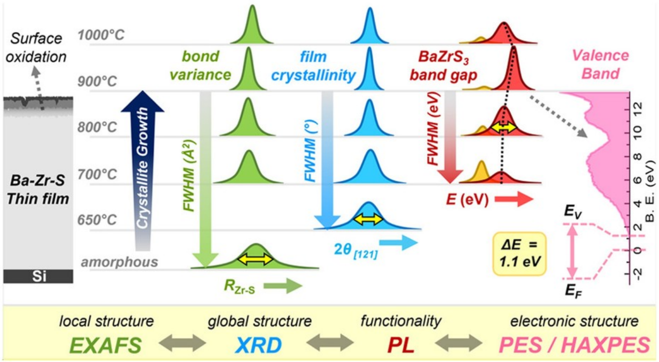

TOC. Temperature control of crystallization, reaction sequence of the $BaZrS_3$ formation and crystal growth in terms of Zr-S disorder (local structure from EXAFS), film crystallinity (global structure from XRD), and their influence on band gap characteristics (electronic structure from PES/HAXPES) and observed material functionality (PL).

O102 - Cryogenic XPS: 20 years probing intact interfaces in nature and life

11. NRG – Energy, Environment, Geology and Heritage

Andrey Shchukarev[1]
Jean-François Boily[1], Madeleine Ramstedt[1]
[1] Department of Chemistry, Umeå University, Sweden

Solid-aqueous solution interfaces are common in nature and can be considered as two-dimensional nanoreactors. These interfaces are responsible for the mediation and catalysis of many (a)biotic environmental processes, including reactions in organisms. Experimental resolution of the composition of interfaces is crucial to our understanding of key phenomena in technology, nature, and life. This can be readily achieved by X-ray photoelectron spectroscopy (XPS), which is an ultra-high vacuum (UHV) based *ex situ* technique for analyzing the composition of solid surfaces. From the start of this century, we have been continuously developing the cryogenic XPS technique [1] in order to secure, identify and quantify the surface and interfacial chemistry on wet, fast-frozen, samples.

We review how the technique was developed from a first set of "proof of principle" studies [2,3]. We then describe how it was followed by applications on (i) the Electrical Double layer (EDL) at mineral/water interfaces in electrolyte solutions [4,5], (ii) bacterial surfaces [6] as well as other microorganisms (algae, fungi, viruses/bacteriophages) [7,8], (iii) atmospheric ice nucleation [9], and (iv) nanomedicine [10].

The key problem in Cryogenic XPS is a reliable and reproducible sample preparation technique. It should ideally make use of UHV-stable samples, with ideally no alterations in the composition and structure of the solid-solution interface, and with a solution layer that is thinner than XPS depth of analysis (*e.g.* ~10 nm). To this end, we present our most recent recommended sample preparation protocols for wet pastes and aqueous solution/gel drops [11], and first bacterial (*Pseudomonas fluorescens* DSM50090) reference set of cryo-XPS spectra [12].

Selected references

1. Shchukarev A, Ramstedt M. Surf. *Interface Anal.* **2017**; *49*: 349-356
2. Shchukarev A, Sundberg B, Mellerowicz E, Persson P. *Interface Anal.* **2002**; *34*: 284-288
3. Ramstedt M, Shchukarev A, Sjöberg S. *Interface Anal.* **2002**; *34*: 632-636
4. Shchukarev A, Rosenqvist J, Sjöberg S. *Electron Spec. Rel. Phenom.* **2004**; *171*: 137-140
5. Kozin Ph, Shchukarev A, Boily J-F. **2013**; *29*: 12129-12137.
6. Ramstedt M et al. J. Biol. **2011**; *286*: 12389
7. Shchukarev A, Gojkovic J, Funk C, Ramstedt M. *Surf. Sci.* **2020**; *526*: 146538
8. Shchukarev A, Backman E, Watts S, Saluting S, Urban CF, Ramstedt M. *Chem.* **2021** *9*:666853
9. Yun J, Kumar A, Removsky N, Shchukarev A, Link N, Boily J-F, Bertram AK. *ACS Earth Space Chem.* **2021**; *5(5)*: 1212-1222
10. Cant DJH, Pei Y, Shchukarev A, Ramstedt M, et al. *Phys. Chem. A* **2023**; 127: 8220-8227
11. Ramstedt M, Shchukarev A. Chapter 16 in *Bacterial Cell Wall Homeostasis: Methods and protocols* (H-J Hong Ed.), Springers protocols, Methods in Molecular Biology 1440. Springer Science+Buisness Media LLC New York, NY. **2016**: 215-223.
12. Ramstedt M, Shchukarev A. *Sci. Spectra* **2022**; *29*: 014010

O103 - Effect of ethylene sulphate on electrode interphases in full cell potassium ion batteries

11. NRG – Energy, Environment, Geology and Heritage

Iurii Panasenko[1]
Leonie Wildersinn[1], Fabian Fabian Jeschull[1]
[1] Karlsruhe Institute of Technology (KIT), Institute for Applied Materials – Energy Storage Systems (IAM-ESS), Germany

The use of the sulphate ester 1,3,2-dioxathiolane 2,2-dioxide (DTD) as electrolyte additive in KIB, was recently suggested to improve the performance of cathode materials in a half-cell[1]. Zhang et al.[2] demonstrated the positive influence of DTD in both half and full cell of sodium-ion batteries (NIBs), through observation of a dense and uniformly distributed surface film. In contrast, in KIBs the additive showed poor compatibility with graphite negative electrodes. Its role in the formation of electrode surfaces in KIB full cell configurations, both the solid electrolyte interphase (SEI) and cathode electrolyte interphase (CEI), and degradation mechanism have so far not been fully understood.

In order to shed more light in the surface chemistry of DTD, we herein present an in-depth X-ray photoelectron spectroscopy (XPS) study on KIB full cells based on graphite negative and Prussian white (PW; $K_2Fe[Fe(CN)_6]$) positive electrodes. As a basis for this study, a detailed XPS study on PW electrodes in battery materials was performed, which will be valuable for future surface investigations. In the following study, the surface film formation at different state-of-charge is investigated, with an emphasis on the differences between the surface layer formation in full-cell and half-cell (i.e. against K-metal). By utilizing DTD in the full cell, a higher discharge capacity can be achieved, making it a suitable choice for KIB with proper tuning. This emphasizes the fact that electrolytes behave differently in full and half-cell K-ion systems, and generalizing findings from one system to another is not effective. The work presented herein is a continuation of our previous study on the surface layers on graphite[3,4] and contributes to a more detailed understanding of the role of DTD at the electrode surfaces of KIB anode and cathode materials.

Selected references

[1] Hosaka *et al.*, *Chem Rev,* **120**, 6358–6466 (2020).
[2] Zhang *et al.*, *Journal of Power Sources*, **541**, 231726 (2022).
[3] Jeschull; Maibach, *Electrochemistry Communications*, **121**, (2020).
[4] Allgayer *et al.*; *ACS Appl Energy Mater,* **5**, 1136–1148 (2022).

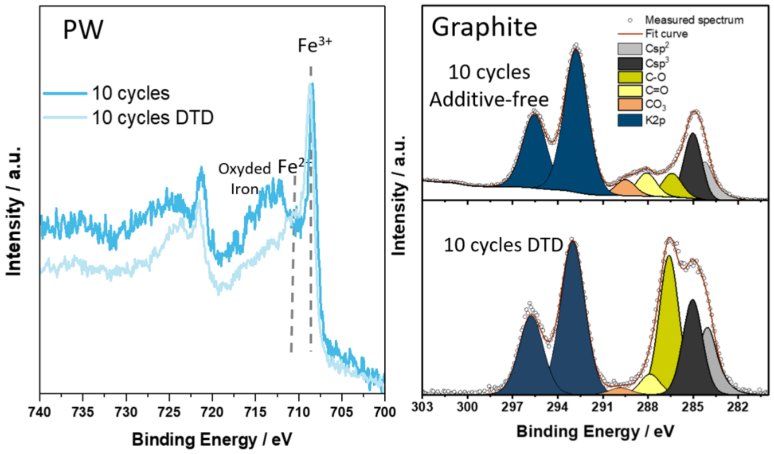

O104 - From the outer surface to the bulk: an overview of Cu(In0.7Ga0.3)Se2 degradation

11. NRG – Energy, Environment, Geology and Heritage

Anna Gagliardi[1]
Olivier Heintz[2], Anna Krystianiak[2], Amelle Rebai[3], Negar Naghavi[3], Arnaud Etcheberry[1], Jean-François Guillemoles[3], Muriel Bouttemy[1], Solène Béchu[1]
[1] Institut Lavoisier De Versailles (ILV), Université De Versailles Saint-Quentin-en-Yvelines, Université Paris-Saclay, CNRS, UMR 8180, Versailles, France
[2] ICB, UMR 6303 CNRS-Université de Bourgogne, Dijon, France
[3] Institut Photovoltaïque d'Île de France (IPVF), CNRS, UMR 9006, Palaiseau, France

Nowadays, one of the flagship solar absorbers is the quaternary alloy Cu(In$_x$Ga$_{1-x}$)Se$_2$ (CIGS), with solar cells reaching up to 23.6% efficiencies[1]. In addition to achieving high efficiencies, the CIGS community is also concerned with the durability of the solar cells. Several studies have been performed on the aging of CIGS solar cells, according to different aging conditions[2], yet only a few papers deal with the interaction of the CIGS absorber itself with the surrounding environment[3,4,5].

Here we propose to investigate the evolution of the CIGS absorber network from the surface to the bulk, when exposed to relative humidity and light, and thus, at different aging times. To this scope, X-ray photoelectron spectroscopy (XPS), hard X-ray photoelectron spectroscopy (HaXPES) and energy-dispersive spectroscopy (EDS) analysis have been performed. On one hand, by the complementary use of two lab X-ray sources, Al Kα (1486 eV) and Cr Kα (5414 eV) we were able to investigate CIGS material from the extreme surface (XPS) up to 20 nm depth probing (HaXPES). Furthermore, by considering different photopeaks along the energy scale but also the take-off angle, and therefore different escape depths, we managed to obtain a precise evolution of the degradation at 3, 8, 15 and 20 nm depth. On the other hand, EDS analysis provided us access to the composition deeper into CIGS material, till ~ 1µm.

These different routes for chemical analyses allowed us to explore the reactivity of our elements when facing drastic aging conditions (80 % relative humidity and different aging times). Starting with the conventional Al Kα X-ray source, we had already evidenced that the formation of oxides is first observed on Ga 2p$_{3/2}$ and In 3d$_{5/2}$ photopeaks, more surface sensitive with their inelastic mean free paths of 3 nm and 5 nm respectively, before affecting Ga 3d and In 4d peaks representative of the subsurface at 8 nm.[4] With the complementary study using the Cr Kα source, slightly higher probing depths were reached and we observed a progressive decrease of the oxygen content in depth, in correlation with the decrease of the oxide phases on the CIGS constitutive elements. To do so, we compared the O 1s photopeak monitored at 45° (15 nm) with the one at 85° (22 nm). This recent result is confirmed with the EDS measurements, where neither modification in the atomic composition, nor oxygen incorporation in the CIGS network has been noticed at 1 µm of depth probing.

Selected references

[1]. From NREL efficiency chart: www.nrel.gov/pv/interactive-cell-efficiency.html
[2]. M. Theelen, F. Daume, *Solar Energy*, **2016**, 586-627, 133
[3]. S. Béchu, *et al.*, *SIA* **2020**, *52*, 275.
[4]. S. Béchu, *et al.*, *Appl. Surf. Sci.* **2022**, *576*, 151898.
[5]. A. Debono, *et al.*, *Prog Photovolt Res Appl.* **2023**,1.

O105 - High-Performance Li-ion Battery negative electrode of porous Silicon Nanowires Modifies with CHx

11. NRG – Energy, Environment, Geology and Heritage

Chafiaa YADDADEN[1]
Noureddine GABOUZE[1], Malika BEROUAKEN[1], Abdelhak CHERIET[1], KATIA Ayouz-Chebout[1], Amar MANSERI[1], Ali MAMERI[1], Lamia TALBI[1], Fatima BOUDEFAR[1]
[1] Centre de Recherche en Technologie des Semi-Conducteurs pour léEnergétique

In this work, porous silicon nanowires of mesoporous types were developed by single-step metal-assisted chemical etching. These porous silicon nanowires have sufficient electronic conductivity along the longitudinal axis and can provide very high capacitance with the addition of carbon. The stability of porous silicon nanowires being the most difficult parameter to control during cycling, we opted for a new energy storage approach that consists of depositing a CHX hydrocarbon on the surface of the latter. The PSiNWs are covered with a CHX layer deposited by methane plasma created in a triode reactor at RF 13.5 MHZ, synchronized under an argon atmosphere on the surface of the porous silicon nanowires. The PSiNWs powder is recovered by ultrasound and then characterized by different characterization methods: FTIR, MEB and XPS. Metallic lithium is a negative electrode, a glass fiber separator, and the electrolyte LP30 (1 M $LIPF_6$ in 1:1 by mass of EC/DMC, (ethylene carbonate and dimethyl carbonate)). Cycling is carried out at 25 °C at a rate of 1 lithium in 10 hours (C/10) with a “loading” of 0.2 mg of silicon per cm^2. Their electrochemical performances will be studied by the CV, CDG, and EIS methods. Galvanostatic discharge was evaluated between 2 and 0.01 V for the two PSiNWs and PSiNWs/CHx electrodes. The evolution of the capacity as a function of the number of cycles makes it possible to exploit a capacity of 2800 mAh/g for the PSiNWs electrode, whereas with the PSiNWs/CHx electrode, the starting capacity is 3700 mAh/g. Furthermore, after a drop in the first cycle in all cases, the capacity is stable over 50 cycles in the case of the PSiNWs/ CHx anode.

O106 - Interface optimization through XPS and UPS in high-efficiency Sb2Se3 solar cells synthesized at high pressure

11. NRG – Energy, Environment, Geology and Heritage

Lorenzo Calvo-Barrio[1]
Maykel Jiménez-Guerra[2], Iván Caño-Prades[2], Joaquim Puigdollers[2], Zacharie Jehl[2], Yudania Sánchez[3], Edgardo Saucedo[2]
[1] Universitat de Barcelona (UB), Department of Electronic and Biomedical Engineering, IN2UB, and CCiTUB – Barcelona (Spain)
[2] Universitat Politècnica de Catalunya (UPC), Photovoltaic Lab, and Barcelona Center for Multiscale Science & Engineering – Barcelona (Spain)
[3] Institut de Recerca en Energia de Catalunya (IREC) – Sant Adrià del Besòs (Spain)

Thin film chalcogenides have established themselves as one of the main photovoltaic technologies complementary to silicon, showing technological and industrial attractiveness due to their high efficiency (> 20% in the case of CIGS or CdTe), stability and versatility. Nevertheless, the potentially unstable supply of scarce elements such as In or Ga, and the toxicity of Cd, have diverted interest towards technologies that involve emerging and abundant materials on Earth. Sb_2Se_3 emerges as a promising candidate for photovoltaic applications, distinguished by its advantageous characteristics such as binary stoichiometry and a suitable bandgap approximately 1.2 eV. This material further exhibits anisotropic electrical properties, which are particularly beneficial when aligned in a "quasi-1D" structure, optimizing light absorption and charge transport. Remarkably, the efficiency of Sb_2Se_3 -based solar cells has experienced a significant leap in less than 10 years, escalating from 0 to over 10%.

To elevate the Sb_2Se_3 technology into its next phase of advancement, it is imperative to devise and implement strategies that meticulously control its crystalline orientation, a key factor for attaining optimal material properties. Furthermore, achieving precise band alignment across various layers is crucial. This alignment significantly influences the movement of photocurrent, thereby enhancing the power conversion efficiency (PCE) of the solar cell. Therefore, we present an innovative approach to synthesise Sb_2Se_3 thin films, employing a co-evaporation method followed by a novel heat treatment process performed at elevated pressures ranging from 2 to 15 atmospheres, for assisting in the good orientation of the material. Subsequent surface modifications, including chemical etching and the application of ozone and UV light treatments, were meticulously executed to improve the efficiency of the resulting films.

We have performed a complete characterization by XRD, XRF and SEM to study grain size, stoichiometric and crystalline orientation, and by XPS and UPS to optimize the different layers and interfaces. Finally, a full optoelectronic characterization, including JV characteristics (dark and under illumination) and external quantum efficiency have been done. Our findings lay the foundation for a new paradigm in the high-efficiency synthesis of Sb_2Se_3 thin films by high-pressure techniques, which could lead to a significant breakthrough in photovoltaic technology.

Selected references

Maykel Jiménez-Guerra, Lorenzo Calvo Barrio et al.
KCN Chemical Etching of van der Waals Sb2Se3 Thin Films Synthesized at Low Temperature Leads to Inverted Surface Polarity and Improved Solar Cell Efficiency.
ACS Applied Energy Materials 2024, 7, 3, 874-884.
https://doi.org/10.1021/acsaem.3c01584
Zhao, Y.; Wang, S.; Li, C.; Che, B.; Chen, X.; Chen, H.; Tang, R.; Wang, X.; Chen, G.; Wang, T.; et al. *Regulating Deposition Kinetics via a Novel Additive-Assisted Chemical Bath Deposition Technology Enables Fabrication of 10.57%-Efficiency Sb2Se3 Solar Cells.*
Energy & Environmenta Science 2022, 15, 5118–5128.
https://doi.org/10.1039/D2EE02261C

O107 - Laser induced plasma spectroscopy as surface analytical tool for quality control gas diffusion layers of fuel cells

11. NRG – Energy, Environment, Geology and Heritage

Indro Biswas[1]
[1] Deutsches Zentrum für Luft und Raumfahrt e.V. (DLR), Pfaffenwaldring 38-40, 70569 Stuttgart, Germany

Hydrogen has gained international attention as energy carrier, as the impact of predominant fossil energies has raised similar attention. At the same time, a hydrogen-based energy economy has significant potential for regulating locally operating renewable energy sources like wind and solar power that are inherently volatile.

Membrane based fuel cells are a highly dynamic and lightweight set piece of a hydrogen-based economy and are in particular applicable in mobile applications. They directly convert the chemical energy of hydrogen and oxygen into electrical energy. The gas diffusion layer (GDL) is one component that has to maintain two opposing requirements in fuel cells: a humidified ion conduction membrane and dry gas supply structure. Typically, it consists of a carbon paper or cloth (the backing) and a micro porous layer (MPL); it is impregnated with PTFE to adjust its hydrophobic properties. Ideally, it has to be functional under a broad range of operational load [1]for dynamic operation [2] and thus a broad range of water production as result of the hydrogen-oxygen reaction, the basic principle of fuel cells.

In an evolving industry, the need for reliable and controllable mass production of fuel components arises. Product quality control is a necessary part of a functional hydrogen economy, and ideal quality control technologies have to be fast, continuous and provide results at the point in time of production.

Laser induced plasma spectroscopy was applied and evaluated regarding its usability for a fast quality control in a conveyor belt production line. The method utilises the emission spectra of material evaporated by short pulsed laser irradiation. Elemental compositions are derived from the resulting spectra. The results of GDL characterisation with this method are compared to other methods regarding availability, precision, applicability and limitations.

Acknowledgement
This work was financially supported by the Federal Ministry for Digital and Transport of Germany (Bundesministerium für Digitales und Verkehr, BMDV) under grant No 03B11016A (QM-GDL).

Selected references

[1] Garcia-Sanchez et al, Analysis of the influence of temperature and gas humidity on the performance stability of polymer electrolyte membrane fuel cells, Journal of the Electrochemical Society 163(3), 2016, F150.
[2] Garcia-Sanchez et al., Local impact of load cycling on degradation in polymer electrolyte fuel cells, Applied Energy 259 (2020) 114210.

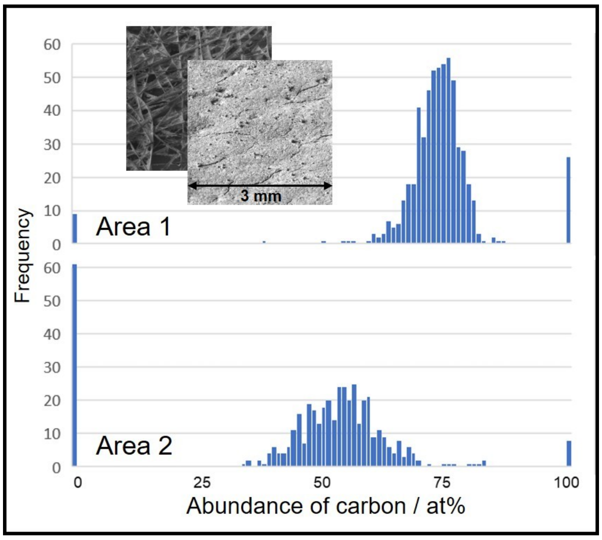

Histogram of LIPS analyses of the carbon abundance in two different areas of a microporous layer (MPL) of a gas diffusion layer (GDL).
The inset shows SEM images of fibre backing (background) and MPL side (foreground) of a an exemplary GDL.

O108 - Potential of thermally evaporated thin Li and Na films for the development of next generation alkali metal batteries

11. NRG – Energy, Environment, Geology and Heritage

Rosalía Cid[1]
Lorenzo Fallarino[1], Begoña Acebedo[1, 2], Gonzalo Salaverri[1, 3], Elena Gonzalo[1], Emanuele Gucciardi[1], Marta Cabello[1], Eider Goikolea[2], Idoia Ruiz de Larramendi[2], Montse Galcerán[1]
[1] Centre for Cooperative Research on Alternative Energies (CIC EnergiGUNE), Basque Research and Technology Alliance (BRTA), Alava Technology Park, Albert Einstein 48, 01510, Vitoria-Gasteiz, Spain
[2] Department of Organic and Inorganic Chemistry, Universidad del País Vasco (UPV/EHU), 48940 Leioa, Spain.
[3] Department of Chemical Engineering, Universidad del País Vasco (UPV/EHU), 48080 Bilbao, Spain

Lithium metal anodes with a theoretical capacity of 3860 mAh g^{-1} and the lowest redox potential (-3.04 V *vs.* SHE) are the preferred option for the next generation of lithium batteries, where high energy density and longer cycle life are required. Sodium metal anodes, with a high theoretical capacity of 1166 mAh g^{-1} and a low reduction potential (-2.71V *vs*. SHE) are emerging as an attractive alternative due to sodium's large availability, low-cost, the possibility of using copper-free current collectors.

However, lithium (Li) and sodium (Na) metal batteries are far from reaching their high theoretical energy densities since it is common to work with a great excess of alkali metal due to irreversible losses and difficulties in processing the metal anodes, especially Na [1, 2]. In fact, a new battery design eliminating the metal anode in the discharged state provides the highest achievable energy density with reduced safety hazards, though this anode-free concept is far from the practical application [2]. On the other hand, the difficulty in processing the Na metal has resulted in a lack of Na thin anodes that at least approach the energy density demands [1].

Here, we show the potential of thermal evaporation towards reaching that target. First, we demonstrate the feasibility of fabricating Na thin anodes < 10 μm by thermal evaporation, achieving a stable cycling in a full battery configuration (as stable as with a thick Na conventional anode and considerably more stable than the anode-less case) [1]. Second, we prove how a thermally evaporated ultrathin Li layer ~ 3 μm enables the platting of a more homogenous Li layer compared to the case of bare copper current collector, while a functional native solid electrolyte interphase (SEI) gives greater protection to the anode/electrolyte interface, leading to a more stable cycling of the battery [2].

Selected references

[1] L. Fallarino, G. Salaverri, R. Cid, E. Gucciardi, M. Cabello, E. Gonzalo, M. Galceran, *On the practical applicability of thermal evaporation technique to fabricate Na thin metal anodes for Na-metal batteries*, Journal of Power Sources Advances, Volume 26, 2024,100137, https://doi.org/10.1016/j.powera.2024.100137.
[2] B. Acebedo, R. Cid, L. Fallarino, G. Goikolea, J. Rikarte, E. Gonzalo, I. Ruiz de Larramendi, *On the role of ultrathin lithium metal anodes produced by thermal evaporation*, under submission.

O109 - Probing electron and ion dynamics of lead halide perovskite single crystals via time-resolved photoelectron spectroscopy

11. NRG – Energy, Environment, Geology and Heritage

Birgit Kammlander[1]
Alberto García-Fernandez[2], Håkan Rensmo[1], Ute B. Cappel[1]
[1] Division of X-ray Photon Science, Department of Physics and Astronomy, Uppsala University, 751 20 Uppsala, Sweden
[2] Division of Applied Physical Chemistry, Department of Chemistry, KTH – Royal Institute of Technology, 100 44 Stockholm, Sweden

Lead halide perovskites have been used as active materials in various opto-electronic applications, such as solar cells, detectors or light emitting diodes. However, the material's instability towards external impacts such as light or moisture remains a challenge to overcome in these devices. Particularly in their application in solar cells, in-depth understanding of the intrinsic behavior of the lead halide perovskites under light is necessary to further their development. This includes a need to understand the intrinsic electron and ion dynamics under light. So far, most studies on behavior under light exposure focused on perovskite thin films. However, slight differences in the preparation of the thin films lead to different grain sizes, which affects the thin film's properties. Studying single crystals instead of thin films excludes these variations and allows to study the intrinsic properties of different compositions. Furthermore, especially the surface and interfaces of the material interact with the environment and possible other device layers. Therefore, there is a need to understand the intrinsic behavior of the surfaces of lead halide perovskites in detail. Therefore, we used the surface-sensitive technique photoelectron spectroscopy (PES) to study compositional and electronic changes of the material's surface.

Here I will present the laser light-induced electron and ion dynamics of two clean lead halide perovskite single crystal surfaces: $CsPbBr_3$ (cesium lead bromide) and $CsFAPbI_3$ (cesium formamidinium lead iodide). To ensure that we are studying the intrinsic properties without effects from adsorbed species on the surface, we cleaved the crystals under ultrahigh vacuum conditions to obtain clean surfaces. By using PES in combination with pulsed green laser light to characterize these crystal surfaces, we were able to follow both compositional and electronic changes and we found distinct behaviors for the different crystal compositions.

O110 - Protein preservation in fossils studied by artificial maturation using ToF-SIMS and N1s-NEXAFS

11. NRG – Energy, Environment, Geology and Heritage

Peter Sjövall[1]
Martin Jarenmark[2], Per Uvdal[3], Anders Sandell[4], Johan Lindgren[2]
[1] RISE Research Institutes of Sweden, Borås, Sweden
[2] Department of Geology, Lund University, Sweden
[3] Department of Chemistry, Lund University, Sweden
[4] Department of Physics and Astronomy, Uppsala University, Sweden

Evidence for preserved proteins in up to 100 million years old fossils have been met with controversy due to analytical difficulties to prove endogeneity and lack of verified mechanisms capable of explaining such long preservation of these relatively labile molecular structures. With its capacity to detect and associate detailed molecular signatures with specific microstructural features, ToF-SIMS has proven to be a powerful method for molecular characterization and identification in fossils, particularly in combination with scanning electron microscopy (SEM) (1-2). However, while ToF-SIMS can provide evidence for molecular structures containing specific amino acids (AA), the technique is typically not capable of verifying the presence of extended peptides or intact proteins. In this work, we use artificial aging/maturation in combination with ToF-SIMS and N1s NEXAFS to study degradation patterns of two common structural proteins, collagen and elastin, and to determine how the protein degradation can be monitored using these techniques, with the final goal to detect and characterize partially degraded protein structures in fossils. Collagen and elastin were matured in a high-pressure cell at high temperatures and inert (Ar) or synthetic air atmospheres, followed by analysis with ToF-SIMS and N1s-NEXAFS. ToF-SIMS analysis was made in a TOFSIMSIV instrument (IONTOF GmbH) using Bi_3^+ primary ions and the N1s NEXAFS measurements were carried out on the FlexPES beamline at the MAXIV synchrotron facility in Lund, Sweden. Degradation of the protein structures was clearly observed in the ToF-SIMS mass spectra for maturation at temperatures above 180-200 °C, and differences between elastin and collagen were gradually diminished to be essentially gone at 250 °C (see score plot from principal components analysis (PCA) in Fig. 1a). The PC loadings reveal that increasing maturation temperatures is associated with reduced intensities of AA-related peaks and increased intensities of N-containing organic fragment ions that may be assigned to so called N-heterocycles, in agreement with previous suggestions for protein degradation in fossils (3). N1s NEXAFS spectra of the same samples show decreasing absorption of a peak assigned to nitrogen in an amide configuration (from the peptide bond) and increasing absorption of pyridine-bonded nitrogen (4) for increasing maturation temperatures (Fig. 1b), in agreement with the ToF-SIMS results. The results of the artificially matured proteins are compared to similar data from bone and teeth fossils of different age, ranging from ~35,000 (Mammoth) to ~70 million (Mosasaur, *Tyrannosaurus Rex*) years old.

Selected references

(1) J. Lindgren, et al., “Molecular preservation of the pigment melanin in fossil melanosomes”, Nat. Commun. 3:824 (2012)
(2) J. Lindgren, et al., “Fossil insect eyes shed light on trilobite optics and the arthropod pigment screen”, Nature 573, 122-125 (2019)
(3) J. Wiemann, et al., “Fossilization transforms vertebrate hard tissue proteins into N-heterocyclic polymers”, Nat. Commun. 9:4741 (2018)

(4) A . Vairavamurthy and S. Wang, “Organic Nitrogen in Geomacromolecules: Insights on Speciation and Transformation with K-edge XANES Spectroscopy”, Environ. Sci. Technol. 36, 3050-3056 (2002)

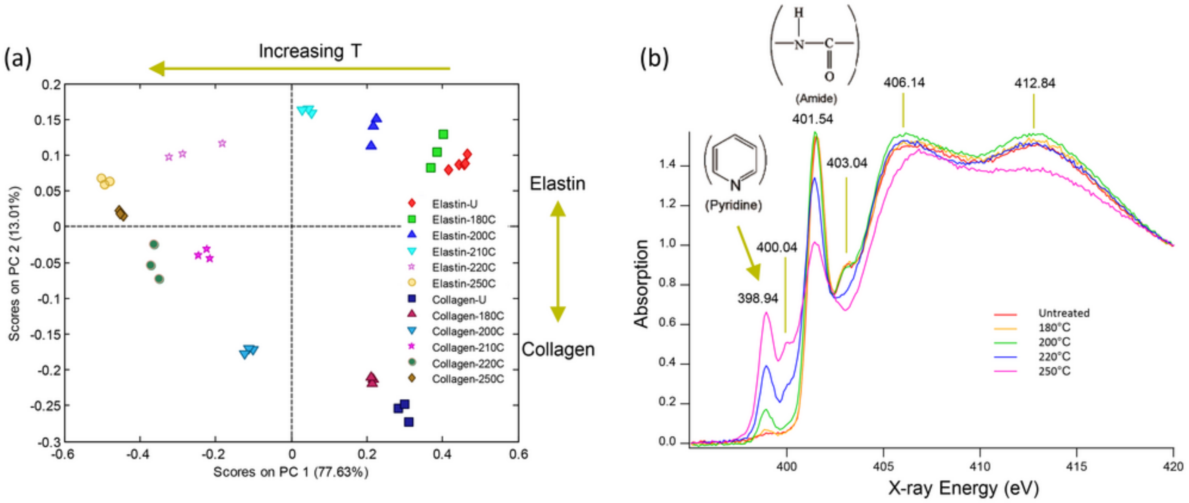

Figure 1 (a) PCA score plot of ToF-SIMS spectra acquired of elastin and collagen after maturation at varying temperatures in a 150 bar argon atmosphere (24 h). (b) N1s NEXAFS spectra of elastin after maturation as in (a).

O111 - Surface analysis of engineered particles for improved battery performance and stability

11. NRG – Energy, Environment, Geology and Heritage

Sarah Zaccarine[1]
Isaiah Oladeji[2], Koukou Suu[2], Jennifer Mann[1], Kateryna Artyushkova[1]
[1] Physical Electronics (PHI USA)
[2] ULVAC Technologies

Next-generation battery materials are needed to achieve high energy density, fast charging times, and long device lifetimes while remaining reliable and low-cost. Lithium metal batteries are a promising alternative to lithium-ion batteries but face stability concerns such as unstable solid-electrolyte interphase (SEI) growth and Li dendrite formation. Similarly, high-energy-density cathode materials like nickel manganese cobalt (NMC) and lithium cobalt oxide (LCO) have stable performance at high potentials but are susceptible to cathode dissolution in the electrolyte as well as unstable SEIs. Engineered particles (Ep) can stabilize electrode interactions, improving battery safety, SEI formation, and performance. However, batteries are multi-layered, complex systems with many components and interfaces that are difficult to handle and characterize. Understanding the chemical composition, distribution, and morphology of Ep-treated anodes/cathodes is necessary to prepare uniform, well-dispersed, high-capacity electrodes for optimized performance.

Developments in X-ray photoelectron spectrometers expand capabilities to address these challenges. X-ray photoelectron spectroscopy (XPS) is ideal for analyzing thin layers and interfaces of battery materials due to its surface (~10nm) and chemical state sensitivity. Multi-technique XPS instruments offer additional operating modes and analytical options to enable the thorough characterization of battery materials. In this talk, a fully automated, multi-technique scanning XPS/HAXPES microprobe was used to address many challenges of analyzing battery materials, including an inert environment transfer vessel for air-free handling; microprobe X-ray source with <5µm spatial resolution for 100% certainty of area selection for small-area spectroscopic analysis and chemical mapping; and the hard X-ray source and cluster ion gun source for analyzing buried interfaces without damaging the chemistry. Combined, these powerful capabilities enable thorough characterization of macro- and microscopic battery materials for a direct link between the chemistry and performance of Ep-treated battery electrodes.

O112 - Understanding and solving the issue of photodecomposition of PEO-LiTFSI polymer electrolytes in XPS analysis

11. NRG – Energy, Environment, Geology and Heritage

Joachim Sann[1, 2]
Yuriy Yusim[1, 2], Yannick Moryson[1, 2], Kevin Seipp[3], Anja Henß[1, 2]
[1] Institute of Physical Chemistry, Justus Liebig University Giessen, Heinrich-Buff-Ring 17, 35392 Giessen, Germany
[2] Center for Materials Research (ZfM/LaMa), Justus Liebig University Giessen, Heinrich-Buff-Ring 16, 35392 Giessen, Germany
[3] Department of Chemistry, Johannes Gutenberg University, Duesbergweg 10–14, 55128 Mainz, Germany

Many efforts worldwide are put into solidstate batteries as the next generation of safe high energy batteries. Among these, polymer electrolyte based batteries are one subgroup that has already been commercialized, i.e. by Blue Solution.

The cycle stability of those poly(ethylene oxide) (PEO) batteries with lithium bis(trifluoromethanesulfonyl)imide (LiTFSI) is, as in most battery technologies, hampered by interfacial decomposition, which is commonly probed through X-ray photoelectron spectroscopy (XPS). However, since these specific polymer materials are also prone to X-ray photodecomposition, it is not straight forward to link decomposition products found in XPS to chemical degradation during cell operation[1].

We investigate X-ray photodecomposition in PEO-LiTFSI systems, often mistaken for chemical decay, including those with NCM cathodes. Our study uncovers heightened photodecomposition when LiTFSI is dissolved, rather than in its pure state. This decomposition is seen in the F1s signal of the samples, which should exhibit only one peak around 688.5 eV for the pristine electrolyte but also show a strongly increasing peak at around 685 eV representing LiF. We present a measurement approaches to reduce the effect of photodecomposition on the result of the analysis and discuss pitfalls in data acquisition.

Notably, we find that cryogenic conditions significantly reduce this degradation, up to almost completely preventing it. This suggests that the photodecomposition reaction is actually limited by transport effects in the polymer. Also, our comprehensive results did not support the presence of LiF-containing decomposition products in pristine PEO-LiTFSI or PEO-LiTFSI in contact with NCM. These insights advance understanding of photodecomposition in XPS and propose a reproducible approach for accurate polymer electrolyte characterization in lithium batteries.

Selected references

[1] I. Shterenberg, M. Salama, Y. Gofer, D. Aurbach, *J. Phys. Chem. C* **2017**, *121*, 3744.

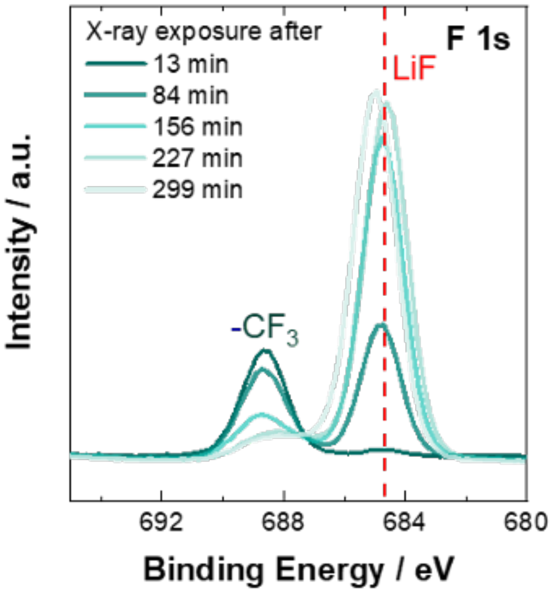
X-ray exposure after
13 min
84 min
156 min
227 min
299 min
F 1s
LiF
-CF$_3$
Intensity / a.u.
692
688
684
680
Binding Energy / eV

O113 - XPS analysis of solid state composite cathodes – discriminating degradation from electric potential gradients

11. NRG – Energy, Environment, Geology and Heritage

Felix Walther[1, 2]
Joachim Sann[1, 2], **Sebastian Leonard Benz**[1, 2], Florian Strauss[3], Xiaohan Wu[4], Boris Mogwitz[1, 2], Jonas Hertle[1, 2], Marcus Rohnke[1, 2], Torsten Brezesinski[3], Jürgen Janek[1, 2, 3]
[1] Institute of Physical Chemistry, Justus Liebig University Giessen, Heinrich-Buff-Ring 17, D-35392 Giessen, Germany.
[2] Center for Materials Research (LaMa/ZfM), Justus Liebig University Giessen, Heinrich-Buff-Ring 16, D-35392 Giessen, Germany.
[3] Battery and Electrochemistry Laboratory, Institute of Nanotechnology, Karlsruhe Institute of Technology (KIT), Hermann-von-Helmholtz-Platz 1, D-76344 Eggenstein-Leopoldshafen, Germany.
[4] BASF SE, Carl-Bosch-Str. 38, D-67056 Ludwigshafen am Rhein, Germany.

All-solid-state batteries still face many obstacles that prevent the application in consumer products. One lingering issue is the chemical instability between common cathode active materials (CAMs) and the highly conductive thiophosphate-based solid electrolytes. To overcome this, various coatings on the CAMs are utilized to prevent or at least reduce the degradation occurring at the solid electrolyte/CAM interface. The coated CAMs and their effect on the degradation phenomena in the composite cathode are regularly analyzed by means of X-ray photoelectron spectroscopy to get an idea of the working principle of the coatings applied, which in turn would be helpful to design more advanced protective coatings.

In this study we report on XPS data collected on $Li_2CO_3/LiNbO_3$-coated $LiNi_{0.6}Co_{0.2}Mn_{0.2}O_2$ (NCM622) particles utilized in a $Li_4Ti_5O_{12}/Li_6PS_5Cl$/Super C65|$Li_6PS_5Cl$|NCM622/$Li_6PS_5Cl$/Super C65 all-solid-state cells and analyzed at different state of charge (SOC) and cycle number. The experiments were conducted within a broader study and the samples were also characterized using time-of-flight secondary ion mass spectrometry (ToF-SIMS), focused ion beam scanning electron microscopy (FIB-SEM) and electrochemical measurements [1]. We were able to show the partial protection of the CAM and the Li_6PS_5Cl solid electrolyte from degradation, but the signals of the coating as well as the CAM bulk signals still show pronounced binding energy shifts for different SOCs. While this could be interpreted as reduction and oxidation processes, we show that the observed shift arises most probably from band-band-interactions of the utilized semiconductor materials resulting in electric potential gradient [2]. We show that such relative binding energy shifts between battery material components can easily result in a misleading interpretation of XPS data and discuss several effects that need to be considered when measuring battery materials with XPS.

Selected references

[1] Walther, F., et al., Chem. Mater. 2021, 33, 2110−2125
[2] Maibach, J., et al., J. Phys. Chem. Lett. 2016, 7, 1775−1780.

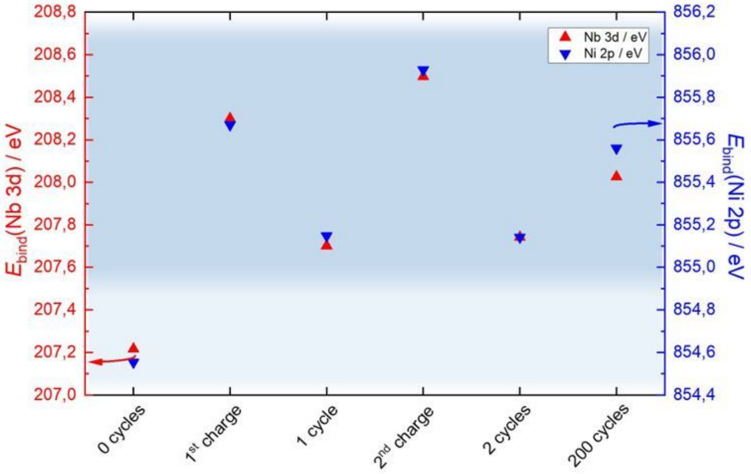

Figure 1: Shown are the mean energy positions of the Nb 3d (red) and Ni 2p (blue) signals of the coated CAM particles after surface cleaning and different stages of cycling. The energy positions were calibrated with the Cl2p-signal of the Li_6PS_5Cl argyrodite surrounding the CAM particles. The graph reveals distinct signal shifts during the first charging step for both signals (light blue area), followed by a partially reversible shift in the subsequent cycles (dark blue area).

12. POL – Polymers

O114 - Optimized surface functionalization of food-grade PVC with polyhexamethylene guanidine for antimicrobial food packaging

12. POL – Polymers

Giulio Casula[1]
Marzia Fantauzzi[1], Laura Brundu[2], Bernard Elsener[1], Antonella Rossi[1]
[1] Dipartimento di Scienze Chimiche e Geologiche, Università di Cagliari, Cagliari, Italy
[2] Laboratorio Chimico Nuorese SRLS,08100 Nuoro, Italy.

The interest toward the development of new food-packaging materials with antimicrobial activity is growing due to the prevention of the proliferation of bacteria that compromises the shelf-life of food products. One route to obtain antimicrobial food-packaging is the surface functionalization of commercially available food-grade polymers with antimicrobial active agents[1]. In this work, the development of an optimized protocol for the surface functionalization of food-grade polyvinyl chloride (PVC) with polyhexametilenguanidine (PHMG) as antimicrobial active agent is presented. The food-grade PVC was functionalized with a bottom-up approach modifying a protocol used on medical-grade PVC reported by Villanueva et alii [2]. Food-grade PVC functionalized with PHMG was obtained immersing 1 cm^2 of the as received PVC in a 10% ethanol solution of (3-mercaptopropyl) trimethoxysilane (MPTMS) for 1 h, followed by the grafting of (3-amminopropil) trietoxyisilane (APTES), glutaraldehyde, and finally with PHMG. The functionalization steps were monitored by ATR-FTIR spectroscopy that allowed confirming the functionalization by assigning the characteristic absorption of the Si-O, NH_2 and S-C bands. X-ray photoelectron spectroscopy (XPS) and angle-resolved XPS (ARXPS) were exploited to determine the surface composition of the functionalized PVC, to assess the lateral homogeneity and estimate the layer thickness. The results obtained by XPS after the first two steps of functionalization with MPTMS and APTES suggest a reaction between the two molecules in ratio 2:1 respectively. Moreover, ARXPS data allowed determining the in-depth disposition of the functional groups by means of the relative depth-plot. The relative depth plot shows (Fig. 1) the NH_2 groups oriented towards the outer layer and the sulphur at the functionalization layer-substrate interface, confirming the theoretical spatial disposition of the functional groups expected. The film thickness calculated from the ARXPS results was found to be 0.5 ± 0.2 nm [3] after the grafting of MPTMS and 1.2 ± 0.3 nm after the grafting of APTES. The results obtained confirmed the functionalization of the PVC and were in good agreement with the literature[2]. The surface analytical results obtained after the four steps will be discussed together with the results on the antimicrobial activity against *Escherichia Coli* and *Staphylococcus Aureus*.

Selected references

1. 1. Bastarrachea, L. J., Wong, D. E., Roman, M. J., Lin, Z. & Goddard, J. M. Active Packaging Coatings. *Coatings* **5**, 771–791 (2015).
2. Villanueva, M. E., González, J. A., Rodríguez-Castellón, E., Teves, S. & Copello, G. J. Antimicrobial surface functionalization of PVC by a guanidine based antimicrobial polymer. *Mater. Sci. Eng. C* **67**, 214–220 (2016).
3. Casula, G., Fantauzzi, M., Elsener, B. & Rossi, A. Surface modification of food-grade PVC monitored by angle-resolved XPS. *Vacuum* 113010 (2024) doi:10.1016/j.vacuum.2024.113010.

Acknowledgement

This research has been supported by the following funding programs:
MIUR- Fondo per lo Sviluppo e la Coesione FSC-Piano Stralcio 2015/2017 for the Ph.D. grant of Giulio Casula (Consortium UniCa and UniSS); University of Cagliari (UniCA) and Fondazione di Sardegna (FdS) for the financial support – Project number CUP J89J20000930001 (2021): “Functionalization of Food Packaging with active antimicrobial agent”.

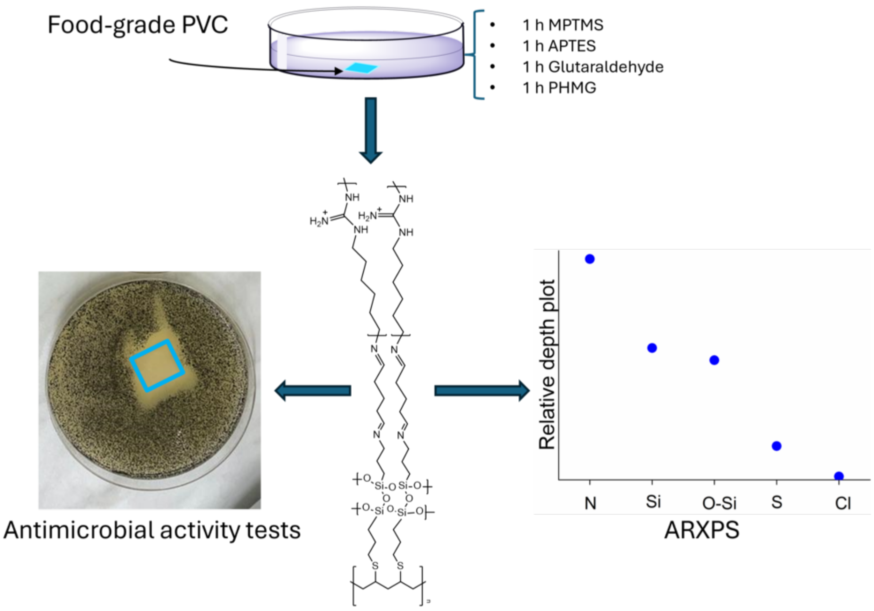

13. TEC – Technical Development and New Instrumentation

O115 - A study on electron spectrum imaging measurements using electron microprobe

13. TEC – Technical Development and New Instrumentation

Noboru Taguchi[1]
Fuyuki Nabeshima[2], Konomi Ikita[2], Tatsuya Uchida[2], Kazushiro Yokouchi[2], Kenichi Tsutsumi[2]
[1] National Institute of Advanced Industrial Science and Technology (AIST)
[2] JEOL Ltd.

In recent years, energy dispersive X-ray spectroscopy (EDX), which can perform elemental analysis at high throughput, has become popular in scanning electron microscopy analysis, and has become a common analysis tool as a visualization technology for elemental distribution in materials analysis. On the other hand, from the perspective of material analysis, more detailed material information needs to be investigated, such as the distinction of chemical states, which is difficult to achieve with EDX analysis. Electron spectroscopy such as X-ray photoelectron spectroscopy (XPS) and Auger electron spectroscopy (AES) are used as surface analysis techniques. By analyzing the electron spectrum, it is possible to analyze not only chemical elements, but also chemical states. In addition, electron spectroscopy is expected to be further utilized as an evaluation technique in materials analysis that can be applied to elements such as Li, which is difficult to evaluate in detail with EDX [1-2]. This means that electron microscopy, which has excellent spatial resolution, can be combined with electron spectroscopy to investigate spatial and local changes in materials in greater detail than ever before.

We have continued to focus on scanning Auger electron spectroscopy (AES), a technique that enables detailed material analysis from both electron microscopy and spectral analysis. Specifically, we are developing materials evaluation techniques using spectrum imaging (hyperspectral images, data cubes) obtained via electron spectroscopy. spectrum imaging methods are very useful in terms of data confirmation, post-processing, and versatility of the analysis process [3-6]. We perform spectrum imaging acquisition using a method that involves continuously acquiring secondary electron images of different energies through beam scanning with a scanning electron microscope, and subsequently generating image stacks. It has been demonstrated that existing commercially available instruments are capable of measuring and analyzing data cubes obtained through post-processing [6].

In this presentation, we will report on our efforts to acquire and analyze spectrum imaging in recent analysis cases (Fig. 1).

Selected references

[1] N. Taguchi et al., J. Electron Spec. Relat. Phenom. 203 (2015) 40
[2] N. Taguchi et al., Surf. Interface Anal. 48 (2016) 1144
[3] M. Prutton et al., Appl. Surf. Sci. 144 (1999) 1
[4] N. Urushihara et al., J. Vac. Sci. Technol. A 26 (2008) 668
[5] D.B. Durham et al., Surf Interface Anal. 50 (2018) 1174
[6] N. Taguchi et al., Ultramicroscopy 233 (2022) 113450

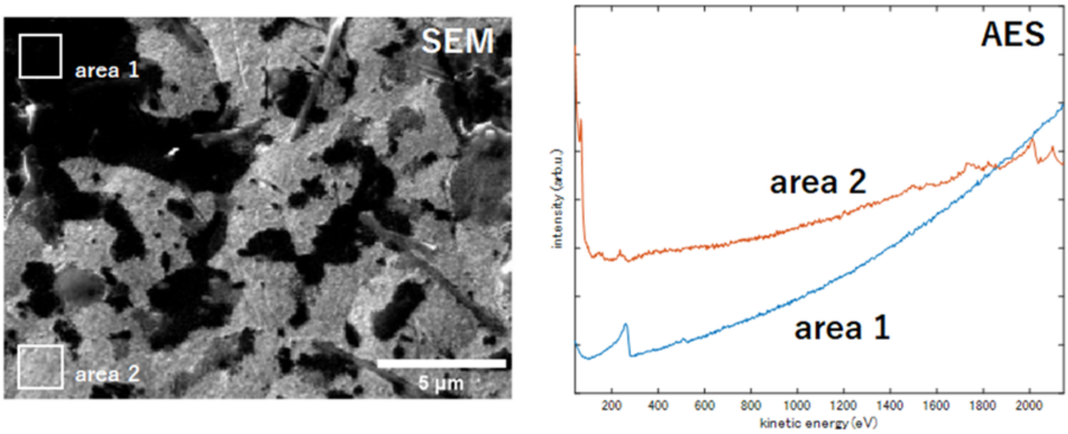

Fig. 1 AES Spectra extracted from data obtained through spectrum imaging of island-like carbon on a gold substrate.

O116 - Battery analysis with high-resolution and high-throughput XPS

13. TEC – Technical Development and New Instrumentation

Jonathan D. P. Counsell[1]
Chris Moffitt[1], **Liam Soomary**[1], Simon Hutton[1], Eric McCalla[1]
[1] Kratos Analytical Ltd.

Various material systems will be examined to provide an in-depth understanding of how X-ray Photoelectron Spectroscopy (XPS) can elucidate the distribution and chemical composition of battery materials. Na-ion batteries, touted as environmentally preferable alternatives to Li-ion batteries, especially for large-scale grid storage due to the abundance of sodium, face challenges in achieving competitive performance. Despite the promise of ternary materials, issues such as poor stability in air and inadequate long-term cycling have hindered progress. Through systematic XPS investigations, the stability in air and moisture is thoroughly explored, offering insights into modifying material stability through informed design strategies. Correlations between chemical assignments, battery performance, and oxidation degradation are established. Additionally, the discussion will encompass the importance of sensitivity and detection limits, comparisons between surface and bulk analyses, and pragmatic approaches for peak fitting difficult elemental lines. Considerations such as etch artifacts and degradation will also be addressed. [Reference: Shipeng Jia et al., J. Mater. Chem. A, 2022,10, 251-265]

Selected references

Shipeng Jia et al., J. Mater. Chem. A, 2022,10, 251-265

O117 - Evaluation of the high energy resolution spectra acquired by newly developed fast hemi-spherical analyzer (f-HSA)

13. TEC – Technical Development and New Instrumentation

Tatsuya Uchida[1]
Konomi Ikita[1], Fuyuki Nabeshima[1], Kenichi Tsutsumi[1], Masahiro Arimitsu[1], Noboru Taguchi[2]
[1] JEOL Ltd.
[2] National Institute of Advanced Industrial Science and Technology (AIST)

Auger electron spectroscopes (AES) and X-ray photoelectron spectroscopes (XPS) are widely used for purposes such as qualitative analysis, quantitative analysis, elemental maps and chemical state analysis. This versatility is derived from a hemispherical analyzer (HSA) which can be changed to variable energy resolution by controlling pass energy, and is generating applications in many academic/industrial fields [1]. On the other hands, it has a big issue that it is too slow to acquire even a spectrum with a reasonable signal-to-noise ratio occasionally taking more than 5 minutes. Therefore, recent developments reported new methods focusing on parallel detection for AES [2, 3]. To decrease such a long acquisition time, we tried to improve the energy scan speed of HSA by a shorter time constant stabilizing the sweeping voltage to inner/outer electrodes. Especially, fast voltage controls from zero to some kV needs completely new hardware design. However, the conventional spectrometer attached to JAMP-9510F manufactured by JEOL Ltd. has a lower limit of dwell time of 10 ms for a wide scan spectrum analysis.

In this presentation, we will report a new hemi-spherical analyzer system which can sweep wide energy range 10 times faster than the commercial Auger instrument, JAMP-9510F. It was called the fast HSA(f-HSA) shown in Figure 1. The spectrometer control unit was redesigned and dedicated to realize a fast and stable voltage control to the inner/outer electrode in f-HSA with a shorter time constant. Figure 2 shows step response difference of the inner electrode voltage between JAMP-9510F (a black line) and f-HSA (a red line). The voltage of f-HSA rises more than 10 times as fast as that of JAMP-9510F. Then, we checked representability of the high energy resolution spectra with the pass energy being 10 eV at constant analyzing energy mode. Figure 3 indicates the electron spectra of copper with different energy sweep rates. The black line was measured with dwell time of 10 ms at each 0.1 eV/step and accumulated 10 sweeps. The red line was acquired with 1 ms at each 0.1 eV/step and accumulated 100 sweeps. These results reveal that the new analyzer can acquire spectra at the faster sweep rate without any problem. Furthermore, we will also demonstrate the possibilities of other applications including spectrum imaging by using f-HSA.

Selected references

[1] N. Taguchi et al., ECASIA (2019)
[2] N. Taguchi, T. Uchida, K. Ikita, A. Tanaka, N. Ikeo, K. Yokouchi, K. Tsutsumi: Ultramicroscopy 233 (2022) 113450
[3] T. Uchida, K. Ikita, A. Tanaka, K. Yokouchi, N. Ikeo, K. Tsutsumi, N. Taguchi: JEOL News 2022, 57, 40-47

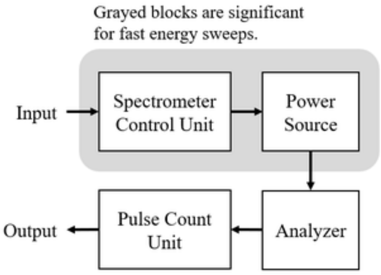

Fig. 1 Redesigned system diagram of f-HSA.

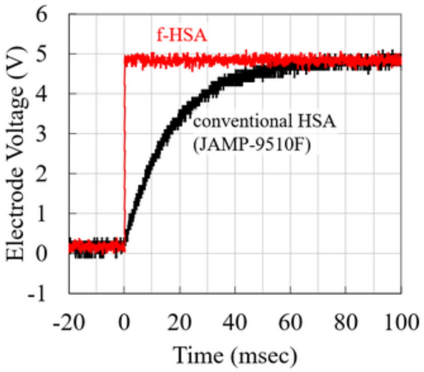

Fig. 2 Step response of power source.

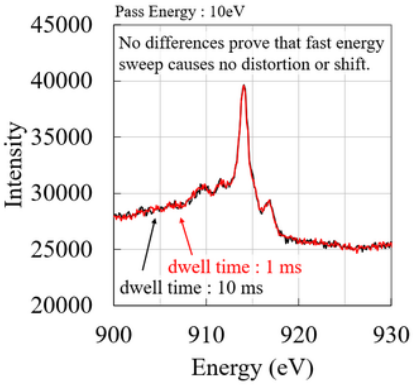

Fig. 3 Electron spectra of Cu KLL.

O118 - Exploring the power of TOF-SIMS by coupling collision-induced dissociation and surface-induced dissociation

13. TEC – Technical Development and New Instrumentation

Jacob Schmidt[1]
Gregory Fisher[1]
[1] Physical Electronics, Inc.

TOF-SIMS with kilo-electron volt collision-induced dissociation (CID) tandem MS is a powerful tool for compositional identification and structural elucidation of molecules, metabolites, and degradation products due to its ability to isolate ions of interest and provide further insights into its molecular structure and composition. TOF-SIMS tandem MS has been used to unambiguously verify analytes and to generate 2D and 3D maps of a brass corrosion inhibitor[1], to image organelles in single cells[2], and to discern the degradation pathway of OLEDs[3].

In this presentation, we will explore the application of surface-induced dissociation (SID) coupled with CID, to assist in the confirmation of molecular assignments. In contrast to CID, which promotes cleavage at every molecular bond, SID is more subtle in that the bond cleavages result predominantly in the observation of functional group chemistry, as shown in Figure 1. The fragmentation energetics between SID and CID are distinct, even at the same kinetic energy. This difference in fragmentation energies can have a significant effect on calibration, which we will address using isotopic abundancies to confirm compositional assignments.

Selected references

1. Finšgar, *Corrosion Science*. **182** (2021) 109269.
2. Agüi-Gonzalez, et. al, *J. Anal. At. Spectrom*. **34** (2019) 1355-1368
3. Sawada, et. al, *SID Symp. Dig. Tec.* **54** (2023) 1291-1293
4.

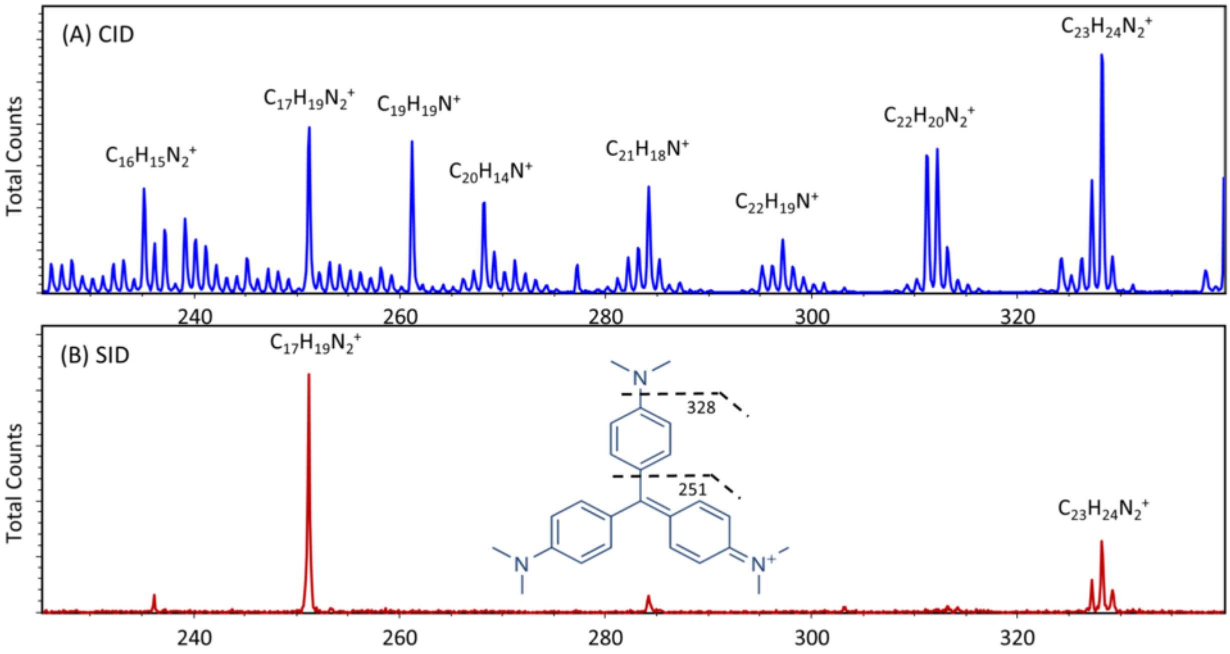

Figure 1 - CID and SID spectra of crystal violet.

O119 - Hard X-ray photoelectron spectroscopy with photon energy up to 30 keV for characterization of semiconductor materials

13. TEC – Technical Development and New Instrumentation

Satoshi Yasuno[1]
Tappei Nishihara[1], Okkyun Seo[1], Yasumasa Takagi[1], Vuong Van Cuong[2], Shin-Ichiro Kuroki[2]
[1] Japan Synchrotron Radiation Research Institute
[2] Hiroshima University

Hard X-ray photoelectron spectroscopy (HAXPES) is a powerful tool for investigating the chemical and electronic states of bulk and buried interfaces non-destructively due to its large probing depth[1]. However, the probing depth of HAXPES of a several tens of nanometers is insufficient to analyze the actual device structure for the semiconductor materials, and in some cases, the thickness of the insulating film or electrode must be reduced for evaluation. Therefore, to obtain a much larger probing depth and measure deeper regions than conventional HAXPES, we have developed a high-energy HAXPES (HE-HAXPES) system excited by photon energies up to 30 keV[2]. This system is achieved by combining an applied bias voltage upon the sample with a conventional hemispherical electron energy analyzer.

By utilizing this system, we successfully observed a Si 1s peak from the bulk-Si substrate underneath the 110-nm-thick SiO_2 film at the photon energy of 30 keV. Figure 1 shows Si 1s spectra of 110-nm-thick SiO_2 film/ n-type crystalline Si-substrate measured by using photon energies from 14 to 30 keV in the 2 keV step. In the spectrum at photon energy of 14 keV, a week signal assigned to a bulk-Si substrate is observed around a binding energy of 1840.5 eV. The signal intensities gradually increased with increasing the photon energy and the Si substrate signal is clearly observed at a photon energy of 30 keV. Additionally, from the Si substrate signals with photon energy over 24 keV, the asymmetric shapes with a shoulder appear at the higher binding energy side. It was suggested that these spectral shapes may originate from the band bending in the Si substrate.
The HE-HAXPES system excited by the photon energy up to 30 keV could be a very useful tool to yield genuine insights into the chemical and electronic states in deeply buried regions. We will also present the results on the application of this method to other semiconductor materials.

Selected references

1. Kobayashi, Nucl. Instrum. Methods Phys. Res. **A601**, 32 (2009)
2. S. Yasuno, O. Seo, Y. Takagi and T. Nishihara, Rev. Sci. Instrum, **94**,115113 (2023).

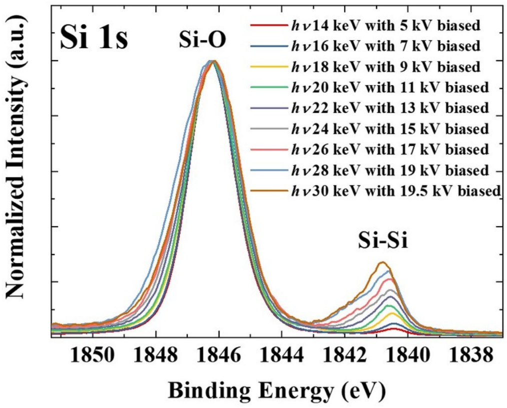

Figure 1. Si 1s spectra of 110-nm-thick SiO_2 film/Si-substrate measured at photon energies from 14 to 30 keV. The photoelectrons emerging from the sample are decelerated to a kinetic energy below 10 keV by the applied bias voltage upon a sample.

O120 - Neural network for high-throughput XPS analysis using the simulation of electron spectra for surface analysis code

13. TEC – Technical Development and New Instrumentation

Florian Simperl[1]
Wolfgang Werner[1]
[1] TU Wien, Institute of Applied Phyiscs, 1040 Vienna, Austria

X-ray photoelectron spectroscopy (XPS) is a surface sensitive (< 10 nm) characterisation technique used to investigate material properties including chemical composition, chemical depth distribution, and electronic structure [1, 2]. Especially in recent years, XPS has become a reliable and advanced experimental technique across various disciplines of science and engineering resulting in the generation of large spectral datasets. Extracting quantitative information from these datasets has traditionally required trained spectroscopists to perform empirical peak-fitting routines for each individual spectrum. For example, to obtain the atomic fraction of a particular element in a sample, the expert needs to determine the integrated peak area from complex fitting routines based on the inelastic scattering background and zero energy loss line shapes and normalize it according to relative sensitivity factors [3].

In response to the increasing demand for reliable and instantaneous spectral analysis, we propose an automated quantitative X-ray photoelectron spectrum analysis pipeline by combining the Simulation of Electron Spectra for Surface Analysis (SESSA) software with a convolutional neural network (CNN). SESSA serves as an important tool in the field of XPS either as a database for material parameter retrieval or as a Monte Carlo-based simulation software for quantitative interpretation of XP spectra or Auger electron spectra (AES) for a variety of materials (bulk, nanostructures, layered spheres, etc.) [4, 5]. In this work SESSA is applied to generate approximately 270’000 spectra for 2500 materials (of varying complexity) and single elements, illustrated by the histogram overlaid with the periodic table in Fig. 1. To increase the variability in the simulated dataset and to reflect experimental conditions we simulated spectra with different chemical shifts, different peak widths, and different peak shapes (Gauss, Lorentz, Doniach-Sunjic).

In a first preliminary study, these simulated spectra together with their corresponding chemical labels were used to train a CNN to classify the chemical abundance. The study aims to investigate the feasibility of applying deep learning models to high-throughput material characterization within XPS. In the future, we plan to compare their performance on experimental data with classical peak-fitting routines and to improve the deep learning model further to predict more complex sample features such as thin film thickness and electronic properties.

Selected references

[1] D. Nanda Gopala Krishna and John Philip. “Review on surface-characterization applications of X-ray photoelectron spectroscopy (XPS): Recent developments and challenges”. In: Applied Surface Science Advances 12 (2022), p. 100332
[2] Grzegorz Greczynski et al. “X-ray photoelectron spectroscopy of thin films”. In: Nature Reviews Methods Primers 3.1 (May 2023), p. 40.
[3] Alexander G. Shard. “Practical guides for x-ray photoelectron spectroscopy: Quantitative XPS”. In: Journal of Vacuum Science & Technology A 38.4 (July 2020), p. 041201
[4] C. J. Powell, W. Smekal, and W. S. M. Werner. “A New NIST Database for the Simulation of

Electron Spectra for Surface Analysis (SESSA): Application to Angle-Resolved X-ray Photoelectron Spectroscopy of HfO2, ZrO2, HfSiO4, and ZrSiO4 Films on Silicon". In: AIP Conference Proceedings 788.1 (Sept. 2005), pp. 107–111.

[5] Wolfgang S. M. Werner and Cedric J. Powell. "Applications of the National Institute of Standards and Technology (NIST) database for the simulation of electron spectra for surface analysis for quantitative x-ray photoelectron spectroscopy of nanostructures". In: Journal of Vacuum Science & Technology A 39.6 (Sept. 2021), p. 063205

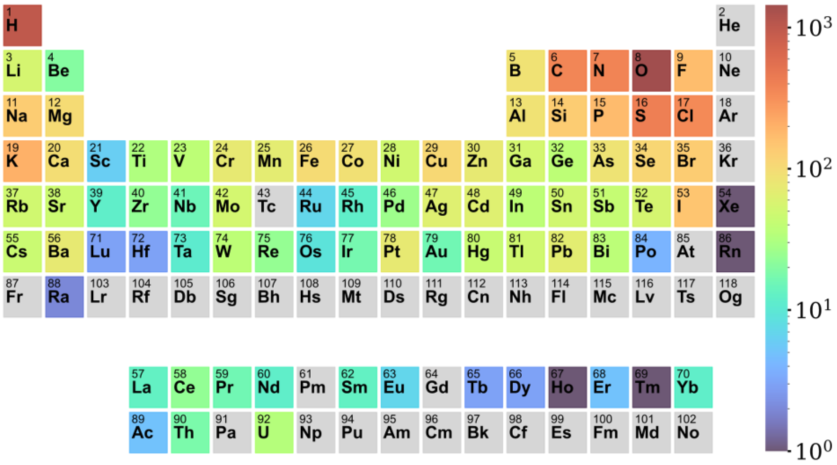

Figure 1: Frequency of elements in the simulated dataset

O121 - Non-destructive depth differentiated analysis of surfaces using Ion Scattering Spectroscopy (ISS), XPS and HAXPES

13. TEC – Technical Development and New Instrumentation

Paul Mack[1]
[1] Thermo Fisher Scientific

Recently there has been renewed interest in probing deeper into surfaces using HAXPES in addition to the more surface sensitive (soft X-ray) XPS. On modern XPS systems, with high sensitivity, the total sampling depth may be somewhere between 10nm and 15nm but HAXPES enables the analyst to look deeper, without having to destructively sputter the surface with ions. For a complementary, more comprehensive analysis, XPS and HAXPES can be combined with Ion Scattering Spectroscopy (ISS). ISS is far more surface sensitive than XPS, typically being thought of as a technique to analyse the top monolayer of a sample for elemental information.

In this work, the combination of XPS, HAXPES and ISS on a single tool has been used to give a non-destructive depth differentiated analysis of a range of samples, including a perovskite and an industrially relevant material containing multiple transition metals. The combination of all three techniques provides insight into the depth distributions of elements and chemical states, from the top monolayer to beyond 20nm into the surface.

O122 - Operando Cells for high-pressure solid-gas and solid-liquid interface analysis

13. TEC – Technical Development and New Instrumentation

Georg Held[1]
David C. Grinter[1], Pilar Ferrer[1], Santosh Kumar[1], James Counter[1, 2], Matthijs van Spronsen[1], Paul Webb[3]
[1] Diamond Light Source, Didcot, UK
[2] University of Reading, Reading, UK
[3] University of St Andrews, St Andrews, UK

The two branch lines of the VerSoX beamline (B07) at Diamond Light Source (UK) deliver medium flux X-rays in the range 45-2800 eV and are dedicated mainly to studies of catalyst surfaces and interfaces under reaction conditions. The beamline has endstations for high-throughput X-ray Photoelectron Spectroscopy (XPS) under ultrahigh vacuum conditions, Near-Edge X-ray Absorption Fine Spectroscopy (NEXAFS) under ambient conditions, and XPS/NEXAFS under near-ambient pressure conditions in the mbar range. This enables studies of a wide range of surfaces and gas-solid interfaces over many decades of pressure, as well as solid-liquid interfaces using custom-built operando cells. We will present the designs of the two cells, a microreactor for NEXAFS measurements at elevated pressures and temperatures up to 1 bar and 400 °C, respectively, and an electrochemical cell with exchangeable windows for both XPS and NEXAFS measurements. First results demonstrate the performance of both cells. Using the Total Electron Yield (TEY) detection mode to probe the first few nanometres of the catalyst sample, the high-pressure microreactor was used to study the Fischer-Tropsch (FT) reaction over Co catalysts. The combination of high temperature, high pressures of toxic and flammable gases, mechanistic complexity, and a product slate comprising both gases and liquids makes this an ambitious and relevant study. The electrochemical cell was used to in a NEXAFS only study of the Cu-redox chemistry and a NAP-XPS and NEXAFS study of water oxidation on a Nafion-based polymer membrane (Nafion/mesoporous C/IrOx catalyst). Both studies are related to electrochemical water splitting.

Selected references

Georg Held, Federica Venturini, David C. Grinter, Pilar Ferrer, Rosa Arrigo, Liam Deacon, Wilson Quevedo Garzon, Kanak Roy, Alex Large, Christopher Stephens, Andrew Watts, Paul Larkin, Matthew Hand, Hongchang Wang, Linda Pratt, James J. Mudd, Thomas Richardson, Suren Patel, Michael Hillman, Stewart Scott, "Ambient-Pressure Endstation of the Versatile Soft X-ray (VerSoX) Beamline at Diamond Light Source", Journal of Synchrotron Radiation 27 (2020) 1153 – 1166; DOI: 10.1107/S1600577520009157

David C. Grinter, Federica Venturini, Pilar Ferrer, Matthijs A. van Spronsen, Rosa Arrigo, Wilson Quevedo Garzon, Kanak Roy, Alexander I. Large, Santosh Kumar, Georg Held, "The Versatile Soft X-ray (VerSoX) Beamline at Diamond Light Source", Synchrotron Radiation News (2022); DOI: 10.1080/08940886.2022.2082181

David C. Grinter, Pilar Ferrer, Federica Venturini, Matthijs A. van Spronsen, Alexander I. Large, Santosh Kumar, Hadeel Hussain, Alex Iordachescu, Andrew Watts, Sven Schröder, Anna Kroner, Federico Grillo, Stephen Francis, Paul Webb, Georg Held, "VerSoX B07-B: A High-Throughput XPS and Ambient Pressure NEXAFS Beamline at Diamond Light Source", Journal of Synchrotron Radiation (accepted); DOI: 10.1107/S1600577524001346

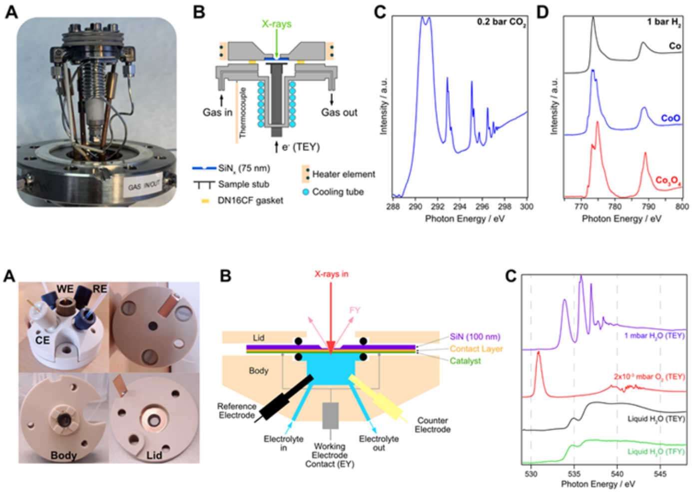

Photographs (A), schematic drawings (B), and representative data (C,D) of the operando microreactor (top) and electrochemical cell (bottom).

O123 - Operando/in-situ coupling of XPS and EIS to study solid-state Li-ion batteries

13. TEC – Technical Development and New Instrumentation

Giulia Serafino[1]
Raf Claessens[1], Benny Wouters[1], Fernand Gauthy[2], Xinhua Zhu[1], Annick Hubin[1]
[1] Research Group Sustainable Materials Engineering SUME , Department Materials and Chemistry, Vrije Universiteit Brussel, Pleinlaan 2, 1050 Brussel, Belgium
[2] SYENSQO, Rue de Ransbeek 310, 1120 Brussel, Belgium

Characterizing and understanding the dynamic processes at the solid/solid interface in solid-state Li-ion batteries SSBs is crucial for designing resilient, durable, and high-energy density SSBs [1][2]. X-ray photoelectron spectroscopy (XPS) is one of the most widely used surface analysis techniques for a broad range of battery materials and provides valuable quantitative and chemical state information from the surface. Unfortunately, the XPS results of SSBs are often convoluted due to the complex chemistry involved. Operando XPS is a combined approach that enables monitoring of the chemical and electronic properties of the electrolyte-electrode interface in SSBs [3][4][5]. Besides the surface analysis techniques, electrochemical impedance spectroscopy (EIS) is a powerful technique for characterizing the state of charge and state of health of battery materials. The in-house developed operando odd random phase EIS (ORP- EIS) allows for achieving valid EIS measurements in dynamic conditions and can reveal the continuous evolution of the interfacial phenomena [6].

In this work, we couple Operando/in-situ XPS with Operando ORP-EIS to study solid-state Li-ion batteries. This approach provides a unique way of exploring dynamic interfacial chemistry concurrently. Cross-section samples on the cross-section of SSBs (full-cell configuration) are prepared to enable access to the buried interfaces. A dedicated electrochemical cell is capable of maintaining a mechanical stuck pressure and heating the cross-section SSB samples. The control over these two parameters allows for more realistic operating conditions during the operando characterizations. This approach remains essential for a better understanding of the interfacial chemistry and future development of next-generation SSB systems.

Selected references

[1] Y. Xiao et al., *Nat Rev Mater*, vol. 5, nº 2, p. 105–126, 2020, doi: 10.1038/s41578-019-0157-5.
[2] M. B. Dixit et al., *Energy Environ Sci*, vol. 14, nº 9, p. 4672–4711, 2021, doi: 10.1039/d1ee00638j.
[3] X. Wu et al., *Physical Chemistry Chemical Physics*, vol. 20, nº 16, p. 11123–11129, 2018, doi:10.1039/c8cp01213j.
[4] A. Benayad et al, *Journal of Physical Chemistry A*, vol. 125, nº 4, p. 1069–1081, 2021, doi:10.1021/acs.jpca.0c09047.
[5] K. N. Wood et al., *Nat Commun*, vol. 9, nº 1, p. 1–10, 2018, doi: 10.1038/s41467-018-04762-z.
[6] X. Zhu et al., *Journal of Power Source*, vol. 544, p. 231852, 2022, doi:10.1016/j.jpowsour.2022.231852.

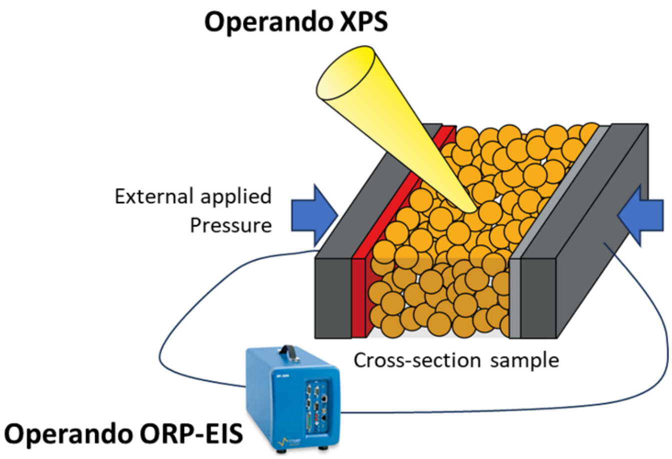

Figure 1. Combined Operando/in situ setup scheme of cross-section of a SSB.

O124 - Photoelectron spectroscopy laboratory at the European XFEL

13. TEC – Technical Development and New Instrumentation

Ivan Arkhipushkin[1]
Manuel Izquierdo[1], Joachim Schulz[1], Elisa Delmas[1], Matthäus Kitel[1], Vasilii Bazhenov[1], Luigi Adriano[1], Serguei Molodtsov[1]
[1] European XFEL

The European XFEL is an X-ray Free-Electron Laser (XFEL) facility providing femtosecond short, extremely intense coherent X-ray pulses for scattering, imaging and spectroscopy. Within the facility, we establish a photoelectron spectroscopy (PES) user laboratory. Here we intended to offer unique possibilities of pre- and post-characterization of samples by means of photoelectron emission microscopy (PEEM) and band probing with ARPES method, along with classic XPS and UPS. The system is equipped with Kreios 150 MM analyzer (SPECS) with MCP DLD detector (Surface Concept), allowing acquisition of 3D data sets of kx/ky images versus energy scale. LHe cryostat and heating post embedded in sample holder allows experiments in the temperature range 500-16 K, now possibility to achieve 4.2 K is examined. Two excitation sources are conventional X-ray twin Al-Mg anode (PreVac) with 600 / 450W peak power and HIS 14 HD UV-source (Focus) with $1.1 \cdot 10^{13}$ Ph/mm^2/s photon density. Setup has preparation chamber with 4-axis manipulator with cryostat for cooling with liquid nitrogen or helium. E-beam heating and Ar ion-sputter gun with energy up to 3 keV allows annealing and sputtering of samples. Spectrometer has RGA head and open ports to install evaporators or custom devices. LEED with MCP screen is used to observe crystal structure and surface purity of samples within preparation cycles. Fast entry lock hosts up to 4 flag-type sample holders and provides installation of vacuum suitcase.

O125 - Quantitative secondary electron spectroscopy using a concentric hemispherical analyzer and Monte-Carlo simulations

13. TEC – Technical Development and New Instrumentation

Marcel Himmerlich[1]
Valentine Petit[1], Sven Mähl[2], Mauro Taborelli[1]
[1] CERN, European Organization for Nuclear Research, 1211 Geneva 23, Switzerland
[2] SPECS Surface Nano Analysis GmbH, Voltastrasse 5, 13355 Berlin, Germany

The quantity of secondary electrons emitted from a surface is an important parameter for the simulation of physical phenomena for applications, where electron multiplication is either desired or detrimental. In such cases, the secondary electron yield (SEY) in dependence of primary electron energy as integrated parameter is utilized for material qualification as its measurement is relatively straight-forward. Nonetheless, for quantitative modeling of electron emission processes, the knowledge of the angular and energy dependence of the number of emitted electrons is necessary. The challenge in measuring these values is the wide range of kinetic energy of the emitted electrons from 0 to 50 eV for the true secondary electrons up to the primary electron energy of several keV. The angle integrated energy distribution of emitted electrons was already studied using hemispherical retarding-field analyzers and assuming an energy independent detection efficiency [1,2]. In this work we utilize a concentric hemispherical electron analyzer for the measurement of the energy-distribution of emitted secondary, backscattered, and elastically reflected electrons in normal emission and in the range from 0 to 1500 eV. Special experimental conditions consider the consequences of Liouville's theorem to define a constant angular acceptance angle, while assuring an analyzer acceptance area larger than the spot size of the impinging electron beam. These measurements are combined with Monte-Carlo simulations to determine the transmission function and detection efficiency correction derived from experimental data, which are essential for a quantitative assessment of the emitted electrons beyond pure spectroscopic considerations. To benchmark the quantitative accuracy of the corrections, the numerical integration of the spectra is compared to classical SEY measurements, and a very good agreement is found. We have conducted such measurements for different materials that are of relevance for electron cloud build-up and its mitigation in particle accelerators, i.e. pure and oxidized copper surfaces, laser-treated and amorphous carbon (a-C) coated Cu, as well as for selected standard crystals with interesting features in the secondary electron spectrum such as HOPG and MoS_2. A detailed analysis of the energy-dependence of the electron spectra of the various surfaces will be presented and reveals differences in the respective contribution of secondary electrons, of the wide range of backscattered electrons and of the elastically reflected electrons to the total electron yield. For example, the two surface modification technologies for SEY reduction, a-C coating and laser-roughening, result in different characteristics in the suppression of low-energy and high-energy electrons.

Selected references

[1] M. Azzolini, M. Angelucci, R. Cimino, R. Larciprete, N. M. Pugno, S. Taioli, and M. Dapor, J. Phys. Condens. Matter 31 (2019), 055901.
[2] S. Schulte, G. Hartung, J. Kröger, M. Himmerlich, V. Petit, M. Taborelli, Phys. Rev. Accel. Beams 23 (2020), 103101.

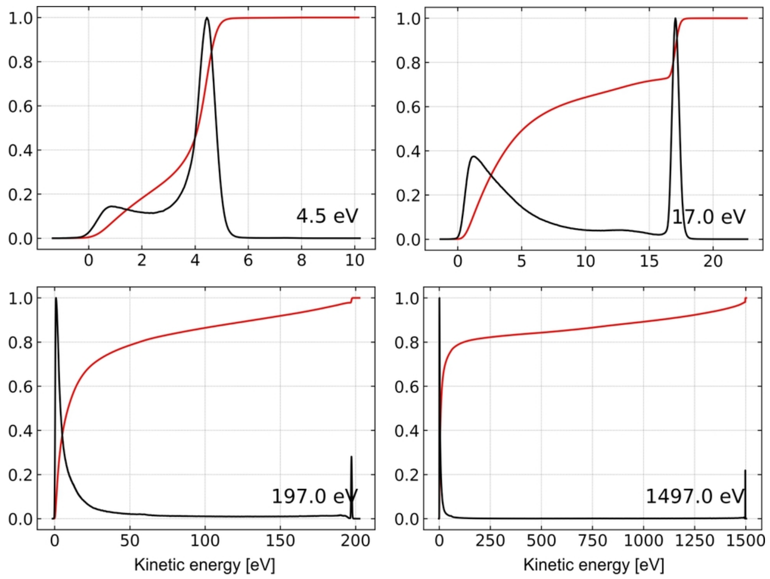

Energy-dependence of the emitted electrons from a sputter-cleaned polycrystalline Cu surface when exposed to primary electrons of different energy (from 5 to 1500 eV). Shown are the transmission-corrected spectra N(E) in black as well as their numerical integration ∫N(E)dE in red.

O126 - Visualization of Fermi level difference at p-n-p junction in transistor device by spectrum image method of AES

13. TEC – Technical Development and New Instrumentation

Konomi Ikita[1]
Fuyuki Nabeshima[1], Tatsuya Uchida[1], Kazushiro Yokouchi[1], Akihiro Tanaka[1], Toshiyuki Ohama[1], Kenichi Tsutsumi[1], Noboru Taguchi[2]
[1] SA business unit, JEOL Ltd.
[2] National Institute of Advanced Industrial Science and Technology (AIST)

Recent semiconductors are designed with the process rules of 10 nm or less, and it is very important to grasp accurately about a p-n junction with high spatial resolution of nanometers. Some people reported to visualize a p-n junction with an electron spectroscopy by the onset position difference of secondary electrons or by the peak position difference in Auger spectra [1][2]. These methods are difficult to obtain reproducibility without controlling surface contamination and oxidation during sample preparation, and furthermore, it is not easy to distinguish the peak shifts from those caused by charging due to beam irradiation. In addition, in the conventional Auger electron spectroscopy (AES), the peak top and background are specified respectively to obtain a mapping of the intensity difference, so that the expected result is often not obtained when the peak position is shifted. In order to solve this problem, we have developed a *spectrum image* method using AES [3]. Using this method, a spectrum measured at any energy resolution in an arbitrary wide energy range including a several peaks in each pixel is stored in cube data format. By postprocessing, it is possible to extract spectra from any area and form an intensity map.

In this presentation, we used the *Spectrum Image* to visualize the Fermi level difference using the peak shift of Si KLL at the p-n junction and evaluated its effectiveness. The sample was a pnp epitaxial planner transistor that was mechanically polished, and p-n junction was exposed. A native oxide layer of 1~2 nm was formed on the surface, so oxide Si and pure Si peaks were detected. The measurement conditions were an acceleration voltage of 20 kV, an irradiation current of 30 nA and an energy resolution of 10 eV for pass energy. Fig.1 (a) shows the spectra extracted from the cube data at the p-typed and n-typed Si areas respectively, and Figs. 1(b) and (c) show the intensity maps calculated by these peak differences. In this result, the work function of the top surface was estimated the same at both p-typed and n-typed area because it was observed no peak shift of the oxide Si KLL peak. On the other hand, it was confirmed only a Si KLL peak shift of about 0.6 eV among both area, which was considered the Fermi level difference of the p-type / n-type silicon in the bulk.

Selected references

[1] R. Pantel, F.Arnaud D'Avitaya, Ph. Ged and D. Bois:Scanning electron microscopy/1982/II 548 SEM Inc., AMF O'hare(Chicago), IL 60666, USA
[2] Y. Sakai, M. Kudo and C. Nielsen. J. Vac. Sci. Technol. A, Vol. 19, No.4 (2001)
[3] Noboru Taguchi, Tatsuya Uchida, Konomi Ikita, AkihiroTanaka, Nobuyuki Ikeo, Kazushiro Yokouchi and Kenichi Tsutsumi, Ultra microscopy, 233,113450 (2022).

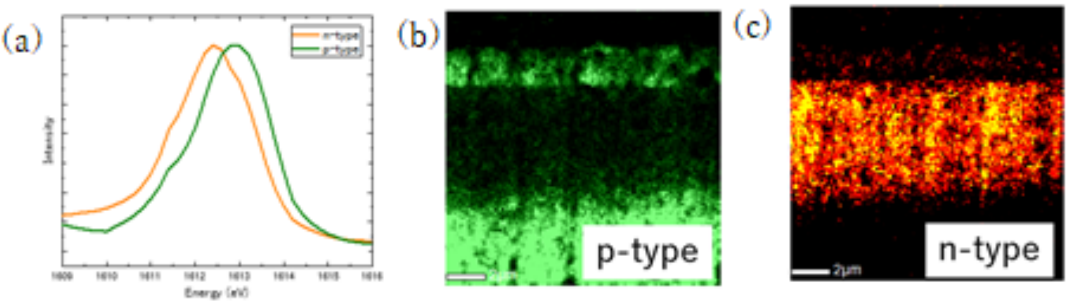

Fig. 1 (a)AES spectra from the p- and n-type area, and (b),(c) maps with these peaks.

Posters

1. ADH – Adhesion and Tribology

P1 - Effects of laser-processed surface texturing on wear behaviors of Ti alloys in contact with ZrO2 for dental applications

1. ADH – Adhesion and Tribology

Masaaki Nakai[1]
Takeshi Iwasaki[1], Kosuke Kisaichi[1], Kosuke Ueki[1]
[1] Kindai University

The effects of surface texturing via picosecond pulsed laser processing on wear behaviors of titanium alloys in contact with zirconia (ZrO_2) was investigated by comparing three different types of alloys. As the α-, α+β-, and β-type titanium alloys, commercially-pure titanium (CP-Ti), Ti-6Al-4V ELI (Ti64), and Ti-29Nb-13Ta-4.6Zr (TNTZ) were used. The wear behaviors of these alloys were dominated by different wear modes, depending on the types of alloys. The abrasive and adhesive wear modes dominated in Ti64 and TNTZ, respectively. On the other hand, adhesion of wear debris was observed in CP-Ti, but the amount of it was smaller than that in TNTZ. The wear debris of Ti64 acted as abrasive particles. The wear debris of TNTZ adhered to the surface easily, and then the adhered wear debris turned into a hard wear-protective layer. The wear debris of CP-Ti were also adhered to the surface, but the amount of them was smaller and the protective effect was weaker than those of TNTZ. These differences in wear debris character leaded to the different effect of surface texturing on wear behaviors of titanium alloys. Because the dimples fabricated on surface can trap the wear debris, they were effective for reducing wear in Ti64 but were detrimental in TNTZ. Similar effects on wear were obtained between the dimples on CP-Ti and TNTZ, but the increase in wear loss due to the presence of dimples was less in CP-Ti than TNTZ.

P2 - Surface coating of graphene oxide/Polyaniline/Cu by co-deposition for improved tribological performance

1. ADH – Adhesion and Tribology

Muhammad Aqeel[1]
Piyatep Ngernklay[1], Jinhua Sun[1]
[1] Department of Industrial and Materials Science, Chalmers University of Technology, 41296 Göteborg, Sweden.

Metal matrix composite coatings represent a cutting-edge approach to surface engineering by combining the robust properties of metal with the exceptional characteristics of ceramics [1]. Graphene emerges as a promising additive for lubricant materials, capable of enhancing tribological characteristics on a micro- and nano-scale [2]. Despite its promise, there are still challenges to homogeneously add graphene into metal matrix with nanoscale distribution. One potential method to address this challenge is the integration of a polymerized conductive polymer to improve the interface interaction of graphene and metal [3]–[5]. However, the co-deposition processes of electroplating metal and electrochemical polymerization inherently hindered each other from their reduction and oxidation natures, respectively. In this work, the crystalline and conductive polyaniline (PANI) nanofibers were grown on the surface of graphene-oxide (GO) (PANI@GO). In tandem with the co-deposition of Cu matrix to form PANI@GO-Cu with controllable thickness and surface properties for the surface coating. The deposition was achieved by electrochemical deposition with various ratios and concentrations. The presence of PANI increases the interaction between graphene and the Cu matrix, leading to a homogeneous distribution of the three components. Structural and morphological information of PANI@GO and PANI@GO-Cu was attained through X-ray diffraction, Fourier transform infrared spectroscopy, Raman spectroscopy, thermogravimetric analysis, scanning electron microscopy, and transmission electron microscopy. The results demonstrate well-grown PANI on GO sheets with worm-like structures. The surface morphology and nanostructures of PANI@GO-Cu composite coatings were significantly affected by PANI content. In addition, tribological tests illustrated the effectively reduced coefficient of friction (CoF) of Cu after the coatings. The lubricant behavior of coatings presented a strong correlation with the GO:PANI ratio, concentration, and applied load. This study presents a novel approach to co-deposit multiple components for surface coating to enhance the tribological performance, providing a critical function in the isolation, connection, and interruption of electrical current.

Selected references

[1] A. Ramakrishnan and G. P. Dinda, "Functionally graded metal matrix composite of Haynes 282 and SiC fabricated by laser metal deposition," *Mater. Des.*, vol. 179, p. 107877, 2019, doi: 10.1016/j.matdes.2019.107877.
[2] F. Jiang *et al.*, "Anti-corrosion behaviors of epoxy composite coatings enhanced via graphene oxide with different aspect ratios," *Prog. Org. Coatings*, vol. 127, no. May 2018, pp. 70–79, 2019, doi: 10.1016/j.porgcoat.2018.11.008.
[3] S. Shahabuddin, N. M. Sarih, M. A. Kamboh, H. R. Nodeh, and S. Mohamad, "Synthesis of polyaniline-coated graphene oxide@SrTiO3 nanocube nanocomposites for enhanced removal of carcinogenic dyes from aqueous solution," *Polymers (Basel).*, vol. 8, no. 9, 2016, doi: 10.3390/polym8090305.

[4] Y. Jafari, S. M. Ghoreishi, and M. Shabani-Nooshabadi, "Polyaniline/Graphene nanocomposite coatings on copper: Electropolymerization, characterization, and evaluation of corrosion protection performance," *Synth. Met.*, vol. 217, pp. 220–230, 2016, doi: 10.1016/j.synthmet.2016.04.001.
[5] Y. C. Yong, X. C. Dong, M. B. Chan-Park, H. Song, and P. Chen, "Macroporous and monolithic anode based on polyaniline hybridized three-dimensional Graphene for high-performance microbial fuel cells," *ACS Nano*, vol. 6, no. 3, pp. 2394–2400, 2012, doi: 10.1021/nn204656d.

2. BIO – Bio-interfaces, Biomaterials and Life Science

P3 - Characterization of the biomedical surface by the XPS and HPXPS

2. BIO – Bio-interfaces, Biomaterials and Life Science

Justyna Kozdemba[1]
Marcin Dzierzega[1], **Lukasz Walczak**[1]
[1] Research and Development Division, PREVAC sp. z o.o., Raciborska 61, 44-362 Rogow, Poland

Nature has developed strategies to produce complex materials. Biomaterials is an important and inspiring field and needs special attention from scientists and engineers to create new reasonable biostructures. X-ray photoelectron spectroscopy (XPS) is valuable for the characterization of biomaterials [1], biointerfaces [2,3], and polymer surfaces [4,5] with detailed chemical and elemental information of the surface composition. We would like to promote the latest equipment, technology solutions, and innovations in the photoelectron spectroscopies field. Here it will be presented an innovative and compact spectrometer for routine X-ray photoemission spectroscopy and ambient pressure photoemission spectroscopy for the study of important phenomena in the current research. The design, construction, and technical parameters of a new X-ray source for imaging of biomedical surfaces with two types of analyser will be presented. We will report the technical solution of the new X-ray source and research results of XPS measurements conducted on the surface chemistry and electronic structures can be investigated, and the elemental composition is obtained in the imaging mode, with a micrometer resolution. Moreover, it will be demonstrated the investigation in ambient pressure conditions.

Selected references

[1] Sara A. M. El-Sayed et. al J Biomed Mater Res. 112 (2024) e35376.
[2] Brittany Foley et. al Appl. Surf. Sci. 647 (2024) 158577.
[3] Anna Taratuta et. al. Vacuum 214 (2023) 112187.
[4] Vanessa de Cassia Gomes Videira et. al. Next Materials 3 (2024) 100071.
[5] Krishna Priya Hazarika & J. P. Borah Scientific Reports 14 (2024) 427.

P4 - Isolation of extracellular vesicles based on functionalized beads and a microfluidic device for biomarkers analysis

2. BIO – Bio-interfaces, Biomaterials and Life Science

Lia Vanzetti[1]
Lorenzo Lunelli[1, 2], Anna Pedrotti[1], Cecilia Pederzolli[1], Cristina Potrich[1, 2]
[1] SD-FBK, Povo (Trento), 38123, Italy
[2] CNR-IBF, Povo (Trento), 38123, Italy

Extracellular vesicles (EVs) are increasingly suggested as innovative biomarkers correlated to the diagnosis, progression and therapy of several diseases. Small EVs, often called exosomes, are possibly the most studied EVs, having a diameter ranging from about 30 – 150 nm and being secreted by almost all type of cells. These vesicles play an important role in cell-to-cell communication, carrying various molecular cargo, which includes proteins, lipids, nucleic acids and metabolites. The EVs cargo varies depending on the physiological and pathological state of the secreting cells and therefore it could be considered as a source of biomarkers informative about the health of an individual. Several techniques have been developed for the specific separation of small EVs, but they are often scarcely efficient and give solutions enriched in vesicles, but still containing other unwanted materials.

New methods for an efficient and reliable isolation of small EVs are therefore desirable. Surface functionalizations can help in setting up new isolation techniques, which can be implemented on-chip once developed. Silicon oxide surfaces were used as starting substrates for functionalization with different divalent cations in order to obtain positively charged surfaces. These surfaces were tested for their efficiency for the capture of small EVS previously purified *via* serial ultracentrifugations of cell supernatants. The two better-performing cations, i.e. Cu^{2+} and Ni^{2+}, were then selected to functionalize magnetic microbeads to be inserted in microfluidic chips. The correct functionalization of microbeads was assessed by X-ray photoelectron spectroscopy (XPS), which allowed quantifying the chemical composition of beads upon the different treatments. The functionalized microbeads were inserted in a microdevice and evaluated for their efficiency in capturing EVs and releasing EVs biomarkers. The best protocol setup was explored for the capture of EVs from cell culture supernatants and for the analysis of EVs biomarkers, i.e. microRNAs, via RT-PCR. The promising results obtained with this on-chip approach allow to move a step forward toward the integration in simple and fast biosensors capable of analyzing the desired biomarkers present in EVs, helping the spread of biomarkers analysis both in clinical settings and in research.

Funding: This work was partially funded by European Union (NextGeneration EU) through the MUR-PNRR project SAMOTHRACE (ECS00000022).

P5 - Surface characterisation of electrically poled polylactic acid using sessile drop method

2. BIO – Bio-interfaces, Biomaterials and Life Science

Kristine O'Dwyer[1]
Ehtsham-Ul Haq Haq[1], Charlie O'Mahony[1], Dinesh Barnana[1], Krittish Roy[1], Daniela Butan[2], Syed A. M. Tofail[1]
[1] Department of Physics, and Bernal Institute, University of Limerick, V94 T9PX, Limerick, Ireland
[2] Technological University of the Shannon Midwest, Moylish Park, V94 EC5T, Limerick, Ireland

Wettability and surface free energy are among the most useful determinants of solid surface morphology and its role in bacterial adhesion. Biofilm formation and encrustation pose significant threat to stented patients with the bio-environment proving hostile through the interface of the material surface and salts contained within urine. is The mitigation of bioburden on urinary stents is observed in bio-coatings such as lubricating or anti-fouling coatings, using low-friction hydrophilic surfaces [1]. Most bacteria possess a negative surface charge, facilitating adhesion. This adhesion is consequential of the interfacial relationship between the bacteria and surface free energy, owing to long-range electrostatic charge, vdW-Ld interactions, and hydrophobic interactions [2]. Polylactic Acid (PLA), a widely utilised hydrophobic biomaterial with extensive functionality is often copolymerised with hydrophilic materials making it more favourable in vivo [3]. Surface charges may be altered through manipulation of the piezoelectric coefficient of the biomaterial. This is achieved through charge injection. Utilising contact poling to manipulate the piezoelectric effect in PLA, surface energy is being investigated through alterations in hydrophobicity via sessile drop method, and quantification of surface potential via the Kelvin probe method. The contact angle (CA) for unpoled PLA is 75° – 85° [4], with poling at 2.2kV in this study resulting in a CA increase from (76.4 – 76.99°) to (87.88 - 87.9°). Surface potential of PLA changed from -77KmV to 86KmV, moving from negative to positive in experiments as expected [5]. The globular protein Lysozyme, identified as displaying significant piezoelectric coefficient, has the ability to catalyse the hydrolysis of the peptidoglycan layer of bacterial cell walls [6]. It is found to possess a piezoelectric coefficient of 6.5pC N^{-1} [6], comparable to that of Glycine, 6.13 ± 1.13 pC N^{-1} [7], with Glycine reported as a suitable candidate for biomedical applications and also possessing antimicrobial properties [8]. PLA and its optical isomers (L and D-lactide)are widely used in medical applications with PLLA being reported to have a D33 value of 7-12 pC N^{-1}. Given these observations, it may be inferred that Lysozyme could be utilised as an antimicrobial and bio-compatible coating for urinary stents, using a multilayered approach. Considering the hostile environment it must perform in, layers prevent biofilm formation in the first instance by peeling away upon bioburden contact to reveal a fresh layer analogous to the preceding layer.

Selected references

[1] Bernasconi, V. T.-N. (2023). 'Comprehensive overview of ureteral stents based on clinical aspects, material and Design' (2023a) *Central European Journal of Urology* [Preprint]. doi:10.5173/ceju.2023.218.
[2] Tofail, S.A. and Bauer, J. (2016) 'Electrically polarized biomaterials', *Advanced Materials*, 28(27), pp. 5470–5484. doi:10.1002/adma.201505403.
[3] Hendrick, E. and Frey, M. (2014) 'Increasing surface hydrophilicity in poly(lactic acid) electrospun fibers by addition of PLA-B-peg co-polymers', *Journal of Engineered Fibers and Fabrics*, 9(2), p. 155892501400900. doi:10.1177/155892501400900219.

[4] Tümer, E.H., Erbil, H.Y. and Akdoğan, N. (2022) ‘Wetting of superhydrophobic polylactic acid micropillared patterns’, *Langmuir*, 38(32), pp. 10052–10064. doi:10.1021/acs.langmuir.2c01708.
[5] Shi, S. *et al.* (2024a) ‘PVTF nanoparticles/PLA electroactive degradable membrane for Bone Tissue Regeneration’, *Coatings*, 14(1), p. 115. doi:10.3390/coatings14010115.
[6] Stapleton, A. *et al.* (2017a) ‘The direct piezoelectric effect in the globular protein lysozyme’, *Applied Physics Letters*, 111(14). doi:10.1063/1.4997446.
[7] Sui, J. *et al.* (2022) ‘Orientation-controlled crystallization of γ-glycine films with enhanced piezoelectricity’, *Journal of Materials Chemistry B*, 10(36), pp. 6958–6964. doi:10.1039/d2tb00997h.

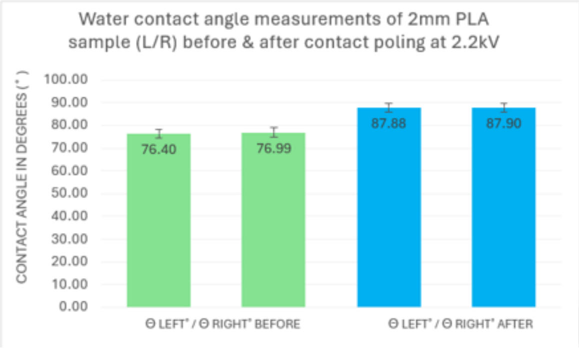

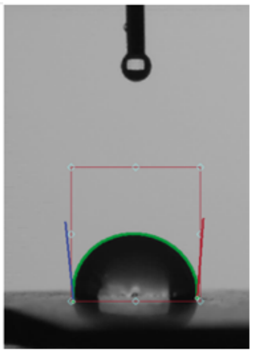

Figure 1: Mean water CA for PLA 2mm sample, before and after contact poling at 2.2kV in ambient conditions for 15 minutes. Measured data shows a difference of 11.48° for ϑ left, making it less hydrophilic, moving towards hydrophobicity. ϑ right measured difference of 10.91°performed similarly suggesting charge injection due to contact poling altered the surface energy of the sample displaying lower adhesion to the water molecules and less wettability. Characteristic activity that may be applied to Lysozyme as a bio-coating when it encounters electronegative bioburden in future studies. Figure 2: CA measurement of water CA on PLA 2mm sample post contact poling captured on the Ossila Goniometer.

P6 - XPS and ToF-SIMS characterization of cholesterol-based nanoparticles for Huntington disease

2. BIO – Bio-interfaces, Biomaterials and Life Science

Marta Valenza[1]
Giovanni Tosi[2], Jason T. Duskey[2], Barbara Ruozi[2], Ilaria Ottonelli[2], Giulia Birolini[1], Angela Vandelli[2], Dora Mehn[3], **Francesco Fumagalli**[3], Elena Cattaneo[1], Giacomo Ceccone[3]
[1] Università degli studi di Milano, Istituto Nazionale di Genetica Molecolare, Milan, Italy
[2] Università di Modena e Reggio Emilia, Department of Life Sciences, Modena, Italy
[3] European Commission, Joint Research Centre, Ispra (VA), Italy

Cholesterol is of a paramount importance in the structure and function of the central nervous system (CNS). The transfer of cholesterol to apolipoproteins and lipoproteins within the CSF plays an important role in brain homeostasis. Moreover, brain Cholesterol (Chol) is the main component of myelin and plays and essential role in neurotransmitter release.[1] Chol in the CNS is almost entirely produced locally and the (BBB) prevents direct transfer of sterols from the blood to the brain, especially when they are contained in lipoprotein particles However, to compensate for the steady-state synthesis of cholesterol within the brain, there is a specific brain clearance mechanism allowing a limited transfer of Chol through the BBB.[2]

The Huntington's disease (HD) is a genetic, adult-onset, neurodegenerative disorder characterized by motor and cognitive defects with loss of striatal and cortical neurons. One dysfunction identified is related to brain cholesterol which is essential for synaptic function. Brain Chol biosynthesis is early reduced in HD animal models and this defect is measured in HD patients by the plasma level of the brain-specific Chol catabolite 24-hydroxy-cholesterol. As reported above, all brain Chol is produced locally and the decreased of Chol biosynthesis in HD brain leads to a lower availability of newly synthesized Chol to satisfy proper synaptic functioning.[3] Since, brain Chol replacement with Chol from circulation is prevented by the BBB, routes to restore cholesterol levels in the brain are investigated. Chol-based nanocarrier formulations to deliver exogenous cholesterol have been successfully applied to reduce the cognitive decline in animal experiments.[4]

In this work, cholesterol loaded brain- permeable nanoparticles (NPs), termed hybrid-g7-NPs, prepared with a hybrid composition of biodegradable poly-lactide-co-glycolide (PLGA) and cholesterol mixture and engineered with a well-known ligand (g7 peptide) for BBB crossing have been synthesized via established protocols.[5] Detailed physico-chemical characterization was performed by means of dynamic light scattering (DLS) and Asymmetric flow-field flow fractionation (AF4) to determine nanoparticles size and size distribution, whilst X-ray photoelectron spectroscopy (XPS) and Time of Flight secondary ion mass spectrometry (ToF-SIMS) were used to assess the surface chemistry of the nanoparticles (Fig. 1).

Selected references

[1] D.H. Mauch, et al. Science, 2001, 294, 1354. doi: 10.1126/science.294.5545.1354
[2] F. Pifferi, et al., Front. Physiol., 2021, 12:645646. doi: 10.3389/fphys.2021.645646
[3] M. Valenza et al., EMBO Mol. Medicine, 2015, 7(12), 1547
[4] A. Passoni, et al., ACS Chem. Neurosci. 2020, 11, 367
[5] G. Birolini, et al., Journal of Controlled Release, 2021, 330, 587

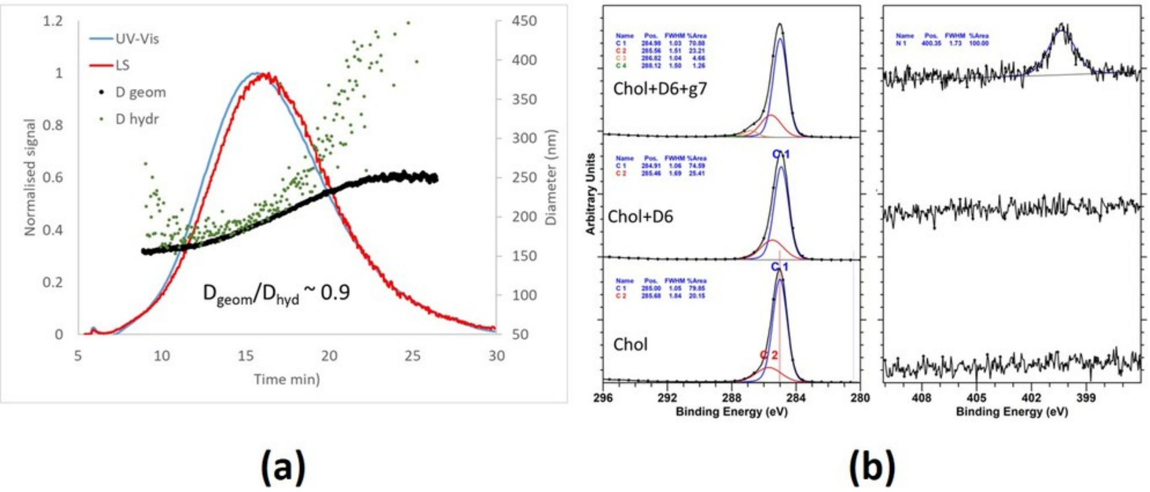

Fig. 1: AF4 with DLS and MALS data of purified hybrid-g7-NPs (a) and C1s and N1s core level spectra purified hybrid-g7-NPs synthesized with deuterated cholesterol (b)

3. CAT – Catalysis and Surface Functionalization

P7 – Combining theory and experiments: spectra validation through DFT studies of metal-phosphonate properties in NU-1000

3. CAT – Catalysis and Surface Functionalization

Roberth Mateo NARVAEZ ADAMS[1, 2]
Jennifer Theissen[3, 4], Nick Gys[1, 3], Elien Derveaux[4], Peter Adriaensens[4], Wouter Marchal[4], Rob Ameloot[3], Ionut Tranca[2], Tom Hauffman[1], Frederik Tielens[2]
[1] Research Group Sustainable Materials Engineering, lab Electrochemical and Surface Engineering (SURF), Vrije Universiteit Brussel.
[2] General Chemistry (ALGC) - Materials Modelling Group, Vrije Universiteit Brussel.
[3] Center for Membrane Separation, Adsorption, Catalysis and Spectroscopy (cMACS), KULeuven.
[4] Analytical and Circular Chemistry (ACC), Institute for Materials Research (IMO) Hasselt University.

Metal-organic frameworks (MOFs) have emerged as a revolutionary class of materials with remarkable versatility and wide-ranging applications across multiple scientific disciplines. MOFs, consisting of metal nodes interconnected by organic linkers, possess exceptional tunability, high surface areas, and intriguing porosity. These distinctive characteristics bestow upon MOFs extraordinary properties, making them highly desirable for diverse applications encompassing gas storage and separation, catalysis, sensing, and drug delivery systems.

Amid the extensive assortment of MOFs, the NU-1000 structure has garnered substantial attention due to its exceptional properties and potential in various fields. NU-1000 is an exceptionally sturdy and highly stable MOF characterized by a well-defined structure comprising 558 atoms (264 C, 180 H, 96 O, 18 Zr) within its unit cell. The deliberate design and synthesis of NU-1000 provide a platform for investigating the fundamental principles governing MOF behavior and offer a pathway for the development of advanced functional materials.

In this study, density functional theory (DFT) calculations are employed to investigate the functionalization of cluster-nodes with a focus on the catalysis, adsorption energies, and structural parameters of the NU-1000 metal-organic framework (MOF) in the presence of phenyl phosphonic acid (PhPA) molecules adsorbed on its metallic nodes. Molecular dynamics simulations, accounting for temperature effects, are utilized to compute infrared (IR) spectra, while nuclear magnetic resonance (NMR) and X-ray photoelectron spectroscopy (XPS) spectra are also calculated. A comparison between the simulated and experimentally measured spectra establishes the reliability of the DFT calculations. This work, conducted as part of the PHOSPORE project, advances the understanding of MOFs and facilitates the tailored design of MOFs for a wide range of applications in catalysis and functional materials.

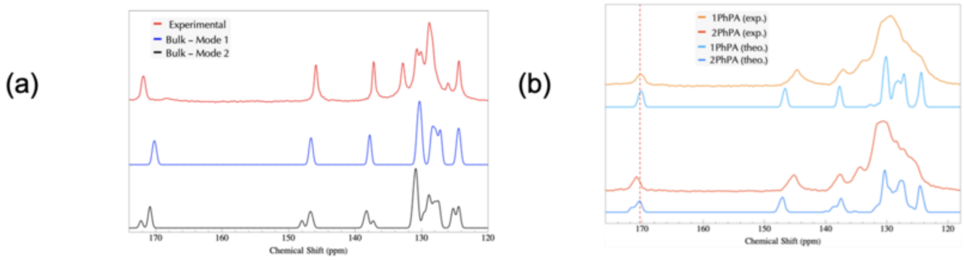

Figure1. Comparison of theoretical-experimental ^{13}C NMR spectra of the bulk structure (a) and in presence of PhPA adsorbed on the cluster-nodes (b).

P8 - Conduction and valence bands investigation of CuInS2@ZnS for gas sensing purposes

3. CAT – Catalysis and Surface Functionalization

Antonio Orlando[1, 2]
Andrea Gaiardo[1], Giorgio Speranza[1], **Lia Vanzetti**[1]
[1] Sensors and Devices Center, Bruno Kessler Foundation, Via Sommarive 18, Trento, 38123, Italy
[2] Faculty of Engineering - Free University of Bozen/Bolzano - Piazza Domenicani 3, 39100 - Bolzano, Italy

Understanding the electronic and optical properties of nanomaterials is essential for tailoring their behaviour as semiconductors, insulators, or conductors. Quantum confinement effects in nanomaterials significantly influence band gap and valence/conduction band energies, offering the potential for tailored electronic transitions and band gap modulation [1]. Manipulating these band energies enables the creation of nanomaterials with specifically designed optical and electrical characteristics, essential for pioneering nanoscale technologies in electronics, sensors, photonics, and energy harvesting. Recently, there has been a growing interest in nanomaterials and quantum dots (QDs) for gas sensors, leveraging their catalytic and chemoresistive properties through photoactivation using radiation energy in the UV-visible wavelength range. This approach enables the development of gas sensors with enhanced specificity and lower power consumption compared to thermally activated devices. However, challenges include low sensitivity and the need for high-energy UV radiation due to the band gap of the material. Recent efforts have concentrated on developing materials and composites with tailored band gaps, particularly exploring the advantages of combining metal oxides with QDs.

In this study, $CuInS_2@ZnS$ quantum dots were synthesized and characterized for their potential to form composite materials with metal oxides. The chemical synthesis process was carried out by a modified procedure of [2], yielding $CuInS_2@ZnS$ formation with a In/Cu ratio of 3:1. The energy values of the valence and conduction bands were estimated through X-ray photoelectron spectroscopy (XPS) and UV-Vis characterization.

The XPS characterization revealed a valence band energy of 0.63 eV for $CuInS_2@ZnS$ quantum dots (Figure 1a). The conduction band energy was determined to be 3.89 eV using a tauc plot obtained from the absorption spectra (Figure 1b-c). These high-energy values suggest that $CuInS_2@ZnS$ quantum dots can facilitate energy-allowed electronic transfer, making them suitable as photo-antennas for the photo-activation of metal oxides using visible light.

To achieve the desired properties in composite materials, the conduction band energy of the metal oxide must be lower than that of the quantum dot, allowing efficient electronic transfer. The study underscores the importance of tailored band gaps in designing composite materials for improved gas sensing applications. Overall, this work contributes to the ongoing efforts in advancing nanomaterials for innovative applications in electronics, sensors, photonics, and energy harvesting.

Selected references

[1] C. Xia, W. Wu, T. Yu, X. Xie, C. van Oversteeg, H. C. Gerritsen, and C. de Mello Donega, ACS Nano (2018), vol. 12, no. 8, p. 8350–836.
[2] W. Hu, S. Yang, and J. Huang, J. Chem. Phys. (2019), vol. 151, no. 21, p. 214705.

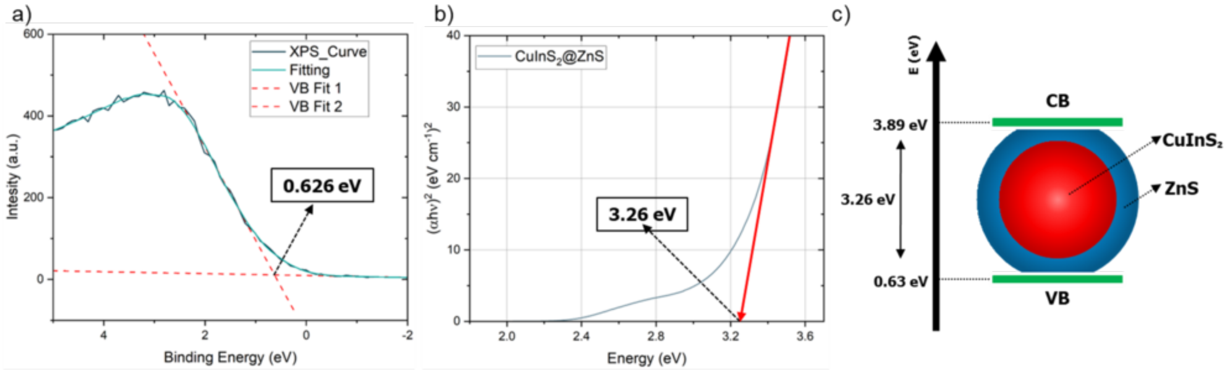

Figure 1. *a) Fitting of the XPS Valence band of the CuInS$_2$@ZnS QDs, b) Tauc Plot of QDs for the estimation of their band gap, c) Energy diagram representation of the band gap of the QDs.*

P9 - Methane dehydroaromatization on Mo/HZSM-5 and Nb doped Mo/HZSM-5 catalysts: A NAP-XPS study

3. CAT – Catalysis and Surface Functionalization

Stephan Bartling[1]
Stefan Peters[1], Ali M. Abdel-Mageed[1], Sebastian Wohlrab[1], Evgenii Kondratenko[1]
[1] Leibniz Institute for Catalysis

The direct conversion of methane to value-added chemicals such as methanol, ethers and aromatics is a key-factor in the efficient use of natural gas resources. Methane can be transformed to hydrogen, ethylene, and aromatics by employing molybdenum-modified zeolite catalysts at elevated temperatures [1]. Rapid catalyst deactivation makes this reaction highly dynamic, while *in situ* reduced Mo oxycarbides and carbides are discussed to be the active species [2]. In this study a laboratory based near ambient pressure X-ray photoelectron spectrometer (NAP-XPS) is used to investigate Mo/HZSM-5 and Nb doped Mo/HZSM-5 catalysts with a nominal Mo loading of 6 wt.% under *operando* non-oxidative methane dehydroaromatization conditions [3,4]. At a reaction temperature of 900 K the evolution of the electronic properties of the catalyst is followed with time on stream under continuous flow of reaction gas (90% CH_4/10% N_2; 2 mbar) revealing a pronounced change of the molybdenum oxidation state. The Mo 3d signal is deconvoluted assuming contributions of Mo^{2+}, Mo^{4+}, Mo^{5+}, and Mo^{6+} using similar peak shapes / FWMH as described by Murugappan et. al [5]. The deconvolution shows a stepwise reduction of Mo^{6+} to Mo^{5+} and Mo^{4+} before a further reduction to Mo^{2+} starts, see Figure 1. The obtained results are discussed in connection with activity measurements under ambient pressure conditions, effect of Nb doping and corresponding *ex situ* and *pseudo in situ* XPS results.

Selected references

1. J. Spivey, G. Hutchings, *Chem. Soc. Rev.* **43** (2014) 792
2. Lezcano-Gonzalez, R. Oord, M. Rovezzi et al., *Angew. Chem., Int. Ed.* **55** (2016) 5215
3. S. Peters, C. Rieg, S. Bartling, M. Parlinska-Wojtan, M. Dyballa, S. Wohlrab, A. M. Abdel-Mageed, *ACS Catal.* **13** (2023) 13056
4. S. Peters, S. Bartling, M. Parlinska-Wojtan, A. Wotzka, A. Guilherme Buzanich, S. Wohlrab and A. M. Abdel-Mageed, *J. Mater. Chem. A*, 2024, Accepted Manuscript
5. Murugappan, E.M. Anderson, D. Teschner, T.E. Jones, K. Skorupska, and Y. Román-Leshkov, *Nat. Catal.* **1** (2018) 960

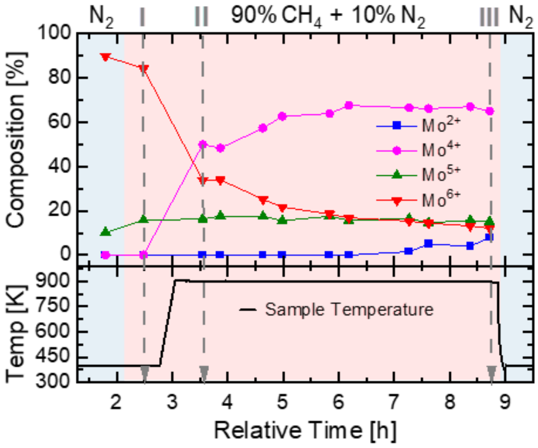

Figure 1. Evolution of the Mo surface species under methane dehydroaromatization conditions in the NAP-XPS at 2 mbar over time.

P10 - XPS, TEM and DFT characterization of mnemonic TiO2 rutile–rutile interfaces triggering spontaneous dissociation of water

3. CAT – Catalysis and Surface Functionalization

Vesna Ribič[1]
Vanja Jordan[1], Sandra Drev[1], **Janez Kovač**[1], Goran Dražič[2], Aleksander Rečnik[1]
[1] Jožef Stefan Institute, Jamova cesta 39, Ljubljana, Slovenia
[2] National Institute of Chemistry, Hajdrihova 19, Ljubljana, Slovenia

Surface mineral–water interactions are decisive for any photocatalytic process. Resolving the atomistic structure of mineral–water interfaces is thus crucial for understanding these processes. In this study, we investigated fibrous rutile TiO_2 mesocrystals grown homoepitaxially on twinned rutile seeds under highly acidic conditions (1). Fibrous rutile grown under such conditions was shown to possess unusual lattice displacements, that trigger spontaneous dissociation of water. Interface translation, atomic structure, and surface chemistry of fibrous rutile were studied using advanced microscopy (HRTEM) and spectroscopy methods (XPS, EDS, EELS) combined with structure modeling and density functional theory calculations. High energy resolution X-ray photoelectron spectra Ti 2p and O 1s were used to identify and quantify the oxidation states of Ti-atoms and the presence of OH and H_2O groups on the rutile surface. XPS data and the band gaps of fibrous TiO_2 were compared to the values obtained for twinned seeds and commercial rutile nanocrystals. Stable fibrous mesostructure that results from hydrothermal growth displays a strong acidic response that is manifested through spontaneous dissociation of interfacial H_2O, which otherwise does not take place on regular {110} rutile surfaces, and an increased bandgap value of 3.25 eV, which surpasses the reported values for rutile. It was shown that TiO_2 fibers while staying in stable separation during their growth, adopt a special crystallographic registry that is controlled by the repulsion forces between fully hydroxylated and protonated (110) surfaces. This specific interface structure can be implemented to induce acidic response in an initially neutral medium when re-immersed, representing the first demonstration of a quantum-confined mineral–water interface, capable of memorizing its past and conveying its structurally encoded properties into a new environment.

Selected references

(1) V. Ribič, V. Jordan, S. Drev, J. Kovač, G. Dražič, A. Rečnik, Mnemonic Rutile–Rutile Interfaces Triggering Spontaneous Dissociation of Water, Adv. Mater. 2024, 36, 2308027, DOI: 10.1002/adma.202308027.

4. CER – Ceramics; Glass; Oxides

P11 - Optical response of 2D waveguides in silicate glass created via ion implantation with varying thick of optical barriers

4. CER – Ceramics; Glass; Oxides

Romana Mikšová[1]
Pavla Nekvindová[2], Petr Aubrecht[3], Anna Macková[1, 4]
[1] Nuclear Physics Institute CAS, Hlavní 130, 250 68 Rez, Czech Republic
[2] Department of Inorganic Chemistry, University of Chemistry and Technology in Prague, 166 28 Prague, Czech Republic
[3] Centre for Nanomaterials and Biotechnology, Faculty of Science, Jan Evangelista Purkyně University in Ústí nad Labem, 400 96 Ústí nad Labem, Czech Republic
[4] Department of Physics, Faculty of Science, University of J. E. Purkyně, Pasterouva 3544/1, 400 96 Ústí nad Labem, Czech Republic

The two-dimensional (2D) waveguides were fabricated through ion implantation, utilizing a photoresist mask, in three types of silicate glasses: S-1, GIL11, and BK7, respectively. The 2D waveguide was formed by the single and the multi-energy C^+ ion implantation with different ion fluences, resulting in 1×10^{16} cm^{-2}. Multi-energy implantation processes were conducted at energies ranging from 0.8 to 1.6 MeV to establish a 1 μm wide barrier for the optical signal, positioned approximately 2 μm below the sample surface. For precise methodology, Rutherford Backscattering Spectroscopy (RBS) was initially employed to ascertain the composition of the photoresist mask and, in conjunction with X-ray fluorescence (XRF) analysis, determine the compositions of the glasses prior to ion implantation. Subsequently, the dimensions of the photoresist mask, glass compositions, and derived glass density values were utilized for SRIM simulations of the C^+ ion projected range. Characterization of the optical waveguides in various glasses was performed using absorption and m-line spectroscopy. The optical modes (TE_0 and TE_1) exhibited significance in S-1 glass, where the carbon ion range was anticipated to be the deepest, resulting in a wider layer. Additionally, a distinction was evident between multi- and single-energy implantation processes: at 473 nm, only one mode of light propagated for single C^+ ion implantation, whereas two modes were observed for multi-energy implantation.

P12 - Influences of Cr contents on oxidation behavior of WC-Co-Ni-Cr cemented carbides at 900℃

4. CER – Ceramics; Glass; Oxides

Jianzhan Long[1, 2]
Tao Xu[1, 2], Ruilin Zeng[1, 2], Jian Yang[1, 2]
[1] State Key Laboratory of Cemented Carbide, Zhuzhou Hunan 412000, China
[2] Zhuzhou Cemented Carbide Group Corp. Ltd., Zhuzhou Hunan 412000, China

Modification of binder composition is an effective way to improve the oxidation resistance of WC-Co-Ni-Cr cemented carbide. Since the adjustment of Ni and Cr contents in the Co-Ni-Cr binder alters the oxidation behavior and oxidation products, WC-Co-Ni-Cr cemented carbide is expected to achieve excellent oxidation resistance in severe service conditions. In this paper, the influences of Cr contents in Co-Ni-Cr binder phase with a fixed total amount of Co and Ni on the oxidation behavior of WC-Co-Ni-Cr cemented carbides at 900 °C was investigated. The oxide morphology and phase distribution were focused. The oxidation mechanism of WC-Co-Ni-Cr cemented carbide was discussed. It has been shown that Co-rich regions are preferentially oxidized in the initial stage of oxidation. As oxidation proceeds (60 min), the dominant oxidation product on the alloy surface is NiO. The oxidation resistance of the WC-Co-Ni-Cr cemented carbide increases with increasing Cr content in the binder. Compared to the series of WC-2Co-11Ni-xCr, WC-6.5Co-6.5Ni-xCr presents a better overall oxidation resistance due to the formation of Cr_2O_5 in the middle of the oxide layer.

5. COR – Corrosion

P13 - Corrosion behavior of low-temperature carburised AISI 304 austenitic stainless steel after hydrogen uptake

5. COR – Corrosion

Xiao Qin[1, 2]
Lars Nyborg[1], Huiqun Liu[2], Yu Cao[1]
[1] Department of Industrial and Materials Science, Chalmers University of Technology, Gothenburg, 41296, Sweden
[2] School of Materials Science and Engineering, Central South University, Changsha, 410083, PR China

Austenitic stainless steel AISI 304 is widely used for hydrogen storage and transportation due to their low hydrogen diffusivity, excellent resistance to hydrogen embrittlement, good corrosion resistance, formability, and weldability [1-4]. However, metastable AISI 304 is susceptible to strain-induced martensitic transformation [5]. This may accelerate the corrosion process, especially in hydrogen-containing environments [6]. Therefore, it is important to investigate the effect of hydrogen on corrosion behavior and develop effective protection methods to reduce the damage of hydrogen on the corrosion resistance of austenitic stainless steels. Low-temperature carburising [7] can improve the surface hardness of ASS without decreasing the corrosion resistance. The present work focuses on the effect of hydrogen uptake on the corrosion behavior of low-temperature carburised AISI 304 austenitic stainless steel in 3.5 wt.% NaCl solution. Low-temperature carburizing treatment introduces super-hard and supersaturated carbon-stabilized austenite (S-phase) with a thickness of ~ 22 μm on the surface of AISI304. Hydrogen uptake reduces the corrosion and pitting potential and accelerates the local corrosion of AISI 304. Hydrogen-induced martensitic transformation and surface cracking lead to reduced corrosion resistance in austenite, while S-phase inhibits martensitic transformation and improves corrosion resistance. XPS results show that hydrogen uptake changes the chemistry of the passivation film on stainless steel. It promotes carbon and chromium depletion and oxide layer destruction.

Selected references

[1] Züttel, Materials for hydrogen storage, Mater. Today 6 (2003) 24-33.
[2] Fukai, H. Sugimoto, Diffusion of hydrogen in metals, Adv.Phys.34 (1985) 263-326.
[3] Michler, Toughness and hydrogen compatibility of austenitic stainless steel welds at cryogenic temperatures, Int. J. Hydrogen Energ. 32 (2007) 4081-4088.
[4] K. Dwivedi, M. Vishwakarma, Hydrogen embrittlement in different materials: A review, Int. J. Hydrogen Energ. 43 (2018) 21603-21616.
[5] K. De, J.G. Speer, D.K. Matlock, et. al, Deformation-induced phase transformation and strain hardening in type 304 austenitic stainless steel, Metall. Mater. Trans. 37 (2006) 1875-1886.
[6] L. Chang, M.G. Burke, K. Mukahiwa, et. al, The effect of martensite on stress corrosion crack initiation of austenitic stainless steels in high-temperature hydrogenated water, Corros. Sci.189 (2021) 109600.
[7] R. Collins, P.C. Williams, S.V. Marx, et. al, Low-temperature carburization of austenitic stainless steels, ASM handbook, 4 (2014) 451-460.

P14 - Dominant characteristic of an anodized NiTi alloy surface that suppress a Ni ion release in biological environment

5. COR – Corrosion

Naofumi Ohtsu[1]
Rino Takada[1], Ryota Kawakami[1]
[1] Faculty of Engineering, Kitami Institute of Technology, Kitami, Hokkaido 090-8507, Japan

A fatal drawback of an almost equiatomic superelastic nickel-titanium (NiTi) alloy when using as a medical implant material is a Ni ion release in a human body. Anodization is the surface modification process that enables to form an oxide layer with a corrosion protective functions, yet have been considered to be inapplicable to NiTi alloy due to the presence of Ni that impedes the layer growth. Our research group found out that selecting an appropriate electrolyte together with applying a pulsed voltage led to the formation of an almost Ni-free TiO_2 layer through the removal of Ni content from the surface[1]. Here, detailed layer characteristics such as surface morphology, and remaining Ni vary depending on the electrolyte and voltage settings, that influences to the suppression efficacy[2]. In this study, thus, we prepared the several types of anodized layer, and characterized through the electrochemical and surface analyses, to discuss the dominant characteristics to suppress Ni ion release.

The NiTi alloy plate was used as the substrate. Electrolytes for anodization were 100 mM HNO_3, H_2SO_4, and H_3PO_4 aqueous solutions, and constant or pulsed voltages (pulse width was 100 ms, and the duty ratio was 50%) was applied to the alloy. Applied voltage was set to 3.5 V, and its duration was 60 min. The resultant surfaces were characterized by XPS and SEM, as well as the electrochemical polarization technique. Also, the anodized alloys were soaked in phosphate buffered saline (PBS) solution for 24 h, and the amount of Ni ion release was determined using graphite furnace atomic adsorption spectrometry.

Overall, the suppression of Ni ion release became prominent when employing the pulsed voltage. Regardless of the electrolyte, the Ni ion release was dropped below half. Among the electrolytes, selecting the H_2SO_4 electrolyte resulted in the lowest Ni-ion release. Nevertheless, SEM images for the H_2SO_4 surface with both the constant and pulsed voltages showed the submicron-scaled bumpy microstructure, that is unbeneficial for the corrosion protection. Also, remarkable difference was not found in the value of passive current density via polarization curve. Apart from these, there was good correlation between the amount of Ni ion release and the Ni content presenting as $Ni(OH)_2$ evaluated by XPS (Fig.). Based on the electrochemical and surface analyses, in conclusion, we elucidated that the dominant characteristic of an anodized NiTi alloy surface that suppress a Ni ion release is the remaining Ni content in the topmost surface.

Selected references

1. N. Ohtsu, K. Yamasaki, H. Taniho, Y. Konaka, K. Tate, Pulsed anodization of NiTi alloy to form a biofunctional Ni-free oxide layer for corrosion protection and hydrophilicity, Surface and Coatings Technology 412 (2021) 127039
2. K. Yamasaki, H. Taniho, K. Tate,N. Ohtsu, Electrolyte effect in pulsed anodization of NiTi alloy to form a Ni-free oxide layer, Surface and Coatings Technology 417 (2021) 127221

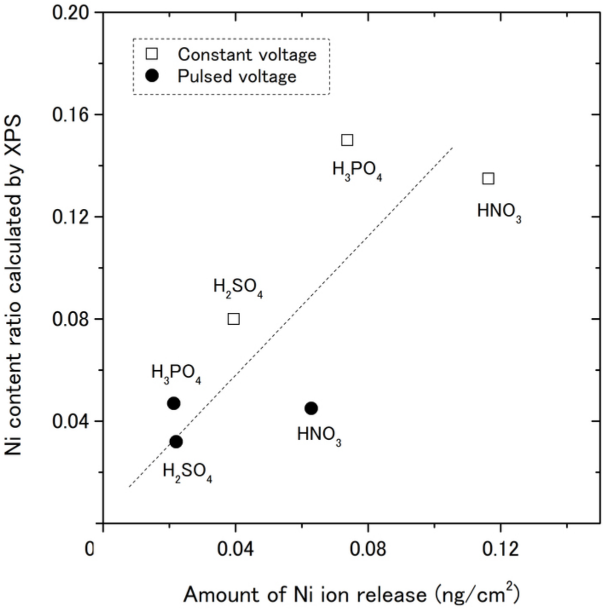

Fig. Ni content ratio in the topmost surface of anodized NiTi surface plotted against the amount of Ni ion release

P15 - Effect of hydrogen on the passivity of steels by an electrochemical-surface analytical approach

5. COR – Corrosion

Chiara Menegus[1]
Jan Philipp Kollender[1], Lars P.H. Jeurgens[1], Claudia Cancellieri[1]
[1] Empa, Laboratory for Joining Technologies & Corrosion, Switzerland

Hydrogen and its associated technologies will play a protagonist role in the ongoing global energy transition. However, as we embrace a hydrogen-driven society, we must confront a relevant number of challenges arising from its interaction with steel across various stages of production, storage, and transportation. Furthermore, the generation and adsorption of hydrogen are unavoidable in many processes such as pickling, cathodic protection, and galvanizing.

While extensive research has been conducted on hydrogen embrittlement, little attention has been paid to the significance of the passive oxide layer naturally forming on the steel surface in a natural or controlled atmosphere. This layer not only can protect steel from corrosion but also serves as a barrier against hydrogen penetration. In this study, an organized methodology and approach is developed for the use of soft and hard X-ray photoelectron spectroscopy (XPS/HAXPES) in the investigation of the effect of hydrogen in passivated steel materials.

To this end, an electrochemical flow cell is specifically designed to electrochemical charge H on one side and passivate on the other side of the thin steel sheets in a controlled way. This cell can also be operated in a glovebox (i.e. an inert Ar atmosphere), as attached to our combinatorial in-situ UHV facilities for thin film deposition (by magnetron sputtering), post-processing (annealing, oxidation, reduction) and in-situ surface analysis using XPS/HAXPES.

After electrochemical charging, a comprehensive analysis of hydrogen's impact on the passive oxide layers of diverse steel types is conducted using XPS/HAXPES to determine features such as the thickness, composition, oxide/hydroxide phase constitution, the Fe^{3+}-to-Fe^{2+} ratio in the oxide films, as well as the chemical state of the elements in the oxide and close to the alloy/oxide interface. Aside from allowing for the direct measurement of the effect of hydrogen on the oxide and its distribution within its thickness, the combined use of Rutherford backscattering (RBS) and elastic recoil detection analysis (ERDA) alongside XPS and HAXPES could facilitate the development of an analytical framework to examine the concentration of hydrogen within the passive layer using only XPS/HAXPES spectra. This framework involves measuring the shift of the peaks and relating it to the chemical state of the elements in the oxide layer. This integrated approach stands as a valuable tool in this field of research, offering possible insights into the intricate processes of hydrogen adsorption, absorption, and penetration within steel materials.

P16 - EIS study of the influence of sputtering parameters of SIN thin films deposited on 316 stainless steel.

5. COR – Corrosion

J. Rafael González-Parra[1]
M. Hernandez[2], A. Barba[2], A Tejeda[3], Arturo Rodriguez[1]
[1] Departamento de Estado Sólido, Instituto de Física, UNAM, 04510, CDMX, México.
[2] CENISA, DIMEI, Facultad de Ingeniería, UNAM, 04510, CDMX, México.
[3] Instituto de Investigaciones en Materiales, UNAM, 04510, CDMX, México.

Silicon Nitride (SiN) is a material with chemical and structural properties that make it a suitable candidate for protecting metallic substrates exposed to corrosive environments and wear. This type of aggressive environment is characteristic of orthopaedic prostheses inside the human body. In addition, SiN has low cytotoxicity, making it a biocompatible material that allows a higher rate of cell growth and integration into the human body. On the other hand, 316L stainless steel is a material commonly used in the medical prosthesis industry, but the corrosion of this alloy can lead to health risks such as metalosis, vascular damage and the reduction of the life span of the prosthesis. Then, the use of a protection system to decrease the corrosion rate of the metallic substrate is necessary to increase the life span of orthopaedic implants and the quality of life of patients. In this study, a SiN nanostructured coating was deposited on 316L stainless steel bars using magnetron RF sputtering technique with different deposition temperatures. The samples were then characterized using scanning electron microscopy, atomic force microscopy, and electrochemical impedance spectroscopy. The samples were immersed in Hanks' solution to mimic human body fluids. The results show that the surface morphology and nanometric features of the thin film are modified with temperature, promoting a higher amount of "cauliflower-like" structures and increasing the roughness. Also, the electrochemical response is modified by the characteristics of the nanostructured coating, increasing the corrosion protection as the barrier film thickness increases

Selected references

S. Varmaziar, M. Atapour, Y. Hedberg, Corrosion and metal release characterization of stainless steel 316L weld zones in whey protein solution, npj Materials Degradation, 6 (**2022**) 1-9. https://doi.org/10.1038/s41529-022-00231-7

U. Majeed, I. Tariq, M. Wasib, M. Mustafa, Surface study of RF magnetron sputtered silicon nitride thin films, Journal of Optoelectronic and Biomedical Materials, 15 (**2023**) 55-64. https://doi.org/10.1521/JOBM.2023.152.55

A. Rao, S. Tiwari, M. Goyat, A. Chawla, Recent developments in magnetron-sputtered silicon nitride coatings of improved mechanical and tribological properties for extreme conditions, Journal of Materials Science, 58 (**2023**) 9755-9804. https://doi.org/10.1007/s10853-023-08575-4

P17 - Influence of current on the surface and corrosion behavior of Ni-obsidian coatings electrodeposited on ductile iron

5. COR – Corrosion

Rafael González-Parra[1]
Miguel Hernandez-Gallegos[1], Raul Valdez[1], Jose Bañuelos[2], Arturo Barba[1]
[1] 1 CENISA, División de Ingeniería Mecánica, Facultad de Ingeniería, UNAM Cd. Universitaria, Av. Universidad 3000, Coyoacán, CDMX, 04510
[2] 2 LUCE, instituto de Ciencias Aplicadas y Desarrollo Tecnológico, UNAM Cd. Universitaria, Av. Universidad 3000, Coyoacán, CDMX, 04510

Ductile iron is a widely used alloy with advantageous mechanical properties compared to other cast irons. Also, represents a sustainable approach in the manufacturing sector due to its recyclability, lower melting temperature and low density. All these characteristics make it suitable for a broad range of applications such as the automotive industry, machinery, aerospace, mining, pumping and piping. In general, this alloy is used in circumstances where the mechanical properties, wear and corrosion resistance are mandatory. In this work, a Ni-Obsidian composite coating was electrodeposited over a ferritic ductile iron for 1 hour to increase corrosion resistance and hardness. The samples were immersed in a solution containing nickel salts, surfactants and obsidian particles. The obsidian particles were obtained by rotary milling. The current density was modified in each case to determine its influence on saline corrosion, micro Vickers hardness and roughness of the coated samples. The results show that as the applied current increases, the corrosion resistance, hardness and roughness of each coating increases. This behavior is related to a higher growth rate, as the higher applied current density enhances the growth kinetics of the coating layer, promoting a higher blocking effect of the Ni deposit. However, adding of obsidian particles results in detrimental corrosion behavior as the cracks formed in the surface coating allow access of aggressive electrolyte. Figure 1 shows the Bode diagram of the nickel coated with and without obsidian particles. The coatings increase the corrosion resistance of the blank ductile iron. However, the composite coating shows a lower impedance modulus and the time constant is shifted towards higher frequencies indicating a higher corrosion activity than the Ni-coated sample. The addition of obsidian particles to the Ni coating allows increasing the hardness and surface roughness of the coating but the corrosion performance is reduced.

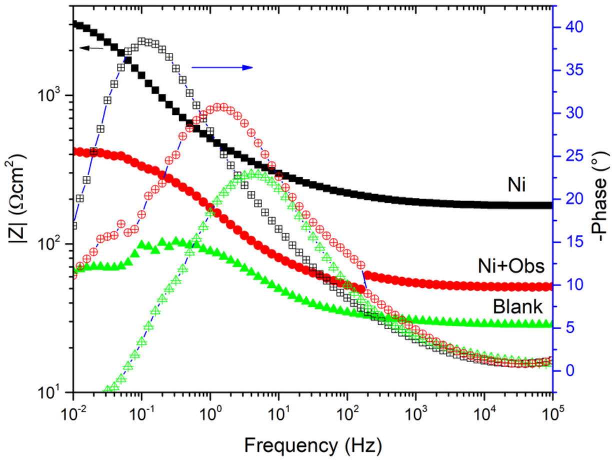

P18 - On the interpretation of the XPS and XAES spectra of Ni compounds

5. COR – Corrosion

Deborah Biggio[1]
Bernhard Elsener[1], Marzia Fantauzzi[1], Antonella Rossi[1]
[1] Dipartimento di Scienze Chimiche e Geologiche, Università di Cagliari, Cagliari, Italy

The interpretation of the X-ray photoelectron spectroscopy (XPS) spectra of Ni-bearing materials is challenging when more than one chemical state is present. The complexity of Ni 2p peaks is due to the presence of peak asymmetries, multiplet splitting, shake-up and plasmon loss structure. Several curve-fitting procedures have been proposed in the literature [1–3] for processing and interpreting the different phenomena involved, necessary for an accurate qualitative analysis and for the quantification of each chemical state.

The aim of this work is the development of an approach for the identification of different chemical states of Nickel that contribute to XPS and XAES spectra. Different approaches for curve-fitting the spectra will be presented and discussed, considering the progresses in data processing programs, the importance of well-defined sample preparation procedures and the characteristics of the instrument. The control of all them allow obtaining accurate results. The XPS analyses of Ni reference compounds were performed with a Theta Probe spectrometer (Thermo Fisher, UK) equipped with a monochromatic Alkα source (hν = 1486.6 eV). The high-resolution spectra were processed using CasaXPS software (v.2.3.25 PR1.0) and applying the Shirley-Sherwood background.

The analysis of the NiO reference sample showed that the O 1s peak exhibits two components, one attributable to NiO, and the second one to the presence of hydroxide species.[2]
The analysis of $Ni(OH)_2$, allowed determining the curve-fitting parameters that provided to obtain the expected stoichiometry on NiO sample, considering also the $Ni(OH)_2$ component in the Ni $2p_{3/2}$ signal (Fig. 1).

The interpretation of the fine structure of the XAES spectra and the calculation of the Auger parameter for all Ni samples analysed will be also discussed.

Selected references

1. Hüfner, S., Photoelectron Spectroscopy, *Springer-Verlag*, **82,** (1995).
2. Biesinger, M.C., Payne, B.P., Lau, L.W.M., Gerson, A. and Smart, R.S.C., *Surf. Interface Anal.* **41**, 324-332 (2009).
3. Addari, D., Mignani, A., Scavetta, E., Tonelli, D. & Rossi, A., *Surf. Interface Anal.* **43**, 816–822 (2011).

Acknowledgement

The financial support of the European Union NextGenerationEU under the National Recovery and Resilience Plan (NRRP) of Ministero dell’Università e della Ricerca (MUR) (Project code PE0000021, Network 4 Energy Sustainable Transition, NEST) is acknowledged.

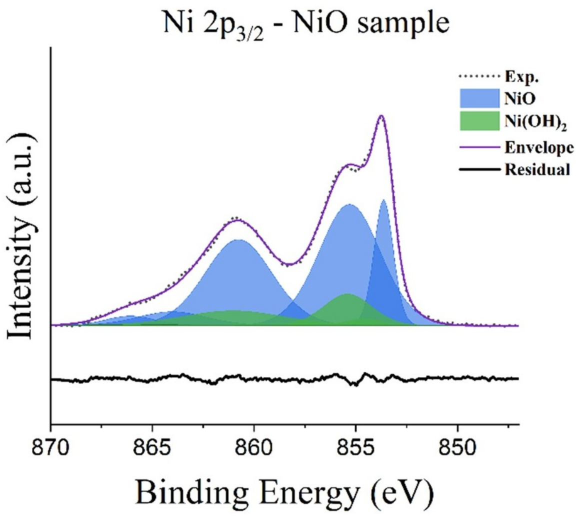

Fig. 1: Ni $2p_{3/2}$ XPS high-resolution spectrum of NiO sample analysed @UniCA.

P19 - Steel oxidation: reaction mechanisms, kinetics and scale morphology

5. COR – Corrosion

Laura Turri[1]
Alexey Koltsov[1], Kanika Anand[1], Nadine Berthelemy[1], Patrice Alexandre[1], Julien Scheid[1]
[1] ArcelorMittal Global R&D, France

Understanding the transformation of steel during the hot rolling process requires a meticulous investigation of the oxidation kinetics and surface morphology, to adapt the process parameters and ensure a good product quality. Moreover, the new production routes for steel process decarbonation require agile and multi-scale approach to understand and provide solutions to key open questions.

In the industrial steel hot-rolling process, the strip is oxidized in the reheating furnace. After unloading, a millimeter scale layer is formed on the strip surface. Oxidation is crucial as it can be at the origin of surface defects.

Oxidation studies require to analyze the influence of the new oxidizing environment and to comprehend the effect of steel composition - presence of residual elements.

To evaluate the kinetic oxidation parameters, thermogravimetric analyses are conducted. These parameters are used to simulate scale growth in reheating furnaces for different heating cycles and temperatures.

For classical steels, the scale is mainly composed of wüstite (FeO) covered by thin layers of magnetite (Fe_3O_4) and hematite (Fe_2O_3) which also depends on the cooling rate. For alloyed steel grades, some compounds might melt especially eutectics as Fayalite. However, external oxidation is not the only phenomenon impairing the steel surface. Among all surface phenomenon, internal and selective oxidation is also observed. It corresponds to the precipitation of oxides from residual elements more prone to oxidation than Fe in the bulk. Internal oxidation can be also located at the grain boundary. In parallel, metal denaturation occurs with the diffusion of carbon, alloying elements and the possible accumulation of residuals elements at the scale/metal interface.

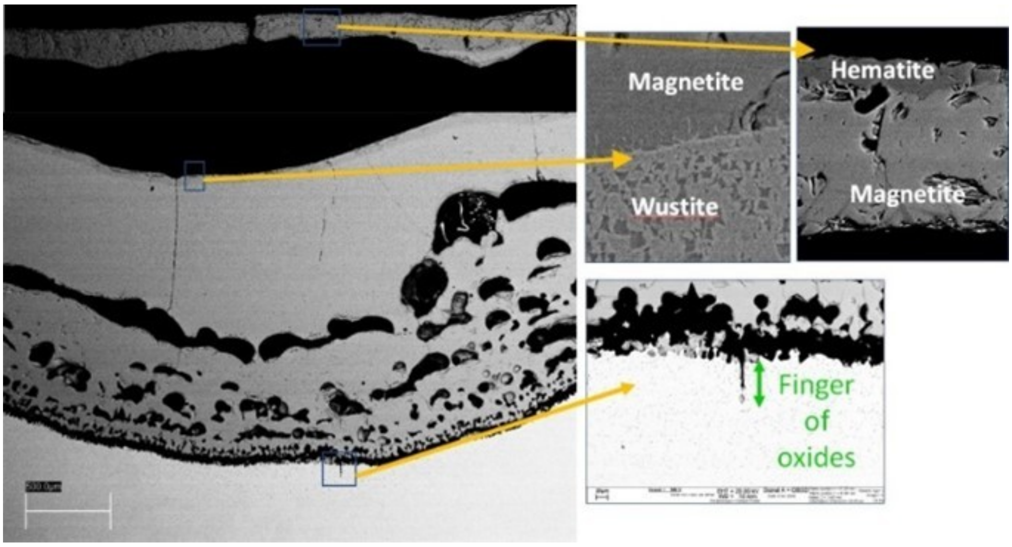

6. DAT – Data Analysis and Metrology

P20 - Correlation analysis for X-ray radiation damage studies on double vacancy ordered halide perovskites

6. DAT – Data analysis and Metrology

Prajna Bhatt[1]
Theo Stucky de Quay[1], Yuhan Liu[1], Tim Evans[1], Orfhlaith McCullough[2], Nathalie Fernando[1], Anna Regoutz[1], Robert Palgrave[1]
[1] University College London
[2] London Metropolitan University

Degradation studies of the ASnX3 perovskites to the A2SnX6 double perovskites have been well researched, but there is a lack of the complete degradation pathway including the degradation undertaken by the double perovskites. We have synthesized and characterized FA-doped (NH4)2SnBr6, (NH4)1−xFAx)2SnBr6 x = 0, 0.03, 0.04, 0.06, 0.09, 1 confirmed by X-ray diffraction and the doping content was quantified using X-ray Photoelectron Spectroscopy (XPS) and elemental combustion analysis. X-ray radiation damage studies were investigated for the FA2SnBr6, $(NH_4)_2SnBr_6$ and $(NH_4)_{1-x}FA_x)_2SnBr_6$ x = 0.03, 0.09 samples to, qualitatively and quantitatively, find degradation mechanisms. Correlation analysis was used to fortify peak fitting models, to understand the degradation. Correlation analysis in general is an established statistical procedure for revealing relationships (which may be causal or coincidental) between variables.[1] For XPS, this was done by comparing shifts in binding energies between two selected elements (phase models) and phase fraction calculations, based on a method used to determine the ratios of intensities two known compounds.[2]

Correlation analysis revealed the degradation of FA into an amine species, that promulgated the degradation in the $(NH_4)_{1-x}FA_x)_2SnBr_6$ solid solution series, depending on the FA doping level. There is also formation of a Sn (II) bromide environment only in FA containing compounds. For $(NH_4)_2SnBr_6$, preferential damaging into NH_4 and Br_2 is suspected.

Selected references

1. P. Bhatt, Y. Liu, M. Isaacs, R. Palgrave, Correlation analysis in X-ray photoemission spectroscopy 2024, doi:10.26434/chemrxiv-2024-m32rt.
2. Shard, A. G., Practical guides for x-ray photoelectron spectroscopy: Quantitative XPS. Journal of Vacuum Science & Technology A 2020, 38 (4).

P21 - Do different XPS systems give the same result?

6. DAT – Data Analysis and Metrology

Lyndi Strange[1]
Donald Baer[1], Mark Engelhard[1], Vaithiyalingam Shutthanandan[1], Alexander Shard[2]
[1] Pacific Northwest National Laboratory, RIchland WA, USA
[2] National Physical Laboratory, Teddington UK

Literature analyses indicate growing use of XPS in multiple disciplines and increasing observations of faulty analysis. To ensure reliable results it is important that care be paid to XPS data acquisition and analysis. Our laboratory has instruments from three vendors, and it may be necessary to collect data from the available instrument. Users increasingly export data for analysis using alternative software. It is useful to know the consistency of data collected on “identical” samples collected on different systems and analyzed using “native” and other software packages. This paper describes a “simple” test of data collection on three different systems and analysis using the native software for each system and analysis when naively “blindly” exported to a non-native analysis package. Copper foil was the test specimen from which survey and high-resolution spectra were collected using Kratos Axis DLD Ultra, Thermo-Fischer NEXSA, and Phi Quantera spectrometers. Using both survey and narrow window data the analyses included: i) comparison of Cu 3p and Cu 2p peak ratios, ii) Cu 3p and Cu 2p atom ratios using native software and iii) when exported to CasaXPS. We also compared the wide scan spectra shapes to the ideal Cu spectra provided by the National Physical Laboratory to obtain an approximate instrument response function. Although simple in concept, these comparisons were found to be less than straightforward. High count rate survey spectra ratioed to the ideal spectra produced unexpected variations in the instrument response functions. These ratios made more sense when count rates were reduced by lowering the X-ray intensity of decreasing the pass energy. Cu 3p and Cu 2p peak ratios were determined using peak intensities after removal of an iterated Shirley background between 58.0 eV and 91.0 eV for Cu 3p and 920.0 eV to 970.0 eV for Cu 2p. Because of variations in the instrument transmission functions, raw peak ratios among the three spectrometers differed by > 2. However, native software analysis on each instrument produced similar amounts of Cu to roughly ± 5%. Note that sensitivity factors are more established for Cu 2p peaks than for Cu 3p peaks which may account for some variation. Naive transfer of data for analysis by non-native software was found to produce results significantly different than expected. This can be due to sensitivity factors or complications related to the instrument response function. These issues can be corrected but require care and verification or incorrect may result.

P22 - HAXPES spectra and quantification of bulk Mo and MoSe2 compound

6. DAT – Data Analysis and Metrology

Olivier Renault[1]
Nicolas Gauthier[1], Eugénie Martinez[1], Kateryna Artyushkova[2]
[1] CEA-Leti, Univ. Grenoble Alpes, F-38000 Grenoble, France.
[2] Physical Electronics, 18725 Lake Dr E, Chanhassen, MN 55317, USA

The HAXPES spectra of bulk Mo and $MoSe_2$ compounds obtained with Cr Ka$_1$ excitation (hn= 5414.8 eV) are presented, with special attention paid to binding energy scale correction, quantification and repeatability aspects [1]. Cr Kα HAXPES allows to ionize all Mo and Se core-levels of principal quantum numbers N=2, 3 and 4.

Empirically determined sensitivity factors (RSFs) were provided by the PHI Multipak software version 9.9.0.8, from the most recently released RSF database. The RSFs were derived from the pure-element relative sensitivity factor as defined in ISO 18118:2015 [2] which were measured on pure element samples using a Cr Kα source. Using the determined pure element RSF's leads to quantification error of ~5% for the $MoSe_2$ compound.

Acknowledgements
This work, carried out on the Platform for Nanocharacterisation (PFNC), was supported by the "Recherche Technologique de Base" and "France 2030 - ANR-22-PEEL-0014" programs of the French National Research Agency (ANR) "

References
[1] P.-M. Deleuze, N. Gauthier, E. Martinez, K. Artyushkova and O. Renault, T. Maindron, *Surf. Sci. Spectra* 31, 014006 (2024).
[2] International Organization for Standardization 2015, Surface chemical analysis - Auger electron spectroscopy and X-ray photoelectron spectroscopy - Guide to the use of experimentally determined relative sensitivity factors for the quantitative analysis of homogeneous materials, ISO 18118:2015.

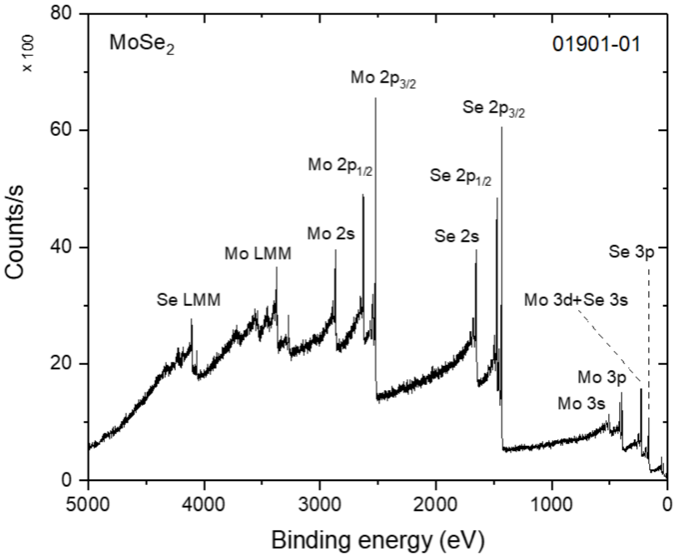

P23 - HAXPES spectra and quantification of bulk W and WSe2 compound

6. DAT – Data Analysis and Metrology

Olivier Renault[1]
Nicolas Gauthier[1], Eugenie Martinez[1], Kateryna Artyushkova[2]
[1] CEA-Leti, Univ. Grenoble Alpes, F-38000 Grenoble, France.
[2] Physical Electronics, 18725 Lake Dr E, Chanhassen, MN 55317, USA

The HAXPES spectra of bulk W and WSe_2 compounds obtained with Cr $K\alpha_1$ excitation (hν= 5414.8 eV) are presented. Cr Ka HAXPES allows to ionize all W and Se core-levels of principal quantum numbers N= 2, 3 and 4.

We emphasize aspects related to binding energy scale correction – which can no longer rely on the C 1s line- and peculiarities of some HAXPES core-level spectra, such as the W 4f core-level spectrum (Fig. 1), compared to the XPS case [1].

The quantification procedure will be presented. It is based on empirically determined sensitivity factors (RSFs) provided by the PHI Multipak software version 9.9.0.8, from the most recently released RSF database. The RSFs were derived from the pure-element relative sensitivity factors as defined in ISO 18118:2015 [2] which were measured on pure element samples using a Cr Kα source.

Acknowledgements
This work, carried out on the Platform for Nanocharacterisation (PFNC), was supported by the “Recherche Technologique de Base” and "France 2030 - ANR-22-PEEL-0014" programs of the French National Research Agency (ANR) ”

Selected references

[1] P.-M. Deleuze, N. Gauthier, E. Martinez, K. Artyushkova and O. Renault, *Surf. Sci. Spectra* **30**, 024029 (2023).
[2] International Organization for Standardization 2015, Surface chemical analysis - Auger electron spectroscopy and X-ray photoelectron spectroscopy - Guide to the use of experimentally determined relative sensitivity factors for the quantitative analysis of homogeneous materials, ISO 18118:2015.

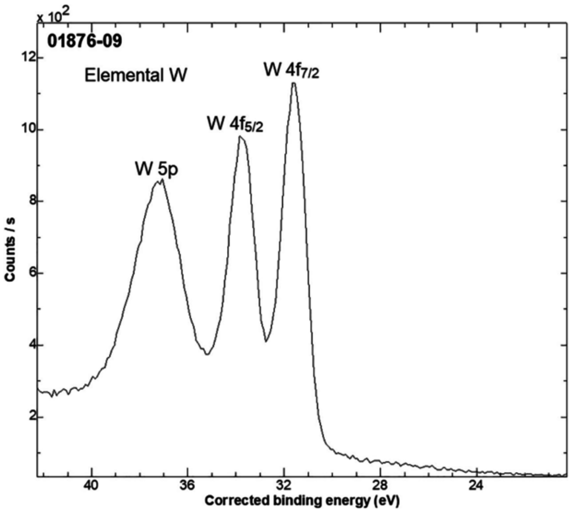

Fig. 1- Cr Kα HAXPES spectrum of W 4*f* core-level.

P24 - Improved estimation of the spectrometer-transmission function with UNIFIT 2022

6. DAT – Data Analysis and Metrology

Ronald Hesse[1]
Reinhard Denecke[1]
[1] Wilhelm-Ostwald-Institut für Physikalische und Theoretische Chemie, Universität Leipzig D-04103 Leipzig, Germany

The recent development of X-ray photoelectron spectroscopy using excitation sources different from the usual lab-source Mg Kα and Al Kα and spectrometers with more sophisticated lense systems (like ambient pressure setups) requires more flexible approaches for determining the transmission function than the well-established ones using reference spectra of noble metals. Therefore, the approach using quantified peak areas (QPA) was refined. A new algorithm allows a more precise estimation of the transmission function which could be shown by comparing the results obtained with the new version with former calculations. Furthermore, reference materials others than Cu, Ag and Au can be used. Ionic liquids can be used as reference for estimating the transmission function at beamlines with variable excitation energies. Comparison between the measured and stoichiometric composition of reference samples shows that a transmission function was determined which allows a reasonable quantification.

Selected references

1. Hesse, R. Denecke, J. Radnik, Surf. Interface Anal., Short Communic., 7131 (2022) 1

P25 - Quantitative investigation of SiP and SiGe binary layers using lab-scale HAXPES & ToF-SIMS

6. DAT – Data Analysis and Metrology

Nicolas Gauthier[1]
Olivier Renault[1], Jean-Paul Barnes[1], Eugénie Martinez[1], Jérôme Richy[1], Joël Kanyandekwe[1]
[1] 1.CEA-Leti, Univ. Grenoble Alpes, 38000 Grenoble, France

Nowadays, “more Moore” and “more than Moore” device architectures have strongly increased the importance of novel materials thereby necessitating the availability of adequate characterization and metrology for reliable process control. For instance, the introduction of SiGe or SiP compounds used in Multi Channel Field Effect devices or raised sources and drain leads to the need for the determination of the exact composition of the resulting films. In this work, the quantification of binary materials such as SiP and SiGe has been investigated using mainly non-destructive Hard X-ray Spectroelectron Spectroscopy (HAXPES) and Time of Flight Secondary Ion Mass Spectrometry (ToF-SIMS). Indeed, while the main obstacle to the use of RBS is the characterization of thin films, techniques with appropriate quantification capabilities like Atom Probe Tomography and Transmission Electron Microscopy are both time consuming and suffer from a lack of sensitivity due to their highly localized analysis volume. For quantitative characterization, the conventional X-ray Photoelectron Spectroscopy (XPS) is a powerful tool. Yet, its low analysis depth remains a major limiting factor to study buried interfaces and especially in this study, since the obtained Si-based layers are oxidized in ambient conditions (or because they should be protected by metallic layers of a few nanometers). A recent lab-based hard x-ray sources was used to investigate both the chemical composition at the binary material surface and the in-depth distribution of SiO_2 within the layer thanks to the increase of the inelastic mean free path of electrons with increasing photon energy (Chromium Kα, $h\nu$ = 5414.7 eV) [1]. To confirm the composition of the materials of interest obtained by HAXPES measurements and to calculate the adequate relative sensitive factor (RSF), the same films were characterized by ToF-SIMS. However, such as for HAXPES, Secondary Ion Mass Spectrometry (SIMS) characterization of SiP/SiGe layers often suffers from matrix effects due to the non-linear variation of ionization yields with P/Ge content. This limitation can be surpassed by analyzing reference samples, by following MCs^{2+} secondary ions or using the full spectrum protocol [2]. Finally, the P and Ge (Si) compositions of the secondary ion beam were calculated and compared with the reference composition as determined by X-ray Diffraction. The repeatability of the measurements and the influence of the layer oxidation were also studied. To conclude, the in-depth composition of the layers and the thickness of surface oxide were accurately evaluated by coupling the HAXPES results with ToF-SIMS.

Selected references

[1] O. Renault et al., *Faraday Disc*. **236**, 288-310 (2022).
[2] M. Py, et al., Rapid Commun. Mass Spectrom. 2011, 25, 629–638

P26 - UNIFIT 2024 – the improved spectrum processing, analysis and presentation software for XPS, AES, XAS, RAMAN Spectroscopy

6. DAT – Data Analysis and Metrology

Ronald Hesse[1]
Reinhard Denecke[1]
[1] Wilhelm-Ostwald-Institut für Physikalische und Theoretische Chemie, Universität Leipzig D-04103 Leipzig, Germany

Main focus of the advancement of UNIFIT 2023/UNIFIT 2024 were the optimization of the saving and loading procedure of Unifit projects and the batch processing sub-routine. For a better and faster operation of the software the common Windows shortcuts were integrated.

The definition and display of the preferences were reworked and newly designed. The dialogue ‘Programme Parameters’ was redesigned and expanded. The definition of the excitation satellites was reworked completely. The pop-up and pull-down commands were improved. The setting options of the X-axis and Y-axis dialogues were refreshed. New export functions were implemented. In order to increase the processing speed of the software, the programme code was reworked and optimized.

P27 - UNIFIT 2025 – the improved spectrum processing, analysis and presentation software for XPS, AES, XAS, RAMAN Spectroscopy

6. DAT – Data Analysis and Metrology

Ronald Hesse[1]
Reinhard Denecke[1]
[1] Wilhelm-Ostwald-Institut für Physikalische und Theoretische Chemie, Universität Leipzig D-04103 Leipzig, Germany

Main focus of the advancement of UNIFIT 2025 was the optimization of the iteration procedure for the estimation of the transmission function *T(E) (IERF)*. Now, the three methods of the *T(E)* estimation, i) Survey Spectra Approach SSA, ii) Quantified Peak-Area Approach QPA and iii) Approach Transmission Function, are clearly separated. The dialogs of the sub-menu 'Calibration Intensity Scale' were reworked. The currently used method, the iteration error and calculation time are displayed. The disadvantage of the QOA method, the very long estimation time, was removed. In order to accelerate the iteration i) the existing programme code (Step by Step) was completely reworked and ii) a new iteration method (Randomize) was implemented. A comparison of both methods will be presented.

Additionally, the dialogue 'Programme Parameters' was redesigned and expanded. The definition of the QPA-iteration method and design option were implemented.

The options of the window-selection dialogue and quantification dialogue were expanded. The selected windows can be activated or deactivated optionally.

The menus 'Plot Energy/Wavenumber Axis' and 'Plot Intensity Axis' have now two new defining options: i) Size of Increments and ii) –DS and +DS for the changing of the dialogue size.

Regarding the dark-mode options of Windows a corresponding dark-mode option was implemented in UNIFIT 2025 software.

7. DPR – Thin films, Coatings and Depth Profiling

P28 - A comparative study of various analytical techniques to investigate Ni-Si thin film characteristics

7. DPR – Thin Films, Coatings and Depth Profiling

Elahe Akbari[1]
Soniya Gahlawat[1], Markus Valtiner[1]
[1] Christian Doppler Laboratory for Surface and Interface Engineering, Institute of Applied Physics, Technische Universität Wien (TU Wien)

Thin film characterization is fundamental across materials science, engineering, and beyond, providing crucial insights into film composition, morphology, crystallinity, and optical properties. This understanding optimizes thin film performance in various applications, enhances fabrication processes, and ultimately advances technology and innovation in diverse industries. Thus, in this study, we aim to systematically investigate the nanoscale structure and chemistry of the Ni-Si layer formed at high temperature using Transmission Electron Microscopy (TEM), Energy Dispersive X-Ray Spectroscopy (EDS), X-ray Photoelectron Spectroscopy (XPS), and Auger Electron Spectroscopy. The evolution of various phases within the Ni-Si layer at high temperatures exhibits critical implications for its structural integrity and functional properties. Initially, during the annealing process, the formation of Ni-Si phases undergoes a sequential transformation, starting with the formation of NiSi, progressing to $NiSi_2$, and ultimately reaching Ni_2Si. Each phase transition is accompanied by distinct changes in microstructure and chemical composition, significantly impacting the layer's mechanical and electrical properties [1].

Our TEM results in conjunction with EDS elemental analysis revealed significant microstructural changes and a mixture of various Ni-Si phases, namely, NiSi, $NiSi_2$, and Ni_2Si. Subsequently, XPS provided chemical information by probing the surface composition and oxidation states of elements within the Ni-Si layer, facilitating the identification of surface species and the monitoring of chemical reactions occurring at elevated temperatures. Finally, AES analysis, with its higher lateral resolution, and enhanced sensitivity to surface elemental compositions, as well as its depth profiling capabilities, confirmed EDS findings and enabled a comprehensive characterization of elemental distribution and diffusion phenomena within the Ni-Si layer.

Selected references

[1] A. M. Thron, P. K. Green, K. Liu, K. van Benthem, "Structural changes during the reaction of Ni thin films with (100) silicon substrates" , Acta Materialia 60 (2012) 2668–2678, doi: 10.1016/j.actamat.2012.01.033

P29 - Characterization of diamond-like carbon (DLC) coatings and effect of sputter depth profiling on these materials

7. DPR – Thin Films, Coatings and Depth Profiling

Vanessa Trouillet[1]
Joachim Faller[2], Dominic Linsler[2]
[1] Institute for Applied Materials (IAM) and Karlsruhe Nano Micro Facility (KNMFi), Karlsruhe Institute of Technology (KIT), 76344 Eggenstein-Leopoldshafen, Germany
[2] Fraunhofer Institute for Mechanics of Materials IWM, Rintheimer Querallee 2b, 76131 Karlsruhe, Germany

Diamond-Like Carbon (DLC) coatings can be used for various applications but play in particular an important role in the field of tribology based on their good resistance to wear and their low friction behaviour [1]. The composition of their surface in terms of sp^2 and sp^3 hybridized carbons as well as hydrogen content is of importance and influence their properties.

A comprehensive characterization approach is necessary and requires the use of different surface analysis techniques in order to identify the different species.

The sp^2/sp^3 ratio can be commonly determined by X-Ray Photoelectron Spectroscopy (XPS). This ratio should also be determined by considering the complementary C KLL X-ray induced Auger spectrum (XAES) in order to determine the D-parameter from the spectrums derivative since its value can be related to the ratio sp^2/sp^3 carbon [2]. Furthermore, Reflection Electron Energy Loss Spectroscopy (REELS) can provide some complementary qualitative information about the hydrogen content.

Not only the first nanometers of the surface are of interest in this study. The effect of mechanical constraints on the composition of DLC under the surface can be followed by use of depth profiling. This demands to proper identify and avoid possible induced effects of the sputtering itself on the composition. For this purpose, different carbon-based materials (like diamond, graphite) are used as model and compared with DLCs for the characterization of the sputter effects in order to determine an adapted depth profiling protocol delivering reliable insights on the near surface material composition.

Selected references

[1] D. K. Rajak, A. Kumar, A. Behera and P. L. Menezes, *Appl. Sci. 2021, 11, 4445*
[2] A. Theodosiou,, B. F. Spencer, J. Counsell, A. N. Jones, *Applied Surface Science, Volume 508, 1 April 2020, 144764*

P30 - Deep probing of buried layers with HAXPES, chemical analysis with bias applied operando setup for electronic devices

7. DPR – Thin Films, Coatings and Depth Profiling

Dick Allansson[1, 2]
[1] Dick Allansson, Scienta Omicron AB, Sweden
[2] Ad Ettema, Scienta Omicron GmbH, Germany

INTRODUCTION

Buried interfaces in electronic devices such as batteries, solar cells, transistors etc. are highly chemically sensitive and reliable instrumentation is necessary for material development. While X-ray photoelectron spectroscopy (XPS) is a powerful method to investigate the chemical nature of surfaces, buried interfaces in device electronics are more difficult to investigate due to scattering. Hard X-rays giving increased information depth, have therefore been increasingly used in the photoelectron spectroscopy field [1].

HAXPES AND XPS APPLICATIONS

Having access to XPS and HAXPES X-ray sources enables measurements of core levels with different resulting kinetic energy of the photoelectrons. With a soft X-ray XPS source, the kinetic energy is low and thus the obtained information is very surface sensitive. With Hard X-rays it is possible to be both surface and bulk sensitive, as electrons stemming from deep core levels will have lower kinetic energy and contain more surface sensitive information. Similarly, electrons stemming from shallow “XPS” core levels will have higher kinetic energy and contain more bulk sensitive information. This is especially valuable when detecting artefacts formed by sample exposure to different environments (e.g. air, moisture, heat, cold etc.) or by preparation steps known to induce chemical changes on the surface (e.g. sputtering). Scienta Omicron’s HAXPES Lab uses both an XPS Al Kα source and a monochromatic Ga Kα MetalJet HAXPES source with excitation energy of 9.25 keV, therefore enabling artefact-free investigations with superior information depth, which clearly extends beyond limits of conventional XPS surface analysis. This unlocks a comprehensive and effective characterisation of layered materials. Combined with a hemispherical electron analyzer with a ±30 degree acceptance angle [2], investigation of buried interfaces, operando devices and real-world samples becomes easily achievable. (Fig.1). Over the years it has proven invaluable in research of semiconductor materials in thin film electronic devices including the operando characterization of bias induced changes in chemical composition of material interfaces [3]. Other applications include polymer materials, metal surfaces and coatings. This presentation will give an overview of HAXPES applications with focus on buried interfaces in electronic devices such as passivation of luminescent quantum dots studied through a 35 nm overlayer, and semiconductor device band alignment by operando measurement with the Si substrate signal as reference detected through 20 nm TiN + 4 nm ZrO stack without sputtering and risk of artifacts.

Selected references

[1] Kalha, J. Phys. Condens. Matter., 33 (2021) 233001
[2] B. Spencer, Faraday Discuss., 236 (2022), 311
[3] T. Hashimoto, Vac. Surf. Sci. 64 (2021) 493

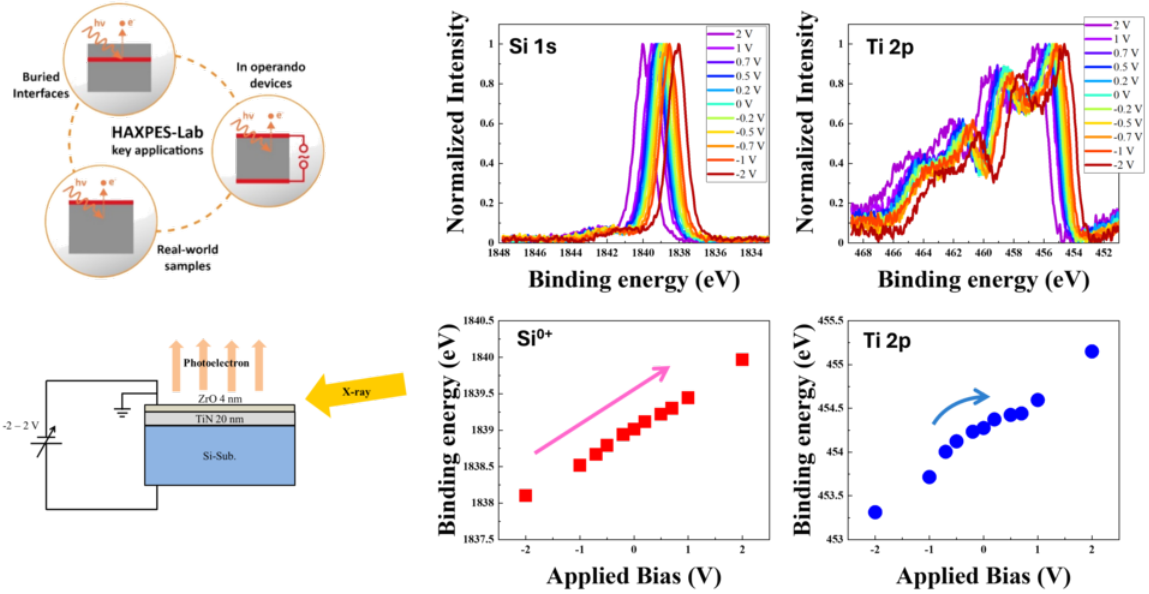

Figure 1. Key applications of HAXPES along with a Bias Applied Operando HAXPES measurement giving insight into the band alignment of a semiconductor device.

P31 – Inelastic background analysis from lab-based HAXPES spectra for critical interfaces in nano-electronics

7. DPR – Thin Films, Coatings and Depth Profiling

Christine ROBERT-GOUMET[1]
Taylor Rose BURE[1, 2], Thierry CONARD[3], Emmanuel NOLOT[2], Nicolas PAULY[4], Olivier RENAULT[2]
[1] Institut Pascal, Univ. Clermont Auvergne, UMR CNRS 6602, Clermont-Ferrand, France
[2] CEA-Leti, Univ. Grenoble Alpes, F-38000 Grenoble, France.
[3] IMEC, Kapeldreef 75, B-3001, Leuven, Belgium
[4] Service de Métrologie Nucléaire, Université libre de Bruxelles, Brussels, Belgium

The framework of this study is nanodevice technology and the need for nondestructive thickness confirmation of the deeply buried layers that make up increasingly complex semiconductor components. X-ray photoelectron spectroscopy (XPS) is widely used as it allows to obtain the chemical environment of an element nondestructively. The limiting factor of XPS measurements, however, is the probing depth of 3xIMFP which is not beyond 9 nm with soft X-ray laboratory sources. Increasing the probing depth through analysis of the inelastic background (IBA) allows to retrieve the depth distribution of deeply buried layers many times past that of core peak analysis. The IBA technique [1] was originally developed for soft X-ray energy.

The goal of this study is to provide a comprehensive study of IBA when applied to lab-based HArd X-ray PhotoElectron Spectroscopy (HAXPES). Two types of novel laboratory spectrometers fitted with Cr K∝ (hv = 5.41472 keV) and Ga K∝ (hv = 9.25174 keV) photon sources have been used which allow the IMFP to increase over 10 nm for many core transitions. Lab-based HAXPES-IBA was tested on bilayer stacks of Al_2O_3 and HfO_2 produced by Atomic Layer Deposition (ALD)[2]. Samples of Al_2O_3 and HfO_2 with increasingly thick overlayers up to 24.4 nm and buried layers of approximately 2.5 nm were measured with Cr K∝ and Ga K∝ sources to give maximum O1s IMFPs of 8.4 and 13.6 nm, respectively. Then, we applied the method to more realistic samples with applications in well-defined technologies: Al_2O_3 deposited over GaN by ALD representative of a recessed gate metal oxide semiconductor channel High Electron Mobility Transistor. Finally, an error correction applied to the IBA solution presented the challenges of a semi-automated method, highlighting the previously presented case studies and comparing the error correction to a visual inspection of the IBA result. IBA results from buried Hf 3d5/2 and Ga 2p3/2 yielded similar solutions for mean squared error (MSE) and visual inspection of the spectra.

Selected references

[1] S. Tougaard, J. Electron Spectrosc. Relat. Phenom. 178–179 (2010) 128–153. doi.org/10.1016/j.elspec.2009.08.005.
[2] Bure, T.R., Renault, O., Nolot, E., Lardin, T., Robert-Goumet, C., Pauly, N., Appl. Surf. Sci. (2023) 609, 155317. doi.org/10.1016/j.apsusc.2022.155317.

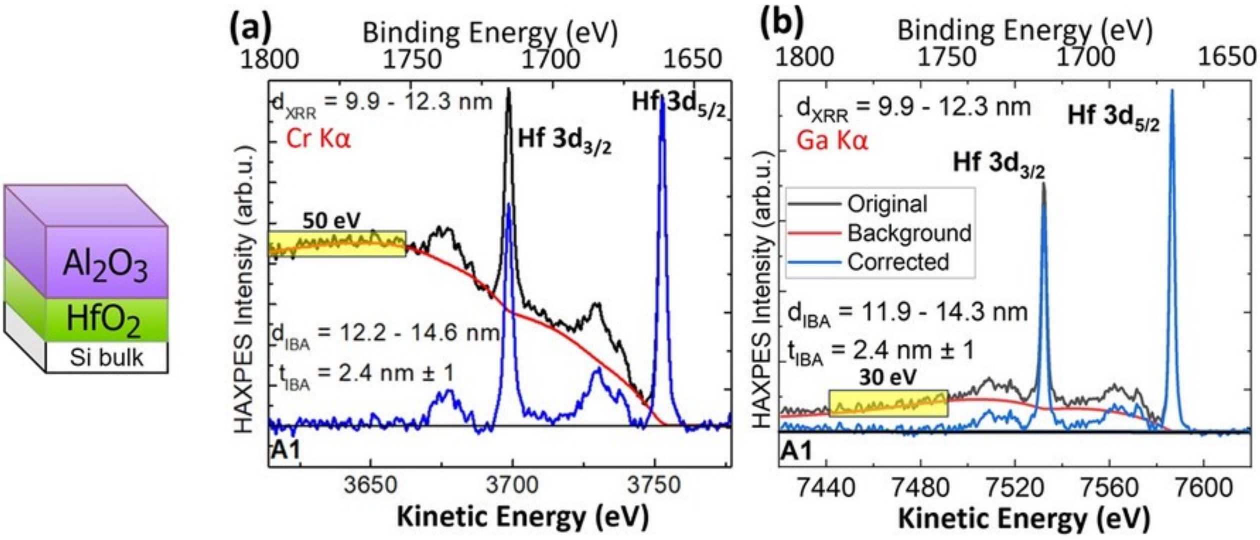

Figure 1: HAXPES-IBA of Hf3d in QUASES-Analyze using $K_{Universal}$ using (a) Cr Kα (hν = 5.41472 keV) and (b) Ga Kα (hν = 9.25174 keV) photon sources, case of Al_2O_3/HfO_2 stacks.

P32 - Metal thin film morphology suitable for multilayer diffusion study

7. DPR – Thin Films, Coatings and Depth Profiling

Antonie Johannes Fourie[1]
Jacobus Johannes Terblans, Hendrik Christoffel Swart[1]
[1] University of the Free State, 205 Nelson Mandela Drive, Park West, Bloemfontein, 9300, SOUTH AFRICA

The diffusion between metal thin films is a valuable research area for a wide range of applications. Typically, two or more different metal layers are deposited in sequence on top of each other. These layers are then subjected to a controlled annealing program that causes diffusion to occur between the two layers. If in-situ heating is possible, only one sample is needed. A depth profile is measured before annealing, and then again after every annealing step. If in-situ heating is not possible, a set of identical samples is prepared; one sample is kept as-deposited, and the rest are annealed at different temperatures and for different time periods, usually in a vacuum. To study the diffusion that happens between the different layers as well as possible, the other factors that cause mixing between the layers should be minimised so that the annealing is the predominant factor that causes the two layers to mix through diffusion. One of the factors that can cause mixing is the morphology of the layers.

In an attempt to produce the absorber layer for a CZTS solar cell, a multilayer of Cu, Zn, and Sn was deposited on a SiO_2 substrate using an electron beam evaporator. Depth profiles were subsequently obtained using an Auger Electron Spectrometer and a Time of Flight Secondary Ion Mass Spectrometer. The depth profiles measured for the unannealed multilayers showed that substantial layer mixing had already occurred. A series of single-layered samples of each element were produced on a SiO_2 substrate in order to look into the reason for the significant premixing of the as-deposited multilayer. These single-layer thin films were studied using a Scanning Electron Microscope, and it was found that Sn, and Zn formed islands on the surface and were not smooth layers. The deposition rate (for the single-layer thin films) was varied while surface morphology was recorded, and it was found that there was a reduction in island formation with an increase in deposition rate for Sn (See Fig. 1).

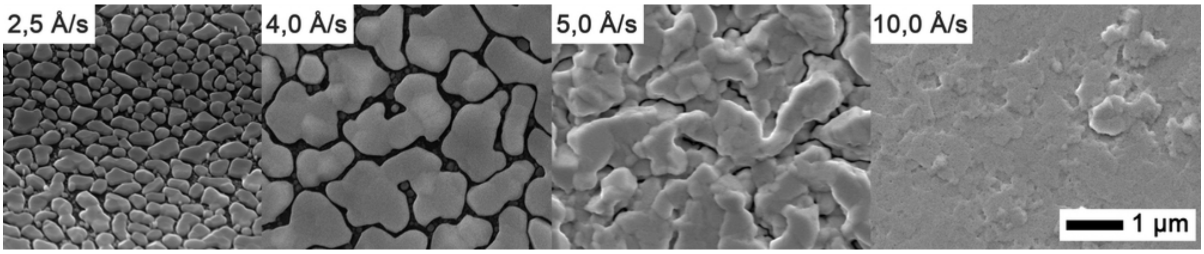

P33 - Surface analysis of the drug-eluting chitosan coatings on 3D-printed TiAl6V4 alloy for orthopedic applications

7. DPR – Thin Films, Coatings and Depth Profiling

Katja Andrina Kravanja[1]
Maša Knez Marevci[1], Željko Knez[1], Matjaž Finšgar[1]
[1] University of Maribor, Faculty of Chemistry and Chemical Engineering, Slovenia

Developing novel multifunctional implantable devices is essential to improve the success rate of orthopedic procedures. Recent studies have shown that the functionalization of implants with drug-eluting bioactive coatings leads to enhanced osteointegration and can alleviate persisting postoperative complications resulting from infection and inflammation at the implantation site. However, the main challenges associated with coating fabrication are attributed to inadequate mechanical durability and adhesion of the coatings, necessary to withstand load-bearing clinical applications [1, 2].

In this study, the 3D-printed TiAl6V4 discs with customizable porosity were prepared by selective laser melting and served as model implants. The pores of the 3D-printed discs were embedded with a combination of biocompatible and biodegradable polymer chitosan and two drugs, i.e., the antibiotic clindamycin hydrochloride and the non-steroidal anti-inflammatory drug ketoprofen. An improved solubility and homogeneous distribution of ketoprofen within the chitosan matrix was achieved by using β-cyclodextrins for drug entrapment. The presented approach was selected as it allows for the development of personalized implants tailored to the patient's anatomy, the perseverance of the drugs within the implant structure during implantation, and controlled localized drug release by altering the pore dimensions [3].

As a part of the initial stage characterization, a variety of surface analytical techniques were employed to investigate the chemical structure, interactions, and morphology of the as-prepared multi-component material. Time-of-flight secondary ion mass spectrometry (ToF-SIMS) and X-ray photoelectron spectroscopy (XPS) analyses were performed to confirm the presence of the two drugs on the surface. Chemically non-destructive sputtering was performed using a gas cluster ion beam (GCIB) combined with ToF-SIMS and XPS to analyze the chemical composition of different species in the coating in depth. Moreover, the acquisition of 3D SIMS images revealed the spatial distribution of the drugs within the polymer matrix. The morphological and topographical properties were investigated using atomic force microscopy on a small scale and 3D profilometry on a larger scale. The performance of the prepared materials was additionally evaluated by *in vitro* drug release tests to determine the drug release kinetics in simulated body fluids. The results demonstrate that the developed materials provide a good foundation for future biocompatibility and bioactivity studies.

Selected references

[1] K.A. Kravanja, M. Finšgar, A review of techniques for the application of bioactive coatings on metal-based implant materials to achieve controlled local release Materials & Design (2022) 110653.

[2] K. Rajesh, M.K. Rangaswamy, C. Zhang, S. Haldar, M. Kumarasamy, A. Agarwal, P. Roy, D. Lahiri, Surface Modified Metallic Orthopedic Implant for Sustained Drug Release and Osteocompatibility, ACS Applied Bio Materials 2(10) (2019) 4181-4192.

[3] Y. Wu, J. Liu, L. Kang, J. Tian, X. Zhang, J. Hu, Y. Huang, F. Liu, H. Wang, Z. Wu, An overview of 3D printed metal implants in orthopedic applications: Present and future perspectives, Heliyon (2023).

P34 - Thermoelectric and structural properties of sputtered AZO thin films with varying Al doping ratios

7. DPR – Thin Films, Coatings and Depth Profiling

Muhammad Isram[1, 2]
Riccardo Magrin Maffei[1], Valeria Demontis[3], Leonardo Martini[4], Stiven Forti[4], Camilla Coletti[4], Vittorio Bellani[5], Andrea Mescola[2], Guido Paolicelli[2], Alberto Rota[1, 2], Stefania Benedetti[2], Alessandro di Bona[2], Carlos J. Tavares[6], Francesco Rossella[1]
[1] Dipartimento di Scienze Fisiche, Informatiche e Matematiche, Università di Modena e Reggio Emilia, Modena, Italy
[2] Istituto Nanoscienze—CNR, Modena, Italy
[3] NEST Laboratory Scuola Normale Superiore, Pisa, Italy
[4] NEST, Istituto Italiano di Tecnologia, Pisa, Italy
[5] Dipartimento di Fisica, Università di Pavia and INFN Sezione di Pavia, Pavia, Italy
[6] Centre of Physics, University of Minho, Portugal

Nanomaterials can be game changers in the arena of sustainable energy production because they may enable highly efficient thermoelectric energy conversion and harvesting. For this purpose, doped thin film oxides have been proven to be promising systems for achieving high thermoelectric performances. A promising material due to its stability over a wide temperature range, high electrical conductivity, and Seebeck (S), is Al-doped ZnO (AZO). With the material benefiting further from the high natural abundance of constituent elements allowing for resource conscience energy harvesting. The deposition of highly uniform and conformal AZO thin films were deposited onto glass substrates by RF magnetron sputtering with an Al doping level in the range of 2–8 at.% In this work, the design, realization, and experimental investigation of the thermoelectric properties exhibited by a set of five Al:ZnO thin films with thicknesses of 300 nm and Al doping levels ranging from 2 to 8 at.% are described, highly uniform and conformal AZO thin films were deposited onto glass substrates by RF magnetron sputtering. Using a multi-technique approach, the main structural and morphological features of the grown thin films are addressed, as well as the electrical and thermoelectrical transport properties. The results show that the samples exhibited a Seebeck coefficient absolute value in the range of 22–33 µV/K, assuming their maximum doping level was 8 at.%, while the samples' resistivity was decreased below 2 × 10-3 Ohm·cm with a doping level of 3 at.%. The findings shine light on the perspectives of the applications of the metal ZnO thin film technology for thermoelectric.

Selected references

M. Isram, et al., Coatings 2023, 13(4), 691; https://doi.org/10.3390/coatings13040691

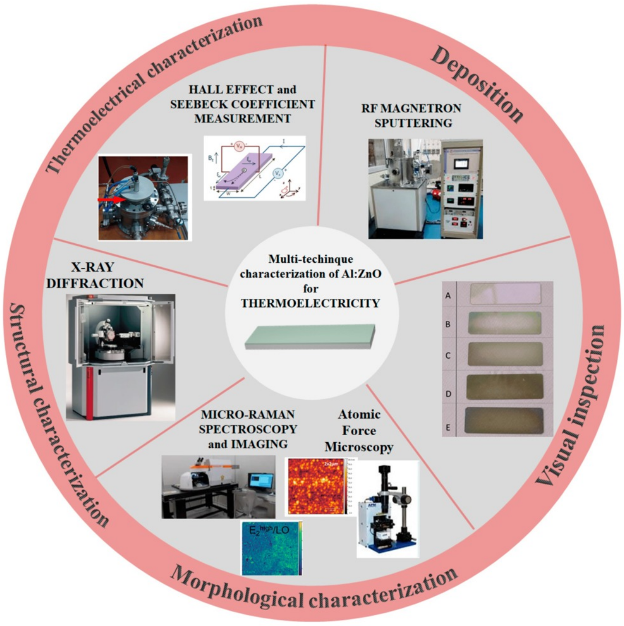
Thermoelectrical characterization
Deposition
Visual inspection
Morphological characterization
Structural characterization
HALL EFFECT and SEEBECK COEFFICIENT MEASUREMENT
RF MAGNETRON SPUTTERING
X-RAY DIFFRACTION
Multi-techinque characterization of Al:ZnO for THERMOELECTRICITY
MICRO-RAMAN SPECTROSCOPY and IMAGING
Atomic Force Microscopy
A
B
C
D
E
2x2μm
E2high/LO

P35 - Tungsten coating as hydrogen permeation barrier: a surface characterization

7. DPR – Thin Films, Coatings and Depth Profiling

Raouaa Hannachi[1]
Deborah Biggio[1], Bernhard Elsener[1], Marzia Fantauzzi[1], Nicoletta Zacchetti[2], Antonella Rossi[1]
[1] 1 Dipartimento di Scienze Chimiche e Geologiche, Università di Cagliari, Cittadella Universitaria, 09042, Monserrato, Cagliari, Italy,
[2] 2 Rina consulting-CSM S.p.A.

In the challenge to reduce emissions globally, hydrogen is one of the possible solutions as energy carrier. Production, storage, and transportation of hydrogen are demanding both for fundamental and applied research. This research focuses on the investigation of tungsten as hydrogen permeation barrier (HPB) on steel X60 to prevent or at least reduce the hydrogen uptake into steel and avoid the phenomenon known as hydrogen embrittlement.

In this context, physical vapor deposition (PVD), was employed to deposit tungsten onto a steel X60 substrate, the surface morphology, and the composition of steel X60 and tungsten-coated steel X60 (W-coated steel X60) were characterized by scanning electron microscopy- energy dispersive X-ray spectroscopy (SEM-EDS), X-ray photoelectron spectroscopy (XPS) and X-ray fluorescence spectroscopy (XRF).Furthermore, the hydrogen permeation test of steel X60 was performed using the Stachurski's cell.

SEM and XPS results confirmed the formation of tungsten coating on steel: The thickness of the tungsten coating is found to be 0.2mm. The preliminary hydrogen electrochemical tests of Steel X60 demonstrated excellent reproducibility. The results from XPS and SEM-EDX analyses will be compared with results of in-situ electrochemistry and discussed.

In overall, this work research provides an important insight for the application of tungsten coating as a promising hydrogen permeation barrier on steel X60.

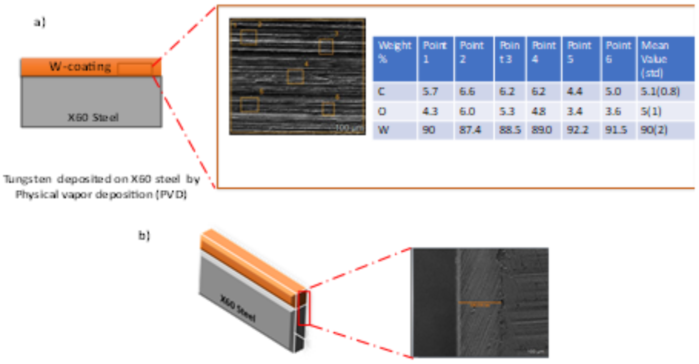

Weight %	Point 1	Point 2	Poin t3	Point 4	Point 5	Point 6	Mean Value (std)
C	5.7	6.6	6.2	6.2	4.4	5.0	5.1(0.8)
O	4.3	6.0	5.3	4.8	3.4	3.6	5(1)
W	90	87.4	88.5	89.0	92.2	91.5	90(2)

Figure: W-Coated X60 Steel analysis through SEM-EDX a) Elemental characterization of W-Coated X60 Steel by SEM-EDX; b) Sectional view of W-Coated X60 Steel examined by SEM.

8. ELC – Micro-, Opto- and Organic Electronics

P36 - Development of plasma surface treatment on GaN analyzed by quasi in-situ pARXPS

8. ELC – Micro-, Opto- and Organic Electronics

Laurent Xu[1]
Sophie Guillemin[1], Jérôme Biscarrat[1], Bernard Pelissier[2]
[1] University Grenoble Alpes, CEA, LETI, F-38000 Grenoble, France
[2] University Grenoble Alpes, CNRS, LTM, Minatec Campus, Grenoble, France

Gallium nitride (GaN) is a wide-gap semiconductor that has attracted increasing attention in recent decades. For power electronic applications, its physical properties enable the fabrication of devices operating at higher voltage, temperature, and frequency compared to mainstream silicon-based devices. However, the difficulty of forming a high-performance ohmic contact on GaN represents today a major challenge to the development of related technologies. An inefficient contact acts as a series resistor within the device, leading to the generation of excess heat and compromising its overall efficiency.

A contact being a metal/semiconductor interface, the properties of the material surface play an important role in the obtained performances. Typically, developing surface preparation schemes that allow the removal of native oxides prior to contact formation is crucial. GaN's native oxide is known to be difficult to remove and tends to regrow rapidly when exposed to air. To overcome these difficulties, inspiration was drawn from previous works on InP and InGaAs [1], adopting the use of a plasma surface treatment chamber directly coupled with an in-situ parallel angular resolved XPS (pARXPS) analysis.

In this paper, the effects of Ar, He, and H_2 plasma on the GaN surface are investigated, focusing on their oxide removal effectiveness and their impact on the substrate surface morphology. The plasma etch step was conducted in a dedicated 300 mm surface preparation chamber. Subsequently, the wafers were transported to the pARXPS chamber using a specific vacuum carrier. This carrier allows the wafer transport from one compatible equipment to another without exposure to air (Fig 1). Thus, eliminating the uncertainty brought by the air-break allows the so-called quasi in-situ characterization [2]. This study on highly air-sensitive GaN surfaces particularly benefits from these specific features.

Selected references

1. Coudurier & al., ECS Trans., 2019, 10.1149/09202.0073ecst
2. Pelissier & al., Micro. Engin., 2020, 10.1016/j.mee.2020.111401

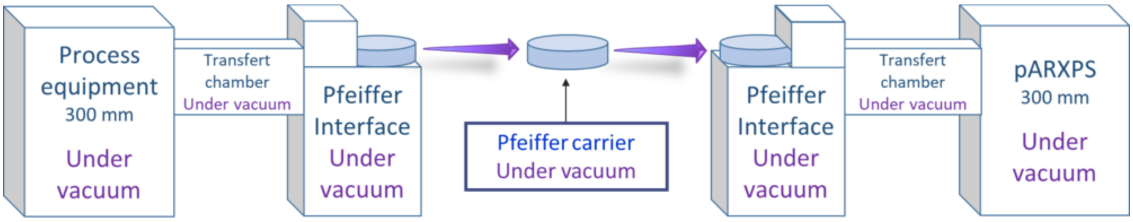

P37 - Microstructures prepared by ion beam writing and ion implantation through mask in graphene derivatives and polymers

8. ELC – Micro-, Opto- and Organic Electronics

Petr Malinsky[1, 2]
Oleksandr Romanenko[1], Vladimir Havranek[1], Josef Novák[1, 2], Eva Stepanovska[1, 2], Jan Luxa[3], Vlastimil Mazanek[3], Zdenek Sofer[3], Anna Mackova[1, 2]
[1] Institute of Nuclear Physics of CAS, v.v.i., Husinec - Rez, 250 68 Rez, Czech Republic
[2] Department of Physics, Faculty of Science, J. E. Purkinje University, 400 96 Usti nad Labem, Czech Republic
[3] Department of Inorganic Chemistry, University of Chemistry and Technology, 166 28 Prague 6, Czech Republic

The ion beam irradiation were used in two ways to prepare micro-scale structures for sensory and electronic application in graphene oxide (GO), reduced graphene oxide (RGO) and polyimide (PI). One way involved ion beam writing, while a second way utilized ion beam implantation through a polymeric mask. The polymeric mask was prepared directly on the surface of substrates by spin coating of PMMA, followed by proton beam writing and development in isopropyl alcohol. After the ion beam implantation, the mask was removed using acetone. The GO, RGO and PI foils were irradiated by 2.5 MeV ion beams with the ion fluence 3.75×10^{14} cm^{-2} (1800 $nC.mm^{-2}$). Subsequently, the shape of the created micro-structures and compositional changes of the irradiated materials were studied using Scanning Electron Microscopy (SEM)/Energy-Dispersive X-ray spectroscopy (EDS) methods, respectively. Complementary structure and compositional changes in the irradiated area were characterized by micro-Raman spectroscopy, X-ray Photoelectron Spectroscopy (XPS), Rutherford Back-scattering Spectroscopy (RBS) and Elastic Recoil Detection Analysis (ERDA) spectroscopy. The electrical and humidity sensing properties of the prepared microstructures were also tested and compared. In this work, we have demonstrated a method to create a structure with comparable properties using both ion beam writing and ion beam implantation through a mask.

9. IMA – Nanomaterials and Imaging

P38 - Comparative chemical analysis of Ni-Fe oxide nanoparticles

9. IMA – Nanomaterials and Imaging

Heydar Habibimarkani[1]
Sarah-Luise Abram[1], Carsten Prinz[1], Vasile-Dan Hodoroaba[1], **Jörg Radnik**[1]
[1] Bundesanstalt für Materialforschung und -prüfung (BAM), Berlin, Germany

Ni-Fe oxide nanoparticles have gained a lot of interest because of their high activity in the oxygen evolution reaction (OER) which is crucial for water splitting. [1] Although there have been great efforts in the last years, the understanding of the synergistic effect between Fe and Ni is still under discussion.

Therefore, we prepared different Ni-Fe oxide nanoparticles with different compositions from pure iron oxide to pure nickel oxide adapting a known procedure. [2,3] Size and morphology of the nanoparticles depend on the composition which was shown with Transmission Electron Microscopy (TEM). The compositions of the nanoparticles were measured with a comparative approach using X-ray Photoelectron Spectroscopy (XPS), Hard X-ray Photoelectron Spectroscopy (HAXPES), and Energy Dispersive X-Ray Spectroscopy (EDS) coupled with the TEM providing detailed chemical information of the nanoparticles in different sample regions. EDS reveals that the different sample regions are dominated by one of the components, Fe or Ni, but a slight mixing between the components can be found (see Figure 1), which was confirmed with X-ray Diffraction (XRD). XPS indicates the enrichment of Fe at the sample surface, while HAXPES and EDS data agree on the stoichiometry of the bulk. High-resolution XPS and HAXPES exhibit some differences in the valence states of Fe and Ni, whereas Ni seems to be easier to reduce than Fe. Further investigations combining these different techniques and additionally Secondary Ion Mass Spectrometry (ToF-SIMS) are ongoing by using *in situ* approaches and coupling cyclic voltammetry to the analytical techniques.

Selected references

[1] J. Zhao, J.-J. Zhang, Z.-Y. Li, X-H. Bu, *Small* 16, 2020, 2003916
[2] S. Noh , W. Na, J. Jang, J.-H. Lee, E. J. Lee, S.H. Moon, Y. Lim, J.S. Shin, J. Cheon *Nano Letter*s 12, 2012, 3716-3721
[3] A. Dong, X. Ye, J. Chen, Y. Kang, T. Gordon, J.H. Kikkawa, C.B. Murray, *J. Am. Chem. Soc.* 133, 2011, 998-1006

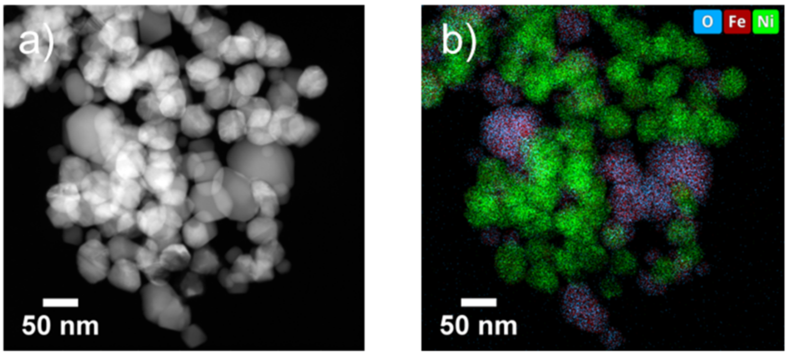

Figure 1: a) HAADF image and b) corresponding EDS elemental mapping of Fe:Ni=2:3 nanoparticles

P39 - Correlative imaging to reveal the nature of different graphene materials

9. IMA – Nanomaterials and Imaging
Robert Schusterbauer[1, 2]
Mario Sahre[1], Elisabeth John[1], Paul Mrkwitschka[1], Thorid Lange[1], Amaia Zurutuza[3], Elliot Jones[4], Ievgen Donskyi[2], Jörg Radnik[1], Vasile-Dan Hodoroaba[1]
[1] Bundesanstalt für Materialforschung und -prüfung (BAM), Berlin, Germany
[2] Freie Universität Berlin, Berlin, Germany
[3] Graphenea Semiconductor SLU, San Sebastián, Spain
[4] Haydale Graphene Industries, Ammanford, Wales

Since the original report in 2004 by Novoselov and Geim[1], Graphene gained incredible attention due to its fascinating properties[2]. In the past 20 years, the synthesis and functionalization of graphene has evolved significantly[3]. Different synthesis techniques were developed which led to other graphene-related materials such as graphene oxide (GO) or elemental-doped graphene[4]. Further chemical functionalization can enhance but also alter or reduce specific properties of the graphene. To reveal the nature of these materials a proper physico-chemical characterization with different analytical techniques is crucial.[5]

Single-layer GO flakes kindly provided by Graphenea (Spain) were prepared for systematic image analysis. These flakes were disposed on an alignment-marked SiO_2 substrate and correlatively imaged by scanning electron microscopy (SEM), atomic force microscopy (AFM), X-ray photoelectron spectroscopy (XPS), time-of-flight secondary ion mass spectrometry (ToF-SIMS) and Raman spectroscopy. The high lateral resolution and/ or extreme surface sensitivity of the mentioned techniques is necessary to explore monolayers. The ToF-SIMS images match well with the SEM and AFM images and provide information about the chemistry. With 2D Raman spectroscopy it is possible to differentiate between the number of stacked single-layer flakes. This is visualized in a 3D image (Figure b). Well-defined GO flakes could be used as a reference material for imaging of graphene-like structures but also of other types of 2D materials.

In addition to these monolayer GO flakes, commercial graphene-containing inks (Haydale) with a more complex morphology were also correlatively imaged. ToF-SIMS and SEM images were merged to identify the origin of different chemical fragments. The findings correlate closely with the expectation that the specific functionalizations (with fluorine and nitrogen as marker elements) are present only on the graphene flakes as presumed from the SEM images. Energy-dispersive X-ray spectroscopy (EDX) supports these results, yet with a much lower sensitivity compared to ToF-SIMS.

Selected references

[1] K. S. Novoselov, A. K. Geim, S. V. Morozov, D. Jiang, Y. Zhang, S. V. Dubonos, I. V. Grigorieva, A. A. Firsov, *Science* **2004**, *306*, 666-669.
[2] R. R. Nair, P. Blake, A. N. Grigorenko, K. S. Novoselov, T. J. Booth, T. Stauber, N. M. R. Peres, A. K. Geim, *Science* **2008**, *320*, 1308-1308; bC. Lee, X. D. Wei, J. W. Kysar, J. Hone, *Science* **2008**, *321*, 385-388.
[3] K. A. Madurani, S. Suprapto, N. I. Machrita, S. L. Bahar, W. Illiya, F. Kurniawan, *Ecs J Solid State Sc* **2020**, *9*.
[4] Z. Jin, J. Yao, C. Kittrell, J. M. Tour, *Acs Nano* **2011**, *5*, 4112-4117.

[5] G. Chemello, X. Knigge, D. Ciornii, B. P. Reed, A. J. Pollard, C. A. Clifford, T. Howe, N. Vyas, V. D. Hodoroaba, J. Radnik, *Adv Mater Interfaces* **2023**, *10*.

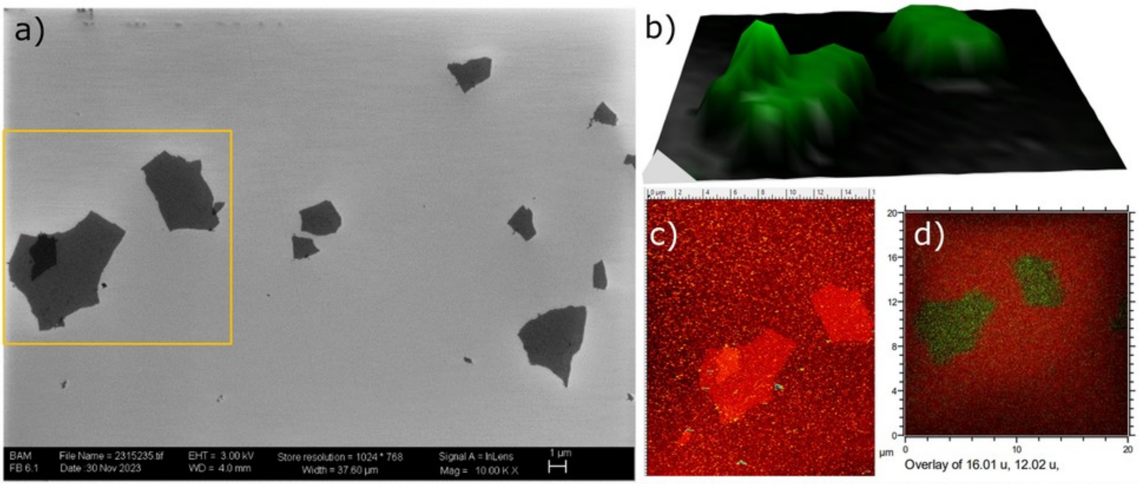

Figure: Correlative images of GO flakes (Graphenea) a) SEM image b) Raman intensity of G peak c) AFM image and d) ToF-SIMS overlay image of O- (red) and C- (green) fragments.

P40 - Correlative XPS & SEM analysis to determine 2D material structures

9. IMA – Nanomaterials and Imaging

Tim Nunney[1]
Paul Mack[1], Robin Simpson[1], Helen Oppong-Mensah[1]
[1] Thermo Fisher Scientific, Unit 1, The Felbridge Centre, Imberhorne Lane, East Grinstead, West Sussex, UK

Single-layer, 2-dimensional materials are actively being investigated across a wide range of fields due to the unique properties they exhibit compared to their bulk equivalents. Materials such as molybdenum disulfide (MoS_2) and graphene, for instance, are seeing potential uses in electronics, medicine, and in materials for engineering. Notably, the properties of 2D materials can be tailored to specific applications through careful modification of their surface chemistry and structure. In order to fully understand these materials and monitor their chemistry, multi-modal observation is often necessary, pairing multiple imaging and analysis techniques to deconvolute molecular-scale changes. In this presentation we show how such a correlative approach can be used to characterise 2D materials deposited on substrates, a sample of MoS_2 which has been applied in an inhomogeneous way onto a silicon substarte, and a BN sample deposited onto a copper foil. The workflow used combines scanning electron microscopy (SEM) and X-ray photoelectron spectroscopy (XPS) instrumentation into a correlated process, enabling the same regions of interest to be investigated; providing both high-resolution imaging and surface analysis from the same positions, even when collected using separate tools. While SEM can easily visualize 2D materials, these layers are typically too thin to be easily characterized with the analytics commonly present on the microscope such as energy dispersive X-ray (EDX) analysis. XPS, meanwhile, cannot easily resolve surface structures at the required resolution, but can clearly detect what material is present at the surface, and quantify any chemical changes that might have occurred. XPS instrumentation typically also incorporates additional analytical techniques, and in the examples presented an in-situ Raman spectrometer, that is coincident with the XPS analysis position, is used to obtain further information.

P41 - Investigation of the MoS2 / substrate interaction using surface analysis techniques

9. IMA – Nanomaterials and Imaging

Francesco Laudani[1]
Jakob Rath[1], Markus Sauer[1], Jakob Hemetsberger[1], Annette Foelske[1]
[1] Technische Universität Wien

Transition metal dichalcogenides (TMDCs) have established as being one of the most studied classes of two-dimensional (2D) materials. Molybdenum disulfide (MoS_2) in particular has gained a lot of interest due to the tunability of its remarkable electronic and optical properties based on the number of layers: the unique band structure changes from an indirect to a direct band gap when going from bulk to single layer and it allows for enhanced light emission and absorption, thus making it promising for nanoscale photonics and optoelectronics. A straightforward method for the deposition of wafer-scale continuous crystalline MoS_2 monolayers is still a challenge for researchers for many reasons, such as achieving high crystallinity, a precise thickness control and homogeneity.

Herein, we report on MoS_2 films deposited in different ways (e.g. mechanical exfoliation, drop casting, spin coating, Chemical Vapor Deposition (CVD), Atomic Layer Deposition (ALD)) and on different substrates (e.g. metal, semimetal, semiconductor) to shed light on how much these parameters influence the quality and properties of the films. In order to obtain a holistic picture, complementary surface analytical tools were applied: X-ray Photoelectron Spectroscopy (XPS) was used to investigate the chemical composition and homogeneity, Auger Electron Spectroscopy (AES) has been used for chemical mapping with high lateral resolution and compared to Secondary Electron Microscopy (SEM) and Energy Dispersion X-ray spectroscopy (EDX) measurements, Low Energy Ion Scattering spectroscopy (LEIS) - as the most surface sensitive technique - was used to probe for contaminations, Atomic Force Microscopy coupled with Raman spectroscopy (AFM-Raman) to conclude on mono-, bi- and multilayer structures and Photoluminescence spectroscopy (PL) to study the films` bandgap.

Main outcome of this comprehensive instigation will be summarized in this contribution.

P42 - Method development for inner-channel surface analysis of quartz nanopipettes with chemical modification

9. IMA – Nanomaterials and Imaging

Lauren Matthews[1, 2]
Mario Sahre[1], René Hesse[1], Robert Schusterbauer[1, 3], Melissa Grant[2], Leonardo Agudo Jácome[1], Tim Albrecht[2], Vasile-Dan Hodoroaba[1]
[1] Bundesanstalt für Materialforschung und -prüfung (BAM), Berlin, Germany
[2] University of Birmingham, Birmingham, United Kingdom
[3] Free University of Berlin, Berlin, Germany

Nanopipettes are a type of solid-state nanopore with needle-like geometry. Their applications range from imaging, sensing, diagnostics, and use as injectors. The response of nanopipette sensors is highly dependent on the size, geometry and chemical properties of the sensing region (1,2). As they are increasingly tuned and modified for specific analytes, a better understanding of the surface chemistry and morphology of the inner channel is necessary. With the aim of developing a comprehensive approach for characterisation of such nanopipettes, this research focuses on combining surface-sensitive analysis methods with advanced sample preparation techniques. Quartz substrates were modified by gas phase silanization, a well-utilised technique in the field to enhance performance of nanopipettes (3), and further functionalised with a metal bis thiolate complex, to aid in chemical analysis (4). The sample characterisation involved scanning electron microscopy (SEM), low-energy dispersive x-ray spectroscopy (EDX), time-of-flight secondary ion mass spectrometry (ToF-SIMS) and Auger electron spectroscopy (AES). Using focused ion beam (FIB) milling under gentle conditions, the inner surface of quartz nanopipettes was exposed whilst preserving the integrity of the overall structure (see figure). Owing to the challenging analysis conditions, modification and analysis of flat quartz substrates has been performed in parallel for optimisation purposes. The results demonstrate the first steps towards full characterisation of nanopipettes at the nanoscale, notably with access to the inner channel. The methods used here can be applied to gain further understanding of the response of these sensors to complex analytes and allow for the study of different surface functionalisations at the all-important sensing region.

Selected references

(1) Albrecht, *Annu. Rev. Anal. Chem.*, 2019, **12**, 371–87.
(2) Y. Y. Loh, C. H. Burgess, D. A. Tanase, G. Ferrari, M. A. McLachlan, A. E. G. Cass, and T. Albrecht, *Anal. Chem.*, 2018, **23**, 14063–14071.
(3) Zhang, M. Li, B. Su, and Y. Shao, *Annu. Rev. Anal. Chem.*, 2018, **11**, 265–86.
(4) Rades, P. Borghetti, E. Ortel, T. Wirth, M. Blanco, E. Gómez, A. Martinez, J. Jupille, G, Martra and V. -D. Hodoroaba*, Surf Interface Anal.,* 2018, **50**, 1200–1206.

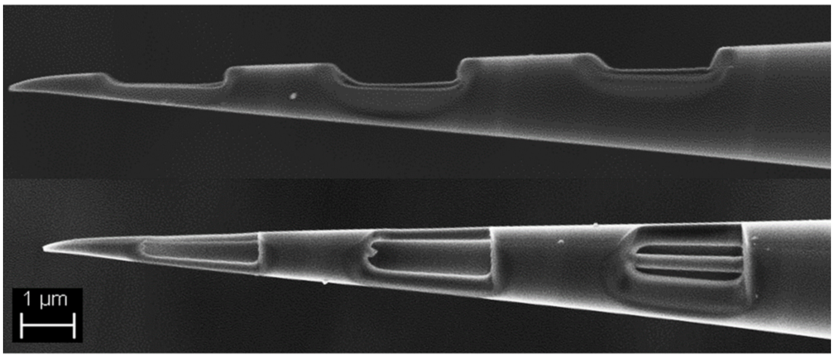
1 µm

P43 - Nanoscale secondary ion mass spectrometry imaging (NanoSIMS) – A new tool to unveil nanostructures in life science, material and environmental science

9. IMA – Nanomaterials and Imaging

Elias Ranjbari[1]
Michael E. Kurczy[2], **Nhu Phan**[1]
[1] Department of Chemistry and Molecular Biology, University of Gothenburg, 41390, Gothenburg, Sweden
[2] DMPK, Research and Early Development, Cardiovascular, Renal and Metabolism (CVRM), BioPharmaceuticals R&D, AstraZeneca, Gothenburg, 43183, Sweden

The NanoSIMS is a unique secondary ion nanoprobe, capable of measuring elemental, isotopic, inorganic, organic, and biomolecular distributions with excellent sensitivity (ppm), and 2D/3D imaging with nanometer spatial resolution (~ 50 nm laterally, 10 nm axially). The instrument is featured with a coaxial optical design for the primary ion beam and secondary ion extraction, along with an innovative magnetic sector mass analyzer with multicollection. NanoSIMS has been increasingly applied in various research fields, especially material, environmental and life science to visualize the nanoscale structure and compositions of samples. NanoSIMS can also be combined with other imaging techniques, such as fluorescence microscopy, electron microscopy, atomic force microscopy to obtain complementary information of sample properties. Moreover, absolute quantification of the compounds or elements of interest can be performed with NanoSIMS. This has been particularly applied as a new approach to assess the absolute accumulation of drugs at the subcellular level, a crucial aspect in therapeutic design.

Here, we provide a showcase of NanoSIMS applications in material, environmental and life science to demonstrate a vast potential of the technology, particularly, characterization of protein turnover in human neural progenitor cells at an organelle level; tracking accumulation and quantification of an antisense oligonucleotide drug in single human hepatocyte cells, 3D imaging of light metal distribution in alloys, visualization of the carbon and nitrogen assimilation in phytoplankton in the central arctic ocean, and examination of uranyl accumulation in hepatic caeca of Daphnia. NanoSIMS imaging, with a capability of correlating with other imaging techniques, offers a new window of opportunity to explore the chemical ultrastructures unravelling complex sample properties, as well as connections between the samples' structures and functions.

P44 - Substrate Effects, Shapes, and Morphologies of Chemical Vapor Deposited 2D WSe2

9. IMA – Nanomaterials and Imaging

Dimitre Dimitrov[1, 2], Krastyo Buchkov[1], Peter Rafailov[1], Nikolay Minev[2], Vladimira Videva[2, 3], Velichka Strijkova[2], **Vera Marinova**[2]
[1] Institute of Solid State Physics, Bulgarian Academy of Sciences 72, Tzarigradsko Chaussee Blvd, 1784 Sofia, Bulgaria
[2] Institute of Optical Materials and Technologies, Bulgarian Academy of Sciences, Acad. G. Bontchev Str. 109, 1113 Sofia, Bulgaria
[3] Faculty of Chemistry and Pharmacy, Sofia University, 1 James Bourchier Blvd., 1164 Sofia, Bulgaria

Owing to their exceptional properties, which are usually determined by growth conditions, 2D transition metal dichalcogenides (TMDCs) offer numerous research directions for applications in spintronics, valleytronics, and optoelectronics. Here, we focus on the chemical vapor deposition (CVD) synthesis of WSe2 (tungsten diselenide) nanoclusters/nanoflakes using a liquid precursor for tungsten (ammonium metatungstate) on Si/SiO2, fused silica, and sapphire substrates. Various WSe2 clusters with different sizes, thicknesses, and geometries were analyzed using optical and atomic force microscopy (AFM) as well as Raman spectroscopy. The observed structures were mostly WSe2 multilayers; however, monolayer formations were also found. They exhibited significant morphological differences, as well as wide nucleation density and size variations, possibly related to precursor/substrate surface interactions under the same CVD synthesis conditions. The largest WSe2 domains, with lateral sizes of up to hundreds of micrometers, were observed on sapphire, likely caused by a higher growth rate of singular nucleation sites. WSe2 domains with irregular and triangular shapes were simultaneously identified on fused silica, whereas multilayered pyramidal WSe2 structures predominated in the case of Si/SiO2 substrates. The application of polarized Raman spectroscopy to precisely determine and differentiate the characteristic vibrational modes (A1g, E2g, and 2LA(M)) enabled the unambiguous identification of 2D mono- and/or multilayered WSe2 formations with a high crystallinity level. The presented comparative analysis of samples prepared under relatively simple synthesis conditions (moderate working temperatures and ambient pressure) lays the foundation for further progress in the facile metatungstate CVD method and provides relevant opportunities for exploring 2D TMDC materials.

Acknowledgment: We acknowledge the support of the Bulgarian Science Fund under the project numbers FNI КП-06-ДО 02/2 and КП-06-ДО 02/3 in the frames of M-ERA program project “Functional 2D materials and heterostructures for hybrid spintronic-memristive devices”.

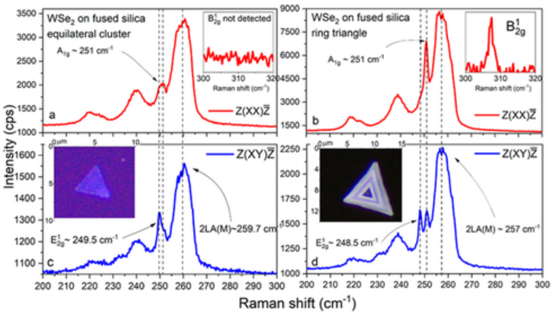

Fig.1. Cross- and parallel-polarized Raman spectra (a–d) of mono- and multilayer WSe2 clusters on fused silica. Insets: optical images of investigated WSe2 flakes.

10. MET – Metallic Materials

P45 - 316L steel prepared by L-PBF: surface effects of plasma low temperature carburizing

10. MET – Metallic Materials

Eleonora Bolli[1]
Saulius Kaciulis[1], Alex Lanzutti[2], Alessio Mezzi[1], Roberto Montanari[3], **Alessandra Palombi**[3], Francesco Sordetti[2], Emanuele Vaglio[2], Alessandra Varone[3], Claudio Verona[3]
[1] ISMN-CNR, P.O. Box 10, 00015 Monterotondo Stazione, Rome, Italy
[2] Polytechnic Department of Engineering and Architecture, University of Udine, Via delle Scienze 208, 33100 Udine, Italy
[3] Department of Industrial Engineering, University of Rome "Tor Vergata", Via del Politecnico 1, 00133 - Roma, Italy

In a previous work [1] 316L steel samples, manufactured by laser powder bed fusion (L-PBF), were submitted to low temperature carburizing treatments assisted by plasma with different gas mixtures (treatment time of 7 hours). All these treatments resulted in a surface layer of expanded austenite (S-phase) with thickness of ~ 25 μm covered by a 2 μm thick DLC over-layer that is brittle and much harder than S-phase. Tribological tests indicated that the DLC over-layer fractures and detaches from the metal surface during the tests and the hard debris take part to the wear process acting as abrasive particles and increasing the wear rate.

In order to optimize tribological behavior, the treatments should induce the formation of S-phase but not of DLC over-layer. Therefore, treatments for shorter time (30, 45, 60, 90, 105 and 120 minutes) by using the plasma gas mixture (2.5% CH_4 + H_2) that allowed to get the best wear resistance, have been carried out and the surface chemical composition of the samples has been then investigated by XPS measurements. Present work illustrates and discusses the results.

Selected references

1- E. Bolli, S. Kaciulis, A. Lanzutti, A. Mezzi, R. Montanari, A. Palombi, F. Sordetti, E. Vaglio, A. Varone, C. Verona, "Surface characteristics and tribological behaviour of 3D-printed 316 L steel after plasma assisted low temperature carburizing", Surface & Coatings Technology (2023) 2024, 477, 130295.

P46 - Impact of gaseous hydrogen on low cycle fatigue performance: Fractographic insights from surface analysis

10. MET – Metallic Materials

Vishnu Anilkumar[1]
Lars Nyborg[1], Yu Cao[1]
[1] Department of Industrial and Materials Science, Chalmers University of Technology, SE-412 96, Gothenburg, Sweden

Hydrogen has the potential to be widely used in various energy systems, such as fuel cells, gas turbines, and internal combustion engines. Materials play a crucial role in the energy transition from conventional fossil fuels to hydrogen [1]. Fuel storage, feeding, and reaction/combustion processes challenge the materials used. It is known that loading metallic material with hydrogen uptake can result in a decrease in the mechanical properties, leading to hydrogen embrittlement (HE). In this study, the low cycle fatigue (LCF) test was performed for a metastable austenitic stainless steel in high pressure gaseous hydrogen in various conditions to examine its effect on embrittlement susceptibility. It was found that exposure to hydrogen significantly reduced fatigue life. The fracture surface investigated using optical microscopy (OM) and scanning electron microscopy (SEM) revealed a different morphology compared to that of air-tested specimens.

Auger electron spectroscopy (AES) is a powerful tool for surface analysis. It was utilized in the present study to examine LCF fracture surfaces tested in-situ in high pressure gaseous hydrogen. Hydrogen-induced segregation of elements was revealed both laterally and in depth. The latter was realized by alternating argon ion sputtering and AES analysis. Comparison with air-tested specimens provided insight into the role of hydrogen in the initiation and propagation of fatigue cracks.

Selected references

[1] Jiaxing Liu, Mingjiu Zhao, Lijian Rong, Overview of hydrogen-resistant alloys for high-pressure hydrogen environment: on the hydrogen energy structural materials, *Clean Energy*, Volume 7, Issue 1, February 2023, Pages 99–115.

P47 - Segregation and crack formation in laser welded IN792 equiaxed superalloy

10. MET – Metallic Materials

Giuseppe Barbieri[1]
Francesco Cognini[1], Alessandra Fava[1], Saulius Kaciulis[2], Alessio Mezzi[2], Massimo Moncada[1], **Roberto Montanari**[3], Maria Richetta[3], Alessandra Varone[3]
[1] ENEA, Department for Sustainability—Research Centre of Casaccia, via Anguillarese 301, Santa Maria di Galeria, 00123 Rome, Italy
[2] ISMN-CNR, P.O. Box 10, 00015 Monterotondo Stazione, Rome, Italy
[3] Department of Industrial Engineering, University of Rome "Tor Vergata", Via del Politecnico 1, 00133, Rome, Italy

Nickel-base superalloys are nowadays widely used in aerospace, aeronautic and energy sectors. Throughout their operational lifespan, the components work in a very hostile environment and are exposed to high temperature and stress which can lead to the formation of cracks compromising their performance. Laser welding is a suitable high-energy density method to repair the damaged parts. The IN792 is a superalloy commonly employed in blades and rotors of jet engines owing to its excellent mechanical properties and corrosion resistance at high temperature. The IN792 alloy with equiaxed grains has been laser welded, however radiographic analyses revealed a significant presence of transverse cracks in samples after bead-on-plate (BoP) tests. Cracks are perpendicular to the welding direction of the laser beam and scanning electron microscopy (SEM) observations showed that some areas of the fracture surfaces exhibit the typical morphological features of intercrystalline fracture mode. Therefore, XPS investigations have been performed to assess possible elemental segregation phenomena which can favour the formation and propagation of cracks. The results are presented and discussed.

P48 - Tailoring Multi-properties of Fe-6.5Si Magnetic Alloys Through Laser Fluence in Powder Bed Fusion Process

10. MET – Metallic Materials

Mukesh Murali[1, 2]
Eduard Hryha[1, 2], Varun Chaudhary[1, 2]
[1] Industrial and Materials Science, Chalmers University of Technology, Gothenburg SE-41296, Sweden
[2] Centre for Additive Manufacturing-Metal (CAM2), Chalmers University of Technology, Gothenburg SE-41296, Sweden

The emergence of electric transportation demands high-performance electric motors with improved efficiency, emphasizing the importance of soft magnetic materials. While traditional silicon steel (Fe-3.2 wt.% Si) suffices for low-frequency applications, its limitations at higher frequencies demand alternatives [1]. High silicon steel (Fe-6.5 wt.% Si) is a promising candidate with superior properties like high electrical resistivity, low iron loss, and near-zero magnetostriction, ideal for reducing energy losses, failure, and noise at high frequencies. However, its brittleness poses manufacturing challenges due to ordered phase formation during conventional methods. Additive manufacturing offers a solution, providing precise control over texture and a high cooling rate to enhance ductility [2]. We investigated the potential of Laser-based Powder Bed Fusion (L-PBF) to produce Fe-6.5wt%Si magnetic materials with improved multi-properties required for high-frequency electric machines. The influence of the surface structure of Fe-6.5Si alloy powders, analyzed by X-ray photoelectron spectroscopy, on powder processibility and the properties of printed components is established. Subsequently, the process parameters for printing highly dense (>99%) and defect-free Fe-6.5Si alloys are optimized. A correlation between part density, microstructure, crystallographic texture, multi-properties such as hardness, electrical resistivity, saturation magnetization, etc., and laser fluence is established. This optimized surface structure and process parameter window for printing defect-free Fe-6.5Si materials using L-PBF can be utilized for developing soft magnetic components required in next-generation real-world applications.

Keywords: Fe-Si alloys, High silicon Steel, Additive Manufacturing, Laser- Powder Bed Fusion, Soft magnetic materials

Selected references

[1] S.M. Varahabhatla *et al.*, Influence of energy density on the microstructure, growth orientation, and anisotropy of magnetic properties in additively manufactured Fe-3.8wt%Si transformer steels, *Materialia*, 30, 101854–101854, 2023.
[2] V. Chaudhary, *et al.*, Additive manufacturing of magnetic materials, *Progress in Materials Science*, 114, 100688, 2020.

P49 - XPS study of Co28Cr6Mo biocompatible alloy

10. MET – Metallic Materials

Alessandra Fava[1]
Saulius Kaciulius[2], Alessio Mezzi[2], Roberto Montanari[3], Alessandra Palombi[3], **Alessandra Varone**[3]
[1] ENEA, Department for Sustainability—Research Centre of Casaccia,Via Anguillarese 301, Santa Maria di Galeria, 00123 Rome, Italy
[2] ISMN-CNR,P.O. Box 10, 00015 Monterotondo Stazione, Rome, Italy
[3] Department of Industrial Engineering, University of Rome “Tor Vergata”,Via del Politecnico, 1, 00133, Rome, Italy

CoCrMo alloys exhibit excellent wear resistance and mechanical strength combined with long-term corrosion resistance thus they are widely used for the production of medical devices such as orthopedic and dental implants. Of particular relevance is the possibility to customize through additive manufacturing (AM) the device for fitting the patient anatomy. Moreover, in the case of Co-based alloys, AM allows to overcome some manufacturing limits typical of conventional processes.

Mechanical Spectroscopy (MS) experiments have been carried out by present authors on an alloy with the following chemical composition: Cr 27.0-30.0, Mo 5.0-7.0, Si < 1.0, Mn < 1.0, Fe < 0.75, Ni 0.25-0.50, C < 0.16, W < 0.20, Ti < 0.10, O < 0.10, Co to balance (wt.%). They evidenced that two main anelastic phenomena occur during heating from room temperature to 800 °C. During the tests part of the metastable γ phase transforms into the stable ε phase. An anelastic phenomenon is due to the sliding of the γ-ε interphase boundaries while the other one has been attributed to surface diffusion of Mo that contributes to the disaggregation of cellular structure.

The sample surface, before and after MS tests, has been investigated by XPS to identify the possible segregation of alloying elements and changes ~~of~~ in chemical distribution. The results of such experiments are illustrated and discussed.

11. NRG – Energy, Environment, Geology and Heritage

P50 - Effects of voltage holds on graphite electrode surfaces layers and X-ray photoelectron spectroscopy post-mortem studies

11. NRG – Energy, Environment, Geology and Heritage

Sofia Reiner[1]
Julia Maibach[1]
[1] Department of Physics, Chalmers University of Technology

Multiple interfaces and interphases are formed in battery cells during operation, and they are imperative for the performance of the cells. Of particular interest is the solid electrolyte interphase (SEI) formed at the contact between the negative electrode and electrolyte during battery cell cycling. This decomposition layer, formed due to the electrochemical instability of the electrolyte at electrode voltage, acts as a passivating film, preventing further decomposition and loss of active species and enables stable cycling. Furthermore, proper characterization of the SEI, identifying the species involved in its formation and evolution during cycling gives important guidance when deciding on chemistries and cycling protocols in battery research.

In previous studies on Lithium-ion batteries, an extended voltage hold during discharge, that is the de-intercalation or de-alloying of lithium from the negative electrode, has been shown to improve capacity retention and therefore extend the cycle life of the cell [1],[2]. In NMC ($LiNi_xMn_yCo_{1-x-y}O_2$) /graphite cells, similar trends have been observed but the mechanisms behind the capacity recovery after voltage holds are not fully understood, and mechanisms connected to the evolution of the SEI cannot be excluded. At the same time, voltage holds are often used in sample preparation for post-mortem XPS studies on cycled battery electrodes to ensure stable electrode potentials. But what if these voltage holds change the SEI or the general surface composition?

Therefore, we study the effect of extended voltage holds on the SEI layer in graphite electrodes with X-ray photoelectron spectroscopy (XPS). Changes in the composition at the graphite electrode surface indicate that the loss and gain of active lithium during cycling and potential holds, respectively, is a result of side reactions or reparations in and of the SEI layer or lithium plating effects and not necessarily the recovery of deeply intercalated lithium from the bulk. Furthermore, we present a study into important factors when measuring battery interphases, such as the SEI and areas of plated lithium on graphite. These include effects of electrode washing as well as the impact of chosen measuring spots and sample homogeneity.

Selected references

[1] F. Lindgren et. al, Adv. Energy Mater. 2019, 1901608.
[2] D. Rehnlund et. al, Energy Environ. Sci., 2017,10, 1350-1357.

P51 - Electron spectroscopic investigations at alkaline-based battery-relevant reference material

11. NRG – Energy, Environment, Geology and Heritage
Steffen Oswald[1]
M. Hantusch[1], T. Schmeida[1], M. Gorbunov[1], A. Thomas[1], D. Mikhailova[1]
[1] Leibniz-IFW Dresden, Helmholtzstr. 20, D-01069 Dresden, Germany

Electron spectroscopy with X-ray photoelectron spectroscopy (XPS) and Auger electron spectroscopy (AES) plays an important role for the characterization of the chemical processes occurring in batteries. The interpretation of the chemical species is not always straightforward because of the high reactivity of the alkaline elements. We therefore performed a series of measurements for reference materials based on the elements lithium (Li), sodium (Na) and potassium (K). All sample preparation was done under glove box atmosphere and with Ar-transfer to the analysis chambers, because otherwise only thick oxide products could be observed. For the thin reaction layers from this preparations never surface charging was observed during the measurements.

Metals
The clean metal samples always were covered by thin reaction layers: mixed oxides, carbonates, (fluorides). Clean metal surfaces were prepared by mechanical scraping or long-time Ar^+ sputtering. The metallic state for Na and K is characterized in XPS by the occurrence of strong plasmon satellite peaks. Short storage on air led in all cases mainly to carbonate formation, never nitrogen could be found. Despite not real charging occurred, all peaks of the surface layers including the C-H contamination and the implanted Ar are shifted stable 3 eV to higher BE values. This was described by a surface “potential barrier” at the alkaline-rich surfaces. AES measurements confirmed the observations, however, for K the overlay of CKLL and KLMM leads to complications.

Intercalated Graphite
Graphite is of interest because it is the mainly used anode material. As reference material highly-oriented graphite (HOPG) was used which was intercalated with the alkaline elements (Li, K) by a thermo-chemical process. The surface oxides were removed by delamination with adhesive tape. Full intercalation could be observed and the XPS C1s peaks of this states were characterized by a shift and an asymmetric shape. Also in the AES spectra such characteristics were found.

Beam damage
During only XPS measurements no spectral changes were observed. Drastic damage could be observed, however, by both ion beams (Ar^+ sputtering) and electron beam (AES). Ion beam led to oxide reduction and to drastic out-diffusion (more than factor 4) of Li and K from the intercalated HOPG. For the electron beam dose-depended oxide reduction and lateral and in-depth diffusion of the alkaline elements were observed.

All these observations must be carefully considered for the interpretation of the surface analytical results in battery research.

Selected references

S. Oswald, Binding energy referencing for XPS in alkali metal-based battery materials research (I): Basic model investigations, Appl. Surf. Sci. 351 (2015) 492-503.

S. Oswald, Auger- and X-ray Photoelectron Spectroscopy at Metallic Li Material: Chemical Shifts Related to Sample Preparation, Gas Atmosphere, and Ion and Electron Beam Effects, Batteries 8 (2022) 24.

S. Oswald, T. Schmeida, D. Mikhailova, Model experiments with Auger electron and X-ray photoelectron spectroscopy at lithiated graphite material: chemical shifts related to ion- and electron-beam effects, Appl. Surf. Sci. 619 (2023) 156776.

S. Oswald, M.V. Gorbunov, D. Mikhailova, Electron spectroscopy investigations of potassium and potassium-intercalated graphite with battery background, Appl. Surf. Sci. 655 (2024) 159614.

P52 - Improvement of magnetic domain structures and magnetic properties of GO FeSi steels by laser surface treatment

11. NRG – Energy, Environment, Geology and Heritage

Ivan Petryshynets[1]
František Kovač[1], Ladislav Falat[1], Ján Füzer[2], Marcela Motýľová[1]
[1] Institute of Materials Research, Slovak Academy of Sciences, Watsonova 47, 04 001 Košice, Slovakia
[2] Institute of Physics, Faculty of Science, P.J. Safarik University, Park Angelinum 9, Kosice 041 54, Slovakia

The FeSi grain oriented (GO) steels are iron - 3% silicon alloys developed with a strong also called the Goss – type texture to provide very low core losses and high permeability in the rolling direction. These steels are predominantly employed for the transformers with high efficiency. With an additional surface treatment after the rolling process, it is possible to improve the magnetic properties of the core material, especially the core losses. At the same time, it is well known that laser radiation influence on domain structure with subsequent decrease of specific power losses.

In the present work the influence of pulse and continuous laser treatment technique on the magnetic domains modification with positive impact on the final magnetic properties of grain-oriented electro-technical steel has been investigated. The conventional GO steel with silicon content 3 % wt, taken from industrial line after final heat treatment, was chosen as an experimental material. The laser scribing at pulse and continuous processing conditions was applied on the material surface in order to induce thermal stresses, which influence on the modification of the internal structure of magnetic domains. The final domain structures were optimized in relation to the minimization of magnetic losses of the experimental material and to the optimization of thermal stresses application on the surface. The magneto-optical Kerr effect was employed to obtain a visible contrast between antiparallel domains. The domain structures showed that domain-walls positions did not repeat precisely from cycle to cycle, particularly at high inductions, and that the average domain-wall spacing decreased with increasing density of laser scribing lines. Also, the samples were subjected to magnetic measurements as well as nano-hardness and EBSD analysis of heat affected zone before and after laser processing. Clear improvements in final magnetic characteristics were observed for all the regimes using the power density of the laser beam up to 24W. A semi quantitative relationship has been found between the domain patterns and the used fiber laser treating method. The magnetic properties of the experimental samples were measured in DC and AC (50Hz) magnetic field. The obtained modified domain structure led to a significant decrease in coercivity measured in DC magnetic field from 20 A/m to 12 A/m.

This work was carried out within the research projects under contract No. APVV-18-0207, APVV-21-0418, and VEGA 2/0092/24.

P53 - Manufacturer discrepancies in potassium metal: Impact on battery performance and detection of sodium traces

11. NRG – Energy, Environment, Geology and Heritage

Leonie Wildersinn[1]
Fabian Jeschull[1]
[1] Institute for Applied Materials, Karlsruhe Institute of Technology (KIT), Hermann-von-Helmholtz-Platz 1, 76344 Eggenstein-Leopoldshafen, Germany

Potassium-ion batteries (PIBs) have emerged as promising candidates for low-cost, high-energy storage systems, driven by their fast ionic conductivity and high operating voltage. To develop high energy and high power PIBs, the performance is often first evaluated in half-cell tests using the highly reactive K metal as anode that often leads to misinterpretation of the results because degradation processes between metal anode and electrolyte components are often neglected. However, the influence of impurities in potassium metal, on the performance remains a critical area requiring investigation. This study investigates the impact of different potassium grades used as negative electrode, on metallurgy softness and overall battery performance in half-cell tests. Using sputter depth profiling X-ray Photoelectron Spectroscopy (XPS) we were able to identify sodium impurities as a major source for different aging behaviors. This discovery is crucial, as these sodium impurities significantly influence the battery performance. This insight informs ongoing research, where the primary challenge lies in scrutinizing the interpretation of aging mechanisms outlined in existing literature, such as the varying aging patterns observed in graphite. This finding highlights the crucial role of analytical methods such as XPS in detecting subtle variations in potassium metals that affect PIB results.

P54 - Probing the solid electrolyte interphases in modified hard carbon-based negative electrodes for sodium ion batteries

11. NRG – Energy, Environment, Geology and Heritage

Sergio Aina[1]
Blaz Tratnik[2, 3], Alen Vizintin[2], **Elena Tchernychova**[2], M. Pilar Lobera[1, 4], María Bernechea[1, 4, 5], Robert Dominko[2, 3]
[1] Instituto de Nanociencia y Materiales de Aragón (INMA) CSIC-Universidad de Zaragoza, Department of Chemical and Environmental Engineering, University of Zaragoza, Campus Río Ebro-Edificio I+D, C/ Mariano Esquillor S/N, 50018 Zaragoza, Spain
[2] National Institute of Chemistry (NIC), Hajdrihova 19, SI 1001, Ljubljana, Slovenia
[3] Faculty of Chemistry and Chemical Technology, University of Ljubljana, Večna pot 113, 1000, Ljubljana, Slovenia
[4] ARAID, Government of Aragon, 50018, Zaragoza, Spain
[5] Centro de Investigación Biomédica en Red de Bioingeniería, Biomateriales y Nanomedicina, Instituto de Salud Carlos III, 50018, Zaragoza, Spain

Upon sodium ion battery (SIB) cycling, solid-electrolyte interphases (SEI) are formed on top of the active electrode's material. These interphases are crucial for enhancing battery performance by ensuring stable and efficient ion exchange between the electrode and electrolyte. Hard carbon (HC) materials stand out as the predominant choice for negative electrodes in SIBs, yet they are affected by notable drawbacks, including diminished initial coulombic efficiency (ICE), inadequate rate performance, and low stability. To address these challenges, the surface of the corn cob-derived hard carbon (HC) materials has been modified utilizing short-chain organic compounds: two that incorporate -SH groups, 3-mercaptopropionic acid (MPA), 1,2-ethanedithiol (EDT), and an oxalic acid (OxA). Prepared electrodes were electrochemically cycled to probe the changes in functional properties and compared to the pristine HC material. *Ex situ* X-ray photoelectron spectroscopy (XPS) analysis following the initial discharge-charge cycle was employed to identify and quantify of the key species constituting the SEI formed on the HC electrode's surface. EDT and MPA treatments, which incorporate -SH groups, lead to increased Na_x-HC content linked to a thinner SEI and reduced -CO_3^{-2}- levels, enhancing ionic conductivity. Conversely, treatments with -COOH group ligands such as OxA increase -CO_3^{-2}- formation, potentially impairing performance. Analysis of O *1s* spectra revealed more Na_2O in MPA and EDT treated samples (14.2% and 10.9% atomic, respectively) compared to pristine HC (9.1%), indicating enhanced stability and Na^+ conductivity. OxA treated sample showed similar but lower Na_2O levels (8.2%) than HC, correlating with its reduced performance. Analysis of F *1s* spectra showed an increased amount of NaF content in all treated samples compared to that identified for HC. Here, thiol containing molecules seem to promote higher content of NaF in MPA- and EDT-treated materials. This in its turn leads to the formation of SEI that is more beneficial in terms of Na^+ ions diffusion and batteries capacity retention.

P55 - Shielding surface for cathode material protection in lithium-ion batteries: Atomic layer fluorination

11. NRG – Energy, Environment, Geology and Heritage

Delphine Flahaut[1, 2]
Hani Fahrat[1, 2], Oumaima Hatim[3], Marc Dubois[4], Lucille Gall[5], Benoit Mortemard[5], Jean-Bernard Ledeuil[1, 2], Dominique Foix[1, 2], Nicolas Louvain[3], Katia Guérin[4]
[1] University of Pau & Pays Adour/E2S UPPA, IPREM UMR 5254, 64000 Pau, France
[2] Electrochemical Energy Storage Network (RS2E) CNRS 3459, F-80039, Amiens cedex, France
[3] Institute Charles Gerhardt Montpellier1919 Rte de Mende, 34293 Montpellier, France
[4] University Clermont Auvergne, CNRS, ICCF F-63000 Clermont–Ferrand, France
[5] Battery company SAFT33074 Bordeaux cedex, France

High-voltage spinel LNMO ($LiNi_{0.5}Mn_{1.5}O_4$) has attracted widespread attention as a promising cathode material for the next generation LIBs[1] due to its numerous advantages such as a 3D spinel structure that improves the flow of lithium ions with open Li^+ sites[2], high operating voltage (~4.7 V vs. Li/Li^+), and energy density[3], with a theoretical capacity of 147 $mAh.g^{-1}$. However, this material faces significant challenges due to electrolyte decomposition and concurrent side degradation reactions at the electrode/electrolyte interfaces. Capacity fading in LNMO/graphite full cells occurs as a result of active Li^+ loss, which has been suggested to be linked to the Mn dissolution problem. Moreover, the Mn^{2+}/Mn^{3+} and Ni^{2+} cations migrate towards the anode, causing detrimental effects on the solid-electrolyte interphase and depleting available Li^+ ions, resulting in the rapid deterioration of battery performance.

Many studies report different way to manage the electrolyte degradations reactions by designing the particles morphology and composition[4]. The ALF method is a fluorination process based on the use of atomic fluorine radicals to modify the surface of materials in a single step at room temperature, and has been successfully applied to negative and positive electrode materials[5] to improve their electrochemical properties.

This study focuses on the surface modification of disordered LNMO using the ALF method, with xenon difluoride as a fluorination agent. Characterization techniques such as XPS, AES, NMR, and SEM confirm the successful fluorination and validate the structural and compositional integrity of the material. Electrochemical tests reveal significant improvements in the battery performance of fluorinated LNMO, including enhanced rate capability and cycling stability. Based on surface characterization probes as X-ray and Auger electron spectroscopies, we highlight the formation of a shell-like fluorinated layer "Li-F" surrounding the LNMO aggregates associated to a reduction of the Mn atom and formation of oxyfluorine species. Surface reactivity of the fluorinated LNMO has been compared to a non-fluorinated LNMO electrode. Under cycling, the ALF method clearly modulates the surface reactivity of the electrode despite a self-consumption-reconstruction of the protection layer.

The results suggest that ALF surface modification, in conjunction with appropriate electrolyte additives, holds promise for optimizing the electrochemical performance of LNMO positive electrodes in lithium-ion batteries, offering potential applications in next-generation energy storage systems.

Selected references

(1) G. Ganas, G. Kastrinaki, D. Zarvalis, G. Karagiannakis, A.G. Konstandopoulos, Mater. Today Proc. 5 2018 27416.
(2) H. Xu, H. Zhang, J. Ma, G. Xu, T. Dong, J. Chen, G. Cui, ACS Energy Lett. 4 2019 2871.
(3) G. Liang, V.K. Peterson, K.W. See, Z. Guo, W.K. Pang, J. Mater. Chem. A. 8 2020 15373.
(4) A. Soloy, D. Flahaut, J.-B. Ledeuil, J. Allouche, D. Foix, G. Salvato Vallverdu, E. Suard, E. Dumont, L. Gal, F. Weill, L. Croguennec, Appl. Energy Mater., 2022, 5 (7) 8669-8685.
(5) Y. Charles-Blin, D. Flahaut, J.-B. Ledeuil, K. Guerin, M. Dubois, M. Deschamps, A.-M. Perbost, L. Monconduit, H. Martinez, N. Louvain, ACS Appl. Energy Mater. 2019, 2, 9, 6681-6692.

P56 - Understanding the surface chemistry of tin halide perovskite thin films

11. NRG – Energy, Environment, Geology and Heritage

Antonella Treglia[1, 2]
Mirko Prato[3], Chun-Sheng Wu[1, 2], E Laine Wong[1], Isabella Poli[4], Annamaria Petrozza[1]
[1] Center for Nano Science and Technology @Polimi, Istituto Italiano di Tecnologia; Milan, Italy
[2] Physics Department, Politecnico di Milano, Piazza L. da Vinci, 32, 20133 Milano, Italy
[3] Materials Characterization Facility, Istituto Italiano di Tecnologia; Via Morego 30, 16163 Genova, Italy
[4] Center for Sustainable Future Technologies @Polito, Istituto Italiano di Tecnologia, Via Livorno, 60, Turin, 10144 Italy

We investigate the role of tin fluoride in defining the complex surface chemistry of tin halide perovskite thin films, prepared via solution processing. We show that oxygen is found on the surface of tin perovskite thin films even if never exposed to ambient air; however, the use of SnF_2 in the precursors solution strongly affects the chemical nature of the found species. Indeed, oxygen primarily binds to tin in the form of SnO_2 only when SnF_2 is added to the precursor solution, while it is mainly due to adventitiuos species when SnF_2 is not used. We therefore highlight that the presence of a predominant single chemical state in the XPS Sn core level does not necessarily correspond only to Sn^{2+} species in the perovskite form but could also indicate the formation of superficial SnO_2. Thanks to spatial mapping of both the local chemical environment and surface photoluminescence, we show that pristine films have higher accumulation of I_2 at the grain boundaries while the addition of SnF_2 allows preserving the perovskite phase and reducing chemical and optical heterogeneities. Finally, we show that SnF_2 does not help in avoiding nor slowing down the degradation of the perovskite film when exposed to ambient air and that oxidation occurs on the whole grain surface. These results provide insightful guidance towards understanding oxidation in tin halide perovskites and elucidate its detrimental effect on material's properties.

12. POL – Polymers

P57 - Controlled tunning of the wettability of aromatic polymers by precise dosing of oxygen atoms

12. POL – Polymers

Alenka Vesel[1]
Rok Zaplotnik[1], Gregor Primc[1], Miran Mozetic[1]
[1] Jozef Stefan Institute, Ljubljana, Slovenia

The wettability of polymers must be just right tuned to ensure the appropriate spreading of liquids and to enable the required adhesion of coatings. A standard ecologically benign method for increasing the polymer wettability is a treatment with a non-equilibrium plasma rich in reactive oxygen species. The basic laws of the evolution of the kinetics of surface wettability of selected aromatic polymers (polystyrene, polyethylene terephthalate, polyetheretherketone, and polyphenylene sulphide) were investigated by exposing polymers to various precisely dosed fluxes of oxygen atoms and measuring the water contact angle (WCA). The O-atom fluxes were varied between $3x10^{20}$ and $1x10^{23}$ $m^{-2}s^{-1}$, and the treatment time was varied between 0.01 and 1000 s. It was found that the kinetics of the evolution of the WCA versus the O-atom fluence (i.e., a product of the O-atom flux and treatment time) for all aromatic polymers followed the same curve. This was not the case if WCA was plotted versus treatment time for various O-atom fluxes. Results clearly show that the most important parameter governing the wettability is the fluence and not treatment time as often reported in the literature. By knowing the general correlation between fluence and WCA, one can foresee the appropriate plasma parameters to achieve the desired wettability for aromatic polymers. The statistically significant decrease of the WCA from the original value of untreated polymers was observed after the fluence of approximately 10^{21} m^{-2}. The WCA stabilized below 20° after the fluence of 10^{23} m^{-2}. The experimental results were interpreted in terms of the available theoretical models of the interaction between oxygen atoms and aromatic polymers.

P58 - In-situ spectroscopic analysis of thin organosilicon plasma film deposition on polylactide substrates

12. POL – Polymers

Sandra Gołębiowska[1]
Hendrik Müller[1], Guido Grundmeier[1]
[1] Technical and Macromolecular Chemistry, Paderborn University, Paderborn, Germany

Polylactide (PLA) is an excellent candidate to replace the conventional, petroleum-based plastics for packaging applications, due to its biodegradable characteristics and small carbon footprint. However, PLA has limited gas barrier properties and therefore enhancing its barrier properties is essential for the use in food packaging. A combination of SiO_x barrier films and thin SiOCH interfacial adhesion layers have been shown to improve the barrier properties of PET and PP substrates. [1, 2] In this work we address the deposition of such thin films on PLA substrates using in-situ polarisation modulation FTIR spectroscopy under grazing incidence (PM-IRRAS).

PLA thin films were deposited on Au coated substrates via spin-coating. Hexamethyldisiloxane was used as precursor gas for the plasma enhanced chemical vapour deposition of ultra-thin SiO_x or SiOCH films in a vacuum chamber with optical windows allowing real time in-situ PM-IRRAS measurements during surface activation and film growth. [3] Relevant surfaces were characterised ex-situ using X-ray photoelectron spectroscopy (XPS). As an example, real-time spectroscopic data of the SiO_x film growth on PLA in combination with the illustration of the in-situ spectroscopic cell are shown in Figure 1. During the SiO_x deposition, a slight shift in the peak maximum could be noticed and attributed to an increasing crosslink density with increasing film thickness. In addition, plasma etching of the PLA coating was recorded during early stages of the deposition process.

The in-situ spectroscopic studies were further complemented by AFM analysis of film nucleation and growth. Deposited films showed promising barrier properties which could be correlated to the film structure.

Selected references

[1] T. de los Arcos, P. Awakowicz, J. Benedikt, B. Biskup, M. Böke, N. Boysen, R. Buschhaus, R. Dahlmann, A. Devi, T. Gergs, J. Jenderny, A. von Keudell, T.D. Kühne, S. Kusmierz, H. Müller, T. Mussenbrock, J. Trieschmann, D. Zanders, F. Zysk, G. Grundmeier, *Plasma Processes & Polymers* **21** (2024).
[2] F. Mitschker, L. Schücke, C. Hoppe, M. Jaritz, R. Dahlmann, T. de los Arcos, C. Hopmann, G. Grundmeier, P. Awakowicz, *J. Phys. D: Appl. Phys.* **51**, 235201 (2018).
[3] M. Maxisch, P. Thissen, M. Giza, G. Grundmeier, *Langmuir the ACS journal of surfaces and colloids* **27**, 6042 (2011).

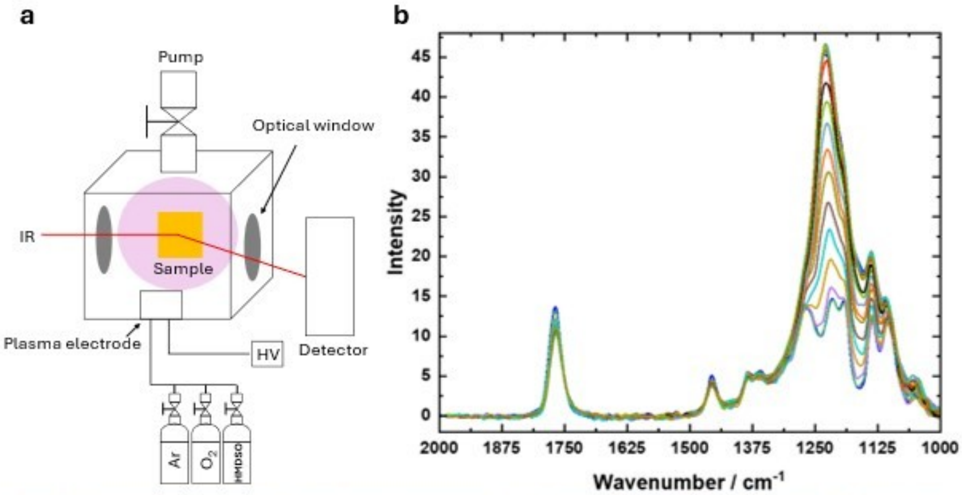

Figure 1. (a) Schematic illustration of the in-situ spectroscopic cell. (b) In-situ real time PM-IRRAS data of the SiO$_x$ film growth on PLA.

P59 - Revealing surface functionalities of micro- and nanoplastic particles' surface by means of XPS

12. POL – Polymers

Dmitri Ciornii[1]
Jörg Radnik[1], Xenia Knigge[1], Vasile-Dan Hodoroaba[1], Andreas Thünemann[1], Roland Drexel[2], Marta Fadda[3], Alessio Sacco[3], Andrea Mario Giovannozzi[3], Korinna Altmann[1]
[1] Bundesanstalt für Materialforschung und -prüfung (BAM), Berlin, Germany
[2] Postnova Analytics GmbH, Landsberg am Lech, Germany
[3] Quantum Metrology and Nanotechnology Division, Istituto Nazionale di Ricerca Metrologica (INRiM), Torino, Itally

Over the last 20 years, many researchers, politicians, and citizens themselves have become increasingly aware of the growing plastic problem of our time. Inadequate recycling concepts, collection points, and careless dumping of plastic products in the environment lead to an accumulation of plastic. External weather influences can cause these to degrade and fractionate, so that today microplastics (1-1000 µm, ISO/TR 21960:2020) [1] of different polymer materials can be detected in all parts of the world.

The precautionary principle applies to microplastics. The particles can break down further to form nanoplastics (<1 µm, ISO/TR 21960:2020) [1]. Whether microplastics or nanoplastics pose a toxicological hazard is being investigated in a variety of ways. Valid results are still pending, however, investigations into the frequency, transport, possible sinks and entry paths must be taken into account. This is why monitoring of microplastics is already required in the revision of the Drinking Water Framework Directive [2]. The same is still pending in the final version of the revision of the Waste Water Framework Directive this year, but is expected.

Nanoplastics are particularly under discussion for having a toxic effect on humans and animals, as these particles are small enough to be absorbed by cells. For targeted toxicological studies, it is important to have test and reference materials that resemble the particles found in the environment. To mimic environmental samples, these materials should also have an irregular shape and show aging at the surface, which can be detected with XPS or SEM/EDS.

BAM in collaboration with the EMPIR project "PlasticTrace" works on a reference material candidate of nano-sized polypropylene (nano-PP) [3]. The nano-PP vials were tested for homogeneity with PTA and further characterized with bulk and surface-sensitive techniques. An SEM image and a corresponding XPS spectrum are presented in Figure 1. Raman measurements as well as XPS indicate an aged surface.

Acknowledgement - The authors thank the PlasticsFatE and POLYRISK Project and European Union's Horizon 2020 Research and Innovation programme for funding from the European Union's Horizon 2020 Research and Innovation programme, under the Grant Agreement number 965367 and 964766. We also acknowledge PlasticTrace Project founded by Euromat/EMPIR under the Grant Agreement number 21GRD07.

Selected references

[1] ISO/TR 21960:2020, Plastics — Environmental aspects — State of knowledge and methodologies (ISO/TR 21960:2020).
[2] https://eur-lex.europa.eu/resource.html?uri=cellar:5c835afb-2ec6-4577-bdf8-756d3d694eeb.0003.02/DOC_1&format=PDF

[3] Hildebrandt, J., Thünemann, A. F., Aqueous Dispersions of Polypropylene: Toward Reference Materials for Characterizing Nanoplastics. Macromol. Rapid Commun. 2023, 44, 2200874. https://doi.org/ 10.1002/marc.202200874

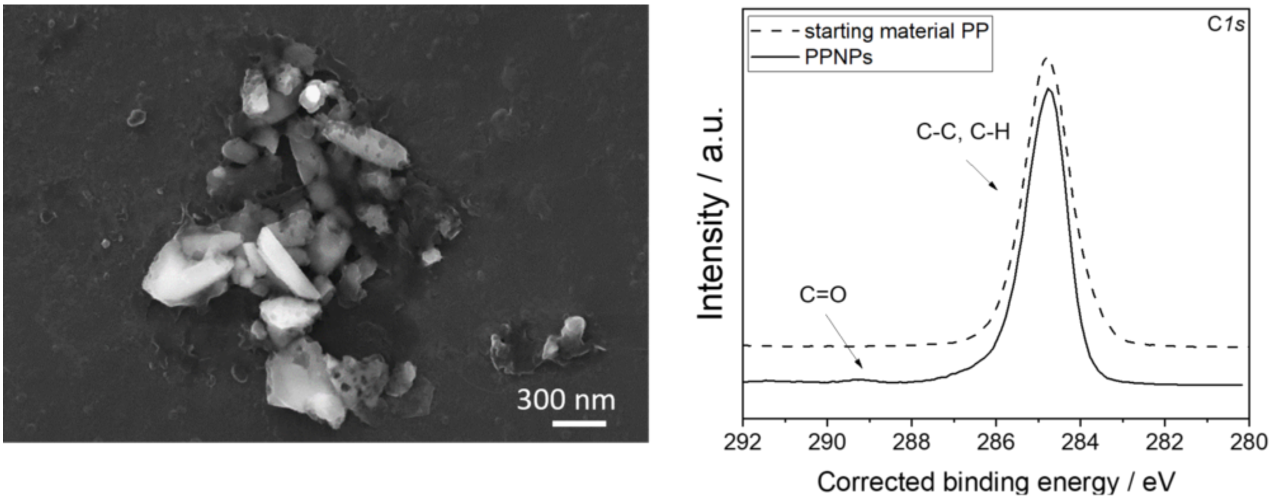

Figure 1: SEM image and XPS spectra of nano-PP as close-to-reality test material

13. TEC – Technical Development and New Instrumentation

P60 - Behavior of aniline molecules in the strong electric field by thermal ionization method

13. TEC – Technical Development and New Instrumentation

Dilshadbek Usmanov[1]
Azim Radjabov[1], Shovkatjon Akhunov[1]
[1] Arifov Institute of Ion-Plasma and Laser Technologies, Uzbekistan Academy of Sciences, Durmon Yoli Street 33, 100125, Tashkent, Uzbekistan

Studying the interactions of molecular particles with solid surfaces is not only of fundamental importance but also crucial for the advancement of various fields such as biotechnology, nanotechnology, heterogeneous catalysis, and gas analytical instrumentation. Consequently, the development of ionization methods, particularly mass spectrometric techniques, holds significant importance in this field.

Thermal or surface ionization (SI) is one of the most informative among many methods for determining the characteristics of the interaction of polyatomic particles with a solid. An important feature of the SI method is the information obtained in the region of high temperatures of the adsorbate, which is difficult to access for other methods. Therefore, the use of SI analysis methods for the study of organic, bioorganic and inorganic compounds will provide the necessary information both on the physicochemical properties of ionizing particles and the ionizing surface, and on the characteristics of their interaction with the surface of a solid.Thermal desorption of polyatomic ions of organic compounds was discovered relatively recently [1]. The method has a high selectivity to the ionization potential of the substances. For example, if the ionization potentials of two compounds differ by 1 eV, their ionization efficiency by surface ionization can differ up to 10^5 times.

In this work, the ionization of aniline molecules in a strong electric field was experimentally studied using the method of surface ionization mass spectrometry in order to reveal the patterns of SI of these molecules.

The experiments were conducted using a serial isotope mass spectrometer MI-1201B, for which the SI ion source underwent modernization to fit the experimental tasks.

The process of thermal ionization of organic molecules involves heterogeneous chemical reactions of molecules adsorbed on the surface of a heated SI emitter through various channels, along with the desorption of chemical reaction products and molecules that have not undergone this process. Initial calculations suggest that a strong electric field can exert influence at each stage of these processes and can be controlled by adjusting the electric field voltage applied to the emitter. Mass spectra and temperature dependencies of aniline ionic currents were obtained at a strong electric field intensity of $E \geq 10^7$ V/sm. Preliminary results indicate that the process of formation and ionization of sample particles is indeed influenced by a strong electric field.

Acknowledgement: This work was supported by the Innovative Development Agency (project IL-5421101794)

Selected references

[1] U.Kh. Rasulev, E.Ya. Zandberg. *Prog Surf Sci.* 28, 3/4 (1988), 181-412.

P61 - Optical Surface Roughness Estimation using Artificial Intelligence Classification

13. TEC – Technical Development and New Instrumentation

Jacob Maxa[1]
Mathias Nowottnick[1]
[1] Rostock University

The use of wind turbines is a core component within Europe's current energy policy. Especially offshore use places high demands on the materials used in terms of stability, service life and processing. Various protective coatings are applied to steel monopiles to prevent corrosion and thus wear of the material. An optimally cleaned and roughened surface is a prerequisite for a well adhering and sealed coating. In the process which is used here, this is produced by blasting with abrasive particles such as corundum.

The following publication presents a system for automatic optical non-contact in-situ analysis of blasted surfaces. The basis of the measuring system is an optical laser triangulation scanner, which was mounted on a precision linear stage (XYZ) on a laboratory scale. This scanner projects a laser line onto the surface to be scanned which, depending on the surface structure, reflects onto a CMOS sensor located at a defined angle. The CMOS sensor calculates the height from this and provides a height profile. In combination with the coordinates of the linear stage, a 3D point cloud is generated.

This data is now processed and analyzed in a specially developed control software and various roughness parameters for lines and planes are calculated. This data serves as the basis for the next process step.

The surface, that the scanner has analyzed, is captured in parallel using a color CMOS camera and correlated with the point cloud in the software. In the next step, an AI model was created and trained using the training data obtained by measuring different prepared surface samples. In the first step, a classic machine learning classifier was created and trained. The overall image of the test surface is split into tiles and a good/bad classification is carried out for each. A good surface is characterized by a uniform reflection pattern or a uniformly chaotic structure. Any imperfections in the blasting process can be represented by existing rust spots or shiny surfaces with little or no reflection. If such a tile is identified as faulty, the AI model recognizes it and marks it for subsequent reworking.

Another current development is the implementation of a CNN (Convolutional Neural Network) for the direct estimation of roughness values from the recorded camera images of the training data. The complete setup is planned to be implemented into an automatic blasting system for large-scale metal structures with an automated detection of defects.

P62 – Surface investigation of Layered Double Hydroxides Grown on the Biodegradable AZ 31 alloy

13. TEC – Technical Development and New Instrumentation

S. Kaciulis[1], **A. Mezzi**[1], R. Montanari[2], R. Narducci[2], A. Palombi[2], M. Richetta[2], A. Varone[2]
[1]ISMN-CNR, PO Box 10, 00015 Monterotondo Stazione, Roma, Italy
[2]Departemnt of Industrial Engineering, University of Rome Tor Vergata, 2Departemnt of Industrial Engineering, University of Rome Tor Vergata

AZ 31 is a biodegradable magnesium alloy for biomedical applications. In orthopaedics, it is adopted for temporary implants thanks to its biocompatibility, osseointegration, and elastic modulus comparable to that of human bone. Furthermore, Mg is essential for the metabolism in biological mechanisms and AZ31 contains a reduced amount of Al. The main drawback is quick degradation in bio-fluids. Corrosive processes lead to a reduction of mechanical properties, compromising its functionality. The growth of LDHs (Layered Double Hydroxides) on alloy surface delays corrosion and also allows to incorporate drugs which can be released in-situ from the implant with local anti-inflammatory, analgesic, and antimicrobial action. This work is aimed to establish the optimal conditions for LDHs growth on the surface of AZ31 alloy and to characterize the coatings.

A

Abdel-Mageed, Ali M.	P9
Abel, Marie-Laure	**O98**
Abram, Sarah-Luise	P38
Acebedo, Begoña	O108
Adriaensens, Peter	O15, P7
Adriano, Luigi	O124
Aggarwal, Garima	O101
Agudo Jácome, Leonardo	P42
Ahlswede, Erik	O100
Aichinger, Laura	O74
Aina, Sergio	P54
Akbari, Elahe	**P28**
Akhunov, Shovkatjon	P60
AL KATRIB, Mirella	O45
Albrecht, Tim	P42
Alexandre, Patrice	P19
Allansson, Dick	**P30**
Altmann, Korinna	P59
Alvarado, Carlos	O72
Alvarado-Chavarin, Carlos	O75
Ameloot, Rob	P7
An, Rui	O15
Anand, Kanika	P19
Anilkumar, Vishnu	**P46**
Aqeel, Muhammad	P2
Arimitsu, Masahiro	O117
Arkhipushkin, Ivan	**O124**
Arlinghaus, Henrik	O88
Artyushkova, Kateryna	O20, **O42**, O111, P22, P23
Aubrecht, Petr	P11
Ayouz-Chebout, KATIA	O105

B

Bacon, Simon	O63, O64
Baer, Donald	**K4**, **P21**

Baert, Kitty	O15, O58
Baker, Mark	O63, **O64**
Bancheva, Pavlina	O32
Barba, A.	P16
Barba, Arturo	O8, O97, P17
Barbieri, Giuseppe	P47
Barnana, Dinesh	O1, P5
Barnes, Jean-Paul	O82, O89, P25
Bartling, Stephan	**P9**
Batenkova, Anastasia	**O24**
Batyrev, Erdni	**O23**
Bayer, Bernhard Christian	O74
Bazhenov, Vasilii	O124
Bañuelos, Jose	O8, P17
BECHU, Solene	**O49**
Beentjes, Peter	O23
Bellani, Vittorio	P34
Bellew, Allen	O89
Belu, Anna	O89
BENAYAD, Anass	**O99**
Benedetti, Stefania	P34
Bennet, Francesca	**O89**
Benz, Sebastian Leonard	**O113**
Bernechea, María	P54
Bernier, Nicolas	O79
BEROUAKEN, Malika	O105
Berthelemy, Nadine	P19
Bertinetti, Daniela	O10
Bhatt, Prajna	**P20**
Biderman, Norbert	O42
BIDEUX, Luc	O40, O86
Biesinger, Mark	**PS3**, **O91**
Biggio, Deborah	**P18**, P35
Birolini, Giulia	P6
Biscarrat, Jérôme	P36
Biswas, Indro	**O107**
BLAIZOT, Alexandre	O45

Blenkinsopp, Paul	O69
Blockhuys, Frank	O15
Boev, Victor	O31
Boily, Jean-François	O102
Bolli, Eleonora	P45
Bomnuter, Jan	O21
Borgschulte, Andreas	O19
BOUDEFAR, Fatima	O105
Bouttemy, Muriel	O36, **O45**, O104
Bozhanova, Nevena	O31
Breitenstein, Daniel	O73
Breugelmans, Tom	O21
Brezesinski, Torsten	O113
Brockhauser, Sandor	O43
Brown-Tseng, Elizabeth	O58
Brundu, Laura	O114
Bucher, Guillaume	O12
Buchkov, Krastyo	P44
BURE, Taylor Rose	P31
Bushell, Adam	O64
Butan, Daniela	P5
Butorin, Sergei	O101
Bábík, Pavel	O14
Béchu, Solène	O36, O104
Bütefisch, Sebastian	O83

C

Cabello, Marta	O108
CACOVICH, Stéfania	O45
Cadot, Stéphane	O79
Caldes, Maria	O33
Calvo-Barrio, Lorenzo	**O106**
Camayang, John Carl	O17
Cancellieri, Claudia	**O57**, O60, P15
Cao, Yu	**O93**, P13, P46
Cappel, Ute	**PS1**
Cappel, Ute B.	O109
Carlos, Emanuel	O30

Carlsson, Per-Anders	O44
Carteret, Cédric	O61
Casula, Giulio	**O114**
Cattaneo, Elena	P6
Cavaco, Afonso	O30
Caño-Prades, Iván	O106
ceccone, giacomo	O9, O12, O89, P6
Chandler, Charlie	**O63**
Chang, Hsun-Yun	**O34**
Chapon, Patrick	**O68**
Chaudhary, Varun	P48
Chemello, Giovanni	O22
CHERIET, Abdelhak	O105
Cid, Rosalía	**O108**
Ciornii, Dmitri	P59
Claessens, Raf	O123
Claesson, Per M.	O71
Clifford, Charles A.	O22
Clingerman, Daniel	O58
Cluzel, Xavier	O23
Coetsee-Hugo, Elizabeth	O27
Cognini, Francesco	P47
Coletti, Camilla	P34
Colin, Marius	O13
Comparotto, Corrado	O101
CONARD, Thierry	P31
Cool, Pegie	O21
Cornette, Pauline	O7
Costa, Dominique	O7
Counsell, Jonathan	O38, O55
Counsell, Jonathan D. P.	O116
Counter, James	O122
Craighero, Mariavittoria	O44
Cristaudo, Vanina	O21, **O58**
cubadda, francesco	O9
Cuong, Vuong Van	O119

D

Dahlin, Andreas	**O11**
DALLY, Pia	O45
Davies, Philip R	O26
DE AVELAR FRANCISCO, Giorgio Fernando	**O6**
de la Fuente, Beatriz	**O21**
de Vito, Eric	O89
DeBeer, Serena	O17
del Moro, Michele	O21
Delcorte, Arnaud	O62, O89
Delmas, Elisa	O124
Demontis, Valeria	P34
Denecke, Reinhard	P24, P26, P27
Derk, Rading	O88
Derveaux, Elien	P7
Deshpande, Rucha	**O28**
Deuermeier, Jonas	**O30**
Devadasan, Dhilan	O63
di Bona, Alessandro	P34
Dias, António	O30
Dietrich, Paul	**O39**
Dimitrov, Dimitre	**O54**, P44
Dimovska Nilsson, Kelly	O5
Dimper, Matthias	O18
Dimtrov, Dimitre	O51
Dobener, Florian	O43
Dominko, Robert	P54
Donskyi, Ievgen	P39
Dražič, Goran	P10
Drev, Sandra	P10
Drexel, Roland	P59
Driessen, Frank	O55
Dubois, Marc	P55
Duchoslav, Jiri	O66, **O77**, O95
Duchoslav, Jiří	O59
Dupont, Christine	O62
Durand, Pierrick	O61
Duskey, Jason T.	P6

Dussaigne, Amélie O79
Dzierzega, Marcin P3

E

Eder, Dominik O74
Ekar, Jernej **O46**
El-Kirat-Chatel, Sofiane O61
Elsener, Bernard O114
Elsener, Bernhard P18, P35
Engelhard, Mark P21
Ernstsson, Marie O53, **O71**
ETCHEBERRY, Arnaud O45, O70, O104
Evans, Tim P20

F

Fabian Jeschull, Fabian O103
Fadda, Marta P59
Fahrat, Hani P55
Fahrnberger, Florian O74
Fairley, Neal O33, O49
Falat, Ladislav P52
Fallarino, Lorenzo O108
Faller, Joachim P29
Fantauzzi, Marzia O114, P18, P35
Fantin, Roberto O99
Fava, Alessandra P47, P49
Fernandez Velasco, Leticia O15
Fernandez, Vincent **O33**
Fernando, Nathalie P20
Ferrand Drake del Castillo, Gustav O11
Ferrer, Pilar O122
Fickl, Bernhard O74
Finšgar, Matjaž P33
Fisher, Gregory O118
Fitl, Premysl O80
Flahaut, Delphine **P55**
Flege, Jan Ingo O72, O75
Fletcher, John O4, **O5**

Foelske, Annette O74, P41
Fogarassy, Zsolt O56
Foix, Dominique P55
Fontaine, Julien O2
Forti, Stiven P34
Fourie, Antonie Johannes P32
Franquet, Alexis O89
Fransson, Alfred O4
Fregnaux, Mathieu O70
Friedlmeier, Theresa O100
Fu, Chongwei O94
Fumagalli, Francesco **O9**, **O12**, O89, **P6**
Fuscaldo, Walter O54
Füzer, Ján P52

G

GABOUZE, Noureddine O105
Gaffar, Kirène **O36**
GAGLIARDI, Anna O49, **O104**
Gahlawat, Soniya P28
Gaiardo, Andrea P8
Galcerán, Montse O108
GALIPAUD, Jules **O2**
Gall, Lucille P55
Gambacorti, Narciso O81
Garcia, Jaime O97
García-Fernandez, Alberto O109
Gardes, Emmanuel O86
Gassilloud, Rémy O79
Gauthier, Nicolas **O79**, P22, P23, **P25**
Gauthy, Fernand O123
Ghasemitabesh, Rezvaneh O10
Ghoreishi, Narges O89
Gianesello, Frédéric O79
Gil-Rostra, Jorge O19, O67
Gilliland, Douglas O89
Gilmore, Ian **AS1**
Giovannozzi, Andrea Mario P59

Goikolea, Eider O108
Gomez, Karla O8
Gonzalez-Elipe, Agustin R. O19
Gonzalo, Elena O108
González, Ramón O67
González-Alva, Patricia O8
González-Elipe, Agustín R O67
González-Parra, J. Rafael **P16**
González-Parra, Rafael **O8**, **O97**, **P17**
Gonçalves, Anne-Marie O70
Good, Kevin O47, O48
Gorbunov, M. P51
Gouder, Thomas O25
Gołębiowska, Sandra **P58**
Gramatte, Simon O60
Grant, Melissa P42
Gregan, Tomas O74
Grill, Stephan **PS2**
Grinter, David C. O122
Groiss, Heiko O59, O95
Grundmeier, Guido P58
Grönbeck, Henrik O29
Guan, Shaoliang **O26**
Gucciardi, Emanuele O108
Guillemin, Sophie P36
GUILLEMOLES, Jean-François O45, O104
Guruprasad Engoor, Gimmi **O3**
Gustafson, Johan O44
Guyot, Claire O82
Guérin, Katia P55
Gys, Nick **O15**, P7
Gökce, Bilal O96

H

Habibimarkani, Heydar P38
Habler, Gerlinde O74
Hafiez, Mahmoud A. O101
Hagenhoff, Birgit O37, O73

Hanisch, Jonas	O100
Hannachi, Raouaa	**P35**
Hantusch, M.	**P51**
Hantusch, Martin	**O16**
Haq, Ehtsham-Ul	**O1**, O87
Haq, Ehtsham-Ul Haq	P5
Hatim, Oumaima	P55
Hauffman, Tom	O15, O21, O52, O58, P7
Havranek, Vladimir	P37
Heintz, Olivier	O104
Held, Georg	**O122**
Heller-Krippendorf, Danica	**O37**, **O73**
Hemetsberger, Jakob	P41
Hempel, Wolfram	**O100**
Henkel, Karsten	O72, O75
Henß, Anja	O112
Herberg, Friedrich W.	O10
Hernandez, M.	P16
Hernandez, Miguel	O97
Hernandez-Gallegos, Miguel	O8, P17
Hertle, Jonas	O113
Hesse, René	P42
Hesse, Ronald	**P24**, **P26**, **P27**
Hetaba, Walid	O43
Himmerlich, Marcel	**O125**
Hinder, Steve	O64
Hinder, Steven	O63
Hodoroaba, Vasile-Dan	O76, O83, O84, P38, P39, P42, P59
HOGGAN, Philip	O40, O86
Holmes, Darcey	O98
Hruska, Martin	O80
Hryha, Eduard	**K7**, **K10**, O92, O96, P48
Hu, Xiaokang	O94
Hubin, Annick	O21, O52, O123
Humbert, Bernard	O33
Hutter, Herbert	O74
Hutton, Simon	**O47**, **O48**, O116

Hyot, Bérangère	O79

I

Iida, Shin-ichi	O34
Ikita, Konomi	O115, O117, **O126**
Ilcheva, Vania	O31
Ionescu, Cornelia	O23
Isram, Muhammad	**P34**
Isufaj, Njomza	O74
Iwasaki, Takeshi	P1
Izquierdo, Manuel	O124

J

J. Tavares, Carlos	P34
Janek, Jürgen	O113
Jarenmark, Martin	O110
Jayantilal Vasa, Nilesh	O3
Jehl, Zacharie	O106
Jeschull, Fabian	P53
Jeurgens, Lars	O57
Jeurgens, Lars P.H.	O24, **O60**, P15
Jiménez-Guerra, Maykel	O106
Jiryaeisharahi, Zahra	O58
Johansson, Fredrik O. L.	O101
John, Elisabeth	**O76**, P39
Jolly, Lionel	O25
Jones, Elliot	O84, P39
Jordan, Vanja	P10
Jouanneaud, Romain	O36, **O40**
Joubert, Olivier	O81
Jungnickel, Harald	O89
Just, Justus	O101

K

Kaciulis, Saulius	O90, P45, P47, P62
Kaciulius, Saulius	P49
Kakko, Katri	K10
Kammlander, Birgit	**O109**
Kang, Liqun	O17

Kanyandekwe, Joël P25
Katsarelias, Dimitrios O5
Kawakami, Ryota P14
Kawala, Wiktor O98
Kawamura, Midori O80
Kayser, Sven O88
Kayser, Yves O17
Kazi, Sofia K10, **O92**
Kentsch, Ulrich O56
Kerdjoudj, Halima O13
Kerner, Zsolt O56
Kiazadeh, Asal O30
KIM, Minjin O45
Kiriakidou, Maria O11
Kisaichi, Kosuke P1
Kitel, Matthäus O124
Kleine-Boymann, Matthias **O88**
Klementiev, Konstantin O101
Knez Marevci, Maša P33
Knez, Željko P33
Knigge, Xenia P59
Kolev, Kolyo O31
Kollender, Jan Philipp P15
Koltsov, Alexey P19
Kondratenko, Evgenii P9
Kosto, Julia O75
Kosto, Yuliia O72
Kotowska, Anna O98
Kovalenko, Maksym O24
Kovač, František P52
Kovač, Janez O46, **P10**
Kozdemba, Justyna P3
Kravanja, Katja Andrina **P33**
Krystianiak, Anna O104
Kumar, Santosh O122
Kurczy, Michael E. P43
Kuroki, Shin-Ichiro O119

Kürnsteiner, Philipp	O95
L	
Laha, Priya	O58
Lakhdar, Mehdi	O62
Lama, Giuseppe Cesare	O90
Lambert, Jean-François	O7
Landoulsi, Jessem	**O7**
Lange, Thorid	O76, P39
Lanzutti, Alex	P45
Laudani, Francesco	**P41**
Lauzin, Clément	O62
Lavorgna, Marino	O90
Ledeuil, Jean-Bernard	P55
Lee, Tae Geol	O89
Lefterova, Elefteria	O31
LEGRAND, Marie	O45
Leidlmair, Daniel	**O59**
Lemaire, Sebastien	O23
Lennon, David	O26
Li, Jun-Xian	O78
Li, Zhixiang	O94
Lin, Chia-Jou	O34
Lin, Wei-Chun	O34, **O78**
Lindgren, Johan	O110
Linsler, Dominic	P29
Liu, Huiqun	P13
Liu, Liang	O13
Liu, Ning	O1
Liu, Yuhan	P20
Lloreda, Javier	O67
Lloreda-Jurado, Pedro Javier	O19
Lobera, M. Pilar	P54
Long, Jianzhan	**P12**
Longo, Filippo	**O19**
Lorenzin, Giacomo	O57
Louvain, Nicolas	P55
Luneau, Mathilde	**O29**

Lunelli, Lorenzo	P4
Luntadila Lufungula, Léon	O15
Luxa, Jan	P37
Lyanage, Manura	O57
Lê-Chesnais, Joanne	O7

M

Macak, Karol	O47, O48
Machata, Peter	O80
Mack, Paul	**O121**, P40
Mackova, Anna	P37
Macková, Anna	P11
Madbouly, Loay Akmal	**O84**
Madelat, Negin	**O52**
Magrin Maffei, Riccardo	P34
Mahlin, Denny	O53
Mahoney, Phillip	K10, O92
Maibach, Julia	**K8**, P50
Maindron, Tony	O82
Malinsky, Petr	**P37**
MAMERI, Ali	O105
Man, Gabriel J.	O101
Mann, Jennifer	**O20**, O111
Mann, Jenny	O42
MANSERI, Amar	O105
Marchal, Wouter	P7
Marchesini, Sofia	O22
Marchfelder, Cornelia	O66
Marcoen, Kristof	O15
Marcus, Philippe	**K2**
Marinova, Vera	**O51**, O54, **P44**
Martin, Mickael	O81
Martinez, Eugenie	P23
Martinez, Eugénie	P22, P25
Martini, Leonardo	P34
Martins, Raquel	O30
Martins, Rodrigo	O30
Mast, Jan	O9

Matouk, Zineb	**O65**
Matthews, Lauren	**P42**
Matulka, Daniel	O74
Maxa, Jacob	**P61**
Mayr, Georg	O59
Mazanek, Vlastimil	P37
McCalla, Eric	O116
McCullough, Orfhlaith	P20
McHardy, Kate	O69
Meeusen, Mats	O52
Mehn, Dora	O12, P6
Menegus, Chiara	**P15**
Menyhard, Miklos	O56
Merker, Daniel	O10
Mescola, Andrea	P34
Meynen, Vera	O15, O21
Mezzi, Alessio	**O90**, P45, P47, P49, P62
Michielsen, Bart	O15
Micusik, Matej	**O80**
Mikhailova, D.	P51
Mikšová, Romana	**P11**
Miles, Alastair	O98
Minev, Nikolay	O51, O54, P44
Mirabella, Francesca	O39
Moellers, Rudolf	O88
Moffitt, Chris	O116
Mogwitz, Boris	O113
Molodtsov, Serguei	O124
Moncada, Massimo	P47
Monier, Guillaume	O36, O40, **O86**
Montanari, Roberto	P45, **P47**, P49, P62
Montserrat-Sisó, Gerard	O29
Morales, Carlos	O72, **O75**
MORCHAIN, Bruno	O6
Morgan, David	**O41**
Morgan, David J	O26
Mortemard, Benoit	P55

Moryson, Yannick	O112
Motýľová, Marcela	P52
Mozetic, Miran	P57
Mrkwitschka, Paul	O84, P39
Mukherjee, Shriparna	**O55**
Mukherjee, Soham	**O101**
Mullens, Steven	O15
Murali, Mukesh	**P48**
Mussi, Valentina	O54
Muthuvijayan, Vignesh	O3
Mähl, Sven	O125
Méthivier, Christophe	O7
Müller, Hendrik	P58

N

Nabeshima, Fuyuki	O115, O117, O126
Naghavi, Negar	O104
Naghdi, Shaghayegh	O74
Nakai, Masaaki	**P1**
Napoleonov, Blagovest	O51
Narayanan Unni, Sujatha	O3
NARVAEZ ADAMS, Roberth Mateo	**P7**
Nastovjak, Alla G.	O86
Navne, Jesper	O28
Neittaanmäki, Noora	O5
Nekvindová, Pavla	P11
Nellessen, Alexander	O44
Ngernklay, Piyatep	**P2**
Nicheva, Denitsa	O31
Nishihara, Tappei	O119
NOLOT, Emmanuel	P31
Normant, Antoine	O2
Novák, Josef	P37
Nowottnick, Mathias	P61
Nunney, Tim	O64, **P40**
Nyborg, Lars	K7, O93, P13, P46

O

O'Donnell, Joseph	O1
O'Dwyer, Krsitine	O1
O'Mahony, Charlie	O1, **O87**, P5
Ohama, Toshiyuki	O126
Ohtsu, Naofumi	**P14**
Oladeji, Isaiah	O111
Olofsson Bagge, Roger	O5
Omastova, Maria	O80
Opitz, Robert	O89
Oppong-Mensah, Helen	P40
Orlando, Antonio	P8
ORY, Daniel	O45
Oswald, Steffen	P51
Ottonelli, Ilaria	P6
Ozcan, Özlem	O18
O’Dwyer, Kristine	**P5**

P

Palgrave, Robert	P20
Palombi, Alessandra	**P45**, P49
Panasenko, Iurii	**O103**
Panjan, Matjaz	O56
Paoli, John	O5
Paolicelli, Guido	P34
Parak, Nick	O74
Park, Helen	O63
Patouillard, Julien	O79
PAULY, Nicolas	P31
Pawlak, Bram	O15
Pederzolli, Cecilia	P4
Pedrotti, Anna	P4
Pelissier, Bernard	**O81**, P36
Peters, Stefan	P9
Petit, Matthieu	O86
Petit, Valentine	O125
Petit-Etienne, Camille	O81
Petkov, Plamen	**O32**
Petkova, Tamara	**O31**, O32

Petrozza, Annamaria	P56
Petryshynets, Ivan	**P52**
Phan, Nhu	**P43**
Phuyal, Dibya	O101
Pielsticker, Lukas	**O17**, **O43**
Pimpinelli, Alberto	O86
Piras, Alessandra	O15
Plate, Kristina	O89
Poleunis, Claude	O89
Poli, Isabella	P56
Politano, Olivier	O25, O60
Pollard, Andrew J.	O22
PONCHE, Arnaud	O6
Popa, Ioana	O25
Popov, Cyril	**O10**
Potrich, Cristina	P4
Prato, Mirko	**P56**
Primc, Gregor	P57
Prinz, Carsten	O18, P38
Průša, Stanislav	**O14**
PUEL, Jean-Baptiste	O45
Puigdollers, Joaquim	O106
Pérez-Dieste, Virginia	O75

Q

Qin, Xiao	**P13**
Quilès, Fabienne	O61

R

Racz, Adel Sarolta	**O56**
Rading, Derk	O89
Radjabov, Azim	P60
Radnik, Jörg	**O22**, O76, O83, O84, O89, **P38**, P39, **P59**
Rafailov, Peter	O54, P44
Ramstedt, Madeleine	**K1**, O102
RANGAYEN, Eva	O45
Ranguis, Alain	O86
Ranjbari, Elias	P43

Rath, Jakob	**O74**, P41
Ravat, Brice	O25
Raynaud, Christine	O79
Raza, Ahmad	K10
Rebai, Amelle	O104
Recupido, Federica	O90
Reed, Benjamen	O38
Reed, Benjamen P.	O22
Reekmans, Gunter	O15
Regoutz, Anna	**K6**, P20
Reiner, Sofia	**P50**
Renault, Olivier	**O82**, **P22**, **P23**, P25, P31
Rensmo, Håkan	O101, O109
Rettig, Laurenz	O43
Rečnik, Aleksander	P10
Rheingans, Bastian	O24
Ribič, Vesna	P10
Richetta, Maria	P47
Richy, Jérôme	P25
Rittinghaus, Silja-Katharina	**O96**
Riva, Stefania	O101
Robert-Goumet, Christine	O36, O40, O86, **P31**
Rodriguez, Arturo	P16
Rohnke, Marcus	O113
Roloff, Alexander	O89
Romanenko, Oleksandr	P37
Rooij-Lohmann, Véronique de	O55
Ros, Eva	O33
Rossella, Francesco	P34
Rossi, Antonella	O114, P18, P35
Rossi, Giovanni E	O26
Rota, Alberto	P34
Roy, Krittish	O1, O87, P5
Rueff, Jean-Pascal	O99
Ruiz de Larramendi, Idoia	O108
Ruozi, Barbara	P6

S

Sacco, Alessio	P59
Sahre, Mario	O76, P39, P42
Salas-Reyes, Antonio	O97
Salaverri, Gonzalo	O108
Sall, Mamour	O86
Sandell, Anders	O110
Sann, Joachim	**O112**, O113
Sano, Naoko	**O69**
Saucedo, Cesar	O20
Saucedo, Edgardo	O106
Sauer, Markus	O74, P41
Schaefer, Andreas	**O44**
Scheid, Julien	P19
Schmeida, T.	P51
Schmidt, Jacob	**O118**
Schmitz, Guido	**PS4**
Schofield, Eleanor	O98
Schubert, Andreas	O72
Schulz, Joachim	O124
SCHULZ, Philip	O45
Schusterbauer, Robert	O84, **P39**, P42
Scragg, Jonathan	O101
Sediqi, Salbin	**O18**
Seipp, Kevin	O112
Selvaraj, Sowmya	O3
Seo, Okkyun	O119
Serafino, Giulia	**O123**
Seth, Malobi	O13
Shard, Alexander	**O38**, P21
Sharif, Reza	O95
Shchukarev, Andrey	K1, **O102**
Shokhen, Victor	O29
Shon, Hyun Kyong	O89
Shutthanandan, Vaithiyalingam	P21
Shwartz, Nataliya L.	O86
Siciliani, Lisa	O9
Siemons, Laurens	O15

Silien, Christophe O1
Silva, Carlos O30
Simonov, Konstantin A. O101
Simperl, Florian **O120**
Simpson, Robin P40
Sjögren Cehajic, Kevin O5
Sjövall, Peter **O53**, **O110**
Smeesters, Lien O21
Sofer, Zdenek P37
Son, Jin Gyeong O89
Soomary, Liam O47, O48, **O116**
Sordetti, Francesco P45
SORET, Etienne O45
Soulimane, Tewfik O1
Soulé, Samantha **O13**, **O61**
Soundarapandiyan, Gowtham O96
Spampinato, Valentina O89
Speranza, Giorgio P8
Stankova, Alice O68
Steely, Lee O58
Stehrer, Thomas O77
Stepanovska, Eva P37
Stifter, David O59, O66, O77, O95
Stockmann, Jörg M. **O83**
Stockmann, Jörg Manfred O76, O84
Strandberg, Linnéa O29
Strange, Lyndi P21
Strauss, Florian O113
Strauß, Bernhard O59
Strijkova, Velichka P44
Stucky de Quay, Theo P20
SUCHET, Daniel O45
Sun, Jinhua P2
Suu, Koukou O111
Swart, Hendrik C **O27**
Swart, Hendrik Christoffel P32
Sweeney, Stephen O64

Syed, Tofail O1
Sánchez, Yudania O106
Säckl, Gary **O66**

T

Taborelli, Mauro O125
Taboryski, Rafael O28
Taguchi, Noboru **O115**, O117, O126
Takada, Rino P14
Takagi, Yasumasa O119
TALBI, Lamia O105
Tallarek, Elke O37
Tam, Eric **O50**
Tam, Pui Lam O96
Tanaka, Akihiro O126
Tang, Jui-Fu O78
Tchernychova, Elena **P54**
Tejeda, A P16
Tentschert, Jutta O89
Terblans, Jacobus Johannes **P32**
Terblans, JJ O27
Terryn, Herman O52, O58
Thalberg, Kyrre O53
Theissen, Jennifer P7
Thissen, Andreas O39
Thomas, A. P51
Thomas, Clémence **O25**
Thünemann, Andreas P59
Tielens, Frederik P7
Tiwary, Chandra **O85**
Tofail, Syed A. M. O87, P5
Tomasetti, Benjamin **O62**
Tosi, Giovanni P6
Tougaard, Sven **K5**
Tranca, Ionut P7
Tratnik, Blaz P54
Treglia, Antonella P56
Trouillet, Vanessa **P29**

Tröger, Jan	O37, O73
Tsamo, Guy	O86
Tschammer, Rudi	**O72**, O75
Tsutsumi, Kenichi	O115, O117, O126
Turlo, Vladyslav	O57, O60
Turri, Laura	**P19**

U

Uchida, Tatsuya	O115, **O117**, O126
Ueki, Kosuke	P1
Usmanov, Dilshadbek	**P60**
Utke, Ivo	O60
Uvdal, Per	O110
Uzoni, Simon	**O4**

V

Vaglio, Emanuele	P45
Valdez, Raul	P17
Valenza, Marta	P6
Valtiner, Markus	P28
Van Doorslaer, Sabine	O15
Van Roekeghem, Ambroise	O99
van Spronsen, Matthijs	O122
Vandelli, Angela	P6
Vanzetti, Lia	**P4**, **P8**
Vaníčková, Elena	O14
Varone, Alessandra	P45, P47, **P49**
Vaxelaire, Nicolas	O79
Verleysen, Eveline	O9
Verona, Claudio	P45
Vesel, Alenka	**P57**
vicentini, olimpia	O9
Videva, Vladimira	P44
VIDON, Guillaume	O45
Villar-Garcia, Ignacio	O75
Visagli, Gianluca	**O70**
Vizintin, Alen	P54

W

Wahl, Tina	O100
Walczak, Lukasz	**P3**
Wallner, Gernot	O66
Wallner, Gernot M.	O59
Walther, Felix	O113
Wang, Fuyi	O89
Wang, Yi-Kai	O78
Wang, Yung-Chen (Andrew)	O89
Watts, John	**K9**
Watts, John Farnham	O98
Webb, Paul	O122
Wei, Xiuyu	O94
Weimann, Thomas	O83
Weise, Matthias	O76
Weiss, Laurent	O13
Welle, Alexander	O12
Wenger, Christian	O72, O75
Werner, Wolfgang	O120
Werner, Wolfgang S.M.	**K3**
Wetzel, Annica	O35
White, Richard	O64
Wickman, Björn	O29
Wildersinn, Leonie	O103, **P53**
Willock, David J	O26
Witt, Julia	O18, O35
Wohlrab, Sebastian	P9
Wolfsjäger, Benedikt	**O95**
Wong, E Laine	P56
Wouters, Benny	O52, O123
Wu, Chien-Ching	O55
Wu, Chun-Sheng	P56
Wu, Jianguo	O94
Wu, Xiaohan	O113
Wyns, Kenny	O15

X

Xu, Laurent	**P36**
Xu, Tao	P12

Y

YADDADEN, Chafiaa	**O105**
Yang, Ji	O94
Yang, Jian	P12
Yasuno, Satoshi	**O119**
Yesilcicek, Yasemin	O35
Yokouchi, Kazushiro	O115, O126
Yuan, Miwen	**O94**
Yubero, Francisco	O19, **O67**
Yun, Jae	O63
Yusim, Yuriy	O112

Z

Zaar, Oscar	O5
Zaccarine, Sarah	O20, **O111**
Zacchetti, Nicoletta	P35
Zakel, Julia	O88
Zaplotnik, Rok	P57
Zeng, Ruilin	P12
Zhang, Kaimin	O15
Zhang, Yongliang	O1
Zhao, Yao	O89
Zhelev, Veselin	O32
Zhirnov, Ivan	O96
Zhu, Xinhua	O123
Zografopoulos, Dimitrios	O54
Zurutuza, Amaia	P39

Ö

Özcan Sandikcioglu, Özlem	**O35**

Š

Šikola, Tomáš	O14